

STARK BROADENING OF ISOLATED ION LINES BY PLASMAS

PETER BREGER

Dissertation submitted for the degree of
Master of Science (Physics),
University of Cape Town

September, 1980

The University of Cape Town has been given
the right to reproduce this thesis in whole
or in part. Copyright is held by the author.

The copyright of this thesis vests in the author. No quotation from it or information derived from it is to be published without full acknowledgement of the source. The thesis is to be used for private study or non-commercial research purposes only.

Published by the University of Cape Town (UCT) in terms of the non-exclusive license granted to UCT by the author.

CONTENTS

	<u>Page</u>
Abstract	i
Preface	iii
 <u>P A R T A</u>	
Introduction	1
 <u>CHAPTER 1 : FROM A QUANTUM MECHANICAL FORMULATION TO A SEMI-CLASSICAL MODEL</u>	 10
1.1 The Impact Approximation	12
1.2 Weak Inelastic Cross-Sections	18
1.3 The Elastic Cross-Sections	21
1.4 Strong Collision Contributions	27
 <u>CHAPTER 2 : RADIATOR STRUCTURE</u>	 29
2.1 The Absorption Oscillator Strength	30
2.2 Correction for Equivalent Electron Configurations	33
2.3 Reduction of Radiator Structure Details	37
2.4 Configuration Interaction	43
2.5 The Completeness Parameter	48
 <u>CHAPTER 3 : THE EFFECTIVE GAUNT FACTOR</u>	 50
3.1 Upper Cut-off of Eccentricity	55
3.2 Lower Cut-off of Eccentricity	63
3.3 Asymptotic Behaviour of \bar{g}	71
i) High-energy Bethe formula	71
ii) Analytical behaviour of \bar{g}	71
iii) Non-zero threshold value for ion scatterers	77
3.4 Extrapolation Below Threshold	78
3.5 The Velocity Average of the Effective Gaunt Factor	81

	<u>Page</u>
<u>CHAPTER 4</u> : <u>FURTHER CONTRIBUTIONS TO THE BROADENING</u>	92
4.1 The Strong Collision Term	92
4.2 Verification of $\beta=1$ in the Unitarity Condition	96
4.3 The Ion Perturber Contribution	103
4.4 The Disentanglement Parameter	106
4.5 The Collision Time Parameter	111
 <u>CHAPTER 5</u> : <u>COMPARISON WITH EXPERIMENTS</u>	 114
5.1 SnII - Radiator Structure Complexities and Stark Widths	114
5.2 Stark Widths of Isolated Oxygen Ion Lines ..	128
5.3 Stark Widths of Isolated Sulphur Ion Lines .	142
5.4 Stark Widths of Isolated Argon Lines	153
5.5 Stark Widths of Isolated Nitrogen Ion Lines	161
5.6 Stark Broadening from Isolated ClIII and FII Ion Lines	168
5.7 Stark Widths of Isolated CIII Ion Lines	175
 <u>CHAPTER 5</u> : <u>CONCLUSION: TRENDS AND REGULARITIES</u>	 181
 <u><u>P A R T</u></u> <u>B</u>	
 <u>SECTION 1</u> : <u>IMPLEMENTATION OF COMPUTER CODES</u>	 196
Program 1 : MTD1	196
Program 2 : MTD2	204
Program 3 : MTD2A	210
 <u>SECTION 2</u> : <u>COMPUTER CODES</u>	 217
 APPENDIX I : Hey and Breger (1980a)	 247
APPENDIX II : Hey and Breger (1980b)	258
APPENDIX III : Hey and Breger (1980c)	280
APPENDIX IV : Data Files BATES. and BATES2.	297
 Bibliography	 301

TABLES and ILLUSTRATIONS

	<u>Page</u>
Table 0.1 : Homologous ion structure	8
Fig. 3.1 : Classical hyperbolic electron orbit	52
Fig. 3.2 : Solution of cubic	62
Fig. 3.3 : Regions of validity of the unitarity condition	76
Fig. 3.4 : Maxwellian average of Gaunt factor	82
Fig. 3.5 : Plot of threshold Gaunt factor vs. change in effective principal quantum number	85
Fig. 3.6 : Energy dependence of Gaunt factor: NV 2s → 2p transition	88
Fig. 3.7 : Energy dependence of Gaunt factor: NV 2s → 3p transition	89
Fig. 3.8 : Ionisation stage dependence of threshold Gaunt factor: 3s → 4p transition	91
Table 4.1 : Effect of β on transition probability	101
Table 4.2 : Effect of β on line widths	102
Table 5.1 : Quantum defects in SnII structure	115
Table 5.2 : Spin orbit splitting factor for the p ² p ⁰ and d ² D series	116
Table 5.3 : Coupling constants calculated from transition probabilities	118
Fig. 5.1 : Spread in coupling constants	119
Table 5.4 : Comparison between measured and calculated widths: SnII	123
Table 5.5 : Experimental uncertainties and agreement of theory with experiment	124
Fig. 5.2 : Effect of configuration interaction	125
Fig. 5.3 : Variations in contributions within multiplets	127
Table 5.21 : Estimated term energies of OII	131
Table 5.22 : Estimated term energies of OIII	132
Table 5.23 : Effect of type of velocity average on line widths	133
Table 5.24 : Comparison between measured and calculated widths: OII	135
Table 5.25 : Comparison between measured and calculated widths: OIII	136

	<u>Page</u>
Table 5.26 : Comparison between various calculational methods: OII	137
Table 5.27 : Comparison between various calculational methods: OIII	138
Table 5.28 : Threshold effective Gaunt factors: OIII ..	139
Table 5.31 : Comparison between measured and calculated widths: SIII, SIV	147
Table 5.32 : Comparison between various calculated line widths: SIII, SIV	148
Table 5.33 : Comparison of various computational methods for SIII line widths	149
Table 5.34 : Threshold effective Gaunt factors: SIII ..	151
Table 5.35 : Threshold effective Gaunt factors: SIII ..	152
Table 5.41 : Estimated term energies of Argon	156
Table 5.42 : Comparison between measured and calculated widths: AIII	157
Table 5.43 : Comparison between measured and calculated widths: AIV	158
Table 5.44 : Comparison of calculational methods of AIII and AIV	159
Table 5.51 : Comparison between measured and calculated widths: NIII, NIV	165
Table 5.61 : Comparison between measured and calculated widths: FII	172
Table 5.62 : Comparison between measured and calculated widths: ClIII	173
Table 5.71 : Comparison between measured and calculated widths: CIII	177
Table 6.1 : Homologous ions	181
Table 6.2 : Transitions within homologous ions: ground term: $ns^2 np^2 \ ^2P^0$	182
Table 6.3 : Transitions within homologous ions: ground term: $ns^2 np^2 \ ^3P$	182
Table 6.4 : Transitions within homologous ions: ground term: $ns^2 np^3 \ ^4S^0$	183
Table 6.5 : Transitions within homologous ions: ground term: $ns^2 np^4 \ ^3P$	184
Table 6.6 : Comparison between theory and measurement .	186
Fig. 6.1 : Dependence of threshold Gaunt factor on change in effective principal quantum number: s-p transitions	190

Fig. 6.2	: Dependence of threshold Gaunt factor on change in effective principal quantum number: p-d transitions	191
Fig. 6.3	: Dependence of threshold Gaunt factor on change in effective principal quantum number: d-f transitions	192
Fig. 6.4	: Plot of threshold Gaunt factor versus $\frac{1}{Z}$...	193
Flowchart 1:	Flow of main program MTD1M	200
Flowchart 2:	Structure of calculations	201
Flowchart 3:	Structure of calculations	207
Flowchart 4:	Gaunt factor integration	214

ABSTRACT

This study focuses on the development and the evaluation of a practical Stark broadening calculation of isolated ion line widths by Hey. In particular, emission profiles produced by optically thin plasma sources are considered.

Despite the development of the fully quantum mechanical theory in the impact regime by Baranger, the semi-empirical and semi-classical approximations by Griem have been widely used in the practical prediction of widths of isolated lines. Whereas these approximations achieved fair success for singly-ionised emitters, discrepancies have been widely reported in the application to the more highly-ionised species.

In order to make use of the advantages offered by the classical path approximation, a new derivation of the effective Gaunt factor appearing in the excitation cross-sections has been carried out. In particular, this function is derived with proper allowance for curvature of the electron (perturber) orbit. Careful examination of the restrictions on a classical path approximation is seen to lead to a Gaunt factor based in spirit on the approach used by Griem, but achieving a continuity as a function of energy for all above-threshold energies, as well as a reduction to the correct limiting behaviour at high energies (Bethe approximation). The extension of the Gaunt factor into the below-threshold energy regime for inclusion of elastic contributions to the broadening is thus facilitated and two methods of achieving this are discussed.

Apart from this major change required in order to deal with the spectra emitted by ions of ionisation stage $Z \geq 2$, it is found that the radiator structure of the emitter plays an important role in the line broadening. Details of the radiator structure required for application of the LS coupling scheme, such as configuration interaction and equivalent electron configurations, are therefore taken into account where necessary.

The derived theory is presented together with its properties and applied to spectral lines of a wide range of ion emitters, namely SnII, OII, OIII, SIII, SIV, AIII, AIV, NIII, NIV, ClIII, FII, CIII. The agreement obtained between theory and experiment is compared with results reported by various authors. Furthermore, attention is paid to the trends and regularities in Stark broadening parameters for iso-electronic and homologous ions, as well as variations within multiplets.

The presented theory is found to yield good agreement for ions of $2 \leq Z < 5$, compares very favourably with some other theoretical approaches in most cases, and is seen to succeed in the improvement of present calculational methods.

PREFACE

The aim of this thesis is the evaluation of a proposed practical procedure by Hey (1979, private communication) for the computation of Stark widths of isolated ion lines, which can be used to correlate experimental data from spectral lines in plasmas. In particular, it is concerned with emission profiles only, normally produced by laboratory plasmas which are optically thin (or require only small corrections for opacity (Griem: 1964)) in the spectral region of interest. Broadening effects specifically associated with radiative transfer in optically thick material, such as stellar atmospheres, are therefore ignored in this investigation.

Line broadening is a direct function of the environment of the radiating atom or ion, and thus offers itself as an attractive non-interfering probe for the measurement of plasma conditions (Baranger: 1962; Griem: 1964, 1974; Cooper: 1966). Such an application is not only of great importance in the determination of the physical state of stellar atmospheres (Mihalas: 1970), but is attaining greater importance with the rapidly increasing demand for the utilisation of high density plasmas in fusion experiments (KWU-report: 1973; Burgess et al.: 1967; Breton et al.: 1977; Hauer: 1980).

The finite width of a spectral line can be ascribed to three mechanisms (Griem: 1964; Traving: 1968):

- (a) the natural line width;
- (b) Doppler broadening;
- (c) pressure broadening.

The natural line width of a line is caused by the interaction of the radiating system with its radiation field (Heitler: 1954) and is usually negligibly small for practical purposes (Baranger: 1958a). The thermal motion of the emitting atom or ion gives rise to Doppler broadening, and the interaction of the emitting atom or ion with surrounding particles causes pressure broadening. The last broadening mechanism can be subdivided into three further categories, depending on the type of surrounding perturbing particles: resonance broadening, van der Waals broadening and Stark broadening (Griem: 1964). Each of these arises from the interaction of the radiator atom with atoms of the same kind, atoms or molecules of a different kind, and charged particles respectively. It is the last category of Stark broadening which is the subject of this thesis, because of its practical importance discussed below. (In addition to the above broadening mechanisms, instrumental broadening is introduced by the scanning spectrometer and has to be accounted for in the analysis of experimental line profiles.)

Of the above mentioned mechanisms, Doppler and Stark broadening are of major practical importance in highly ionised plasmas (Wiese: 1965; Griem: 1964). Since Doppler broadening is caused directly by the thermal motion of the radiator, it can be used to determine the temperature of the radiating system. Stark broadening (pressure broadening) is

however relatively insensitive to temperature and, unlike Doppler broadening, depends directly on the pressure of the system. Stark broadening thus becomes the dominant broadening mechanism at large pressures, as is seen when comparing widths of lines from glow discharges with those from high pressure arcs (Marr: 1968). Since these two mechanisms give rise to two different line profiles (Doppler broadening causes a Gaussian shape, whereas Stark broadening gives rise to a Lorentzian profile for isolated lines in the impact approximation), de-convolution techniques can be applied to experimental data to yield the separate line profiles. Since Stark broadening predominates in high pressure plasmas, the perturber densities (usually free electron densities) can thus be deduced. This use of Stark broadening as a practical probe has been particularly applied to spectral lines from hydrogen and hydrogenic ions, as these are strongly sensitive to Stark broadening effects (Baranger: 1962; Griem: 1964, 1974).

A minor disadvantage of the Stark broadening analysis is the required knowledge of the kinetic temperature of the plasma (Wiese: 1965). Since the Doppler width is usually much smaller than the Stark width, line profile analysis does not provide a useful means of obtaining kinetic temperatures. Use is therefore often made of total (integrated) line intensity ratios and line-to-continuum ratios for this purpose (Griem: 1964). Stark widths are also experimentally more difficult to obtain than Stark shifts of the line, since the latter require wavelength calibration only, whereas widths

require an additional intensity calibration (Wiese: 1965). Calculation difficulties associated with the line shifts (Griem: 1964, 1968, 1974) make this simple measurement however less reliable, and width measurements are favoured (Wiese: 1965). For ionic lines, additional shifts from plasma polarisation make accurate predictions of density from shift measurements difficult (Griem: 1974; Volonté: 1978). Apart from free electron density determination in dense plasmas, other applications are possible. For plasmas of known pressure in local thermodynamic equilibrium (LTE), both the temperature and electron density can be obtained (Wiese: 1965; Griem: 1964). Alternatively, the use of Stark width measurements as a means of checking the existence of LTE as well as a means of correcting line and continuum intensities has been suggested (Wiese: 1965). Examples of such diagnostic use of Stark widths are the analysis of a laser produced plasma by Burgess et al. (1967) and the determination of the electron density from the HeII line $\lambda = 3203 \text{ \AA}$ by Bogen (1972).

The lines from hydrogen and hydrogenic ions are subject to linear (quasi-static) Stark effects and are therefore far wider than the isolated impact-broadened lines. This has been the reason for the major part of attention devoted to these ion lines. While isolated impact-broadened lines are therefore of less interest for diagnostic purposes, they provide a direct test of our knowledge of the structure of complex atomic systems (Hey: 1977a, 1978). Whereas comparison between theory and experiment for the singly-ionised

radiators has yielded good results (Griem: 1974; Jones et al.: 1974) the state of theory for multiply-charged ions has remained unsatisfactory (Hey and Bryan: 1977). Some discrepancies for individual linewidth calculations by various authors have been reported as follows:

CIII	$\frac{W_m}{W_c} \sim 2$	Bogen (1972)
NIII	$\frac{W_m}{W_c} \sim 2$	Hey and Bryan (1977)
NIV	$\frac{W_m}{W_c} \sim 5$	Källne et al. (1979)
OIII	$\frac{W_m}{W_c} \sim 2$	Hey and Bryan (1977)
SIII	$\left\{ \begin{array}{l} \frac{W_m}{W_c} \sim 0.5 \\ \frac{W_m}{W_c} \sim 2.0 \end{array} \right.$	Platiša et al. (1979)

$\frac{W_m}{W_c}$ denotes the ratio of measured to calculated linewidth. These reported discrepancies therefore provide an incentive for further investigation of the existing computational techniques, one of which is developed in detail in this thesis.

ACKNOWLEDGMENTS

I wish to express my thanks to the University of Cape Town for providing me with the necessary financial assistance from the Joseph Stone and Janet Goldblatt bursaries during 1979, and the Siri Johnson and Twamley post-graduate bursaries during 1980. My thanks also go to the Physics Department for providing me with a post-graduate assistantship during both years.

I also wish to thank Miss L. Jennings for typing my manuscript and Ms R.A. Hill for her proof-reading and help with compilation of this work.

The extensive calculations done during this research were performed at the Computer Centre of the University of Cape Town.

Those references cited as private communication in the text were communicated to me through my supervisor, Dr. John Hey. I should like to thank these people for their helpful comments.

My deepest debt of gratitude is owed to my supervisor, Dr. John Hey, for his unstinting aid over the last two years.

INTRODUCTION

With the large acquisition in the last decade of experimental data on Stark widths from isolated ion lines for the determination of electron densities (Konjević and Wiese: 1976) , a critical re-evaluation of theoretical developments of Stark broadening has become imperative. Despite the fully quantum mechanical solution of the line broadening problem obtained by Baranger (1958a, c), classical collision concepts have remained an essential feature of the analysis of the broadening mechanism (Griem: 1974). The reason for this feature has been the inadequacy of the quantum mechanical formulation in providing a readily computable programme for calculation of the many collision cross-sections required in the determination of the line shape. For example, in the distorted-wave calculation (Davis, Kepple and Blaha: 1976) this failure can be specifically attributed to the large number of partial waves that normally need to be analysed laboriously for each single cross-section, thus giving rise to prohibitive lengths of computing times when large numbers of line widths are required. Quantum mechanical calculations of widths have thus become available only relatively recently, and the accuracy of these is potentially well within the agreement obtained by semi-classical theories (Bely and Griem: 1970; Barnes and Peach: 1970; Hey and Blaha: 1978) combining classical collision statistics with quantum mechanical radiator structure details. The success obtained by Griem (1974), using a semi-classical method for the calculation of Stark

broadening of singly ionised ion lines thus encourages the further development of semi-classical methods for use in the determination of Stark widths from ions of higher ionisation stages. Such a development of the semi-empirical theory by Griem (1968) has been undertaken by Hey (1979, private communication) and this thesis forms part of the evaluation and improvement of this development.

As already mentioned (see Preface), Stark broadening is caused by the interaction between the radiator ion and surrounding charged particles. This broadening mechanism is thus an extension of the well-known Stark effect; the splitting and polarisation of spectral lines parallel and perpendicular to an applied electric field (Herzberg: 1937; Bethe and Salpeter: 1957). In the case of hydrogen, one obtains, for example, a pattern of components symmetrically disposed around the position of the unperturbed line (Condon and Shortley: 1935). The collision of charged particles in a plasma with the radiator will thus impose a varying electric field, and thus a perturbation, giving rise to a rapidly varying pattern of components, which is observed as a broadening effect. The second order Stark effect, however, gives rise to an asymmetrical splitting, and thus the line is not only broadened, but also shifted (Marr: 1968).

As a starting point for the analysis of such a line profile, the following expression for the power spectrum obtained from all possible transitions in the radiator needs to be considered (Baranger: 1958a, b, c):

$$P(\omega) = \frac{4\omega^4}{3c^3} \sum_{if} \delta(\omega - \omega_{if}) |\langle f | \underline{d} | i \rangle|^2 \rho_i \quad (0.1)$$

Here ω_{if} denotes the angular frequency of a spectral line resulting from a transition from state $|i\rangle$ to $|f\rangle$

($\hbar\omega_{if} = E_i - E_f$), \underline{d} is the dipole moment operator, and ρ_i is the probability of occurrence of state $|i\rangle$. In the case of isolated lines, interest is confined to a small region $\omega_{if} \pm \Delta\omega$ about the unperturbed frequencies, and it is thus sufficient to regard:

$$F(\omega) = \sum_{if} \delta(\omega - \omega_{if}) |\langle f | \underline{d} | i \rangle|^2 \rho_i \quad (0.2)$$

as the line shape. Taking the Fourier transform of the line shape, one readily obtains an expression for the auto-correlation function of the light amplitude, which can be rewritten in terms of the quantum mechanical states of the system of radiator and perturbers (Baranger: 1958a):

$$\mathbb{V}(s) = \int_{-\infty}^{\infty} F(\omega) e^{-i\omega s} d\omega \quad (0.3)$$

$$\begin{aligned} &= \sum_{if} \rho_i e^{-i\omega_{if}s} |\langle f | \underline{d} | i \rangle|^2 \\ &= \text{Tr}[\underline{d} T^+(s) \cdot \underline{d} T(s) \rho] \end{aligned} \quad (0.4)$$

Tr denotes the trace of the quantum mechanical operators \underline{d} , $T(s)$ (time evolution operator in the Schrödinger picture) and the density matrix ρ :

$$T(s) = e^{-\frac{i}{\hbar} H_0 t} U(s)$$

where

$$H = H_A + \sum_j K_j + \sum_j V_j$$

$$= H_0 + \sum_j V_j ;$$

$$\sum_j K_j \equiv \text{kinetic energies of the } N \text{ perturbers;}$$

$$H_A \equiv \text{atomic Hamiltonian;}$$

$$\sum_j V_j \equiv \text{perturbation potential arising from the interaction between perturbers and radiator } (H_1(s));$$

$$U(s) \equiv \text{time evolution operator in the interaction picture}$$

$$= \sum_{n=0}^{\infty} \frac{1}{(i\hbar)^n} \int_0^s ds_1 \int_0^{s_1} ds_2 \dots \int_0^{s_{n-1}} ds_n H_{\text{I}}(s_1) \dots H_{\text{I}}(s_n) \quad (0.5)$$

$$(s \geq s_1 \dots \geq s_{n-1})$$

In order to make use of a classical path approximation, and thereby assuming that the perturbers move along a fixed orbit about the radiator, one needs to neglect the back reaction of the atom on the perturbers. This assumes that the density matrix ρ remains the same at all times, thus placing a restriction of short times s on the collision intervals of importance (Baranger: 1958b). It is then possible to separate out the averaging procedure over the radiator and

the perturbers by writing:

$$\mathbb{W}(s) = \text{Tr} [\underline{d}T^+(s), \underline{d}T(s)]_{AV} \quad (0.6)$$

where the trace facilitates the average over the radiator states and the subscript AV denotes an independent average over the perturber velocities. Since the latter is readily obtainable from an integration over the Maxwellian velocity distribution, the situation is greatly simplified. As has been shown by Baranger (1958b), the above approximation regarding the important collision intervals s is just the impact approximation. This approximation, which is examined in detail in Chapter 1, is also known from the classical picture obtained from the interpretation of the Fourier integral 0.3. It amounts to saying that the auto-correlation function $\phi(s)$ differs appreciably from its unperturbed value only in times much longer than the average collision time, a situation analysed classically by Lorentz (1906). In consideration of the Fourier integral 0.3, the opposite extreme to the impact approximation is known as the quasi-static approximation, meaning that the auto-correlation function $\phi(s)$ varies rapidly within a single collision interval (Baranger: 1962). This situation has been analysed classically by Holtsmark (1919), but a quantum mechanical analogue does not exist (Baranger: 1958a, c). Since the major contribution to the broadening of the isolated lines arises from electron perturbers (Baranger: 1962; Griem: 1964, 1974), it is the impact approximation which remains of

interest for the development of the line width calculation in this thesis (Baranger: 1958a, b, c; Griem: 1974).

The separation of the line width problem into two parts, as in eq. 0.6, and the resultant analysis of the problem in a quantum mechanical treatment of the radiator on the one hand, and the classical treatment of the perturbing electrons on the other, is examined carefully in Chapter 1. It is this separation which is central to the semi-empirical method developed by Griem (1968), which forms the starting point for the calculations presented in this thesis.

In the semi-empirical calculations of Stark widths (Griem: 1968), the estimation of the collision cross-sections relies on the validity of the effective Gaunt factor approximation for excitation cross-sections (van Regemorter: 1962; Seaton: 1962a, b). The use of the empirical data by van Regemorter (1962) in calculation of Stark widths of several singly-ionised ion lines has achieved limited success (Griem: 1968; Hey: 1976, 1977a, c, d, 1978; Hey and Bryan: 1977). For multiply ionised radiators, the empirical values suggested by van Regemorter (1962) and Seaton (1962a, b), as well as the functional form suggested by Griem (1968), were found to be inadequate. Improved versions have been discussed by Griem (1974), but even these failed to predict Stark widths of lines for multiply ionised species adequately (Dimitrijević and Konjević: 1980a). Therefore, a universal effective Gaunt factor should be derived, which combines the already obtained success for singly ionised ions with predictive abilities for higher ionisation stages as well.

The derivation of such an effective Gaunt factor is presented in Chapter 3, and is based on the simple model by Griem (1968, 1974). The expression obtained is found to be continuous for all above-threshold energies and also dispenses with the independent specification of a threshold value required by the earlier model by Griem (1974). The model presented here thus lends itself to extrapolation below threshold for the evaluation of the dipole elastic contributions to the broadening - a procedure originally suggested by Griem (1968). Two methods of extrapolation below threshold for the inclusion of the elastic contributions are discussed in Chapter 3, and their success has been repeatedly tested in the calculations performed in Chapter 5. Further insight is thus gained into the various methods of inclusion suggested in the literature (Griem: 1968; Fleurier et al.: 1977).

Apart from the improvement obtained by extension of the semi-empirical procedure into the high-Z regime, the details of the radiator structure have been included - a feature which is particularly lacking in the partially successful semi-classical model by Griem (1974, eq. 526). In particular, the following points are examined in Chapter 2:

- (a) the validity of the LS coupling scheme;
- (b) the inclusion of equivalent electron configurations; and
- (c) the allowance for configuration interaction in the radiator structure.

The importance of such effects in the prediction of variations

within multiplets, for example, has been repeatedly pointed out by Hey (1977b, d, 1978) and Hey and Blaha (1978).

A further point of investigation in this thesis is the possibility of regularities of Stark widths with respect to atomic structure. The regularities obtained in the atomic oscillator strengths (Wiese and Weiss: 1968) have led to investigations of similar trends in the Stark widths (Purić et al.: 1974, 1978, 1979a, b, 1980) as the width depends directly on the atomic oscillator strength (Hey: 1977b; see also Chapter 2). The ion lines investigated in Chapter 5 have thus also been chosen with the outer electron structure in mind, and are tabulated below in Table 0.1:

TABLE 0.1
HOMOLOGOUS ION STRUCTURE

ground term	ion
$ns^2 \ ^1S$	CIII, NIV
$ns^2 np \ ^2P^0$	NIII, SIV, SnII
$ns^2 np^2 \ ^3P$	OIII, SIII
$ns^2 np^3 \ ^4S^0$	OII, ClIII, AIV
$ns^2 np^4 \ ^3P$	FII, AIII

Apart from inclusion of "weak" collisions (Baranger: 1958a, b, c) in the Gaunt factor approximation of collision cross-sections, the inclusion of "strong" collisions is required. Instead of including these contributions in the formulation of the effective Gaunt factor (Griem: 1968, 1974), a separate line width term has been obtained in Chapter 4 for

CHAPTER 1FROM A QUANTUM MECHANICAL FORMULATIONTO A SEMI-CLASSICAL MODEL

The need for a quantum mechanical theory for the estimation of the line width arises when the distance between the radiator and the nearest perturber is of the same order as the de Broglie wavelength of one of the two (Baranger: 1958a). Since the wavelength of electron perturbers is appreciable on the scale of distances under consideration, breakdown of classical treatments may occur for a non-negligible fraction of the total number of collisions between the perturber and radiator systems. Furthermore, the energy exchange in the collision must be much less than the kinetic energy of the perturber, in order for a treatment of the line broadening problem by classical mechanics to be valid (Baranger: 1958a, 1962). Provided that certain criteria are satisfied, one may approximate the fully quantum mechanical result obtained by Baranger (1958c) by the classical path theory. (See in particular Chapter 3 on the effective Gaunt factor.) As discussed in the Introduction, the large number of collision cross-sections required make a fully quantum mechanical calculation impractical, and hence the need for classical path approximations arises (Griem: 1968). In this approximation, the perturbers are assumed to travel along classical paths about the radiator and to interact with the radiator constituents via a changing

electric field (Baranger: 1958b). In order to facilitate an analysis of this problem, the complexities of the radiator structure and the complexity of the statistics of the collision processes can be separated by dividing the calculation up into two terms, each to be treated by appropriate approximations.

A detailed quantum mechanical development of Stark broadening (Baranger: 1958a, c) yielded the following expression for the full width at half maximum (FWHM) of an isolated line $|i\rangle \rightarrow |f\rangle$ in wavelength units (Baranger: 1958c):

$$W_e = N_e \frac{\lambda^2}{2\pi c} \left\{ v \left[\sum_{i'} \sigma_{i'i} + \sum_{f'} \sigma_{f'f} + \int |\phi_i - \phi_f|^2 d\Omega \right] \right\}_{AV} \quad (1.1)$$

where $N_e \equiv$ perturber (electron) density;

$v \equiv$ electron speed;

$\{ \}_{AV}$ denotes the average over a Maxwellian velocity distribution of the perturbers;

$\sigma_{i'i}; \sigma_{f'f} \equiv$ inelastic cross-sections for collisional transitions to levels i' (f') from initial state $|i\rangle$ and final state $|f\rangle$ of the optical transition;

$\phi_i; \phi_f \equiv$ elastic scattering amplitudes for the two states of the perturbed system; the integration being performed over all scattering angles $d\Omega$.

This quantum mechanical expression is valid in the impact approximation (Baranger: 1958a, b, c), which is a weak coupling approximation.

1.1 THE IMPACT APPROXIMATION

It is the nature of this weak coupling that needs to be examined carefully before this quantum mechanical result (eq. 1.1) can be applied to a particular line broadening problem. Apart from a quantitative validity criterion for the above expression, an interpretation of "weak" collisions as opposed to "strong" collisions is given by Baranger (1958b, c) in the consideration of a Dyson expansion of the time evolution operator of the radiator system. Whereas "weak" collisions can be treated by a first order Dyson expansion over times involved in the collision process (see also expression 0.5 for time evolution operator given in the Introduction):

$$|\psi(t)\rangle_I = |\psi(t_0)\rangle_I + \frac{1}{i\hbar} \int_{t_0}^t dt_1 H_{1I}(t_1) |\psi(t_0)\rangle_I \quad (1.2)$$

(where $|\psi(t)\rangle_I \equiv$ radiator wave function in the interaction picture;

$H_{1I} \equiv$ perturbation Hamiltonian for $t > t_0$),

higher orders are appreciable for strong collisions. In order to disentangle (Baranger: 1958c; Feynman: 1951) the resultant higher order terms, the impact approximation needs to be applied to these strong collisions. This approximation

requires that the strong collisions be sufficiently separated in time for the following inequality to hold (Baranger: 1958a, b, c):

$$W \ll \frac{1}{\tau} \quad (1.3)$$

where τ is the duration of a typical collision and W the width of the resultant (impact broadened) line profile. It is in this form that this criterion for the impact approximation is known from classical treatments of the line broadening problem (Breene: 1957; Baranger: 1962), namely as the opposite to the quasi-static approximation (Holtmark: 1919) which does not arise in the quantum mechanical analysis by Baranger (1958a, b, c).

An additional criterion for the impact approximation is obtained by combining the expression 1.3 with the Heisenberg Uncertainty Principle:

$$\tau \gtrsim \frac{\hbar}{\epsilon} \quad (1.4)$$

thus yielding:

$$W \ll \frac{\epsilon}{\hbar} \quad (1.5)$$

where ϵ is the incident electron energy. Since the major contribution to the broadening of the isolated lines arises from the free electron perturbers (Baranger: 1962; Griem: 1964, 1974), any effects associated with radiator motion are

neglected in the following discussion, and the perturbers are considered to be electrons. Corrections owing to ion perturbers are dealt with in Chapter 4.3.

This thesis is restricted to strictly isolated (non-overlapping) lines, and one has thus the additional requirement that:

$$W \lesssim \text{minimum} \left[\frac{\Delta E_{i'i}}{\hbar}, \frac{\Delta E_{f'f}}{\hbar} \right] \equiv \frac{\Delta E}{\hbar} \quad (1.6)$$

where the $\Delta E_{i',i}$ and $\Delta E_{f',f}$ denote the separation in the energy level (term) diagram between the initial (i) and final (f) levels of the spectral line under consideration and the "interacting" or "perturbing" levels i', f' to or from which optically allowed transitions can occur.

In order to apply a classical path treatment (Baranger: 1958b, 1962; Griem, Kolb and Shen: 1959) to the quantum mechanical result 1.1, one requires that the distance between the radiator and the perturber be larger than the (reduced) de Broglie wavelength of the perturber ($\chi = \frac{\hbar}{mv}$) (Baranger: 1958a). Since the orbital angular momentum quantum number l of the perturber is just the impact parameter ρ in units of χ , this is equivalent to the requirement that the relevant l values be large (Baranger: 1962):

$$l = \frac{\rho}{\chi} \gg 1 \quad (1.7)$$

or estimating the collision time $\tau \sim \frac{2\rho}{v}$ (Spitzer: 1940):

$$\tau \gg \frac{\hbar}{\epsilon} \quad (1.8)$$

which indeed implies eq. 1.5 within the impact approximation. Furthermore, the classical path approximation assumes:

$$\epsilon \gg \Delta E \quad (1.9)$$

which contains the condition for inelastic collisions that:

$$\epsilon \gg \Delta E$$

This restriction (inequality 1.9) on the perturber energies allows one to extend the original definition of "weak" collisions by Baranger (1958a, b, c) to include a weak coupling approximation in spatial wavefunctions: apart from the first order Dyson integral (time dependence) applied above, a first order (spatial) Born approximation can be made. Since one is, however, dealing with a charged scattering centre, Coulomb waves need to be employed rather than plane waves. In the high energy limit, both types of first order approximations - the Born I and Coulomb-Born I approximation - tend to the Bethe approximation (Seaton: 1962a, 1975). This high energy limit (Bethe: 1930) is usually considered as the simplification of the Born I approximation (van Regemorter: 1960):

$$|\psi_k^{(\pm)}(\underline{r})\rangle = \left[e^{i\underline{k}\cdot\underline{r}} - \frac{1}{4\pi} \int \frac{e^{\pm i\underline{k}|\underline{r}-\underline{r}'|}}{|\underline{r}-\underline{r}'|} U(\underline{r}') e^{i\underline{k}\cdot\underline{r}'} d^3r' \right]$$

by the expansion:

$$e^{i(\underline{k}-\underline{k}')\cdot\underline{r}} = 1 + i(\underline{k}-\underline{k}')\cdot\underline{r}$$

where $\frac{1}{2} \underline{k}^2 = \frac{1}{2} m \underline{v}^2$

and the unprimed quantities refer to the incident perturber electron and the prime denotes the wave vector of the scattered electron. The Bethe approximation is thus equivalent to the classical path approximation.

Combining these various conditions applicable to isolated lines in the impact regime treated by the classical path approximation, one obtains the following order for the times in question:

$$W \ll \frac{\Delta E}{\hbar} \ll \frac{1}{\tau} \ll \frac{\epsilon}{\hbar} \quad (1.10)$$

For extremely isolated lines this could have the form:

$$W \ll \frac{1}{\tau} < \frac{\Delta E}{\hbar} \ll \frac{\epsilon}{\hbar} \quad (1.11)$$

As an upper limit for the impact parameter, the following criterion will be applied (Griem: 1968, 1974) in Chapter 3 on the Gaunt factor. As formulated originally by

Spitzer (1940), the "adiabatic" cut-off is given by:

$$\rho_{\max.} \simeq \frac{\hbar v}{\Delta E} \quad (1.12)$$

$$\Rightarrow \frac{1}{v} > \frac{\Delta E}{\hbar} \quad (1.13)$$

which is entirely consistent with condition 1.9 for the Bethe approximation (see also Seaton: 1975; Hey and Breger: 1980b; Chapter 3.3). From inequalities 1.11, the following sequence of times could be applicable for extremely isolated lines:

$$W \ll \frac{1}{\tau} \lesssim \frac{\Delta E}{\hbar} \ll \frac{\epsilon}{\hbar} \quad (1.14)$$

This particular regime corresponds to the adiabatic approximation (Baranger: 1962; Spitzer: 1940):

$$\Delta E \gtrsim \frac{\hbar v}{\rho} \quad (1.15)$$

Since collisions in this regime are too slow to induce transitions (Spitzer: 1940; Schiff: 1955), the ordering of inequalities given by 1.14 is not applicable to the present calculations, in which collision-induced transitions play an important role (Baranger: 1962). Excluding thus the sequence of times given by 1.11, one is left with the time ordering given in expression 1.10, which is required for the validity of:

- (a) the impact approximation;
- (b) the classical path approximation;
- (c) the Bethe approximation (equivalent to (b));
- (d) broadening by inelastic collisions.

In order to compute also the contribution from elastic processes (see section 3 of this Chapter), the ordering in 1.10 will have to be relaxed to the less stringent form:

$$W \lesssim \frac{\Delta E}{\hbar} \lesssim \frac{1}{\tau} \lesssim \frac{\epsilon}{\hbar} \quad (1.10a)$$

This is in order to deal, in particular, with perturber energies in the vicinity of threshold ($\epsilon \sim \Delta E$), where elastic processes become important (Gailitis: 1963; Bely: 1969). It is in this attempt to extend the classical path, impact approximation into the threshold regime, that the major difficulties with the present theoretical approach have been encountered in the past (Griem: 1968, 1974; Hey and Breger: 1980a, b).

The calculation of line widths from eq. 1.1 can thus be subdivided into the calculation of inelastic and elastic cross-sections, as well as into two groups of collisions: weak and strong collisions.

1.2 WEAK INELASTIC CROSS-SECTIONS

Since the inelastic collisions contribute the major part of the line width at high perturber velocities (Griem: 1968), these cross-sections will be dealt with first. As the

summation in eq. 1.1 extends over all levels i' (f') above and below levels i (f) to which collision-induced transitions can occur, one has to deal with cross-sections for both excitation and de-excitation. It is convenient at this point to introduce the dimensionless collision strength $\Omega(i, i')$ (Hebb and Menzel: 1940; Seaton: 1958) which is symmetrical in the labels i', i . The inelastic cross-sections can then be written as (Hebb and Menzel: 1940):

$$\sigma_{i'i} = \pi a_0^2 \frac{E_H}{\frac{1}{2} m v^2} \frac{\Omega(i, i')}{\tilde{\omega}_i} \quad (1.16)$$

where $\tilde{\omega}_i \equiv$ statistical weight of level i ;
 $v \equiv$ initial electron velocity.

For the evaluation of the collision strengths, further assumptions need to be made. For high perturber energies, the weak coupling approximation is appropriate and the first order Born approximation is usually made, or, to include slower perturbers, a distorted wave approximation. Replacing the interaction potential by the monopole-dipole term leads to the Bethe approximation of the inelastic cross-sections (Seaton: 1962a). This replacement can be justified by the fact that the allowed dipole transitions are the predominant sources of optical radiation in laboratory plasmas. Defining the effective Gaunt factor as done by Seaton (1962a) yields (van Regemorter: 1962):

$$\Omega(i, i') = \frac{8\pi}{\sqrt{3}} \frac{E_H}{\Delta E_{i'i}} \tilde{\omega}_i f_{i'i} \bar{g} \quad (1.17)$$

where $E_H \equiv$ Rydberg constant for infinite nuclear mass;
 $\bar{g} \equiv$ effective Gaunt factor;
 $f_{i',i} \equiv$ absorption (emission) oscillator strength
 for level i' lying above (below) level i .

In this expression for the collision strength (symmetrical in labels i',i) the oscillator strength introduces the asymmetry in labels i',i of the cross-section, the effective Gaunt factor $\bar{g}(i',i)$ being also symmetrical in labels i',i .

This simplified form of the collision strength (which also ignores exchange terms (Seaton: 1975)) thus yields for the inelastic cross-sections:

$$\sigma_{i'i} = \frac{8\pi^2}{\sqrt{3}} \frac{2E_H^2 a_0^2}{\Delta E m v^2} \bar{g} f_{i'i} \quad (1.18)$$

This expression is equivalent to the form of the Bethe limit used by Griem (1968):

$$\sigma_{i'i} = \frac{8\pi^2}{3\sqrt{3}} \frac{E_H}{E} |\langle i' | \mathbf{r} | i \rangle|^2 \bar{g} \quad (1.19)$$

but any ambiguity about the exact definition of the matrix element has so far been avoided by employing a general parameter, the collision strength.

The expansion of the collision strength (and thus oscillator strength) in terms of the detailed matrix elements required can thus be left to a separate treatment (Chapter 2).

It is at this point that a division of the line width

calculation into:

- (i) radiator structure complexities;
- (ii) collision statistics;

has been achieved. Details about the radiator structure are now contained in the oscillator strength $f_{i,i}$ whereas the complexity of the collision between the radiator and the perturbers can be treated classically (subject to 1.10) in the determination of the effective Gaunt factor \bar{g} (Chapter 3). It is this separation into a quantum mechanical treatment and a classical treatment that makes the semi-classical approach suggested by Griem (1968, 1974) so successful.

1.3 THE ELASTIC CROSS-SECTIONS

As stated earlier, the calculation of eq. 1.1 can be subdivided into the calculation of weak and strong inelastic/elastic contributions of the linewidth. From the above discussion of the weak inelastic cross-sections, one requires as part of the full linewidth the weak inelastic contribution:

$$W_e^{(i)} = N_e \left\{ v \sigma_{vi} \right\}_{Av} \quad (1.20)$$

where the average is an integration over a Maxwellian velocity distribution of the incoming electron perturbers:

$$f(v)dv = 4\pi \left(\frac{m}{2\pi kT} \right)^{3/2} v^2 \exp \left[-\frac{mv^2}{2kT} \right] \quad (1.21)$$

Using the expansion 1.18 for the inelastic excitation cross-sections ($E_{i'} > E_i$) one obtains thus:

$$N_e \left\{ v \sigma_{i'i} \right\}_{AV} = N_e \frac{32 \pi^2}{\sqrt{3}} \frac{E_H^2 a_0^2}{\Delta E kT} \left(\frac{m}{2 \pi kT} \right)^{1/2} f_{i'i} \int_{v_{\min}}^{\infty} v \bar{g} \exp \left[-\frac{m v^2}{2 kT} \right] dv \quad (1.22)$$

Integration from a lower limit v_{\min} is required, since incident electrons of energy less than $\frac{1}{2} m v_{\min}^2 = \Delta E_{i',i}$ will not induce transitions. A more convenient form is obtained by changing the variable of integration to:

$$z = \frac{m v^2}{2 kT}$$

thus imposing the condition:

$$z \gg z_{i'i} = \frac{\Delta E_{i'i}}{kT}$$

This yields for eq. 1.22:

$$N_e \left\{ v \sigma_{i'i} \right\}_{AV} = N_e \frac{16 \pi^2}{\sqrt{3}} \frac{\hbar^2}{m^2} \frac{E_H}{\Delta E} \left(\frac{m}{2 \pi kT} \right)^{1/2} f_{i'i} \int_{z_{i'i}}^{\infty} \bar{g}(z) \exp(-z) dz \quad (1.23)$$

where one can denote now the excitation rate integral by:

$$\langle v \sigma_{i'i} \rangle = f_{i'i} \int_{z_{i'i}}^{\infty} \bar{g}(z) \exp(-z) dz \quad (1.24)$$

To obtain $N_e \{ v \sigma_{i',i} \}_{AV}$ for de-excitation (superelastic) processes, the principle of detailed balance can be used (Tolman: 1938; Hey and Bryan: 1977):

$$N_i \langle v \sigma_{i'i} \rangle = N_{i'} \langle v \sigma_{ii'} \rangle \quad (1.25)$$

in terms of the LTE level populations of i and i' . Using a Boltzmann distribution law:

$$\frac{N_{i'}}{N_i} = \frac{\tilde{\omega}_{i'}}{\tilde{\omega}_i} \exp \left[-\frac{\Delta E_{i'i}}{kT} \right] \quad (1.26)$$

one has for the de-excitation rate:

$$\langle v \sigma_{ii'} \rangle = \exp \left[\frac{\Delta E_{i'i}}{kT} \right] f_{i'i'} \int_{z_{i'i}}^{\infty} \bar{g}(z) \exp(-z) dz \quad (1.27)$$

Changing the variable of integration such that the integration is performed instead from zero to infinity and retaining the notation z for the dummy variable, one obtains:

$$\langle v \sigma_{ii'} \rangle = f_{i'i'} \int_0^{\infty} \bar{g} \left(z + \frac{\Delta E_{i'i}}{kT} \right) \exp(-z) dz \quad (1.28)$$

The reason for writing the de-excitation rate in this form (eq. 1.28) is to compare it with the excitation rate given by eq. 1.24, which will be modified by extending the integration down to zero, i.e.:

$$\langle v \sigma_{i'i} \rangle = f_{i'i} \int_0^{\infty} \bar{g}(z) \exp(-z) dz \quad (1.29)$$

in order to include the elastic collision contributions to the linewidth. The suggestion to include the elastic parts of the width, given in eq. 1.1 by:

$$\int |\phi_i - \phi_f|^2 d\Omega \quad (1.30)$$

by extrapolating the excitation rates below threshold, has been made by Griem (1968) and can be justified as follows. Making a classical path approximation, Baranger (1958b) obtains for the line width:

$$W_e = \int (1 - \text{Re } S_i S_f^*) d\nu \quad (1.31)$$

where S_i, S_f are the classical path scattering matrix elements appropriate for the upper and lower states of the line, and the collision frequency element:

$$d\nu = \left\{ N_e v 2\pi f d\rho \right\}_{Av} \quad (1.32)$$

Combining eqs. 1.31 and 1.32 one obtains the expression given by Griem (1968):

$$W_e = N_e \left\{ 2\pi v \int f d\rho (1 - \text{Re } S_i S_f^*) \right\}_{Av} \quad (1.33)$$

Expanding the scattering matrices in terms of a Dyson series, and replacing the actual interaction in the Schrödinger picture by the dipole-monopole interaction (the same approximation was made in the estimation of the cross-sections by eq. 1.18), one finds that the first order and negative interference terms vanish (Griem: 1968, 1974). One thus retains to second order:

$$W_e \approx N_e \left\{ 2 \pi v \int \rho d\rho \frac{1}{\hbar^2} \operatorname{Re} \left[\sum_{i'} \left| \langle i' | \int_{-\infty}^{\infty} \tilde{V}(t) dt | i \rangle \right|^2 + \sum_{f'} \left| \langle f' | \int_{-\infty}^{\infty} \tilde{V}(t) dt | f \rangle \right|^2 \right] \right\}_{AV} \quad (1.34)$$

For an expansion of $\sigma_{i',i}$ in the form given by eq. 1.18, the definition of a cross-section by Seaton (1962a) has been utilised:

$$\sigma_{i'i} = 2 \pi \int P_{i'i} \rho d\rho \quad (P_{i'i} \ll 1) \quad (1.35)$$

which is written as (Griem: 1968; Seaton: 1962a):

$$\sigma_{i'i} \approx 2 \pi \int_0^{\infty} \frac{1}{\hbar^2} \left| \langle i' | \int_{-\infty}^{\infty} \tilde{V}(t) dt | i \rangle \right|^2 \rho d\rho \quad (1.36)$$

Comparing eqs. 1.36 and 1.34 with the quantum mechanical expression 1.1 thus suggests the inclusion of the elastic collision terms by extrapolating the inelastic excitation cross-sections below threshold. The validity of such an approximation has been discussed by Bely (1969), who used the result by Gailitis (1963) that "the discontinuities due to the inelastic cross-sections are exactly compensated for by the discontinuities of the elastic cross-sections" (Bely: 1969). Bely comes to the conclusion that this quantum mechanical consequence of the continuity of the collision cross-section averaged over the resonances below threshold is applicable for all practical cases.

Including the elastic cross-sections in this fashion, one thus obtains the form for the collision strengths for

excitation and de-excitation:

$$\left\{ \Omega(i' i') \right\}_{Av} = \frac{8\pi}{\sqrt{3}} \frac{E_H}{\Delta E} \tilde{\omega}_i f_{i'} \langle \bar{g}(i' i') \rangle \quad (1.37)$$

where the average Gaunt factor is given by

$$\langle \bar{g}(i' i') \rangle = \int_0^{\infty} \bar{g}(z) \exp(-z) dz \quad (1.38)$$

for excitation

$$\langle \bar{g}(i' i') \rangle = \int_0^{\infty} \bar{g}\left(z + \frac{\Delta E_{i' i'}}{kT}\right) \exp(-z) dz \quad (1.39)$$

for de-excitation.

Since the effective Gaunt factor \bar{g} is often a very slowly varying function of energy (Griem: 1968; Hey and Bryan: 1977), the difference between eq. 1.38 and eq. 1.39 has often been neglected (Griem: 1968), and the average of the Gaunt factor has often been approximated by the computation of (Griem: 1968):

$$\left\langle \bar{g}\left(\frac{\Delta E}{kT}\right) \right\rangle \equiv \bar{g}\left(\frac{\bar{E}}{kT}\right) \quad (1.40)$$

where \bar{E} is the average energy $\langle \frac{1}{2} m v^2 \rangle = \frac{3}{2} kT$. In a calculation by Hey and Bryan (1977), the approximation was made of a constant threshold value of \bar{g} of 0.2 for all transitions, as proposed by van Regemorter (1962). The resultant underestimation of the threshold Gaunt factor lead to underestimates of the line widths calculated for OIII (Hey and Bryan: 1977), as already mentioned in the Preface.

A calculation involving the evaluation of eq. 1.38 and eq. 1.39 for each transition in question for the same OIII lines has been done in the course of this investigation (see Chapter 5.2; Hey and Breger: 1980b). Much better agreement between theory and experiment has been obtained using a rigorous averaging procedure.

1.4 STRONG COLLISION CONTRIBUTIONS

Having included the weak inelastic and elastic collision contributions to the line width, an estimate for the remaining strong collision contributions in eq. 1.1 has to be made. For these, higher orders of the Dyson series (eq. 1.2) are not negligible, but because of the impact approximation (Baranger: 1958a, b, c) these collisions are well separated in time. This additional term is usually assumed to take the form (Weisskopf: 1933; Griem et al.: 1959; Griem: 1964, 1974):

$$W_S = 2\pi N_e \langle v \rho_{\min}^2 \rangle \quad (1.41)$$

(compare with eq. 1.33), where ρ_{\min} is chosen to be consistent with the lower cut-off employed in the calculation of the weak inelastic cross-sections. A modification of this relation for hyperbolic perturber trajectories has been proposed by Hey (1979, private communication). It is this modified form that is employed below (see also Chapter 4.1).

Summarising the above discussion, the transformation of the quantum mechanical expression 1.1 to the following semi-

classical result has been achieved (Hey: 1977):

$$\begin{aligned}
 W_e &= N_e \frac{32\pi^2}{\sqrt{3}} \frac{\lambda^2}{2\pi c} \frac{E_H a_0^2}{m} \left(\frac{m}{2\pi kT} \right)^{\frac{1}{2}} \left[\sum_{i'} \frac{E_H}{\Delta E_{i'i}} f_{i'i} \langle \bar{g}(i'i) \rangle \right. \\
 &\quad \left. + \sum_{f'} \frac{E_H}{\Delta E_{f'f}} f_{f'f} \langle g(f'f) \rangle \right] + W_S \\
 &= \frac{\alpha \lambda^2 a_0^2}{\sqrt{\pi}} N_e \left(\frac{E_H}{kT} \right)^{\frac{1}{2}} \left[\sum_{i'} \frac{\langle \Omega(i'i) \rangle}{\tilde{\omega}_i} \right. \\
 &\quad \left. + \sum_{f'} \frac{\langle \Omega(f'f) \rangle}{\tilde{\omega}_f} \right] + W_S \quad (1.42)
 \end{aligned}$$

where in the latter expression (given for comparison with eq. (1) in Hey and Breger (1980a)):

$$\alpha \equiv \text{fine-structure constant } \frac{e^2}{\hbar c}$$

$$a_0 \equiv \text{Bohr radius } \frac{\hbar^2}{me^2} .$$

In expression 1.42 the Stark width resulting from interactions with surrounding ions has been neglected. As is shown in Chapter 5, this is indeed permissible as the contributions remain of the order of 1% in most cases.

CHAPTER 2RADIATOR STRUCTURE

The semi-classical expression for the spectral line width (eq. 1.42) obtained in Chapter 1 is seen to depend on the atomic absorption oscillator strength $f_{i',i}$. The importance of this parameter in determining the Stark width has been pointed out repeatedly (Hey: 1977b; Hey: 1978; Hey and Blaha: 1978; Behringer and Thoma: 1978) as it is through this quantity that the line broadening mechanism is explicitly dependent on the internal structure of the ion emitter. It is thus important to allow sufficient details of the radiator structure to remain explicitly in the expression used for the oscillator strength in order to include the traits (such as variations within multiplets, configuration interaction) of the ion under consideration. For the correct evaluation of the matrix elements involved, one thus requires the knowledge of a reliable system of atomic energy values and classifications (Griem: 1964, 1974). Since there is often a shortage of known data on a particular radiator structure, a careful balance has to be struck between reducing (simplifying) the oscillator strengths to include less detail on the one hand and the difficulty of obtaining reliable radiator structure data on the other.

2.1 THE ABSORPTION OSCILLATOR STRENGTH

As a general starting point, the definition of the oscillator strength as formulated by Sobel'man (1972) is used in order to facilitate a unified notation. The absorption oscillator strength is defined in terms of the line strength and is positive for a transition $\gamma \rightarrow \gamma'$ where γ' is above level γ :

$$f(\gamma J; \gamma' J') = \frac{2m}{3\hbar e^2} \frac{\omega_{\gamma J, \gamma' J'}}{2J+1} S(\gamma J; \gamma' J') \quad (2.1)$$

and

$$S(\gamma J; \gamma' J') = S(\gamma' J'; \gamma J) \\ = \sum_{MM'} |\langle \gamma JM | \underline{D} | \gamma' J' M' \rangle| \quad (2.2)$$

$$\equiv |(\gamma J \| \underline{D} \| \gamma' J')| \quad (2.3)$$

where $\omega_{\gamma J, \gamma' J'} = \frac{1}{\hbar} (E_{\gamma' J'} - E_{\gamma J})$;

$\underline{D} = -e\underline{r} \equiv$ dipole moment operator;

$J(J')$ \equiv total angular momentum of level $i(i')$;

$\gamma(\gamma')$ \equiv any remaining quantum numbers required for level specification.

In order to proceed, one requires the choice of a suitable coupling scheme. For the ions under consideration in this investigation, as for most applications, the LS

coupling approximation was found to be valid (see also Chapter 5). For other ions, the spin-orbit term may not be sufficiently small to warrant such a choice, and other coupling schemes need to be employed. Such an exception occurs in the case of NII, where highly excited terms occur in pairs. As discussed by Hey (1977b), the application of a LK coupling scheme is applicable and can be facilitated by a correction factor multiplied into the LS coupled line strength. The use of a LS coupled line strength would remain more appropriate for special cases of transitions in which this correction factor reduces to unity (Hey: 1977b).

Making use, thus, of the LS coupling scheme, one employs a quantum number description of $\gamma SLJM$ so that the line strength (eq. 2.3) becomes:

$$\begin{aligned}
 S(\gamma SLJ; \gamma' S' L' J') &= \left| (\gamma SLJ \| D \| \gamma' S' L' J') \right|^2 \\
 &= (2J+1)(2J'+1) \left\{ \begin{matrix} L & J & S \\ J' & L' & 1 \end{matrix} \right\}^2 \left| (\gamma L \| D \| \gamma' L') \right|^2 \quad (2.4)
 \end{aligned}$$

where $L(L')$ = total orbital angular momentum of $i(i')$;
 S = total spin;
 $\{ \}$ \equiv 6-j symbol.

From the triangular conditions of the 6-j symbol one obtains the selection rules:

$$\begin{aligned}
 \Delta S &= 0 \\
 \Delta L &= 0, \pm 1 \quad L + L' \geq 1. \quad (2.5)
 \end{aligned}$$

Employing furthermore the parentage scheme approximation, thus considering a transition:

$$\propto S_1 L_1 l S L \rightarrow \propto S_1 L_1 l' S' L'$$

one obtains

$$\left| \langle \delta L \| D \| \delta' L' \rangle \right|^2 = (2L + 1)(2L' + 1) \left\{ \begin{matrix} L & L & L_1 \\ L' & l' & 1 \end{matrix} \right\}^2 \left| \langle l \| D \| l' \rangle \right|^2 \quad (2.6)$$

and

$$\left| \langle l \| D \| l' \rangle \right|^2 = l_{>} e^2 a_0^2 \left(R_{n', l'}^{n, l} \right)^2 \quad (2.7)$$

where $l_{>} = \max(l, l')$;

$R_{n', l'}^{n, l}$ = radial integral (in units of a_0).

Collecting equations 2.1, 2.4, 2.6 and 2.7, one obtains the following form of the oscillator strength usually quoted (Hey: 1977b):

$$f_{ij} = \frac{1}{2J + 1} \frac{|E_{j'} - E_i|}{3E_H} \frac{S(J, J')}{a_0^2 e^2} \quad (2.8)$$

and

$$\frac{1}{2J + 1} \frac{S(J, J')}{a_0^2 e^2} = l_{>} (2L + 1)(2L' + 1)(2J' + 1) \left\{ \begin{matrix} L & L & L_1 \\ L' & l' & 1 \end{matrix} \right\}^2 \left\{ \begin{matrix} L & J & S \\ J' & l' & 1 \end{matrix} \right\}^2 \left(R_{n', l'}^{n, l} \right)^2 \quad (2.9)$$

The radial integral can be evaluated for ions with a single outer electron using the Coulomb method by Bates and

Damgaard (1949) with sufficient degree of accuracy (Griem: 1962a, 1964, 1974; Hey: 1977b; Warner: 1968):

$$\left(R_{n'l'}^{nl}\right)^2 = \left(\frac{3n_{l'}^*}{2Z}\right)^2 \left(n_{l'}^{*2} - l_{l'}^2\right) \Phi^2 \quad (2.10)$$

where

$$n_i^* \equiv \sqrt{\frac{Z^2 E_H}{E_\infty - E_i}} \equiv \text{effective principal quantum number of level } i;$$

E_∞ = ionisation energy relevant to the appropriate parentage scheme;

$n_{l'}^*$ = n^* of level with larger l value;

Φ = Bates-Damgaard factor (Bates and Damgaard: 1949; see also revised tables by Oertel and Shomo: 1968).

To date, this approximation has also been employed successfully for individual equivalent electron transitions (Hey and Breger: 1980a, b, c), but this is, however, not strictly valid, and a Thomas-Fermi radial integral (Thomas: 1927) should be employed for equivalent electron levels (Warner: 1968d). (Due to the limitations imposed on this particular investigation, such an alteration has to be left for future work.)

2.2 CORRECTION FOR EQUIVALENT ELECTRON CONFIGURATIONS

As stressed by Sobel'man (1972), the above formalism of the line strength (and thus oscillator strength) is not

applicable to transitions in which an equivalent electron configuration participates. Apart from the cases where one of the levels giving rise to the broadened line corresponds to an electron configuration containing equivalent electrons (henceforward called simply "equivalent electron level") as in the example of SnII (see Chapter 5), it is often found that the lower level of the transition is sufficiently near to equivalent electron levels to give rise to non-negligible matrix elements between the transition level and an equivalent electron level. For the calculations done in this investigation, this range of important near perturbing levels is defined to correspond to about $\Delta n^* < 1.3$. Equivalent electron levels were found to lie within this range from transition levels in several lines of SIII, AIV, NIII, ClIII and FII (see Chapter 5).

Two cases of oscillator strengths need thus to be considered:

$$f(\alpha l^N SLJ \rightarrow \alpha l^{N-1} S_1 L_1 l' S' L' J') \quad (2.11)$$

and

$$f(\alpha l^{N-1} S_1 L_1 l' S' L' J' \rightarrow \alpha l^N SLJ) \quad (2.12)$$

depending on which is the lower level, since the absorption oscillator strength is defined as $f(\ell \rightarrow u)$. From the previous section, 2.1:

$$f(\alpha S_1 L_1 l S L J \rightarrow \alpha S_1 L_1 l' S L' J') \quad (2.13)$$

and

$$f(\alpha S_1 L_1 l' S L' J' \rightarrow \alpha S_1 L_1 l S L J) \quad (2.14)$$

are already known. The relationship between an absorption oscillator strength and the corresponding emission oscillator strength is:

$$\tilde{\omega}_l f(l \rightarrow u) = \tilde{\omega}_u f(u \rightarrow l) \quad (2.15)$$

where $\tilde{\omega}_l$ and $\tilde{\omega}_u$ denote statistical weights of the lower and upper levels, respectively, or for configurations:

$$\tilde{\omega}(l^{N-1} l') f(l^{N-1} l' \rightarrow l^N) = \tilde{\omega}(l^N) f(l^N \rightarrow l^{N-1} l') \quad (2.16)$$

In order to obtain equations 2.11 and 2.12 in terms of equations 2.13 and 2.14 respectively, use can now be made of the correction for the equivalent electron oscillator strengths as formulated by Sobel'man (1972, p. 314, equations 31.55, 31.49, 31.27) to yield for the oscillator strength 2.11:

$$f(\alpha l^N S L J \rightarrow \alpha l^{N-1} S_1 L_1 l' S L' J') = N |G_{S_1 L_1}^{S L}|^2 f(\alpha S_1 L_1 l S L J \rightarrow \alpha S_1 L_1 l' S L' J') \quad (2.17)$$

where N = number of equivalent electrons;
 $G_{S_1 L_1}^{S L}$ = fractional parentage coefficient
 (Sobel'man: 1972, pp. 105-112; Shore and Menzel: 1968, pp. 385-390).

The oscillator strength 2.12 can be derived analogously to eq. 2.17 by making use of eq. 2.16. However, care needs to be taken in the detailed consideration of the hierarchical procedure involved in formulating an oscillator strength for configurations, terms and levels. One thus obtains for configurations that:

$$\begin{aligned} f(l^{N-1}l' \rightarrow l^N) &= \frac{\tilde{\omega}(l^N)}{\tilde{\omega}(l^{N-1}l')} N f(l \rightarrow l') \\ &= \frac{\tilde{\omega}(l^N)}{\tilde{\omega}(l^{N-1}l')} \frac{\tilde{\omega}(l')}{\tilde{\omega}(l)} N f(l' \rightarrow l) \end{aligned} \quad (2.18)$$

Evaluating the thus defined equivalent electron correction factor explicitly yields:

$$\frac{\tilde{\omega}(l^N)}{\tilde{\omega}(l^{N-1}l')} \frac{\tilde{\omega}(l')}{\tilde{\omega}(l)} N = \frac{4l+3-N}{2(2l+1)} \quad (2.19)$$

for the oscillator strength averaged over all terms corresponding to a configuration. Rewriting this relationship for oscillator strengths of terms (eq. 2.18) for atomic levels (eq. 2.12) one obtains the same form as for eq. 2.11, namely:

$$f(\alpha l^{N-1} S_L L_l' S_L' J' \rightarrow \alpha l^N S L J) = N \left| G_{S_L' L_l'}^{S_L} \right|^2 f(\alpha S_L L_l' S_L' J' \rightarrow \alpha S_L L_l S L J) \quad (2.20)$$

The correct relationship between eqs. 2.20 and 2.18 as elucidated in the following section.

In the case of SnII (Hey and Breger: 1980a) an even more complicated type of transition occurs: oscillator strengths of the type:

$$f(l'^{N-1} l^P \rightarrow l'^N l^{P-1})$$

are required. Accepting the formulation by Sobel'man (1972, p. 318) one has for configurations:

$$f(l'^N l^{P-1} \rightarrow l'^{N-1} l^P) = \frac{NP}{2} \frac{\tilde{\omega}(l^P)}{\tilde{\omega}(l^{P-1})} \frac{1}{(2l'+1)} f(l \rightarrow l') \quad (2.21)$$

and for atomic levels (Sobel'man: 1972, equation 31.60):

$$\begin{aligned} f(l^N [S_1 L_1] l'^{P-1} [S_2 L_2] S L J \rightarrow l'^{N-1} [S'_1 L'_1] l'^P [S'_2 L'_2] S L' J') \\ = NP \left| G_{S'_1 L'_1}^{S_1 L_1} \right|^2 \left| G_{S'_2 L'_2}^{S_2 L_2} \right|^2 f(S'_1 L'_1 [S_1 L_1] l'^{P-1} [S_2 L_2] S L J \rightarrow S'_1 L'_1 l'^{P-1} [S_2 L_2] l' [S'_2 L'_2] S L' J') \end{aligned}$$

The multiplicative factor in equation 2.21 reduces to:

$$\frac{P}{2} \left(\frac{4l' + 3 - N}{2l' + 1} \right) \quad (2.22)$$

For $P = 1$, this reduces to the equation 2.19 as it should.

2.3 REDUCTION OF RADIATOR STRUCTURE DETAILS

The reduction of the equivalent electron oscillator strength for levels (eq. 2.17) to the corresponding total oscillator strength of the set of transitions $l^N \rightarrow l^{N-1} l'$ has been discussed in detail by Sobel'man (1972, pp. 314, 315) and the result obtained is:

$$f(l^N \rightarrow l^{N-1} l') = N f(l \rightarrow l') \quad (2.23)$$

The result proposed for a transition $\ell^{N-1}\ell' \rightarrow \ell^N$ is (eq. 2.20):

$$f(\gamma'J' \rightarrow \gamma J) = \frac{|E_{\gamma'} - E_i|}{3E_H} N |G_{S,L}^{SL}|^2 l_{>} (2L+1)(2L'+1)(2J+1) \\ \times \left\{ \begin{matrix} L & L & L \\ L' & L' & 1 \end{matrix} \right\}^2 \left\{ \begin{matrix} L & J & S \\ J' & L' & 1 \end{matrix} \right\}^2 (R_{n'l'}^{nL})^2 \quad (2.24)$$

and it remains to be shown that this reduces correctly to equation 2.23 by making use of the relationship between absorption and emission oscillator strengths (eq. 2.16).

If the spin-orbit term is sufficiently small, or the J value is restricted to one value by the triangular conditions of the 6- j symbol, this expression 2.24 can be reduced to the oscillator strength for terms, which is defined by Sobel'man (1972, p. 309):

$$f(\gamma'SL' \rightarrow \gamma SL) = \frac{1}{(2L'+1)(2S+1)} \sum_{J'} (2J'+1) f(\gamma'J' \rightarrow \gamma J) \quad (2.25)$$

with the corresponding sum rules:

$$\sum_J (2J+1) \left\{ \begin{matrix} L & J & S \\ J' & L' & 1 \end{matrix} \right\}^2 = \frac{1}{2L'+1}$$

and

$$\sum_{J'} (2J'+1) = (2L'+1)(2S+1)$$

One thus obtains after summation over J and J' :

$$f(\gamma'SL' \rightarrow \gamma SL) = N |G_{S,L}^{SL}|^2 \frac{|E_{\gamma'} - E_i|}{3E_H} l_{>} (2L+1) \left\{ \begin{matrix} L & L & L \\ L' & L' & 1 \end{matrix} \right\}^2 (R_{n'l'}^{nL})^2 \quad (2.26)$$

As a next simplification, one needs to consider the oscillator strength between all terms of a particular parent S_1L_1 in a given configuration. One can thus define analogously to eq. 2.25:

$$f(S_1L_1l' \rightarrow S_1L_1l) = \frac{1}{\tilde{\omega}_{S_1L_1}} \sum_{\substack{S_1L_1 \\ \text{(for given } S_1L_1)}} (2L'+1)(2S+1) f(\gamma'SL' \rightarrow \gamma SL)$$

where

$$\sum_{\substack{L'S \\ \text{(for given } S_1L_1)}} (2L'+1)(2S+1) = \tilde{\omega}_{S_1L_1}$$

defines the corresponding statistical weight and the sum rule:

$$\sum_{L'} (2L'+1) \left\{ \begin{matrix} l & L & L \\ L' & l' & 1 \end{matrix} \right\}^2 = \frac{1}{2l+1}$$

is obeyed. As stated by Sobel'man (1972, p. 315), a general summation over L is however not possible due to the L -dependence of the fractional parentage coefficient.

Following thus the approach outlined by Sobel'man, only the summation over L' is performed to yield:

$$f(S_1L_1l' \rightarrow S_1L_1l) = N \frac{|E_v - E_i|}{3 E_H} \frac{l_y}{2l+1} \left(R_{nl'}^{nl} \right)^2 \frac{1}{\tilde{\omega}_{S_1L_1}} \times \sum_{SL} (2L+1)(2S+1) |G_{S_1L_1}^{SL}|^2 \quad (2.27)$$

The mean oscillator strength for the configuration is now obtained by summation over the various parents possible. One defines again analogously to eq. 2.25:

$$f(l^{N-1}l' \rightarrow l^N) = \frac{1}{\tilde{\omega}(l^{N-1}l')} \sum_{S_1 L_1} \tilde{\omega}_{S_1 L_1} f(l^{N-1} S_1 L_1 l' \rightarrow l^N)$$

where the statistical weights are related by:

$$\tilde{\omega}(l^{N-1}l') = \sum_{S_1 L_1} \tilde{\omega}_{S_1 L_1}$$

One thus obtains for configurations that

$$f(l^{N-1}l' \rightarrow l^N) = N \frac{|E_{i'} - E_i|}{3E_H} \frac{l_{>}}{2l+1} \left(R_{n'l'}^{nl}\right)^2 \frac{1}{\tilde{\omega}(l^{N-1}l')} \\ \times \sum_{S_1 L_1 S_L} (2L+1)(2S+1) |G_{S_1 L_1}^{SL}|^2$$

(It should be noted that reduction of the oscillator strength given by eq. 2.17 along the same lines as above yields:

$$f(l^N \rightarrow l^{N-1}l') = N \frac{|E_{i'} - E_i|}{3E_H} \frac{l_{>}}{2l+1} \left(R_{n'l'}^{nl}\right)^2 \frac{1}{\tilde{\omega}(l^N)} \\ \times \sum_{S_1 L_1 S_L} (2L+1)(2S+1) |G_{S_1 L_1}^{SL}|^2$$

which is almost identical to the above expression with the exception of the statistical weight $\tilde{\omega}$ factors.)

Making use now of the sum rule for fractional parentage coefficients (Sobel'man: 1972):

$$\sum_{S_1 L_1} |G_{S_1 L_1}^{SL}|^2 = 1$$

one obtains readily (compare with eq. 2.18):

$$\begin{aligned}
 f(l^{N-1}l' \rightarrow l^N) &= N \frac{|E_f - E_i|}{3E_H} \frac{l_{>}}{2l+1} \left(R_{n'l'}^{nl}\right)^2 \frac{\tilde{\omega}(l^N)}{\tilde{\omega}(l^{N-1}l')} \\
 &= N \frac{\tilde{\omega}(l^N)}{\tilde{\omega}(l^{N-1}l')} \frac{\tilde{\omega}(l')}{\tilde{\omega}(l)} f(l' \rightarrow l) \quad (2.28)
 \end{aligned}$$

Furthermore, application of equation 2.16 shows clearly that this result is entirely consistent with the result obtained by Sobel'man (1972, p. 315): the total oscillator strength of the set of transitions $l^N \rightarrow l^{N-1}l'$ is N times greater than the oscillator strength of the single electron transition $l \rightarrow l'$.

Using this simple correction for equivalent electrons, the factor N can be introduced into the results obtained for the line width using a single electron oscillator strength as follows. By the dipole selection rules, the angular l values are restricted to:

$$l' = l \pm 1$$

and after separation into $\Delta n = 0$ and $\Delta n \neq 0$ transitions one obtains using equation 2.28 and the expression for the line width (eq. 1.42) for the FWHM:

$$\begin{aligned}
W_e = & \frac{8}{3} \left(\frac{\pi}{3} \right)^{\frac{1}{2}} \frac{h a_0}{m} N_e \left(\frac{E_H}{kT} \right)^{\frac{1}{2}} \left[\frac{l_i}{2l_i+1} R_{l_i l_{i-1}}^2 \langle \bar{g}(i, i) \rangle \right. \\
& + \frac{l_i+1}{2l_i+1} R_{l_i l_{i+1}}^2 \langle \bar{g}(i, i) \rangle + \frac{l_f}{2l_f+1} R_{l_f l_{f-1}}^2 \langle \bar{g}(f, f) \rangle \\
& + \frac{l_f+1}{2l_f+1} R_{l_f l_{f+1}}^2 \langle \bar{g}(f, f) \rangle + \sum_{j'} \frac{l_j}{2l_j+1} (R_{n'l_j}^{nl_j})_{n \neq n'}^2 \langle \bar{g}(i, i) \rangle \\
& \left. + \sum_{f'} \frac{l_{f'}}{2l_{f'}+1} (R_{n'l_{f'}}^{nl_{f'}})_{n \neq n'}^2 \langle \bar{g}(f, f) \rangle \right] + W_S \quad (2.29)
\end{aligned}$$

This reduced form contains little detail about the actual ion structure, but has nevertheless been employed with varying success by Griem (1974) in obtaining his semi-classical line width formula equation (526) and also in a recent modified application to several ions by Dimitrijević and Konjević (1980a). The latter investigation deals with similar ions to those of this thesis (see also Chapter 5). The simplification of complex spectra by description of the bound states merely by their effective principal quantum number and orbital angular momentum of the outermost electron results, however, in a loss of the dependence of the line broadening mechanism on variations within multiplets, deviations from the LS coupling scheme and the possibility of imperfections in the level classification such as configuration interaction. That variations within multiplets, as predicted by Hey (1978), are in some cases (AII) of measurable magnitude was illustrated by Behringer and Thoma (1978). Appreciable variations within multiplets were also found in the calculation of SnII linewidths (Hey and Breger: 1980a;

Chapter 5). The difficulty of the inclusion of the correction factor for equivalent electron levels in the simple hydrogenic matrix element sum $\sum_{i,j} R_{l_i l_j}^2$ for cases with initial states with equivalent electrons has been pointed out by Dimitrijević and Konjević (1980a) who included fractional parentage coefficients only for cases where perturbing levels were of the equivalent type. The resultant error in the hydrogenic sum in the case of SnII calculations was found to be negligible, where the additional terms were less than ten percent (see Chapter 5; Hey and Breger: 1980a). A lack of reliability when reducing the radiator structure to an average over the parentage (i.e. from eq. 2.27 to eq. 2.28) has also been reported in the calculation of radial integrals for the calculation of lifetimes of excited levels in Al by Zurro et al. (1973).

2.4 CONFIGURATION INTERACTION

Apart from the unequal contribution of various members of a perturbing term to the line width observed (Behringer and Thoma: 1978; Hey: 1978), the shift of energy levels due to interactions between configurations was expected to affect the line broadening mechanism (Hey: 1977d), particularly in the case of ionised silicon. This effect was also detected in the investigation of several SnII lines, where several strong "forbidden (two-electron)" transitions were observed (Miller et al.: 1979; Wujec and Musielok: 1976) due to the strong interaction of the terms denoted $5s 5p^2 \ ^2D$ and $5s^2 5d \ ^2D$. (See also Chapter 5; Hey and Breger: 1980a). Using this particular case as an example, the modifications required to

the line broadening calculation can be illustrated as follows.

Denoting the two levels $5p^2 \ ^2D$ and $5d \ ^2D$ as tabulated in the energy level tables (Moore: 1958):

$$\Upsilon_{\text{I}}(^2D) \equiv 72\,000 \text{ cm}^{-1} \quad (\text{labelled } 5d)$$

$$\Upsilon_{\text{II}}(^2D) \equiv 58\,000 \text{ cm}^{-1} \quad (\text{labelled } 5p^2)$$

one has in terms of the "pure" energy eigenfunctions:

$$\Upsilon_{\text{I}}(^2D) = \alpha_{11} \Upsilon(d) + \alpha_{12} \Upsilon(p^2) \quad (2.30)$$

$$\Upsilon_{\text{II}}(^2D) = \alpha_{21} \Upsilon(d) + \alpha_{22} \Upsilon(p^2) \quad (2.31)$$

where for normalised wavefunctions:

$$|\alpha_{11}|^2 + |\alpha_{12}|^2 = 1 \quad (2.32)$$

$$|\alpha_{21}|^2 + |\alpha_{22}|^2 = 1 \quad (2.33)$$

In the calculation of the line width, one calculates matrix elements of the type:

$$|\langle \Upsilon_{n\ell m} | \mathcal{L} | \Upsilon_{\text{pert}} \rangle|^2$$

where $\psi_{n\ell m}$ corresponds to the transition level perturbed by ψ_{pert} . Two cases need to be considered now, depending on which of the two ($\psi_{n\ell m}$ or ψ_{pert}) is the mixed wavefunction.

Case 1: ψ_{nlm} is pure, $\psi_{\text{pert.}}$ is mixed.

In this case, suppose that ψ_{nlm} is perturbed according to the dipole selection rules by $\psi(d)$. Then, since both $\psi_I(^2D)$ and $\psi_{II}(^2D)$ contain this character, both

$$|\langle \Upsilon_{nlm} | \underline{r} | \Upsilon_I(^2D) \rangle|^2$$

and

$$|\langle \Upsilon_{nlm} | \underline{r} | \Upsilon_{II}(^2D) \rangle|^2$$

need to be calculated. From equations 2.30 and 2.31 one thus finds:

$$\begin{aligned} |\langle \Upsilon_{nlm} | \underline{r} | \Upsilon_I(^2D) \rangle|^2 &= |\alpha_{11}|^2 |\langle \Upsilon_{nlm} | \underline{r} | \Upsilon(d) \rangle|^2 \\ &\quad + |\alpha_{12}|^2 |\langle \Upsilon_{nlm} | r | \Upsilon(p^2) \rangle|^2 \\ &= |\alpha_{11}|^2 |\langle \Upsilon_{nlm} | \underline{r} | \Upsilon(d) \rangle|^2 \end{aligned} \quad (2.34)$$

and

$$|\langle \Upsilon_{nlm} | \underline{r} | \Upsilon_{II}(^2D) \rangle| = |\alpha_{21}|^2 |\langle \Upsilon_{nlm} | \underline{r} | \Upsilon(d) \rangle| \quad (2.35)$$

similarly. Hence the calculated oscillator strengths need to be multiplied by $|\alpha_{11}|^2$ and $|\alpha_{21}|^2$ respectively in order to obtain the correct contribution to the line width. If ψ_{nlm} is perturbed via the dipole selection rules by the p^2

character rather than the d character, the weighting constants in equations 2.34 and 2.35 would be $|\alpha_{12}|^2$ and $|\alpha_{22}|^2$ respectively.

Case 2: ψ_{nlm} is mixed, $\psi_{\text{pert.}}$ is pure.

In this case, the state $|\psi_{nlm}\rangle$ would be perturbed by two sets of perturbing levels. The following two matrix elements then enter into the sum over all contributions to the line width for $\psi_{nlm} \equiv \psi_I(^2D)$:

$$\begin{aligned} |\langle \Upsilon_I(^2D) | \underline{r} | \Upsilon_{\text{pert.}} \rangle|^2 &= |\alpha_{11}|^2 |\langle \Upsilon(d) | \underline{r} | \Upsilon_{\text{pert.}} \rangle|^2 \\ &\quad + |\alpha_{12}|^2 |\langle \Upsilon(p^2) | \underline{r} | \Upsilon_{\text{pert.}} \rangle|^2 \\ &= |\alpha_{11}|^2 |\langle \Upsilon(d) | \underline{r} | \Upsilon_{\text{pert.}}^{(1)} \rangle|^2 + |\alpha_{12}|^2 |\langle \Upsilon(p^2) | \underline{r} | \Upsilon_{\text{pert.}}^{(2)} \rangle|^2 \end{aligned} \quad (2.36)$$

and if $\psi_{nlm} \equiv \psi_{II}(^2D)$:

$$\begin{aligned} |\langle \Upsilon_{II}(^2D) | \underline{r} | \Upsilon_{\text{pert.}} \rangle|^2 &= |\alpha_{21}|^2 |\langle \Upsilon(d) | \underline{r} | \Upsilon_{\text{pert.}}^{(1)} \rangle|^2 \\ &\quad + |\alpha_{22}|^2 |\langle \Upsilon(p^2) | \underline{r} | \Upsilon_{\text{pert.}}^{(2)} \rangle|^2 \end{aligned} \quad (2.37)$$

where the superscripts (1) and (2) denote members of the set of perturbing levels which are permitted by the dipole selection rules.

The mixing constants α_{11} , α_{12} and α_{21} , α_{22} need therefore to be known to use the above outlined correction for line broadening calculations. By the selection of accurate measurements of

the atomic transition probabilities between the states $\psi_I(^2D)$ (and $\psi_{II}(^2D)$) and other levels, comparison of theoretical and measured values could yield these constants α_{ij} . The relationship between transition probabilities and the line strength is (Griem: 1964):

$$A_{lu} = \frac{8 \pi^2 \alpha^2 a_0}{c} \frac{(E_u - E_l)^2}{h^2} \frac{\tilde{\omega}_l}{\tilde{\omega}_u} f_{ul} \quad (2.38)$$

and

$$f_{ul} = \frac{1}{\tilde{\omega}_l} \frac{(E_u - E_l)^2}{3 E_H} \frac{S(J, J')}{a_0^2 e^2} \quad (2.39)$$

In this particular example of SnII, the following term transition probabilities would be applicable:

$$\begin{array}{lll} 5s 5p^2 \ ^2D - 6p \ ^2P^\circ & \text{yielding} & |\alpha_{21}|^2 = \frac{(A_{lu})_m}{(A_{lu})_c} \\ 5s 5p^2 \ ^2D - 4f \ ^2F^\circ & \text{yielding} & |\alpha_{21}|^2 \\ 5d \ ^2D - 4f \ ^2F^\circ & \text{yielding} & |\alpha_{11}|^2 \end{array}$$

Using the J-splitting within the terms, the consistency of the obtained values $|\alpha_{ij}|^2$ can be checked. The remaining two values of $|\alpha_{22}|^2$ and $|\alpha_{12}|^2$ can then be obtained from the normalisation conditions equations 2.32 and 2.33 (see also Chapter 5).

2.5 THE COMPLETENESS PARAMETER

From the reduced form (eq. 2.28) of the oscillator strength:

$$f_{i' i} = \frac{|E_{i'} - E_i|}{3 E_H} \frac{l_{>}}{2l+1} (R_{n'l'})^2$$

the following sum rule is obeyed for hydrogenic ions:

$$\begin{aligned} \sum_{n'l'} \frac{l_{>}}{2l+1} (R_{n'l'})^2 &= \frac{l}{2l+1} \sum_{n'} (R_{n'l-1})^2 + \frac{l+1}{2l+1} \sum_{n'} (R_{n'l+1})^2 \\ &= \frac{l}{2l+1} \langle nl | \frac{r^2}{a_0^2} | nl \rangle + \frac{l+1}{2l+1} \langle nl | \frac{r^2}{a_0^2} | nl \rangle \\ &= \langle nl | \frac{r^2}{a_0^2} | nl \rangle \\ &= \frac{n^2}{2Z^2} (5n^2 + 1 - 3l(l+1)) \end{aligned}$$

(Condon and Shortley: 1935) (2.40)

In order to check the completeness of the sets of perturbing levels used in the calculation, the parameter $\frac{\Delta S_i}{S_i}$ is evaluated:

$$\frac{\Delta S_i}{S_i} = \frac{\sum_{i'} |\langle i | r | i' \rangle|^2 - \frac{n_i^2}{2Z^2} (5n_i^2 + 1 - 3l_i(l_i+1))}{\frac{n_i^2}{2Z^2} (5n_i^2 + 1 - 3l_i(l_i+1))} \quad (2.41)$$

where:

$$\sum_{i'} |\langle i | r | i' \rangle|^2 = \sum_{l'} \frac{l_{>}}{2l_i+1} (R_{n'l'})^2$$

and $(R_{n'l'})^2$ is calculated, as pointed out earlier, in the Coulomb approximation (Bates and Damgaard: 1949).

A somewhat similar quantity used by Jones, Benett and Griem (1971) and Griem (1971) is an effective completeness parameter for both the upper and lower levels of a particular spectral line, taken together. This quantity has also been used by Platisă et al. (1977).

CHAPTER 3THE EFFECTIVE GAUNT FACTOR

The semi-classical model (eq. 1.42) suggested in Chapter 1 treats the electron perturbers as particles travelling along classical trajectories about the radiating ion. As such, all possible paths and collisions have to be included in the evaluation of the line width. In order to simplify the resultant complexity of this diverse picture, the details of these collisions with regard to their trajectories and their statistical occurrence have been isolated in a single quantity: the effective Gaunt factor \bar{g} .

The definition of this quantity \bar{g} has been based on a development of the original concept of the Kramers-Gaunt factor g (Kramers: 1923; Gaunt: 1930). Gaunt (1930) considered the problem of continuous absorption and defined a factor g which can be used to calculate also excitation cross-sections for dipole transitions (Seaton: 1962a; Baranger: 1962; van Regemorter: 1962):

$$\sigma_{\nu i} = \frac{8 \pi^2}{\sqrt{3}} \frac{E_H^2 a_0^2}{\Delta E \frac{1}{2} m v^2} g f_{\nu i} \quad (3.1)$$

The definition of the effective Gaunt factor \bar{g} as given by eq. 1.18 (Seaton: 1962; van Regemorter: 1962) seems to be identical at first sight; there, however, the cross-sections are assumed to be known, and the effective Gaunt factor is thus an empirical quantity obtained by:

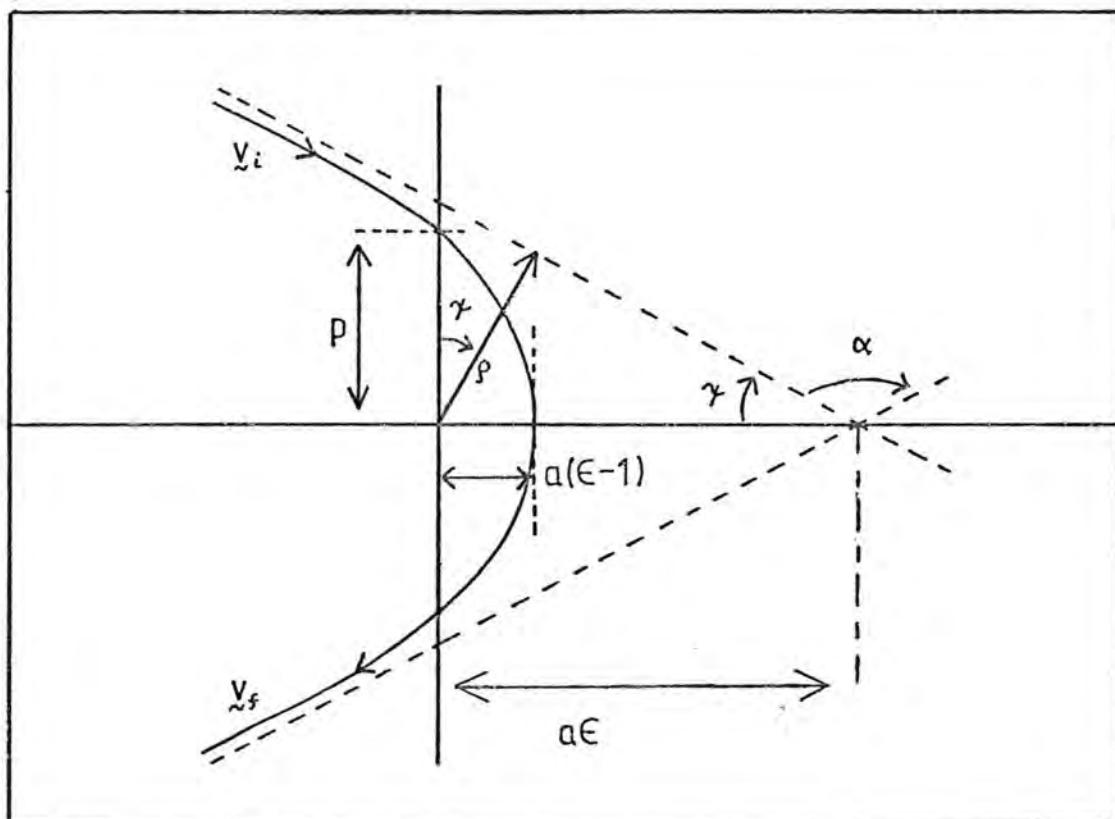
$$\bar{g}_{li} = \sigma_{li} \frac{\sqrt{3}}{8\pi^2} \frac{\Delta E \frac{1}{2} m v^2}{E_H^2 a_0^2 f_{li}} \quad (3.2)$$

specifically for collisions not involving exchange and treated within the dipole approximation. The value of \bar{g} is thus not given by a fixed theoretical expression, but is based on deductions "from the best observations and the best computations available" (van Regemorter: 1962, p. 907). Any attempts to formulate an expression for this factor \bar{g} (as in this chapter) are thus attempts to fit the empirical data available. Such an evaluation of the effective Gaunt factor has been made by van Regemorter (1962) and Seaton (1962a), who proposed numerical values for \bar{g} on the basis of the atomic data available at the time. These values were considered to be applicable to a general ion within an average accuracy of a factor of two, and have been applied to the line broadening problem. Limited success has been achieved in predicting experimental values of the line widths (Griem: 1968; Hey: 1976b; Hey and Bryan: 1977; Hey: 1977a, b). Various other values for \bar{g} , particularly to replace the threshold value of 0.2 given by Seaton (1962a) and van Regemorter (1962), have been suggested for particular ions to improve the above estimates (Blaha: 1969; Davis: 1974). A convenient functional form of the effective Gaunt factor relating it to the classical path of the electron perturber around the ion has been obtained by Griem (1968). Since this formula has been found to disagree with experiment for the more highly ionised species, a new derivation of \bar{g} on the basis of the classical path

approximation has been undertaken in this study.

For electrons colliding with a positive ion of ionisation stage Z , the path described by the electron will be a hyperbolic orbit with the ion scatterer at the focus:

Fig. 3.1: Classical hyperbolic electron orbit



where

- α \equiv scattering angle;
- ϵ \equiv eccentricity of orbit;
- a \equiv semi-axis of hyperbola;
- $2p$ \equiv latus rectum of the orbit;
- ρ \equiv impact parameter;
- v_i \equiv incident electron velocity;
- v_f \equiv outgoing electron velocity;
- O \equiv focus of hyperbola.

For such an orbit, the following relationships can be deduced:

$$a = \frac{(Z-1)e^2}{m v^2} \quad (3.3)$$

$$p = a(\epsilon^2 - 1) \quad (3.4)$$

$$\rho = a(\epsilon^2 - 1)^{1/2} \quad (3.5)$$

$$\sin \alpha/2 = \cos \gamma = \frac{1}{\epsilon} \quad (3.6)$$

$$\text{perihelion distance} = a(\epsilon - 1) \quad (3.7)$$

In order to obtain the collision cross-section from such an orbit, the definition by Seaton (1958, 1962a) of a cross-section can be used (Griem: 1968):

$$\sigma_{i'i} = 2\pi \int P_{i'i} \rho d\rho \quad (P_{i'i} \leq 1) \quad (3.8)$$

where the integration is over all possible impact parameters, and $P_{i',i}$ is the transition probability of a collision at impact parameter ρ . As already discussed in Chapter 1, a monopole-dipole expansion of the interaction is sufficient, thus yielding (Seaton: 1962b; Griem: 1968; see also eq. 1.36):

$$P_{i'i} = \frac{4}{3} \left(\frac{m v}{(Z-1)\hbar} \right)^2 \sin^2(\alpha/2) \left| \langle i' | \mathcal{L} | i \rangle \right|^2 \quad (3.9)$$

In order to obtain an expression now for the effective

Gaunt factor from eq. 3.2, the transition probability needs to be integrated over all possible impact parameters to yield:

$$\bar{g}_{li} = \frac{\sqrt{3}}{\pi} \int_0^{\infty} \frac{\rho}{\rho^2 + a^2} d\rho \quad (3.10)$$

This integral, however, diverges, and suitable upper and lower limits for the impact parameter have to be introduced in order to yield a finite effective Gaunt factor. Denoting these limits ρ_{\max} and ρ_{\min} , the above integral yields the "quasi-classical" effective Gaunt factor (Griem: 1968, p. 260):

$$\begin{aligned} \bar{g}_{li} &= \frac{\sqrt{3}}{2\pi} \ln \left[\frac{\rho_{\max}^2 + a^2}{\rho_{\min}^2 + a^2} \right] \\ &= \frac{\sqrt{3}}{\pi} \ln \left(\frac{\epsilon_{\max}}{\epsilon_{\min}} \right) \end{aligned} \quad (3.11)$$

The necessary choice of the cut-off parameters ρ_{\max} and ρ_{\min} gives rise to the major criticisms of the above method of calculating cross-sections (Davis et al.: 1976; Hey and Breger: 1980b). Griem et al. (1959) suggest that the cut-off be made at the minimum impact parameter below which strong collisions, rather than weak collisions, take place, and at the maximum impact parameter above which the collisions are screened (i.e. $\rho_{\max} = \rho_D$, the Debye length for screening of ions by electrons). The validity of such a definition of the cut-off parameters in the impact regime has been further discussed by Lewis (1961). Where correlations between electron perturbers occur, $\rho_{\max} = 1.1 \rho_D$ has been suggested (Griem et al.: 1962a; Baranger: 1962). In the case of non-degenerate

ions rather than hydrogen, the upper limit needs to be reduced, such that an evaluation of the cross-section (eq. 1.36) by eq. 3.9 is valid (Griem: 1966, 1968). For such an evaluation, the classical path perturbation Hamiltonian \tilde{V} in the interaction picture was assumed approximately to be the same as the actual interaction in the Schrödinger picture (which is in fact an equivalent assumption to the impact approximation applied to isolated lines, see eqs. 1.10 and 1.11), and thus:

$$\frac{1}{\beta} \gg \frac{|\Delta E_{i,i}|}{\hbar v} \quad (3.12)$$

Adopting this "adiabatic" cut-off (Spitzer: 1940) as the upper limit of the impact parameter, the lower cut-off needs to be obtained from the "demarcation" of the strong and weak collision regimes (Lewis: 1961; Griem *et al.*: 1959) as well as the validity of the semi-classical approach as discussed in Chapter 1.

3.1 UPPER CUT-OFF OF ECCENTRICITY

In order to ascribe the broadening of isolated lines to the impact of unshielded perturbers, one requires (Griem: 1962b):

$$|\Delta E_{i,i}| > \hbar \omega_p \approx \frac{\hbar v}{\beta_D}$$

where $\hbar \omega_p$ is the plasmon energy. For ions in a plasma with electron density 10^{+17} cm^{-3} , the energy separation $\Delta E_{i,i}$ would have to remain larger than 94.7 cm^{-1} in order for the above

criterion to be valid. For such energy separations, one thus has a shielding distance of:

$$f_D > \frac{\hbar v}{|\Delta E_{\ell\ell}|} = f_{\max}^{\text{adiabatic}}$$

and the adiabatic cut-off occurs thus for impact parameters below the Debye shielding distance. Since the energy separations in practice (see Chapter 5) are usually much larger than 94.7 cm^{-1} , the following cut-off can be used (Griem: 1966, 1968, 1974):

$$f_{\max} = \frac{\hbar v}{|\Delta E_{\ell\ell}|} \quad (3.13)$$

This cut-off is, however, not sufficient, as it neglects the effect of the curvature of the hyperbolic orbit traversed (Griem: 1966, 1968, 1974).

Applying conservation of angular momentum for the unperturbed trajectory in a Coulomb field (Griem: 1966):

$$f v = f' v' \quad (\text{primes denote perihelion distance where transition occurs}) \quad (3.14)$$

one obtains:

$$f_{\max} = \frac{\hbar v}{|\Delta E_{\ell\ell}|} \left(\frac{v'}{v} \right)^2 \quad (3.15)$$

The correction to the straight classical path has to be

obtained from considerations of conservation of energy of the unperturbed classical path (Griem: 1966):

$$\frac{1}{2} m v^2 = \frac{1}{2} m v'^2 - \frac{(Z-1)e^2}{f'} \quad (3.16)$$

$$\Rightarrow \left(\frac{v'}{v}\right)^3 - \left(\frac{v'}{v}\right) - \frac{2(Z-1)e^2 \Delta E}{m v^3 \hbar} = 0 \quad (3.17)$$

where the level separation $|\Delta E_{i',i}|$ has been abbreviated as ΔE .

Using expression 3.5, one thus obtains:

$$\epsilon_{\max}^2 = 1 + \frac{m^2 v^4}{(Z-1)^2 e^4} \frac{\hbar^2 v^2}{(\Delta E)^2} \left(\frac{v'}{v}\right)^4 \quad (3.18)$$

or denoting:

$$\frac{(Z-1)e^2 \Delta E}{m v^3 \hbar} = \sum_{n'l'} \frac{n'l'}{3_{nl}} \quad (3.19)$$

as introduced by Griem (1968, eq. 16):

$$\epsilon_{\max}^2 = 1 + \left(\sum_{n'l'} \frac{n'l'}{3_{nl}}\right)^{-2} \phi^4 \quad (3.20)$$

where ϕ is the solution $\left(\frac{v'}{v}\right)$ of the cubic eq. 3.17, which is written as:

$$\phi^3 - \phi - 2 \sum_{n'l'} \frac{n'l'}{3_{nl}} = 0 \quad (3.21)$$

In order to solve this cubic, both an analytical as well as an iterative process can be applied. The analytical

solution of the cubic:

$$x^3 + px + q = 0$$

as discussed by Littlewood (1958, p. 188), is presented below for the special case (eq. 3.21) under consideration here. Two different methods for the solution of a cubic of the above form are required, depending on the sign of the discriminant:

$$D = 4p^3 + 27q^2$$

which becomes in the case of eq. 3.21:

$$D = \xi^2 - \frac{1}{27}$$

Case 1: $D > 0$ and thus $\xi^2 > \frac{1}{27}$

In this case, the cubic will have one real root only. For eq. 3.17 this would correspond to the condition:

$$\frac{\Delta E}{E_H} < \frac{27}{4} (Z-1)^2$$

which will apply in most practical cases (see Chapter 5). As a first step in the solution of eq. 3.21, one substitutes:

$$\phi = y + z$$

to obtain instead of eq. 3.21:

$$y^3 + z^3 + (3yz - 1)(y + z) - 2\sqrt[3]{3} = 0$$

Making the choice now of y or z such that $3yz = 1$, one derives the following two equations for y and z :

$$y^3 + z^3 = 2\sqrt[3]{3} \quad (3.21b)$$

$$y^3 z^3 = 1/27 \quad (3.21c)$$

For a quadratic of form:

$$a\lambda^2 + b\lambda + c = 0$$

one can derive the following equations for the roots λ_1 and λ_2 of the quadratic:

$$\lambda_1 + \lambda_2 = -b/a$$

$$\lambda_1 \lambda_2 = c/a$$

One can thus deduce from eqs. 3.21b and 3.21c that y^3 and z^3 must be the solutions of the quadratic:

$$\lambda^2 - 2\sqrt[3]{3}\lambda + \frac{1}{27} = 0$$

The variables y^3 and z^3 can thus be solved for, and since $\phi = y + z$, one obtains:

$$\phi = \left[\xi + \sqrt{\xi^2 - \frac{1}{27}} \right]^{1/3} + \left[\xi - \sqrt{\xi^2 - \frac{1}{27}} \right]^{1/3} \quad (3.22)$$

as the solution of the single real root.

Case 2: $D < 0$ and thus $\xi^2 < \frac{1}{27}$

In this case all three roots are real but only one positive. One substitutes:

$$\phi = k \cos \theta$$

into eq. 3.21 and rewrites the result as:

$$4 \cos^3 \theta - \frac{4}{k^2} \cos \theta = \frac{8}{k^3} \xi$$

Use can now be made of the trigonometric identity:

$$\cos 3\theta = 4 \cos^3 \theta - 3 \cos \theta$$

by choosing k such that $\frac{4}{k^2} = 3$. One thus obtains that:

$$\theta = \frac{1}{3} \arccos \sqrt{27} \xi$$

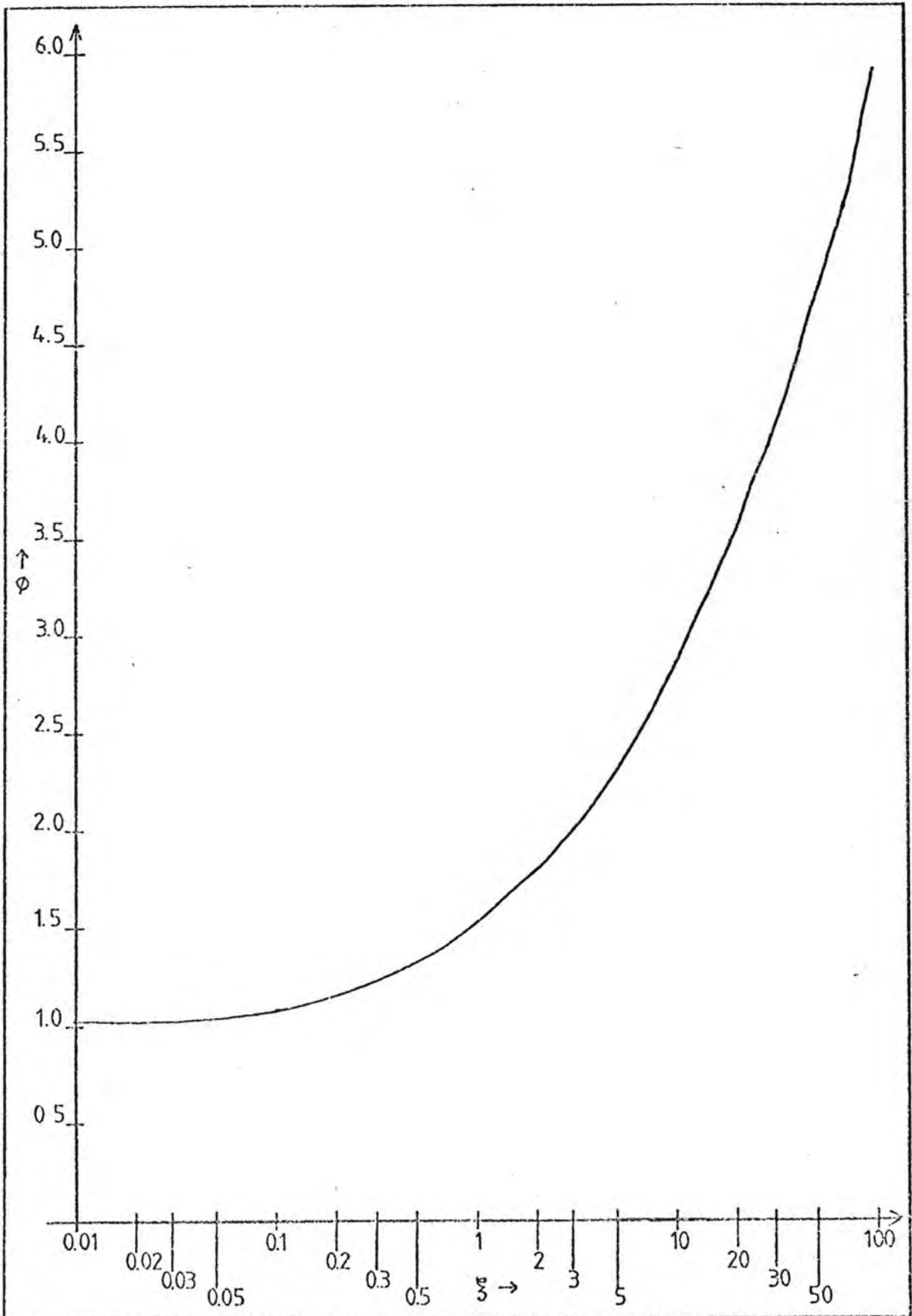
and since $\phi = k \cos \theta$, the solution for the only positive root can be written as:

$$\phi = \frac{2}{\sqrt{3}} \cos \left[\frac{1}{3} \arctan \sqrt{\frac{1}{27} \xi^2 - 1} \right] \quad (3.23)$$

This form involving arc tan rather than the simpler expression using arc cos had to be chosen in order to make evaluation on the computer possible.

Using the above two methods of evaluating the roots of the cubic (eq. 3.21), the maximum eccentricity ϵ_{\max} (eq. 3.18) can now be evaluated readily.

The effect of the curvature correction in the ϵ_{\max} term on the \bar{g} factor has been investigated for several transitions of NV, as well as for the process 2s-2p of the iso-electronic sequence of NV. For large incident electron velocities, the error introduced by omitting this correction was found to be very small, but erroneous \bar{g} are obtained for low velocities, as was expected (Griem: 1968). Some typical values obtained

Fig. 3.2: Solution of cubic

were:

$$\frac{\bar{g}}{g_c} \approx 0.995 \quad \text{for} \quad \frac{1}{2} m v^2 = 100 \Delta E$$

$$\frac{\bar{g}}{g_c} \approx 0.05 \quad \text{for} \quad \frac{1}{2} m v^2 = \Delta E$$

where \bar{g} and \bar{g}_c are calculated without and with introduction of the curvature correction ϕ into the numerator (ϵ_{\max}) respectively.

In order to allow estimates of the effective Gaunt factor to be made without the elaborate exact solution of the cubic (eq. 3.21), a plot of ϕ versus ξ is presented in Fig. 3.2.

3.2 LOWER CUT-OFF OF ECCENTRICITY

Since the effective Gaunt factor is evaluated using classical perturber orbits, one requires, as pointed out in Chapter 1, that the de Broglie wavelength of the electron perturbers must be small with respect to the impact parameter. Thus (Baranger: 1962; Griem: 1966, 1968):

$$f \gg f' = \frac{\hbar}{mv} \quad (3.24)$$

Furthermore, a dipole approximation was employed and, as already assumed in Chapter 1, the Coulomb interaction did not contain a monopole-monopole term. For the case of charged radiators, i.e. ions, such an omission is valid only when the perturber remains outside the orbit of the bound electrons

of the ion (Griem: 1974, pp. 24, 51, 269). One thus requires:

$$f > \rho_2' = d_{i',i} a_0 \quad (3.25)$$

where $d_{i',i}$ is the dipole matrix element. In other words, the dipole moment of the incoming electron with respect to the ion should remain larger than the dipole moment of the ion-bound electron system. Griem (1974, p. 269) estimates this ρ_2 to be of the order of $\frac{n^2 a_0}{Z}$, but, as will be discussed in the following sections, a more accurate estimate needs to be used. The appropriate estimate will be seen to be (see also Chapter 2) the Coulomb approximation:

$$d_{i',i}^2 = \frac{1}{3} \frac{l_{>}}{2l_{n_{<}} + 1} \left(\frac{3n_{l_{>}}^*}{2Z} \right)^2 (n_{l_{>}}^{*2} - l_{>}^2) \Phi^2 \quad (3.26)$$

where $l_{>}$ \equiv the larger of the two angular momenta of i', i ;

$l_{n_{<}}$ \equiv the angular momentum of the lower level of the pair;

n^* \equiv effective principle quantum number;

Φ \equiv Bates-Damgaard factor.

As already mentioned above, the lower impact parameter limit must correspond to the limit between weak and strong collisions. A further requirement that needs to be met, is the unitarity of the S-matrix. Several values for this impact parameter have been suggested (Griem et al.: 1962;

of the ion (Griem: 1974, pp. 24, 51, 269). One thus requires:

$$f > \beta'^2 = d_{i',i}^2 a_0 \quad (3.25)$$

where $d_{i',i}$ is the dipole matrix element. In other words, the dipole moment of the incoming electron with respect to the ion should remain larger than the dipole moment of the ion-bound electron system. Griem (1974, p. 269) estimates this ρ_2 to be of the order of $\frac{n^2 a_0}{Z}$, but, as will be discussed in the following sections, a more accurate estimate needs to be used. The appropriate estimate will be seen to be (see also Chapter 2) the Coulomb approximation:

$$d_{i',i}^2 = \frac{1}{3} \frac{l_{>}}{2l_{n_{<}}+1} \left(\frac{3n_{l_{>}}^*}{2Z} \right)^2 (n_{l_{>}}^{*2} - l_{>}^2) \Phi^2 \quad (3.26)$$

where $l_{>}$ \equiv the larger of the two angular momenta of i', i ;

$l_{n_{<}}$ \equiv the angular momentum of the lower level of the pair;

n^* \equiv effective principle quantum number;

Φ \equiv Bates-Damgaard factor.

As already mentioned above, the lower impact parameter limit must correspond to the limit between weak and strong collisions. A further requirement that needs to be met, is the unitarity of the S-matrix. Several values for this impact parameter have been suggested (Griem et al.: 1962;

Cooper and Oertel: 1969; Griem: 1974), but all cut-off parameters are found to be of the order of:

$$\rho > \rho'_3 = \beta d_{i'i} \frac{\hbar}{mv} \quad (3.27)$$

for rectilinear trajectories, where β is a numerical factor of order unity.

Having obtained various minimum impact parameters that need to be exceeded, one still needs to apply curvature corrections in a similar fashion as for the maximum impact parameter.

For the first condition, the impact parameter had to remain larger than the reduced de Broglie wavelength:

$$\rho > \rho_1 = \frac{\hbar}{mv} \quad (3.28)$$

Applying $\rho v = \rho' v'$ to this expression just yields the same form.

The second condition required that the dipole moment of the perturber-ion remains larger than the bound electron-ion dipole moment:

$$\rho > \rho_2 = d_{i'i} a_0$$

Applying again conservation of angular momentum and energy (eqs. 3.14 and 3.16) (Griem: 1966):

$$\begin{aligned}
\rho^2 > \rho_2^2 &= \rho_2'^2 \left(\frac{v'}{v} \right)^2 \\
&= \rho_2'^2 \left(1 + \frac{2(Z-1)e^2}{\rho_2' m v^2} \right) \\
&= \frac{\hbar^2}{m^2 v^2} d_{i'i}^2 \left[\frac{m v^2}{2 E_H} + \frac{2(Z-1)}{d_{i'i}} \right]
\end{aligned} \tag{3.29}$$

Since the third condition of unitarity has been obtained for a rectilinear trajectory (Griem: 1974, p. 79), curvature corrections need to be made, applying:

$$\rho_{str}^2 = \rho_c^2 + a^2 \tag{3.30}$$

where $\rho_{str.}$ = straight path impact parameter;

ρ_c = curved path impact parameter,

$$\begin{aligned}
\Rightarrow \rho^2 > \rho_3^2 &= (\beta d_{i'i})^2 \frac{\hbar^2}{m^2 v^2} - \frac{(Z-1)^2 e^4}{m^2 v^4} \\
&= \frac{\hbar^2}{m^2 v^2} \left[\beta^2 d_{i'i}^2 - \frac{(Z-1)^2 E_H}{\frac{1}{2} m v^2} \right]
\end{aligned} \tag{3.31}$$

So far the constant β has been assumed to be a numerical factor, indicating that ρ_3 should be of the order of the above value. As will be discussed in Chapter 4.2, this constant may be taken as unity without appreciable error in \bar{g} . For slow velocities and large $d_{i,i}^2$ the above lower limit of the impact parameter can turn negative. Since such values are meaningless, this criterion will be neglected when such a sign reversal occurs (Griem: 1968; Cooper and Oertel: 1969).

Since the two cut-off conditions ρ_2 and ρ_3 are just

indications of the order of magnitude of the lower limit of the impact parameter (as was emphasised by the factor β in ρ_3), a different approach to the one by Griem (1968, 1974) for the evaluation of ϵ_{\min} will be adopted. It would certainly be correct to evaluate the ρ_{\min} by using the following form (Griem: 1968, 1974):

$$\rho_{\min} = \max [\rho_1; \rho_2; \rho_3] \quad (3.32)$$

but to avoid an underestimation of ρ_{\min} by the wrong scaling factor for each criterion (i.e. β in the case of ρ_3) it is advantageous to estimate ρ_{\min} by:

$$\rho_{\min} = (\rho_1^2 + \rho_2^2 + \rho_3^2)^{1/2} \quad (3.33)$$

and for the case of negative ρ_3^2 :

$$\rho_{\min} = (\rho_1^2 + \rho_2^2)^{1/2} \quad \text{for} \quad \beta^2 d_{ii}^2 < \frac{(Z-1)^2 E_H}{\frac{1}{2} m v^2} \quad (3.34)$$

Having defined ρ_{\min} in such a way, the factor β will be taken as unity in the following discussion. The validity of this estimate will be considered in Chapter 4.2.

Using this prescription of a lower limit to the impact parameter integration, one obtains for:

$$\begin{aligned} \epsilon_{\min}^2 &= 1 + \frac{m^2 \rho_{\min}^2 v^4}{(Z-1)^2 e^4} \\ &= 1 + \frac{\frac{1}{2} m v^2}{(Z-1)^2 E_H} \left[1 + d_{ii}^2 \left[1 + \frac{\frac{1}{2} m v^2}{E_H} + \frac{2(Z-1)}{d_{ii}} \right] - \frac{(Z-1)^2 E_H}{\frac{1}{2} m v^2} \right] \end{aligned} \quad (3.35)$$

for all $d_{i'i}^2 \geq \frac{(Z-1)^2 E_H}{\frac{1}{2} m v^2}$, and otherwise:

$$E_{\min}^2 = 1 + \frac{\frac{1}{2} m v^2}{(Z-1)^2 E_H} \left[1 + d_{i'i}^2 \left[\frac{\frac{1}{2} m v^2}{E_H} + \frac{2(Z-1)}{d_{i'i}} \right] \right] \quad (3.36)$$

It is convenient at this point to define:

$$x = \sqrt{\frac{\frac{1}{2} m v^2}{\Delta E}} \quad (3.37)$$

$$y = \sqrt{\frac{E_H}{\Delta E}} \quad (3.38)$$

Using these parameters, the threshold condition is given by $x = 1$ and comparison with the van Regemorter values (1962), discussed earlier, as well as other suggested \bar{g} values is facilitated.

From eq. 3.11 one thus obtains for the effective Gaunt factor:

$$\bar{g} = \frac{\sqrt{3}}{2\pi} \ln \left[\frac{1 + \frac{4x^6}{(Z-1)^2 y^2} \phi^4}{1 + \frac{x^2}{(Z-1)^2 y^2} \left[1 + d_{i'i}^2 \left[1 + \frac{x^2}{y^2} + \frac{2(Z-1)}{d_{i'i}} \right] - \frac{(Z-1)^2 y^2}{x^2} \right]} \right] \quad (3.39)$$

and when:

$$d_{i'i}^2 < \frac{(Z-1)^2 y^2}{x^2} \quad (3.40)$$

$$\bar{g}_t = \frac{\sqrt{3}}{2\pi} \ln \left[\frac{1 + \frac{4x^6}{(Z-1)^2 y^2} \phi^4}{1 + \frac{x^2}{(Z-1)^2 y^2} \left[1 + d_{i,i}^2 \left[\frac{x^2}{y^2} + \frac{2(Z-1)}{d_{i,i}} \right] \right]} \right] \quad (3.41)$$

should be employed, where the subscript t denotes that a "truncated" version of the \bar{g} factor is employed.

Neglecting the curvature corrections in both numerator and denominator of eq. 3.39, and employing the estimate of $d_{i,i}$ as suggested by Griem (1974), one obtains ($\beta = 1$, $d_{i,i} = \frac{n^2}{Z}$):

$$\bar{g}_{S_n} = \frac{\sqrt{3}}{2\pi} \ln \left[\frac{1 + \frac{4x^6}{(Z-1)^2 y^2}}{1 + \frac{x^2}{(Z-1)^2 y^2} \left[1 + \frac{n^{*4}}{Z^2} \left[1 + \frac{x^2}{y^2} \right] \right]} \right] \quad (3.42)$$

Despite the earlier demonstration of the large error introduced in the numerator by neglecting curvature effects, this crude estimate has been employed with success for the calculation of several SnII line widths (Hey and Breger: 1980a). So far, however, no reference to the correct limiting behaviour of the effective Gaunt factor has been made: it is precisely for this reason that the simple form of \bar{g}_{S_n} had to be abandoned in favour of the expressions 3.39 and 3.41. The effective Gaunt factor obtained by consideration of the collision processes along classical paths should satisfy the following criteria:

- i) The Bethe approximation formula of \bar{g} should be obtained in the high-energy limit ($x \gg 1$). This limit can be obtained in a suitable form from Seaton (1975) for the Bethe approximation:

$$\Omega(i,i') = \frac{8}{3} \frac{S(i,i')}{a_0^2 e^2} \ln \left[\frac{2 a_0^2 k}{r_0} \frac{E_H}{\Delta E} \right] = \frac{8\pi}{3\sqrt{3}} \bar{g}_B \frac{S(i,i')}{a_0^2 e^2} \quad (3.43)$$

where $\hbar k = mv$;

$r_0 =$ "classical distance of closest approach"
 $= \rho_{\min}$

Thus:

$$\bar{g}_B = \frac{\sqrt{3}}{\pi} \ln \left[\frac{\hbar v}{\rho_{\min} \Delta E} \right] \quad (3.44)$$

- ii) The effective Gaunt factor must remain an "analytical" - continuous in energy (i.e. well-behaved) - function for y large, even for small x (threshold limit 1^+).
- iii) Since broadening of ion lines is considered here, a non-zero threshold value must be obtained under all circumstances (Seaton: 1962). A zero \bar{g} factor is obtained for all cases where the argument of the logarithm $\lesssim 1$. The case where $\rho_{\min} > \rho_{\max}$ is thus artificially interpreted to give $\bar{g} = 0$ on physical grounds (Griem: 1966, 1968; Cooper and Oertel: 1969).

3.3 ASYMPTOTIC BEHAVIOUR OF \bar{g}

i) High-energy Bethe formula:

Since the curvature correction for the ρ_{\max} was given by ϕ where:

$$\phi^3 - \phi - \frac{2(Z-1)e^2\Delta E}{m v^3 \hbar} = 0$$

this correction can be neglected in the high velocity limit.

Furthermore:

$$\epsilon = \left[1 + \frac{m^2 \beta^2 v^4}{(Z-1)^2 e^4} \right]^{1/2}$$

$$\rightarrow \frac{m \beta v^2}{(Z-1) e^2} \quad \text{for large } v.$$

Thus:

$$\bar{g} \rightarrow \frac{\sqrt{3}}{2\pi} \ln \left[\frac{\beta_{\max}^2}{\beta_{\min}^2} \right]$$

which, for the upper limit $\rho_{\max}^2 = \frac{\hbar^2 v^2}{(\Delta E)^2}$, becomes:

$$\bar{g} \rightarrow \frac{\sqrt{3}}{\pi} \ln \left[\frac{\hbar v}{\beta_{\min} \Delta E} \right] = \bar{g}_B$$

which is the correct limit (Seaton: 1975).

ii) Analytical behaviour of \bar{g} :

For all values of y and $x \geq 1$, the derived effective Gaunt factor should be continuous and remain positive. Thus

the difficulty of interpretation (Griem: 1966, 1968; Cooper and Oertel: 1969) for the case where ρ_{\min} exceeds ρ_{\max} is avoided in the above threshold regime. To verify this analytical behaviour, the high energy regime of the Gaunt factor is examined, as well as the exact nature of the ratios $\frac{\rho_1}{\rho_{\max}}$, $\frac{\rho_2}{\rho_{\max}}$, $\frac{\rho_3}{\rho_{\max}}$ in the near-threshold regime.

For large values of x , the curvature correction ϕ for the upper impact parameter tends to unity, since it obeys the relation:

$$\phi^3 - \phi - \frac{(Z-1)y}{x^3} = 0 \quad (3.45)$$

For high energies and $x \gg y$, a finite positive \bar{g} value requires for both eqs. 3.39 and 3.41:

$$\frac{4x^4}{1 + d_{li}^2 \left[\frac{x^2}{y^2} + \frac{2(Z-1)}{d_{li}} \right]} > 1 \quad (3.46)$$

which can be further approximated for $x \gg 1$:

$$\frac{4x^2}{\left(\frac{d_{li}^2}{y^2} \right)} > 1 \quad (3.47)$$

At this point it is important to note that (Sobel'man: 1972, p. 315; see also Chapter 2):

$$d_{li}^2 \frac{1}{y^2} = \frac{1}{3} \frac{l_y}{2l_y+1} R_{li}^2 \frac{\Delta E_{li}}{E_H} = f_{li} \lesssim 1 \quad (3.48)$$

Since values of $x \geq 1$ are considered, the effective Gaunt factor is seen to remain analytical for large x . The above

relation 3.48 is not necessarily satisfied if one estimates (Griem: 1964, 1974):

$$d_{i'i} \approx \frac{n^2}{Z} \quad (3.49)$$

as was done in the calculation of \bar{g}_{Sn} . Following a similar procedure for \bar{g}_{Sn} as for the above \bar{g} high energy behaviour, one obtains the requirement:

$$4x^4 > \frac{n^4}{Z^2} \left[\frac{x^2 + y^2}{y^2} \right] \quad (3.50)$$

which may break down for small values of y . More serious, however, was a breakdown of this approximation near threshold x discussed below under section iii).

It still remains to be verified that the proposed \bar{g} formulae 3.39 and 3.41 remain analytical (continuous) in the near threshold regime. For this, it is most convenient to consider each ρ_1 , ρ_2 and ρ_3 separately.

Case I: $\frac{\rho_{max}}{\rho_1}$

Including the curvature corrections at low x , ρ_{max} was written as:

$$\rho_{max} = \frac{\hbar v}{\Delta E} \left(\frac{v'}{v} \right)^2$$

and

$$\rho_i = \frac{\hbar}{m v}$$

Thus:

$$\frac{\rho_{\max}}{\rho_1} = 2x^2\phi^2$$

and:

$$\left(\frac{\rho_1}{\rho_{\max}}\right)^2 = \frac{1}{4x^4\phi^4} < \frac{1}{4} \quad (3.51)$$

Case II: $\frac{\rho_{\max}}{\rho_2}$

$$\rho_2^2 = \left(\frac{\hbar}{mv}\right)^2 d_{ii}^2 \left[\frac{mv^2}{2E_H} + \frac{2(Z-1)}{d_{ii}} \right]$$

from eq. 3.29, thus yielding:

$$\left(\frac{\rho_{\max}}{\rho_2}\right)^2 = \frac{4x^4\phi^4}{x^2 \frac{d_{ii}^2}{y^2} + 2(Z-1)d_{ii}}$$

and using condition 3.48:

$$\left(\frac{\rho_2}{\rho_{\max}}\right)^2 < \frac{x^2 + 2(Z-1)y}{4x^4\phi^4}$$

For large x , this is clearly < 1 . For large y , ϕ can be estimated as $\sim \left[(Z-1) \frac{y}{x^3}\right]^{1/3}$ and:

$$\left(\frac{\rho_2}{\rho_{\max}}\right)^2 \sim \frac{1}{2(Z-1)^{1/3} y^{1/3}} < 1$$

For intermediate values, $\phi^3 = \phi + (Z-1) \frac{y}{x^3}$ and:

$$\left(\frac{\rho_2}{\rho_{\max}}\right)^2 < \frac{\frac{1}{x} + \frac{2(Z-1)y}{x^3}}{2 \left[2\phi + \frac{2(Z-1)y}{x^3} \right] \phi x} < \frac{1}{2\phi x} < 1 \quad (3.52)$$

Case III: $\frac{\rho_{\max}}{\rho_3}$

$$\rho_3^2 = \left(\frac{\hbar}{mV}\right)^2 \left[d_{i'i}^2 - \frac{(Z-1)^2 E_H}{\frac{1}{2}mV^2} \right]$$

from eq. 3.31. Thus:

$$\begin{aligned} \left(\frac{\rho_3}{\rho_{\max}}\right)^2 &= \frac{d_{i'i}^2 - \frac{(Z-1)^2 y^2}{x^2}}{4x^4 \phi^4} \\ &< \frac{y^2 \left[1 - \frac{(Z-1)^2}{x^2}\right]}{4x^4 \phi^4} \end{aligned} \quad (3.53)$$

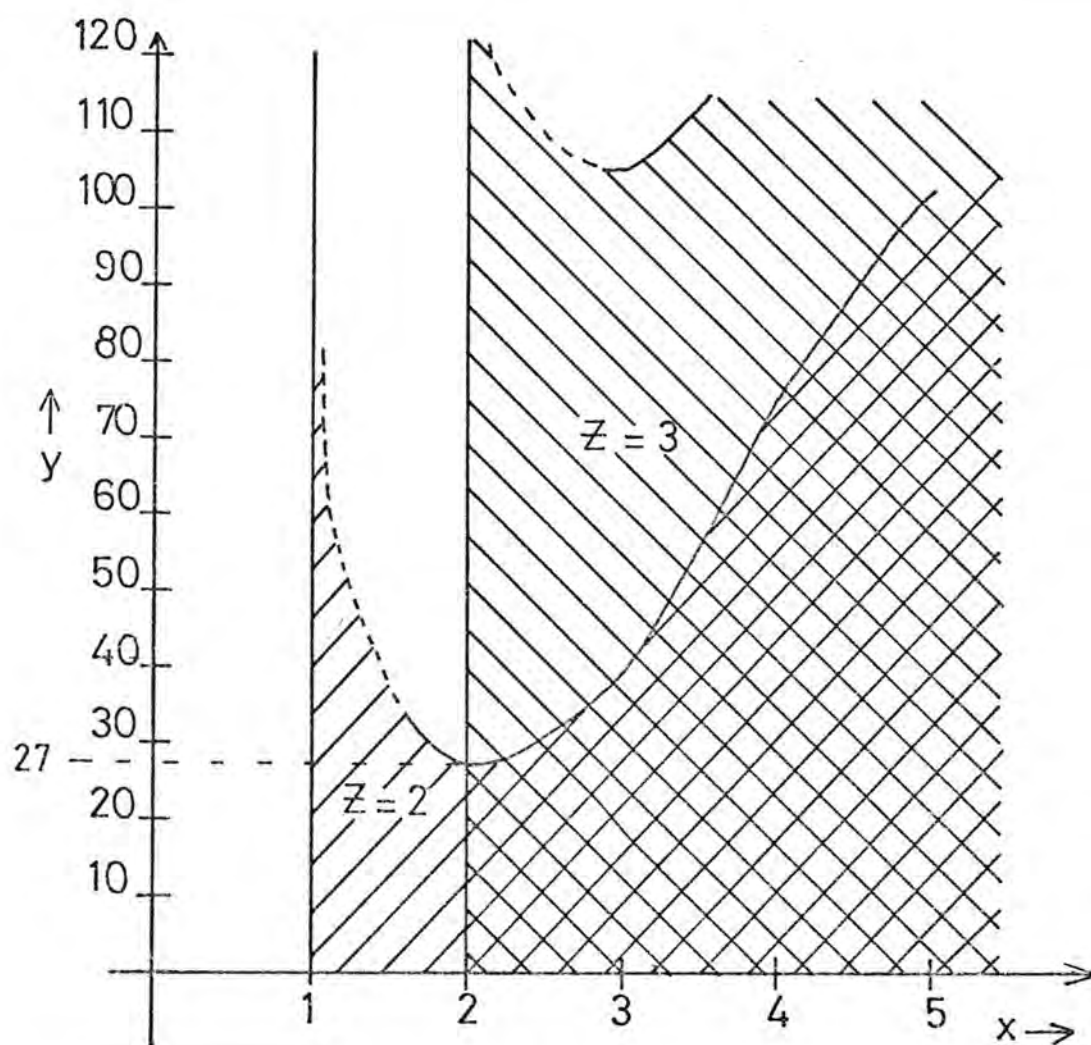
Deductions about this ratio are difficult to make and a numerical investigation was thus employed to establish whether this ratio remains less than unity. Since this cut-off should be applied only when:


$$d_{i'i}^2 \geq \frac{(Z-1)^2 y^2}{x^2}$$


and one has $d_{i,i}^2 \leq y^2$ from eq. 3.48, it is important to note that the unitarity condition enters in the expression for \bar{g} only at threshold ($x = 1$) when $Z = 2$. For values of x larger than $(Z-1)$, the following diagram (fig. 3.3) has been obtained from a numerical analysis of eq. 3.53, indicating the conditions under which breakdown of the Gaunt factor occurs.

As can be seen from the diagram, a non-zero effective Gaunt factor using the unitarity condition is obtained for all $y < 27$. From the definition of $y = \sqrt{\frac{E_H}{\Delta E}}$, this observation means that the effective Gaunt factor expression 3.39 for \bar{g} is valid for all:

Fig. 3.3: Regions of validity of the Unitarity condition



Key:  regime in which $\frac{\rho_{\max}}{\rho_3} > 1$ for $Z = 2$

 regime in which $\frac{\rho_{\max}}{\rho_3} > 1$ for $Z = 3$

Note: The vertical boundary of $Z = 2$ field at $x = 1$ is due to use of \bar{g}_{tr} below $x = 1$; similarly for $Z = 3$ the unitarity condition is not applied for $x < 2$.

$$\Delta E > 150 \text{ cm}^{-1}$$

This conclusion really requires:

$$\frac{\rho_1^2 + \rho_2^2 + \rho_3^2}{\rho_{\max}^2} < 1 \quad (3.54)$$

but for $\left(\frac{\rho_3}{\rho_{\max}}\right)^2 \rightarrow 1$, $\frac{\rho_1^2}{\rho_{\max}^2}$ and $\frac{\rho_2^2}{\rho_{\max}^2}$ are very small, allowing the extension of $\left(\frac{\rho_3^2}{\rho_{\max}^2}\right) < 1$ to eq. 3.54.

In practice, the condition of $\Delta E > 200 \text{ cm}^{-1}$ is easily met by most ions (Hey and Breger: 1980a, b, c). For $Z > 2$, the unitarity cut-off is dropped at threshold (for $x < 2$) and a non-zero value is obtained for values of $y < 100$, i.e. $\Delta E > 11 \text{ cm}^{-1}$.

It should, however, be noted that for such small energy separations (less than $\sim 100 \text{ cm}^{-1}$) the effect of shielding will become significant (see discussion at beginning of section 3.1).

iii) Non-zero threshold value for ion scatterers:

From eqs. 3.51, 3.52 and fig. 3.3 it is apparent that the effective Gaunt factor can be calculated from eq. 3.39 and a fortiori from eq. 3.41. Since an increase in ionisation stage Z will increase the curvature factor ϕ , the condition of non-zero threshold values is even better maintained for higher ionisation stages.

This success at threshold cannot be claimed by the expression 3.42 for \bar{g}_{Sn} , not even when this is corrected for

curvature. One obtains at $x = 1$ the requirement:

$$\frac{4 \phi^4}{1 + \frac{n^4}{Z^2} \left[\frac{1 + y^2}{y^2} \right]} > 1$$

For small values of y , the correction factor $\phi \rightarrow 1$ (see eq. 3.45) and the denominator varies as $\sim \frac{1}{y^2}$. Breakdown does thus occur at threshold, unless the matrix element $d_{i,i}$ contains a ΔE dependence. It is thus not advisable to replace $d_{i,i}$ by $\frac{n^2}{Z}$, but rather to retain the whole eq. 3.26, so that an equality of type 3.48, ($\frac{d_{i,i}^2}{y^2} \leq 1$) is obtained.

3.4 EXTRAPOLATION BELOW THRESHOLD

In the foregoing discussion, the validity of the proposed effective Gaunt factor (eqs. 3.39, 3.41) above threshold has been verified. As already discussed in Chapter 1, the effective Gaunt factor approximation of inelastic collision cross-sections can be extended to include elastic contributions to the line broadening (Griem: 1968) by extrapolation into the below-threshold energy regime. Below threshold, the elastic contributions are predominantly dipole, whereas above threshold, the major elastic contribution is assumed to be quadrupole (Hey and Blaha: 1978). The inclusion of elastic contributions by extrapolation of the Gaunt factor into the regime of energies below $\Delta E_{i,i}$ thus omits the quadrupole elastic contributions to the line width. This approximation is discussed by Hey and Blaha (1978), who supplemented a semi-empirical calculation with the formally more correct distorted-wave calculation of cross-sections. It was found that, in

the case investigated ($\lambda = 4041.3 \text{ \AA}$ line in the NII spectrum), some 81% of the line width could be ascribed to dipole contributions. The attention given to the dipole elastic terms, rather than to the quadrupole terms, seems thus justified.

For these dipole elastic collisions below threshold, the incoming electron can be captured into an unstable state, giving rise momentarily to a doubly excited auto-ionising ion (or neutral) state (Gailitis: 1963; Bely: 1969). These states form a converging Rydberg series of resonances in the collision strength, which, in turn, converge to the threshold energy. In order to extrapolate the effective Gaunt factor below threshold, an average over these resonances is required (Bely: 1969; see also Chapter 1). Such an average has been derived by Gailitis (1963), showing that this average gives rise to a collision strength continuous with respect to energy. Bely (1969) discusses this aspect with respect to the line broadening calculations as suggested by Griem (1968) and arrives at the conclusion that the collision strength "will be continuous when averaged over resonances, provided there exist no (levels) k and k' such that":

$$\Delta E_{ik} = \Delta E_{fk'} \quad (3.55)$$

In the case of the ions considered in this investigation, such a restriction was found to be of no consequence, as this equality 3.55 never arose. Details of the method that one should employ to obtain an averaged \bar{g} below threshold are

found to vary widely in the literature (Bely and Griem: 1970; Barnes and Peach: 1970; Petrini: 1970; Fleurier et al.: 1977). Griem (1968) suggests that one should maintain $\bar{g} = \bar{g}_{th}$ for all energies below threshold. Various other methods have been investigated by Fleurier et al. (1977), namely using an unaltered collision strength expression below threshold, as well as applying two types of corrections for cases where there are a great number of resonances and when there are a few resonances to be averaged over below-threshold. Although non-negligible differences in the calculated line widths were obtained (Fleurier et al.: 1977), results of the same order of magnitude as the ones using the semi-empirical method of Griem (1968) were obtained.

In order to investigate this uncertainty with regard to the exact extrapolation procedure below threshold, two "extreme" approaches have been tested for various ion lines (Hey and Breger: 1980b, c; see also Chapter 5). The elastic contributions have been estimated using:

- (a) the same expression for \bar{g} below as above threshold, accepting that the valid \bar{g}_{min} possible should be zero (method I);
- (b) employing the threshold value of \bar{g} for all energies below threshold (method II).

In the two cases of oxygen and sulphur (Hey and Breger: 1980b, c; see Chapter 5), the latter approach led to an overestimate of the measured line width for the lower ionisation stages; whereas employing method I of

extrapolation yielded better consistency with experimental results.

3.5 THE VELOCITY AVERAGE OF THE EFFECTIVE GAUNT FACTOR

As discussed in Chapter 1, the average effective Gaunt factor (eqs. 1.38, 1.39):

$$\langle \bar{g}(\check{i}, i) \rangle = \int_0^{\infty} \bar{g}(z) \exp(-z) dz \quad (3.56)$$

(excitation)

$$\langle \bar{g}(\check{i}, i) \rangle = \int_0^{\infty} \bar{g}\left(z + \frac{\Delta E_{i'i}}{kT}\right) \exp(-z) dz \quad (3.57)$$

(de-excitation)

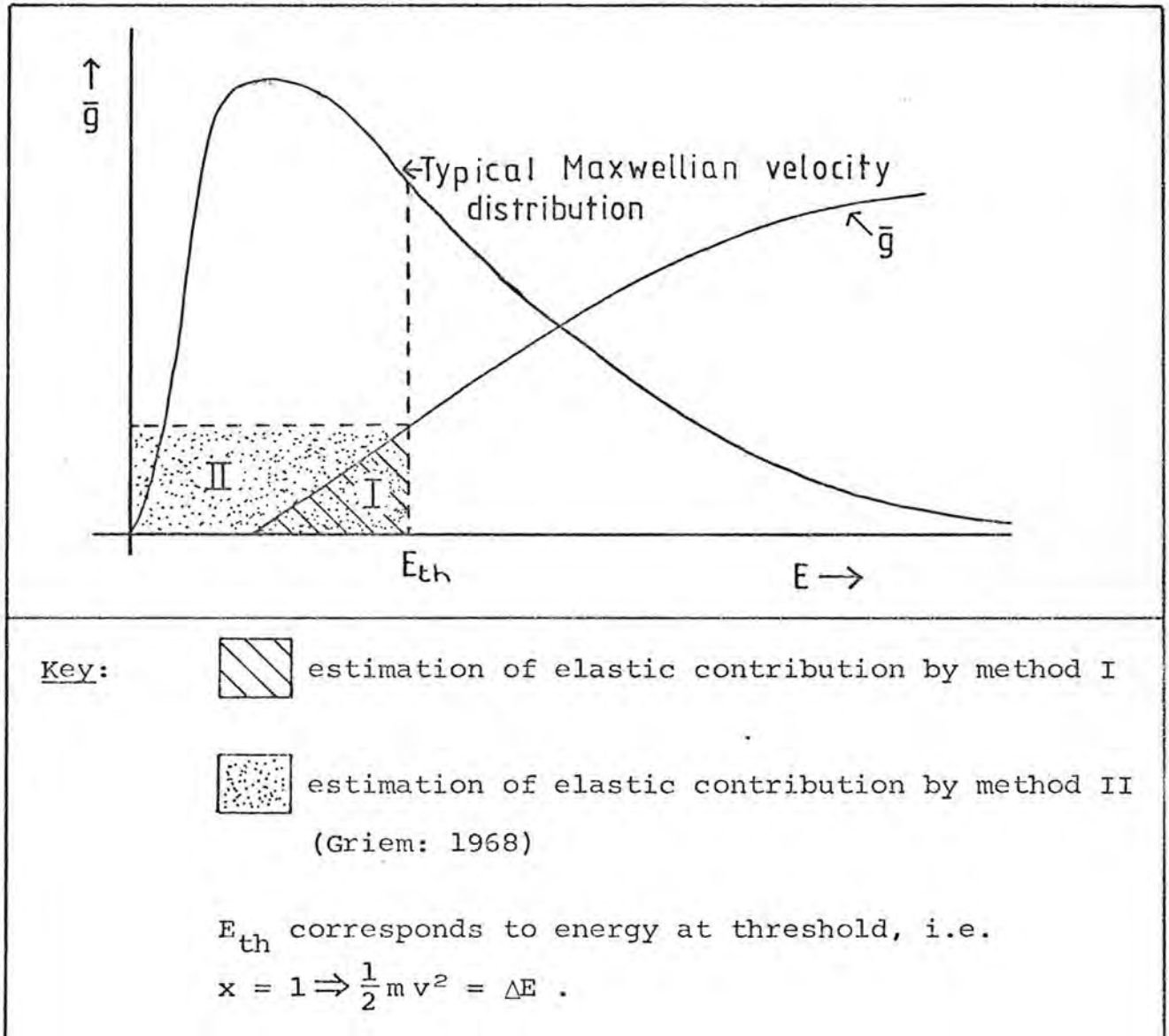
with $z = \frac{1}{2} \frac{m v^2}{kT}$ are required to obtain the collision strength of a particular perturber collision. Since the \bar{g} expressions (eqs. 3.39, 3.41) derived above yield mathematically cumbersome integrations, numerical methods have been employed to evaluate eqs. 3.56, 3.57. Such an integration needs to be done only when the assumption that \bar{g} is a slowly varying function of energy fails, and thus the approximation of:

$$\left\langle \bar{g}\left(\frac{E}{kT}\right) \right\rangle = \bar{g}\left(\frac{\bar{E}}{kT}\right)$$

(as employed in the use of \bar{g}_{Sn} in Hey and Breger: 1980a) is not valid any longer. This was found to be the case in OII and OIII (Hey and Breger: 1980b), making numerical integration essential. The discussion of the two methods (method I and II) of extrapolation below threshold can then be illustrated

by the following diagram (fig. 3.4):

Fig. 3.4: Maxwellian average of Gaunt factor



The ratio of inelastic to (dipole) elastic contribution to the line width is thus directly obtainable from the evaluation of the integrals (eq. 3.56) above and below threshold respectively. It was found that the elastic contribution thus obtained exceeded the simpler estimate made by Griem (1968), who evaluated this simply by taking:

$$W_{el} = W_{TOTAL} \left[1 - \exp\left(-\frac{\Delta E}{kT}\right) \right]$$

where $W_{el} \equiv$ elastic contribution to line width;

$W_{TOTAL} \equiv$ elastic plus inelastic contributions.

3.6 COMPARISON OF \bar{g} BY 3.39 AND 3.41 WITH PUBLISHED DATA

Since the model for line broadening calculations in this investigation can be regarded as an extension of the semi-empirical model by Griem (1974), it is thus of interest to see how the suggested form of eqs. 3.39 and 3.41 compare with Griem's effective Gaunt factor. The Gaunt factor, as used by Griem, has been employed in a slightly modified form by Dimitrijević and Konjević (1980a) for similar ions to those in this investigation. An alternative form of the effective Gaunt factor has been suggested by Davis (1974) and this form has also been found by Younger (1979), Younger and Wiese (1979). For comparison purposes, the different effective Gaunt factors can be summarised as follows:

$$\begin{array}{l} \text{Davis (1974)} \\ \text{Younger (1979) for } \Delta n = 0 \end{array} \quad \bar{g} = A + \frac{B}{x^2} + C \ln x^2 \quad (3.58)$$

$$\begin{array}{l} \text{Younger + Wiese (1979)} \\ \text{for } \Delta n = 0 \text{ transitions} \end{array} \quad \bar{g} = \left(1 - \frac{1}{Z_e}\right) \left(0.7 + \frac{1}{n}\right) (0.6 + 0.25 \ln x^2) \quad (3.59)$$

$Z_e =$ effective charge

$$\begin{array}{l} \text{Dimitrijević + Konjević (1980a)} \\ \text{for } \Delta n = 0 \text{ (Griem (1974))} \end{array} \quad \bar{g} = 0.7 - \frac{1.1}{Z} + g(x) \quad (3.60)$$

$g(x) = 0.2, 0.24, 0.33, 0.56, 0.98$
for $x^2 = 1, 3, 5, 10, 30$

$$\text{Griem (1974)} \quad \Delta n = 0: \quad \bar{g} = \frac{\sqrt{3}}{\pi} \ln \left(5 - \frac{4.5}{\sqrt{Z}} + \frac{2x^3}{(Z-1)y} \left[1 + \frac{n^2 x^2}{Z(Z-1)y^2} \right]^{-1} \right) \quad (3.61)$$

$$\Delta n \neq 0: \quad \bar{g} = \frac{\sqrt{3}}{\pi} \ln \left(1.4 + \frac{n^3 x^3}{Z^2(Z-1)y^3} \left[1 + \frac{n^2 x^2}{Z(Z-1)y^2} \right]^{-1} \right) \quad (3.62)$$

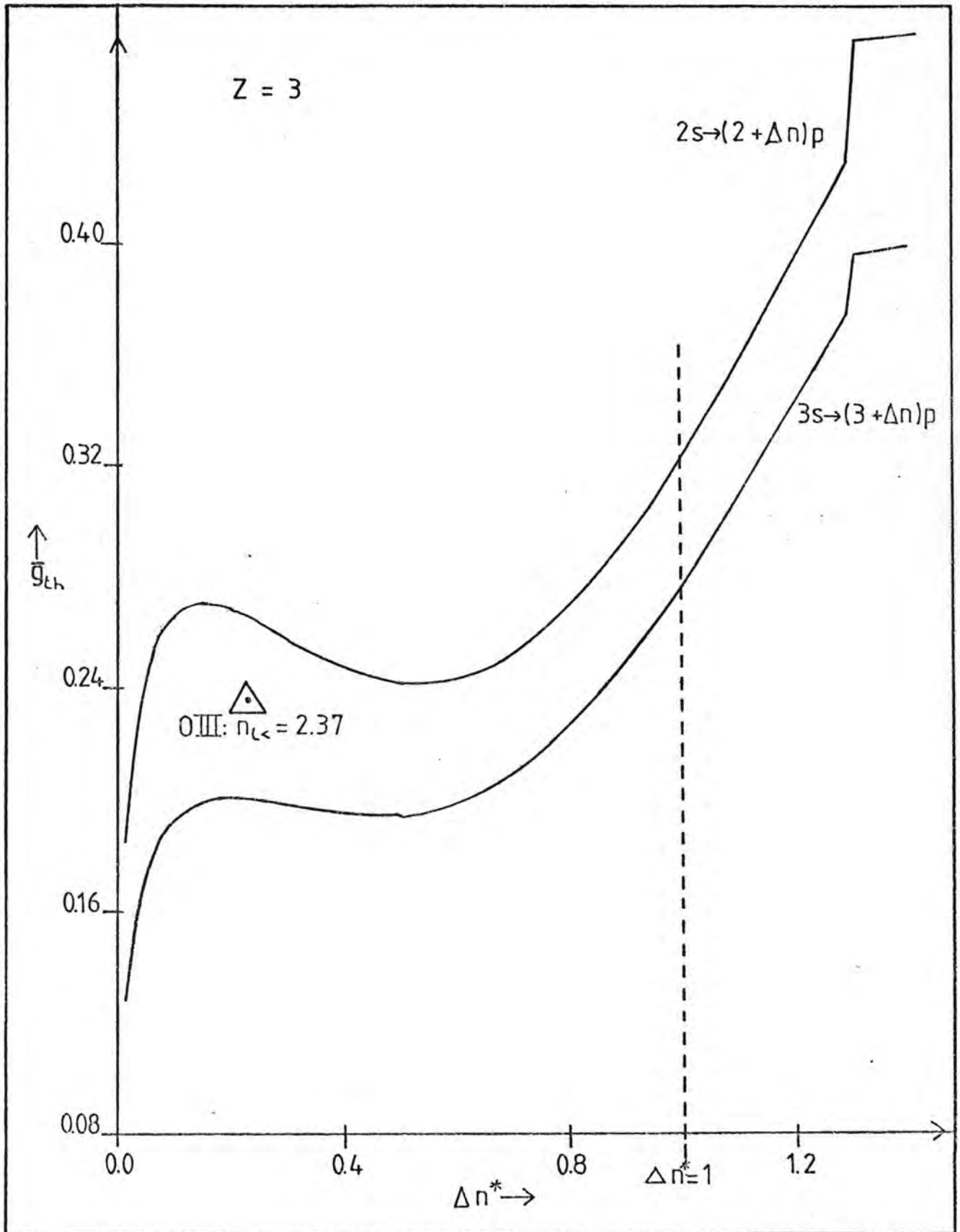
All of the above authors distinguish between $\Delta n = 0$ and $\Delta n \neq 0$ types of transition. Generally, the Gaunt factor for $\Delta n \neq 0$ is found to be more rapidly varying with energy (x) than for $\Delta n = 0$ transitions. Except for the case of eq. 3.59, no explicit allowance is made for the difference in structure between real ions and the highly idealised model of the hydrogenic ion which predicts integral principal quantum numbers. The inclusion of the observed quantum defect (alternatively, the definition of an effective charge Z_e) is only partially possible in the equations 3.61 and 3.62 suggested by Griem (1974), by setting $n \equiv n_{<}^*$ (where $n_{<}^*$ denotes the lower of the two effective principal quantum numbers). As discussed also in Chapter 6, this neglect of structure of the actual ion involved signifies a major difference between the form suggested by Griem (1974) (eqs. 3.61, 3.62) and the form presented in this investigation. For a transition:

$$2s \rightarrow (2 + \Delta n^*)p$$

$$\text{and } 3s \rightarrow (3 + \Delta n^*)p$$

in an ion of $Z = 3$, the following plot (fig. 3.5) of threshold

Fig. 3.5: Plot of threshold Gaunt factor vs. change in effective principal quantum number



Gaunt factor versus change in effective principal quantum number ($\Delta n^* = n_{l_>}^* - n_{l_<}^*$) is obtained using eqs. 3.39 and 3.41. (Here $n_{l_>}^*$ and $n_{l_<}^*$ denote the effective principal quantum number of the level with larger and smaller orbital angular momentum respectively.)

For example, the transition $3s \ ^3P_1 \rightarrow 3p \ ^3S_1$ in OIII is in fact a transition of $(2.37)s \rightarrow (2.37 + 0.23)p$ in terms of effective principal quantum number, and the resultant \bar{g}_{th} has been indicated on fig. 3.5.

It would thus appear as though the classification of transitions into categories $\Delta n = 0$ and $\Delta n \neq 0$ (Griem: 1974; Younger: 1979) is an oversimplification of the complexity of the ion radiator, of the same nature as the reduction of the fine structure details in the oscillator strengths to a function of orbital angular momenta and principal quantum number only. This point has been discussed already in detail in Chapter 2.

From the graph (fig. 3.5) it becomes clear that the suggested calculation of the threshold effective Gaunt factor (Hey and Breger: 1980b, c) is valid only for non-zero level separations; for cases where Δn^* vanishes, the \bar{g}_{th} factor is not valid. This was found in the discussion of the analytical behaviour of \bar{g} where a minimum ΔE was established in the paragraph following fig. 3.3. For a radiator with degenerate bound states, such as a hydrogenic ion, reductions of the complexity of the radiator structure is justified, and the semi-empirical theory by Griem (1974) is applicable.

In order to compare the energy dependence of the suggested

Gaunt factor with previously established behaviour, the graph in fig. 3.6 was obtained for a NV transition $2s \rightarrow 2p$, as well as $2s \rightarrow 3p$ in fig. 3.7.

The curves plotted are:

DAVIS - from Davis (1974) using eq. 3.58;

D & K - from Dimitrijević and Konjević (1980a) using eq. 3.60;

GRIEM $n_{<}$ - using eq. 3.61 with $n = 2$;

GRIEM $n_{<}^*$ - using eq. 3.61 with $n = n^* = 1.864$;

H & B - eqs. 3.39 and 3.41 with $n^* = 1.864$, $n^* = 1.967$;

BLAHA - single value from Blaha (1969).

As is apparent from the graphs, the calculation using a method of the same form as Davis (1974) can be employed for $x \geq 1$ only, as it diverges below threshold. For values of $x > 2$, the suggested Gaunt factor eqs. 3.39 (3.41) is consistent with the tabulated alternatives. Comparing the graphs in fig. 3.6 and fig. 3.7 for the $2s \rightarrow 3p$ transition, where good agreement is obtained near threshold, it would appear as if the classification of transitions into $\Delta n = 0$ and $\Delta n \neq 0$ leads to an overestimate and an underestimate, respectively, of the actual situation of $\Delta n^* \text{ never} = 0$. Correction of the formulae of Griem (1974) by setting n equal to the effective principal quantum number introduces a slight change in \bar{g} only.

Fig. 3.6: Energy dependence of Gaunt factor:
NV 2s \rightarrow 2p transition

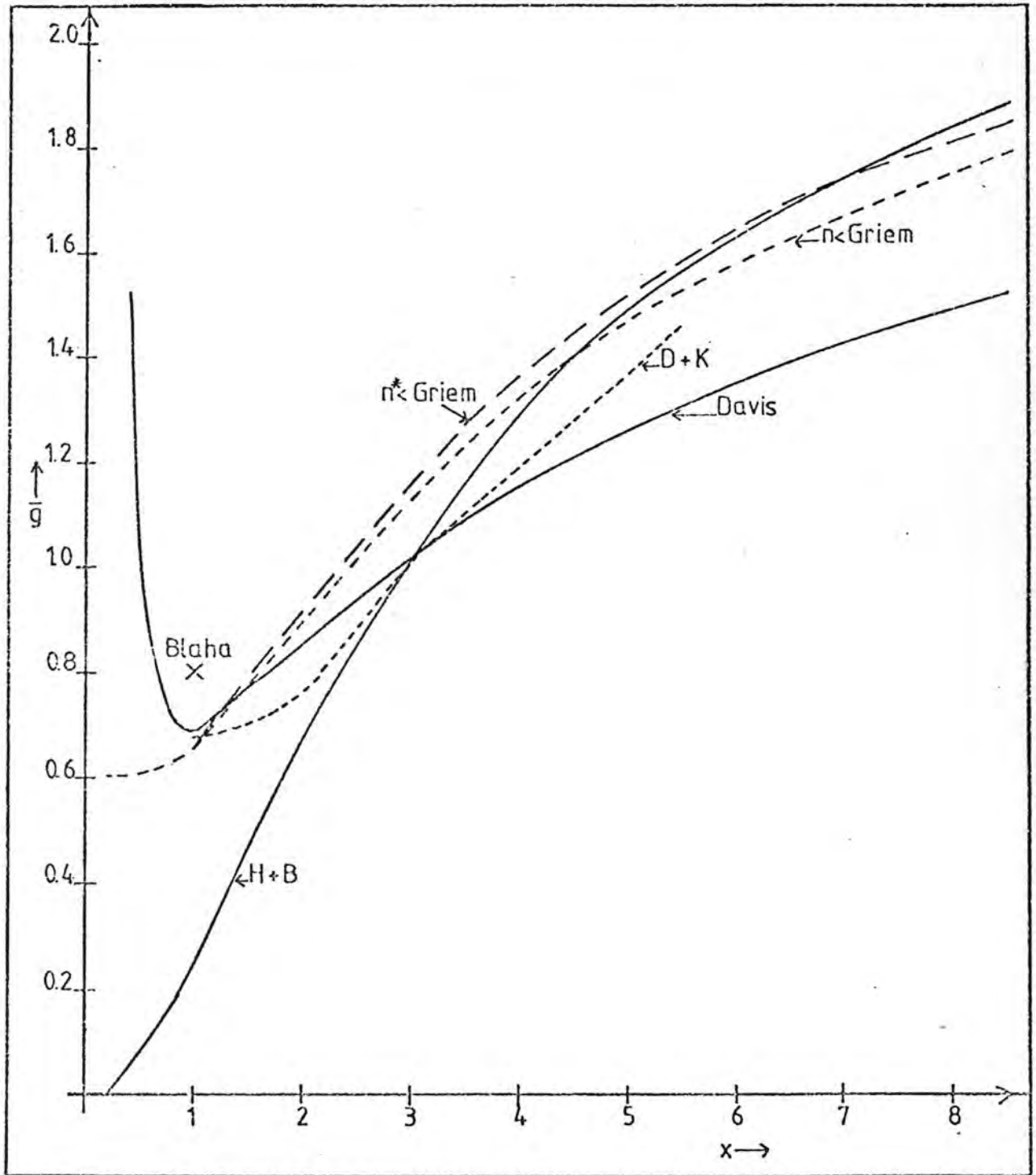
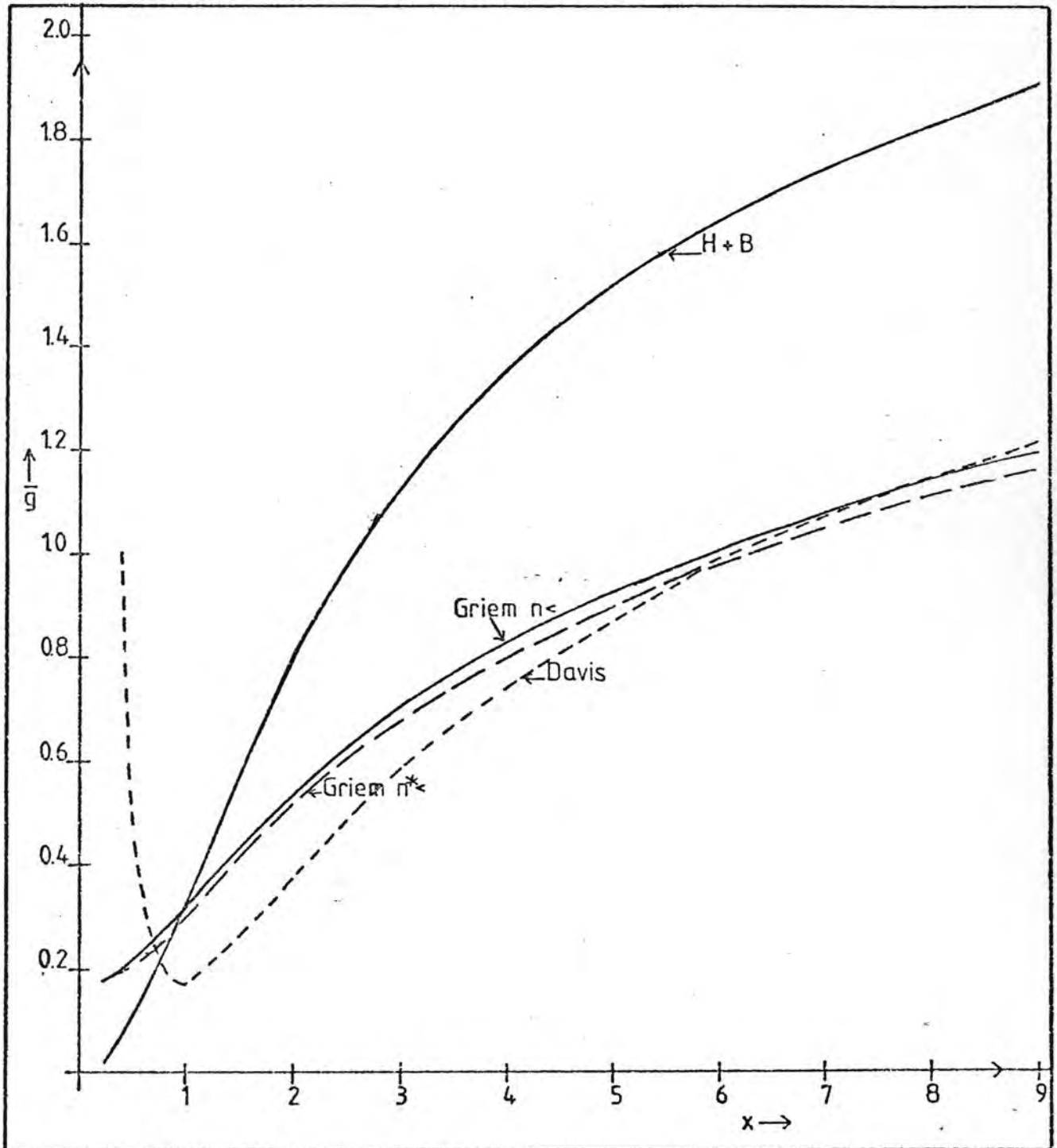


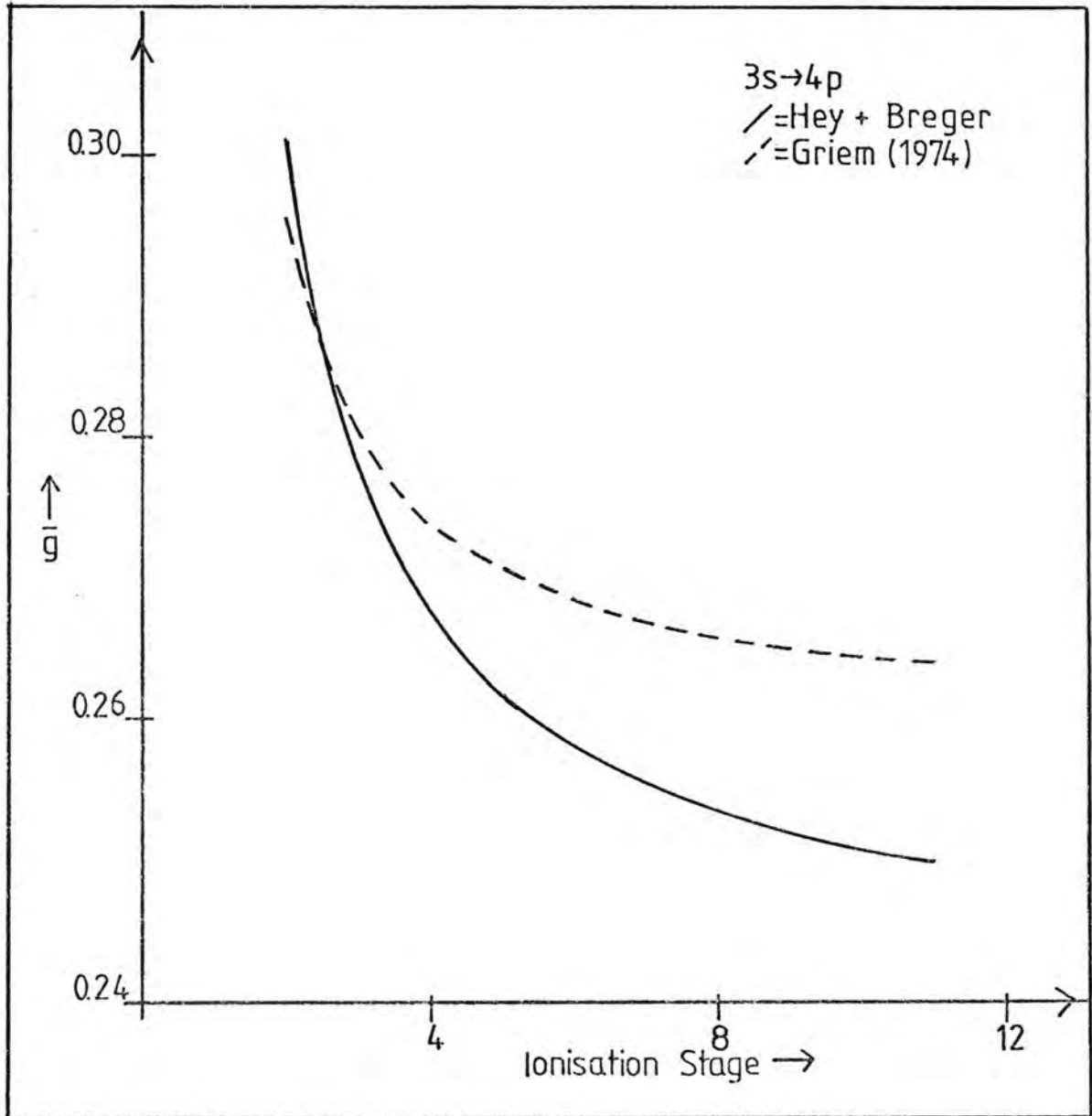
Fig. 3.7: Energy dependence of Gaunt factor:
NV 2s \rightarrow 3p transition



Comparison of the Gaunt factor as predicted by Griem (1974) and Hey and Breger (1980) for various ionisation stages for the ideal transition $3s \rightarrow 4p$ shows a similar decrease with increasing Z (fig. 3.8). Introducing the quantum defect into this comparison, the values by Griem would be lowered (see fig. 3.7) and the resultant increase in Δn^* would lead to an increase in the plotted \bar{g} values by eqs. 3.39 (3.41) thus leading to an even better correlation.

It should, however, be noted that comparisons of the above nature are not strictly valid, as a fundamental difference in the approach to inclusion of the radiator structure complexities makes the derived \bar{g} (eqs. 3.39 (3.41)) incompatible with the other values quoted above. Furthermore, the application of the above Gaunt factor is made after integration over a Maxwellian velocity distribution, thus introducing a further incompatibility between the various Gaunt factors used in the literature. Care needs to be taken also in the compatibility of the definition of the effective Gaunt factor - the expressions derived in this chapter do not include any estimates of strong collision contributions. These higher order terms are included in a separate term to the line width (see Chapter 1, eq. 1.42; also Chapter 4.1). A meaningful comparison is thus limited to the calculated line widths only, which forms the topic of Chapter 5 (see also Hey and Breger: 1980b, c).

Fig. 3.8: Ionisation stage dependence of threshold Gaunt factor: $3s \rightarrow 4p$ transition



CHAPTER 4FURTHER CONTRIBUTIONS TO THE BROADENING4.1 THE STRONG COLLISION TERM

As already pointed out in Chapter 1, this term needs to incorporate the higher orders of both the Dyson series and the multipole expansion of the interaction potential, which are not negligible, but still well separated in time within the impact approximation. This contribution is usually estimated using the Lorentz-Weisskopf formulation (Weisskopf: 1933; Griem, Kolb and Shen: 1959; Griem: 1964, 1974):

$$W_S = 2 \pi N_e \left\{ v \rho_s^2 \right\}_{Av} \quad (4.1)$$

where ρ_s is the strong collision cut-off for the impact parameter of the colliding electron. Since the quantum mechanical cross-section equals twice the classical cross-section in the classical limit (Merzbacher: 1961), the above estimate would become for a quantum mechanical calculation:

$$W_S = N_e \left\{ v \sigma_s \right\}_{Av} \quad (4.2)$$

which is consistent with the result obtained by Baranger (1958a). In order to preserve consistency, the impact parameter ρ_s has to be chosen as the lower limit used for the calculation of the weak inelastic cross-sections (Lewis: 1961). Thereby it is hoped that the resultant matching of the "weak"

and "strong" regimes would reduce any inaccuracies in the exact definition of the border between the two. The parameter ρ_s has thus to be consistent with the parameter ρ_{\min} discussed in Chapter 3. To do this, one needs to note that the parameter ρ_s , as it appears in the expression 4.1, is really a rectilinear path impact parameter and needs to be corrected for hyperbolic orbits (Hey: 1979). To do this, expression 3.30 is again employed:

$$\rho_{\text{str}}^2 = \rho_c^2 + a^2 \quad (3.30)$$

Hence the strong collision term for a particular transition between $|i\rangle$ and $|i'\rangle$ becomes:

$$W_S = 2\pi N_e v \left[\frac{(Z-1)^2 e^4}{m^2 v^4} + \rho_{\min}^2 \right] \quad (4.3)$$

From Chapter 3, the minimum impact parameter for weak collisions was:

$$\begin{aligned} \rho_{\min}^2 &= \rho_1^2 + \rho_2^2 + \rho_3^2 \\ &= \left(\frac{\hbar}{m v} \right)^2 \left[1 + d_{i'i}^2 \left[1 + \frac{m v^2}{2E_H} + \frac{2(Z-1)}{d_{i'i}} \right] - \frac{(Z-1)^2 E_H}{\frac{1}{2} m v^2} \right] \end{aligned} \quad (4.4)$$

for $d_{i',i}^2 \geq \frac{(Z-1)^2 E_H}{\frac{1}{2} m v^2}$; for smaller $d_{i',i}^2$ one has:

$$\rho_{\min}^2 = \left(\frac{\hbar}{m v} \right)^2 \left[1 + d_{i'i}^2 \left[\frac{m v^2}{2E_H} + \frac{2(Z-1)}{d_{i'i}} \right] \right] \quad (4.5)$$

In eq. 4.5, the unitarity condition was excluded from the minimum impact parameter since the relationships (eqs. 3.30, 3.31) used became questionable on physical grounds. For this reason, eq. 4.3 should not be employed in a regime where eq. 4.5 becomes valid, but a different estimate using eqs. 4.2 and 4.5 could be obtained.

However, the strong collision term should now be made representative for all possible types of transitions $|i\rangle \rightarrow |i'\rangle$ that can occur. By the impact approximation (Baranger: 1958a, b, c) only one transition $|i\rangle \rightarrow |i'\rangle$ will be strong at a particular time. Since these collision-induced transitions are here assumed to be independent, an average over all perturbing levels i' needs to be taken. It is sufficient to consider expression 4.4 only, since this is the correct form for most perturbing levels under consideration, and amounts to the validity of:

$$\overline{d_{i'i}^2} \geq \frac{(Z-1)^2 E_H}{\frac{1}{2} m v^2} \quad (4.6)$$

The overbar indicates the following average over n perturbing levels:

$$\overline{d_{i'i}^2} = \frac{1}{n} \sum_{i'} d_{i'i}^2 \quad (4.7)$$

$$\overline{d_{i'i}} = \frac{1}{n} \sum_{i'} d_{i'i} \quad (4.8)$$

With this definition of an average over the set of perturbing levels employed, the strong collision term becomes

In eq. 4.5, the unitarity condition was excluded from the minimum impact parameter since the relationships (eqs. 3.30, 3.31) used became questionable on physical grounds. For this reason, eq. 4.3 should not be employed in a regime where eq. 4.5 becomes valid, but a different estimate using eqs. 4.2 and 4.5 could be obtained.

However, the strong collision term should now be made representative for all possible types of transitions $|i\rangle \rightarrow |i'\rangle$ that can occur. By the impact approximation (Baranger: 1958a, b, c) only one transition $|i\rangle \rightarrow |i'\rangle$ will be strong at a particular time. Since these collision-induced transitions are here assumed to be independent, an average over all perturbing levels i' needs to be taken. It is sufficient to consider expression 4.4 only, since this is the correct form for most perturbing levels under consideration, and amounts to the validity of:

$$\overline{d_{i'i}^2} \geq \frac{(Z-1)^2 E_H}{\frac{1}{2} m v^2} \quad (4.6)$$

The overbar indicates the following average over n perturbing levels:

$$\overline{d_{i'i}^2} = \frac{1}{n} \sum_{i'} d_{i'i}^2 \quad (4.7)$$

$$\overline{d_{i'i}} = \frac{1}{n} \sum_{i'} d_{i'i} \quad (4.8)$$

With this definition of an average over the set of perturbing levels employed, the strong collision term becomes

(in units of angular frequency):

$$W_S = 2\pi N_e v \left(\frac{\hbar}{m v} \right)^2 \left[1 + 2(Z-1) \overline{d_{i'i}^2} + \overline{d_{i'i}^2} \left[1 + \frac{m v^2}{2 E_H} \right] \right] \quad (4.9)$$

In addition, the average over the Maxwellian electron velocity distribution needs to be obtained. Using the standard results:

$$\left. \begin{aligned} \left\langle \frac{1}{v} \right\rangle &= \left(\frac{2m}{\pi kT} \right)^{1/2} \\ \langle v \rangle &= \left(\frac{2m}{\pi kT} \right)^{1/2} \frac{2kT}{m} \\ \langle v^2 \rangle &= \frac{3kT}{m} \end{aligned} \right\} \quad (4.10)$$

one obtains in wavelength units:

$$W_S = \frac{2\alpha \lambda^2 a_0^2}{\sqrt{\pi}} N_e \left(\frac{E_H}{kT} \right)^{1/2} \left[1 + 2(Z-1) \overline{d_{i'i}^2} + \overline{d_{i'i}^2} \left[1 + \frac{kT}{E_H} \right] \right] \quad (4.11)$$

where the constants have been grouped to make comparison with the remaining expression of the width (see eq. 1.42) possible.

The total strong contribution to the line width should now be obtained by adding the above expression for both the upper and lower transition levels. So far, however, no allowance has been made for resultant (elastic) interference terms between the upper and lower states in the dipole approximation. Based on the discussion on p. 97 of Griem (1974), the lower state strong contributions and the elastic interference term have been treated as cancelling, reducing

the strong contributions to an upper state term of the above form (eq. 4.11) only. The good agreement between experimental data and calculated line widths (see Chapter 5) employing this rather crude incorporation of the negative interference term seems to verify this choice, but further work in developing a formally more correct inclusion of the strong contributions to the line width is required (Hey and Breger: 1980b, c).

4.2 VERIFICATION OF $\beta = 1$ IN THE UNITARITY CONDITION

Having obtained the above method of inclusion of any strong collision contribution to the broadening, the validity of the assumption of $\beta = 1$ in the unitarity condition can be discussed. The unitarity condition amounted to limiting the weak collision term to impact parameters such that (eq. 3.31):

$$b^2 > b_3^2 = \left(\frac{\hbar}{m v} \right)^2 \left[\beta^2 d_{i'i}^2 - \frac{(Z-1)^2 E_H}{\frac{1}{2} m v^2} \right] \quad (4.12)$$

where only positive values of b_3^2 were regarded as physically meaningful. From Seaton (1958, 1962a, b) one has for weak collisions:

$$\sigma_{i'i} = \int_0^{\infty} P_{i'i}(\rho) 2\pi \rho d\rho \quad P_{i'i} \leq 1 \quad (4.13)$$

where $P_{i'i}$ is the probability of a collision-induced transition $|i\rangle \rightarrow |i'\rangle$ for particular ρ . This definition of a collision cross-section has been employed throughout. However, including the possibility of strong collisions, one

has a minimum ρ below which weak coupling is not applicable, since the failure of the perturbation theory (Born approximation) leads to an overestimate of the collision cross-section (Seaton: 1962b; Griem: 1968). This requires the modified form for the estimation of collision cross-sections (Seaton: 1962b):

$$\sigma_{i'i} = \sigma_s + \int_{\rho_{\min}}^{\infty} P_{i'i}(\rho) 2\pi \rho d\rho \quad (4.14)$$

where collisions below ρ_{\min} are regarded as strong. In Seaton (1962b), the value of ρ_{\min} is determined by the condition:

$$P_{i'i}(\rho_{\min}) = \frac{1}{2} \quad (4.15)$$

In the formulation of the effective Gaunt factor, Griem (1968) and Sahal-Bréchet (1969b) employ the restriction:

$$\sum_{i'} P_{i'i} \leq \frac{1}{2} \quad (4.16)$$

in contrast to eq. 4.15.

This procedure is different from the development used in this investigation, where a single transition is unitarised, which can be justified on the following grounds.

Consider several weak collisions $i \rightarrow i'$ occurring at one particular time together with one strong collision, which is the impact approximation (Baranger: 1958a, b, c; see Chapter 1). Since for "weak" collisions the transition probabilities

must remain small (this was the requirement for the first order perturbation methods employed in Chapter 1), it is only the strong collisions which need to be restricted by the form of eq. 4.16. Since, however, only one strong collision occurs at one time, unitarisation of a single transition remains sufficient.

It has, however, been suggested (Griem: 1980, private communication) that a treatment of the present theory to higher order in the Dyson series would lead to an expression for the $P_{i',i}$ which involves intermediate states i'' . In such an expression, one would no longer be able to unitarise, as done here, for an individual process $|i\rangle \rightarrow |i'\rangle$, but only for the sum over all such collision-induced transitions. This circumstance would probably prevent the derivation of a \bar{g} , as here, which is continuous in energy (see Chapter 3.3).

In order to decide on the applicability of the unitarity condition, the maximum value of the transition probability needs thus to be examined in more detail.

The transition probability evaluated in the impact parameter approximation becomes (Seaton: 1962b; Griem: 1968):

$$P_{i'i} = \frac{4}{3} \left(\frac{m v}{\hbar(Z-1)} \right)^2 \left| \langle i' | \underline{r} | i \rangle \right|^2 \sin^2 \alpha/2 \quad (4.17)$$

where α = scattering angle as defined in fig. 3.1.

Replacing the above matrix element by quantities as defined earlier (eqs. 1.18, 1.19, 2.27, 3.26, 3.6), one obtains:

$$P_{i'i} = \frac{4}{3} \left[\frac{m v}{\hbar(Z-1)} \right]^2 3 a_0^2 d_{i'i}^2 \frac{1}{\epsilon^2} \quad (4.18)$$

where the maximum value is now obtained from:

$$(P_{i'i})_{\max} = \frac{4}{3} \left[\frac{m v}{\hbar(Z-1)} \right]^2 3 a_0^2 d_{i'i}^2 \frac{1}{\epsilon_{\min}^2} \quad (4.19)$$

and:

$$\epsilon_{\min}^2 = 1 + \frac{m v^2}{2E_H(Z-1)^2} \left[1 + d_{i'i}^2 \left[\beta^2 + \frac{m v^2}{2E_H} + \frac{2(Z-1)}{d_{i'i}} \right] - \frac{(Z-1)^2 2E_H}{m v^2} \right] \quad (4.20)$$

in the regime of a non-trivial unitarity condition:

$$\beta^2 d_{i'i}^2 \gg \frac{(Z-1)^2 E_H}{\frac{1}{2} m v^2} \quad (4.21)$$

Introducing the parameter $X = A v^2 = \frac{\frac{1}{2} m v^2}{E_H}$ one obtains:

$$(P_{i'i})_{\max} = \frac{4 d_{i'i}^2}{1 + d_{i'i}^2 (\beta^2 + A v^2) + 2(Z-1)d_{i'i}} \quad (4.22)$$

Suppose $(P_{i'i})_{\max} \leq \gamma$ is required. This is satisfied for all velocities such that:

$$X \gg X_c = \left(\frac{4}{\gamma} - \beta^2 \right) - \frac{2(Z-1)}{d_{i'i}} - \frac{1}{d_{i'i}^2} \quad (4.23)$$

and thus definitely for all velocities such that:

$$A v^2 > \frac{4}{\gamma} - \beta^2 \quad \left(A = \frac{m}{2E_H} \right) \quad (4.24)$$

From eq. 4.21, the unitarity condition is non-trivial only for values such that:

$$A v^2 \geq \frac{(Z-1)^2}{\beta^2 d_{i,i}^2} \quad (4.25)$$

and criterion 4.23 is thus automatically satisfied for all $d_{i,i}$ such that:

$$X_c \geq \frac{(Z-1)^2}{\beta^2 d_{i,i}^2} \quad (4.26)$$

Using this last condition to define a critical value $d_{i,i}^c$, one has conditions $(P_{i,i})_{\max} \leq \gamma$ and criterion 4.25 satisfied for all $d_{i,i}$ such that:

$$d_{i,i} \leq d_{i,i}^c = \frac{(Z-1) \left(\pm \sqrt{(Z-1)^2 + \left(\frac{4}{\gamma} - \beta^2\right) \left(1 + \frac{(Z-1)^2}{\beta^2}\right)} \right)}{\left(\frac{4}{\gamma} - \beta^2\right)} \quad (4.27)$$

To summarise: the effective Gaunt factor including the unitarity condition will yield $(P_{i,i})_{\max}$ less than a maximum value imposed (γ) for all velocities exceeding a critical value $A v_c^2 (= X_c)$. Since this effective Gaunt factor is applied for a range of velocities which depend upon the dipole matrix $d_{i,i}$, there will be a critical $d_{i,i}^c$ below which the velocity automatically exceeds $A v_c^2$. Substitution of values for the example of $Z = 3$ yields table 4.1 ($A = \frac{m}{2E_H}$).

In the example of an OIII calculation of line widths, it was found that $d_{i,i}$ never exceeds 1.69 in the program. Typical values were about 1.6 and 0.5. This implies that $(P_{i,i})_{\max}$ was less than 0.8 for $\beta = 1$.

$(P_{i,i})_{\max} < 1$ requires $Av^2 > (4-\beta^2)$ true for all $d_{i,i} < d_{i,i}^c$		
$\beta = 1$	$Av^2 > 3$	$d_{i,i} < 2.1$
$\beta = 2$	all velocities	all $d_{i,i}$
$(P_{i,i})_{\max} < 0.5$ requires $Av^2 > (8-\beta^2)$ true for all $d_{i,i} < d_{i,i}^c$		
$\beta = 1$	$Av^2 > 7$	$d_{i,i} < 1.2$
$\beta = 2$	$Av^2 > 4$	$d_{i,i} < 1.4$
$\beta = 2.828$	all velocities	all $d_{i,i}$

Table 4.1: Effect of β on transition probability

In order to test the dependence of the line width calculation on the parameter β , four OIII lines were calculated for $\beta = 1$ and $\beta = 2$. The results are presented in table 4.2. The classification method II refers to the type of below threshold Gaunt factor employed (see Chapter 3.4 and Chapter 5; Hey and Breger: 1980b).

Putting $\beta = 2$ thus decreased the weak inelastic width (W_{IN}) by about 5% of the total line width. The strong contribution is seen to increase drastically to contribute about half of the calculated line width. General agreement with measured line width deteriorates. The large change in the strong contribution arises due to the direct dependence on β^2 :

$$W_S = \frac{2 \alpha \lambda^2 a_0^2}{\sqrt{\pi}} N_e \left(\frac{E_H}{kT} \right)^{1/2} \left[1 + 2(Z-1) \overline{d_{i,i}} + \overline{d_{i,i}^2} \left[\beta^2 + \frac{kT}{E_H} \right] \right] \quad (4.28)$$

(compare with eq. 4.11).

	method II	
	$\beta = 1$	$\beta = 2$
$2p(^2P^0)3s - 3p\ ^3P_1^0 - ^3D_2$		
$\frac{W_m}{W_e}$	0.94	0.76
W_{IN}/W_e	23%	22%
W_s/W_e	38%	50%
$2p(^2P^0)3s - 3p\ ^3P_3^0 - ^3P_2$		
$\frac{W_m}{W_e}$	1.10	0.93
W_{IN}/W_e	26%	20%
W_s/W_e	33%	45%
$2p(^2P^0)3p - 3d\ ^3D_2 - ^3F_3^0$		
$\frac{W_m}{W_e}$	1.02	0.84
W_{IN}/W_e	31%	25%
W_s/W_e	36%	47%
$2p(^2P^0)3p - 3d\ ^3P_2 - ^3D_3^0$		
$\frac{W_m}{W_e}$	0.84	0.70
W_{IN}/W_e	32%	26%
W_s/W_e	34%	46%

Table 4.2: Effect of β on line widths

From the foregoing discussion of the effectiveness of β in the example of OIII, the following conclusion can be made: the unitarisation of the transition probabilities is achieved by setting the factor $\beta = 1$, and an even safer margin can be obtained by putting $\beta = 2$. With the present evaluation of the strong collision term, strong contributions to the line widths are overestimated using $\beta = 2$ in the unitarity condition, as this would lead to the major part of the line width to be due to strong collisions instead of an estimated 30% (Baranger: 1962). Given the small dependence of the weak inelastic contribution on the application of $\beta \neq 1$ as well as the predominance of the other cut-off impact parameters over the unitarity condition in most practical calculations, it thus suffices to use $\beta = 1$ consistently in both the estimates of weak and strong contributions. As already pointed out, this consistency in demarcation of the weak and strong regimes (Lewis: 1961) is hoped to reduce the error made by overestimating the one in favour of the other. As has been shown already in table 4.2, the present demarcation can be justified on grounds of the excellent agreement obtained for comparisons with experimental data (Hey and Breger: 1980a, b, c; see also Chapter 5).

4.3 THE ION PERTURBER CONTRIBUTION

This additional contribution to the line width due to the perturbation of the radiator ion by surrounding ions in the plasma can be regarded as small compared with the dominating electron impact broadening (Griem: 1964, 1974).

Usually, values of the order of a few percent (Griem: 1962a; Platina et al.: 1977; Hey: 1977c) up to the rather large value (12%) obtained by Fleurier et al. (1977). Unlike for the electron perturbers, second order dipole and quadrupole interactions have to be considered in either the quasi-static or impact approximation (Griem: 1974; Sahal-Brechot: 1969b). Furthermore, at large densities, the importance of ion-ion correlations and Debye shielding by electrons are found to be significant. However, since this mechanism of line broadening is far less significant than the previously discussed mechanisms of electron broadening, crude estimates of ion broadening suffice (Griem: 1974) for the ions considered in this investigation.

For the quadrupole interactions, the problem of characterising collisions as either quasi-static or within the impact approximation regime is much simplified by the fact that both types of calculations yield very similar results (Griem: 1974, pp. 95, 98). Adopting Griem's (1974, p. 98) estimate of this quadrupole contribution, one obtains in units of angular frequency (FWHM):

$$W_i^q = 4\pi N_p \left[(n_i^{*2} - n_f^{*2})^2 \frac{\hbar a_0}{Z^2 m} \right] Z_p \quad (4.29)$$

Assumption of the condition of quasi-neutrality, i.e.:

$$N_e = \sum_p N_p Z_p \quad (4.30)$$

allows the reduction of eq. 4.29 for all types of ion

perturbers by summation, thus yielding in wavelength units:

$$W_i^q = \frac{2 \alpha \lambda^2 a_0^2}{Z^2} N_e (n_i^{*2} - n_f^{*2})^2 \quad (4.31)$$

where the superscript q denotes the quadrupole nature of this estimate.

For second order dipole collisions, simple addition of a broadening contribution as for the quadrupole terms is not possible, since the quadratic Stark broadening depends on the magnetic quantum number "to the extent of being zero on the average over corresponding orientations" (Griem: 1974, p. 96). Furthermore, the classification of these collisions as quasi-static or within the impact regime does not yield similar results - a choice of either has thus to be made. Defining the quasi-static approximation as the inverse of the impact approximation (eq. 1.3) and thus:

$$W\tau > 1 \quad (4.32)$$

one obtains, according to Griem (1974), the following criterion for validity of the quasi-static regime:

$$\frac{kT}{E_H} < 6 \left(\frac{m_p}{m} \right)^{1/2} \frac{n_i^{*4}}{Z^2} \frac{N_e}{N_p^{1/3}} a_0^2 \quad (4.33)$$

where the typical impact parameter has been taken as the average interparticle distance $N_p^{-1/3}$, the electron and ion temperature as equal, and thus the kinetic energy of both equivalent to about $\frac{3}{2} kT$. Evaluating this criterion for

typical plasma parameters under consideration (Hey and Breger: 1980a, b, c) shows that the quasi-static condition is marginally satisfied for ion perturbers, and not at all for proton perturbers. This is of little consequence for the estimation of the quadrupole contribution, as these are very similar in either approximation, but for the second order dipole approximation this leads to difficulties. Adopting, however, the procedure used by Griem (1974), one can regard these quadratic contributions as much smaller than the quadrupole contributions. Since it is found that:

$$W_i^q \ll W_e$$

the electron broadening completely predominates and the evaluation of W_i^q by the present method (Griem: 1974) is a valid estimation of the ion contributions to the spectral line width for isolated lines.

4.4 THE DISENTANGLEMENT PARAMETER

In all of the foregoing development of the line broadening calculation, the impact approximation was assumed valid for electron perturbers. As discussed in Chapter 1, this vital approximation is equivalent to assuming strong collisions occurring between the electrons and the radiator ion as separated in time, thus leading to disentanglement of the Dyson series (Baranger: 1958a, b, c). As discussed by Baranger, this formal statement of the impact approximation is equivalent to the formulation of the impact approximation as:

$$W\tau \ll 1 \quad (4.34)$$

It remains thus to be shown how well this disentanglement of strong collisions in time is really satisfied in the calculations performed. Estimating a collision time as:

$$\tau = \frac{2\rho}{v} \quad (4.35)$$

one thus has the requirement that:

$$\tau_{\text{strong}}(v) \lesssim \frac{2\rho_{\text{min}}(v)}{v} \quad (4.36)$$

The mean rate at which close collisions occur is given by:

$$R^c = \int_0^{\infty} N_e f(v) \pi \rho_{\text{min}}^2 v \, dv \quad (4.37)$$

where $f(v)$ is the Maxwellian velocity distribution:

$$f(v) = 4\pi \left(\frac{m}{2\pi kT} \right)^{3/2} v^2 \exp\left(-\frac{mv^2}{2kT}\right) \quad (4.38)$$

The mean collision time for strong collisions is:

$$\bar{\tau}_s = \int_0^{\infty} \frac{2\rho_{\text{min}}}{v} f(v) \, dv \quad (4.39)$$

and the impact approximation can thus be stated as:

$$\tau_s \ll \frac{1}{R^c} \quad (4.40)$$

Collecting eqs. 4.37, 4.38, 4.39, this statement of disentanglement becomes:

$$8\pi \left(\frac{m}{2\pi kT} \right)^{3/2} \int_0^{\infty} v \rho_{\min} \exp\left(-\frac{mv^2}{2kT}\right) dv \ll \left[4\pi^2 \left(\frac{m}{2\pi kT} \right)^{3/2} \right]^{-1} \frac{1}{N_e} \left[\int_0^{\infty} v^3 \exp\left(-\frac{mv^2}{2kT}\right) \rho_{\min}^2 dv \right]^{-1} \quad (4.41)$$

Defining the parameter:

$$z = \frac{mv^2}{2kT} \quad (4.42)$$

criterion 4.41 can be written as:

$$8N_e \int_0^{\infty} \rho_{\min} \exp(-z) dz \int_0^{\infty} \rho_{\min}^2 z \exp(-z) dz \ll 1 \quad (4.43)$$

where the LHS is defined as a "disentanglement parameter".

From the discussion in Chapter 3, ρ_{\min} has two forms:

$$\rho_{\min}^2 = \frac{\hbar^2}{m^2 v^2} \left[1 + d_{i'i}^2 \left[1 + \frac{\frac{1}{2}mv^2}{E_H} + \frac{2(Z-1)}{d_{i'i}} \right] - \frac{(Z-1)^2 E_H}{\frac{1}{2}mv^2} \right] \quad (4.44)$$

and for:

$$d_{i'i}^2 - \frac{(Z-1)^2 E_H}{\frac{1}{2}mv^2} < 0 \quad (4.45)$$

$$\rho_{\min}^2 = \frac{\hbar^2}{m^2 v^2} \left[1 + d_{i'i}^2 \left[\frac{\frac{1}{2}mv^2}{E_H} + \frac{2(Z-1)}{d_{i'i}} \right] \right] \quad (4.46)$$

Rewriting eqs. 4.44, 4.46 in terms of the parameter z as defined by eq. 4.42, one obtains:

$$\rho_{\min}^2 = a + \frac{b}{z} - \frac{c}{z^2} \quad (4.47)$$

and:

$$\rho_{\min}^2 = a + \frac{e}{z} \quad (4.48)$$

respectively, where:

$$\left. \begin{aligned} a &= a_0^2 d_{ii}^2 \\ b &= \frac{E_H a_0^2}{kT} \left[1 + d_{ii}^2 + 2(Z-1)d_{ii} \right] \\ c &= \frac{(Z-1)^2 E_H^2 a_0^2}{(kT)^2} \\ e &= b - \frac{c}{z_d} \end{aligned} \right\} \quad (4.49)$$

and z_d is defined by eq. 4.45

$$z_d = \frac{(Z-1)^2 E_H}{d_{ii}^2 kT}$$

Evaluation of the disentanglement parameter (eq. 4.43) thus requires the integrals:

$$\int_0^{\infty} \rho_{\min} \exp(-z) dz = \int_0^{z_d} \left(a + \frac{e}{z} \right)^{1/2} \exp(-z) dz + \int_{z_d}^{\infty} \left(a + \frac{b}{z} - \frac{c}{z^2} \right)^{1/2} \exp(-z) dz \quad (4.50)$$

and:

$$\begin{aligned}
\int_0^{\infty} \rho_{\min}^2 z \exp(-z) dz &= \int_0^{z_d} (az + e) \exp(-z) dz \\
&\quad + \int_{z_d}^{\infty} \left(az + b - \frac{c}{z} \right) \exp(-z) dz \\
&= a_0^2 \left[d_{i'i}^2 + \frac{E_H}{kT} \left[1 + 2(Z-1)d_{i'i} \right] \right] \\
&\quad + a_0^2 \frac{E_H}{kT} d_{i'i}^2 \exp(-z_d) - (Z-1)^2 a_0^2 \frac{E_H^2}{(kT)^2} \int_{z_d}^{\infty} \frac{1}{z} \exp(-z) dz \quad (4.51)
\end{aligned}$$

Evaluation of eqs. 4.50 and 4.51 is, however, not readily possible by analytical means, and evaluation of the disentanglement parameter needs to be done by numerical means for particular line width calculations (see Chapter 5). It was found by crude estimation of the above integrals as well as by application to particular ions that the disentanglement parameter is usually of the order of 10^{-5} and thus well satisfied.

In the high temperature limit, however, the following simplifications occur:

$$\begin{aligned}
z_d &\rightarrow 0 \\
b, c \text{ and } e &\rightarrow 0
\end{aligned}$$

and criterion 4.43 collapses to:

$$8 N_e a_0^3 d_{i'i}^3 \ll 1 \quad (4.52)$$

Regarding $a_0^3 d_{i'i}^3$ as the atomic dimension of the radiator, only a very small amount of perturbers is allowed within this

radiator volume for the disentanglement to remain valid. It thus confirms the description of the impact approximation as a low density or high velocity approximation by Baranger (1958a, p. 482).

4.5 THE COLLISION TIME PARAMETER

In Chapter 1 the impact approximation was enforced by considering a regime for which (Baranger: 1958a, b, c):

$$W\tau \ll 1$$

Having checked how well this criterion ensures disentanglement between strong collisions, it is of interest to know how well an average collision which occurs in the line width calculation obeys this criterion. In particular, the calculation allows collision times with:

$$\tau_{\max} = \frac{2 \rho_{\max}}{v}$$

to be included. The average of such collision times would be given by:

$$\tau_{\max} = 2 \int_0^{\infty} \frac{\rho_{\max}}{v} f(v) dv \quad (4.53)$$

where $f(v)$ is the Maxwellian velocity distribution (eq. 4.38).

Employing again parameter:

$$z = \frac{m v^2}{2kT}$$

one obtains:

$$\bar{\tau}_{\max} = \frac{4}{\sqrt{2\pi}} \left(\frac{m}{kT} \right)^{1/2} \int_0^{\infty} \rho_{\max} \exp(-z) dz \quad (4.54)$$

For comparison with the line width in wavelength units, it is convenient to obtain $\bar{\tau}_{\max}$ in units of cm^{-1} and thus:

$$\bar{\tau}_{\max} = 8\pi \left(\frac{m}{2\pi kT} \right)^{1/2} \frac{c}{\lambda^2} \int_0^{\infty} \rho_{\max} \exp(-z) dz \quad (4.55)$$

Now, from Chapter 3.1:

$$\rho_{\max} = \frac{\hbar\nu}{\Delta E_{i'i}} \phi^2 \quad (4.56)$$

where ϕ is the solution of:

$$\phi^3 - \phi - \frac{2(Z-1)e^2 \Delta E}{\hbar m v^3} = 0 \quad (4.57)$$

or, in terms of parameter z :

$$\rho_{\max} = \frac{\hbar}{\Delta E} \left(\frac{2kT}{m} \right)^{1/2} \phi^2 \sqrt{z} \quad (4.58)$$

Substitution thus yields with λ , ΔE in (inverse) wavelength units:

$$\bar{\tau}_{\max} = \frac{4}{\sqrt{\pi}} \frac{1}{\lambda^2} \frac{1}{\Delta E} \int_0^{\infty} \phi^2 \sqrt{z} \exp(-z) dz \quad (4.59)$$

Evaluation of this quantity by numerical methods for particular line width calculations (see Chapter 5) yields

typically:

$$W\bar{\tau}_{\max} \sim 10^{-3} \quad (4.60)$$

and the impact approximation is thus well satisfied.

CHAPTER 5COMPARISON WITH EXPERIMENTS5.1 SnII - RADIATOR STRUCTURE COMPLEXITIES AND STARK WIDTHS

This ion has been chosen for further investigation as it shows similar deviations from an ideal LS coupling model for a singly ionised ion as SiIII, for which several problems arose in the calculation of the required oscillator strengths owing to considerable configuration interaction (Hey: 1977c; Hey and Breger: 1980a). From recent experiments (Wujek and Musielok: 1976; Miller et al.: 1979) it is apparent that configuration interaction gives rise to several strong lines from "forbidden two-electron" transitions in the observed spectrum. Application of the semi-empirical calculations of Griem (1968) to some measured line widths were found to lead to satisfactory results for the widths of those lines allowed by LS-coupling, whereas no theoretical estimates could be advanced for the two-electron transitions (Miller et al.: 1979).

In the latter investigation, the following lines were identified:

$$\begin{array}{lll}
 5s \ 5p^2 \ ^2D_{5/2} - 4f \ ^2F_{5/2}^0 & \lambda = & 3352.0 \text{ \AA} \\
 5s \ 5p^2 \ ^2D_{3/2} - 4f \ ^2F_{3/2}^0 & \lambda = & 3283.1 \text{ \AA} \\
 5s \ 5p^2 \ ^4P_{5/2} - 6p \ ^2P_{3/2}^0 & \lambda = & 4816.3 \text{ \AA}
 \end{array}$$

indicating the perturbation of the $5s \ 5p^2$ configuration by

some other member of the energy spectrum. Examination of the quantum defect $\Delta = n - n^*$ (Condon and Shortley: 1935) of the level structure (Moore: 1958) tabulated in table 5.1 shows an extremely regular structure (and thus no appreciable configuration interaction), with the exception of the $5d \ ^2D$ term, which is considerably shifted upwards by an amount of about 3000 cm^{-1} due to interaction with the neighbouring

config.	Δ	config.	Δ	config.	Δ	config.	Δ	config.	Δ
						4f $\ ^2F^0$	0.091		
		5p $\ ^2P^0$	3.048	5d $\ ^2D$	1.918	5f $\ ^2F^0$	0.110		
6s $\ ^2S$	3.320	6p $\ ^2P^0$	2.908	6d $\ ^2D$	2.020	6f $\ ^2F^0$	0.109	6g $\ ^2G$	0.022
7s $\ ^2S$	3.281	7p $\ ^2P^0$	2.881	7d $\ ^2D$	2.020			7g $\ ^2G$	0.023
8s $\ ^2S$	3.269	8p $\ ^2P^0$	2.872	8d $\ ^2D$	2.018			8g $\ ^2G$	0.023
9s $\ ^2S$	3.263	9p $\ ^2P^0$	2.861	9d $\ ^2D$	2.016			9g $\ ^2G$	0.023
10s $\ ^2S$	3.260			10d $\ ^2D$	2.013			10g $\ ^2G$	0.023
11s $\ ^2S$	3.257	.						11g $\ ^2G$	0.023

Table 5.1: Quantum defects in SnII structure

$5p^2 \ ^2D$ term (see also Chapter 2). The regularity of the remaining structure is apparent from the following general trends in the quantum defects as listed in table 5.1:

$$\Delta(np \ ^2P^0) = 2.88 - 0.01 (n-7) \quad (n > 6)$$

$$\Delta(nd \ ^2D) = 2.02 \quad (n > 5)$$

$$\Delta(nf \ ^2F^0) = 0.11 \quad (n > 4)$$

$$\Delta(ng \ ^2G) = 0.023 \quad (n > 5)$$

Except for the $5d \ ^2D$ term, pure LS coupling is thus expected to be applicable. This is further substantiated if

one considers the spin-orbit splitting for one-electron atoms (Condon and Shortley: 1935, p. 123):

$$\Delta E_{SO} \propto \frac{1}{n^3 l(l+1)(2l+1)} \quad (l \neq 0)$$

For a many-electron atom with a single electron in the outer orbital, a relation of this type may be expected (Sobel'man: 1972, p. 166), provided the principal quantum number n above is replaced by the effective principal quantum number n^* for the particular term. The proportionality factor is expected to be a constant within a particular series. Tabulating the proportionality constant:

$$C_{SO} = \Delta E_{SO} n^{*3} l(l+1)(2l+1) \times 10^{-5}$$

for the $np \ ^2P^0$ series and $nd \ ^2D$ series (table 5.2) indicates again the general applicability of LS coupling except for the perturbed $5d \ ^2D$ term, thus confirming the configuration

config.	C_{SO}	config.	C_{SO}
5p $^2P^0$	1.9	5d 2D	5.6
6p $^2P^0$	1.6	6d 2D	2.1
7p $^2P^0$	1.5	7d 2D	2.0
8p $^2P^0$	1.5	8d 2D	2.0
		9d 2D	1.9
		10d 2D	1.8

Table 5.2: Spin orbit splitting factor for the $p \ ^2P^0$ and $d \ ^2D$ series

interaction hypothesis.

The necessary corrections thus applicable to the line broadening calculation for the inclusion of the $5d \ ^2D$ and $5p^2 \ ^2D$ terms into the LS coupling calculations have been discussed in Chapter 2.4. One defines:

$$\Upsilon_{\underline{I}}(^2D) = \alpha_{11} \Upsilon(d) + \alpha_{12} \Upsilon(p^2)$$

$$\Upsilon_{\underline{II}}(^2D) = \alpha_{21} \Upsilon(d) + \alpha_{22} \Upsilon(p^2)$$

to correspond to the tabulated energy levels (Moore: 1958) and introduces the correction factor $|\alpha_{ij}|^2$ into the calculation of the atomic oscillator strengths. Since measured transition probabilities for such affected transitions are available (Miller et al.: 1979), it was hoped that the correction factors $|\alpha_{ij}|^2$ would be obtainable from:

$$(A_{lu})_m = (A_{lu})_c |\alpha_{ij}|^2$$

where the subscripts m and c denote measured and calculated quantities respectively. Table 5.3 lists the results obtained from such a comparison.

Representation of the data in table 5.3 graphically (fig. 5.1) shows that the large spread of possible $|\alpha_{ij}|^2$, due to large experimental errors, makes a definite assignment of value for $|\alpha_{ij}|^2$ impossible.

Rather than deciding on the values for $|\alpha_{ij}|^2$ from the measured transition probabilities, several "mixtures" between

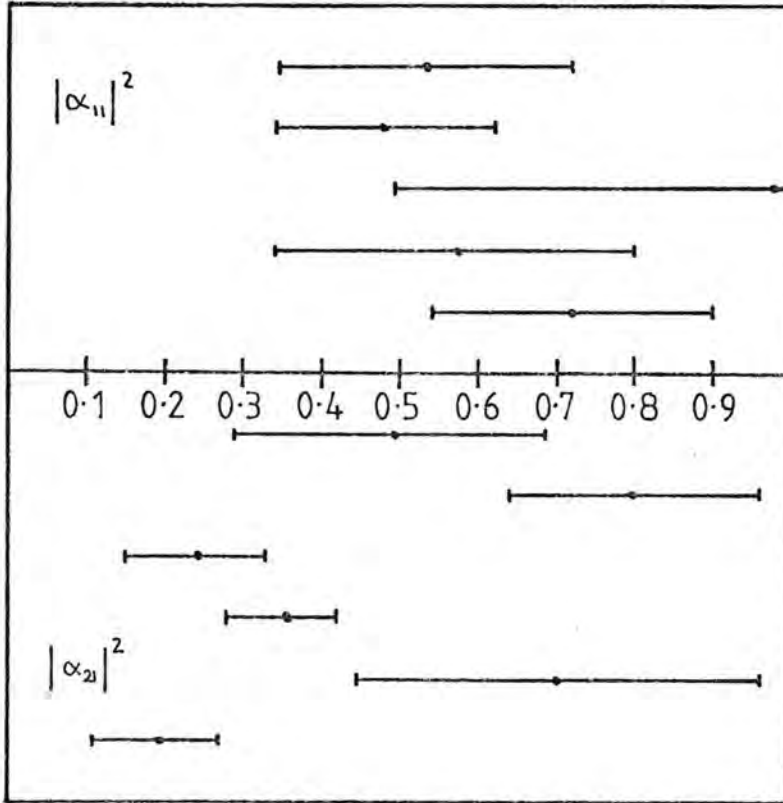
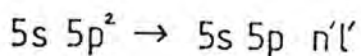


Fig. 5.1: Spread in coupling constants

light on structural details of complex atoms, as suggested by Hey (1978). Indeed, the results obtained strongly indicate a 50% mixing of the $\mathcal{Y}(d)$ and $\mathcal{Y}(p^2)$ wavefunctions and thus values of $|\alpha_{11}|^2 = |\alpha_{22}|^2 = 0.5$ (see table 5.4 and fig. 5.2).

A further complication that needs to be incorporated in the correct calculation of atomic oscillation strengths is the correction for equivalent electrons, when considering collision-induced transitions of the type:



Applying the procedure outlined in Chapter 2.2 leads to the following relation for the oscillator strength (Sobel'man: 1972):

$$f(5s 5p^2 \rightarrow 5s 5p n'd) = 2f(5p \rightarrow n'd)$$

and:

$$f(5s 5p^2 \rightarrow 5s 5p n's) = 2f(5p \rightarrow n's)$$

For transitions to the ground configuration one obtains from eq. 2.22:

$$\begin{aligned} f(5s 5p^2 \rightarrow 5s^2 5p) &= \left[\frac{4l' + 3 - 2}{2l + 1} \right] f(5p \rightarrow 5s) \\ &= f(5p \rightarrow 5s) \end{aligned}$$

Attention needs to be drawn now to the fact that a slightly different method for the calculation of line widths to eq. 1.42, with oscillator strengths given by eq. 2.8 and averaged Gaunt factors from eqs. 3.39 and 3.41, was employed here. The exact details of this less refined method are contained in Part B, method MTD1, and have been published (Hey and Breger: 1980a; see also Appendix I). At the time, the application of a general threshold Gaunt factor of 0.2 and an effective Gaunt factor \bar{g}_{Sn} without curvature correction, evaluated at mean kinetic energy $\frac{1}{2} m \bar{v}^2 = \frac{3}{2} k T$, was found to be adequate for the calculations for this ion. Eq. 1.42 is

thus calculated using:

$$W_e = \frac{\alpha \lambda^2 a_0^2}{\sqrt{\pi}} N_e \left(\frac{E_H}{kT} \right)^{1/2} \left[\sum_{i'} \frac{\langle \Omega(i,i') \rangle}{2J_i + 1} + \sum_{f'} \frac{\langle \Omega(f,f') \rangle}{2J_f + 1} \right] + W_S \quad (5.1)$$

where:

$$\begin{aligned} \sum_{i'} \frac{\langle \Omega(i,i') \rangle}{2J_i + 1} &= \frac{8\pi}{3\sqrt{3}} \left[\left\langle i \left| \frac{\Gamma^2}{a_0^2} \right| i \right\rangle \bar{g}_{th} \right. \\ &\quad \left. + \sum_{i'} \left(\bar{g}(i,i') \Big|_{\frac{3}{2}kT} - \bar{g}_{th} \right) \frac{1}{2J_i + 1} \frac{S(J,J')}{a_0^2 e^2} \right] \quad (5.2) \end{aligned}$$

and:

$$\bar{g}(i,i') \Big|_{\frac{3}{2}kT} \equiv \bar{g}_{Sn} \text{ evaluated @ } x = \sqrt{\frac{3kT}{2\Delta E_{i'i}}} \quad (\text{see eq. 3.42}) \quad (5.3)$$

$$\left\langle i \left| \frac{\Gamma^2}{a_0^2} \right| i \right\rangle = \frac{n^{*2}}{2Z^2} (5n^{*2} + 1 - 3l(l+1)) \quad (5.4)$$

The strong collision term used is calculated analogously to the contribution derived in Chapter 4.1 with no corrections for hyperbolic curvature of the perturber orbit applied (see eq. 4.11), namely:

$$W_S = \frac{2\alpha \lambda^2 a_0^2}{\sqrt{\pi}} N_e \left(\frac{E_H}{kT} \right)^{1/2} \left[1 + \bar{d}_{i'i}^2 \left[1 + \frac{kT}{E_H} \right] \right] \quad (5.5)$$

and:

$$\bar{d}_{i'i}^2 = \frac{n_i^{*4}}{Z^2} \quad (\text{Griem: 1974}) \quad (5.6)$$

In order to incorporate the equivalent electron correction

derived above for transitions to the ground state correctly in expression 5.2, one needs to sum eq. 2.27 to obtain:

$$\begin{aligned}
 & \sum_{n'l'} \frac{E_H}{\Delta E_{i'i}} f_{i'i} \\
 &= \frac{1}{3} N \frac{l}{2l+1} \left(R_{n'l'}^{nl} \right)^2 \\
 &= \frac{1}{3} \left[N \frac{l+1}{2l+1} \sum_{n'} \left(R_{n'd}^{5p} \right)^2 + \frac{N l}{2l+1} \sum_{n' \neq 5} \left(R_{n's}^{5p} \right)^2 + \frac{l}{2l+1} \left(R_{5p}^{5s} \right)^2 \right] \\
 &= \frac{1}{3} \left[N \left\langle 5p \left| \frac{r^2}{a_0^2} \right| 5p \right\rangle - \frac{(N-1)l}{2l+1} \left(R_{5p}^{5s} \right)^2 \right] \\
 &= \frac{2}{3} \left[\left\langle 5p \left| \frac{r^2}{a_0^2} \right| 5p \right\rangle - \frac{1}{6} \left(R_{5p}^{5s} \right)^2 \right]
 \end{aligned}$$

Evaluation of the negative term inside the brackets reveals that an error of less than 10% is made by neglecting this term and thus sufficient correction for equivalent electrons is made by multiplying eq. 5.2 by 2, considering the uncertainties in the individual matrix elements involved.

Application of this formalism by Hey (1979, private communication) to the measurements performed by Miller *et al.* (1979) as well as two additional multiplet members of $5s^2 6s \ ^2S - 5s^2 6p \ ^2P^0$ and $5s 5p^2 \ ^2D - 5s^2 4f \ ^2F^0$ leads to the results tabulated in table 5.4. The calculations were performed at 11000°K and a normalised electron density of 10^{17} cm^{-3} . The effect of the experimental uncertainty in temperature has been investigated and is plotted for the $6s \ ^2S_{1/2} - 6p \ ^2P_{1/2}^0$ line in fig. 5.2. The widths (FWHM) are all given in units of Å and the unshifted wavelengths are given

Table 5.4: Comparison between measured and calculated widths: SnII

Key:

- W_m - measured FWHM
- W_e - calculated FWHM
- η - percentage purity of interacting configurations
- $\frac{W_s}{W_e}$ - per unit strong collision contribution
- $\frac{W_i}{W_e}$ - per unit ion perturber contribution (neglected)
- $\frac{W_e}{W_m}$ - per unit agreement

Transition Array	Designation	Unshifted λ (Air)	W_m (Å)	$\frac{W_e(\text{Å})}{\eta = 100\%}$	$\frac{W_e(\text{Å})}{\eta = 50\%}$	$\eta = 50\%$		
						$\frac{W_e}{W_m}$	$\frac{W_s}{W_e}$	$\frac{W_i}{W_e}$
5s ² 6s - 5s ² 6p	² S _{1/2} - ² P _{1/2} ^o	6843.49	4.2 ± 1.7	6.21	4.44	1.06	0.23	0.005
	² S _{1/2} - ² P _{3/2} ^o	6453.41	-	4.32	3.38	-	0.22	0.007
5s ² 6p - 5s ² 6d	² P _{3/2} ^o - ² D _{5/2}	5561.37	5.1 ± 0.7	6.11	5.41	1.06	0.34	0.023
	² P _{1/2} ^o - ² D _{3/2}	5332.48	5.3 ± 0.7	6.66	5.58	1.05	0.30	0.021
5s ² 5d - 5s ² 4f	² D _{5/2} - ² F _{7/2} ^o	5799.39	4.2 ± 1.2	4.95	4.32	1.03	0.43	0.026
	² D _{3/2} - ² F _{5/2} ^o	5589.29	3.8 ± 1.0	5.02	4.27	1.12	0.40	0.026
5s ² 6p - 5s ² 7s	² P _{1/2} ^o - ² S _{1/2}	6761.42	5.5 ± 1.5	8.86	7.13	1.30	0.29	0.013
5s ² 6p - 5s ² 7d	² P _{3/2} ^o - ² D _{5/2}	3575.27	3.0 ± 1.0	5.64	5.36	1.79	0.35	0.056
5s 5p ² - 5s ² 4f	² D _{3/2} - ² F _{5/2} ^o	3283.32	2.3 ± 0.8	1.19	1.21	0.53	0.49	0.056
	² D _{5/2} - ² F _{7/2} ^o	3352.20	2.5 ± 0.8	1.25	1.26	0.50	0.49	0.055
	² D _{5/2} - ² F _{5/2} ^o	3351.53	-	1.25	1.26	-	0.49	0.055
5s 5p ² - 5s ² 6p	⁴ P _{5/2} - ² P _{3/2} ^o	4618.22	1.6 ± 0.5	1.97	1.48	0.93	0.32	0.055

for air (C. de Witt Coleman et al.: 1960). The parameter η denotes the degree of configuration mixing employed:

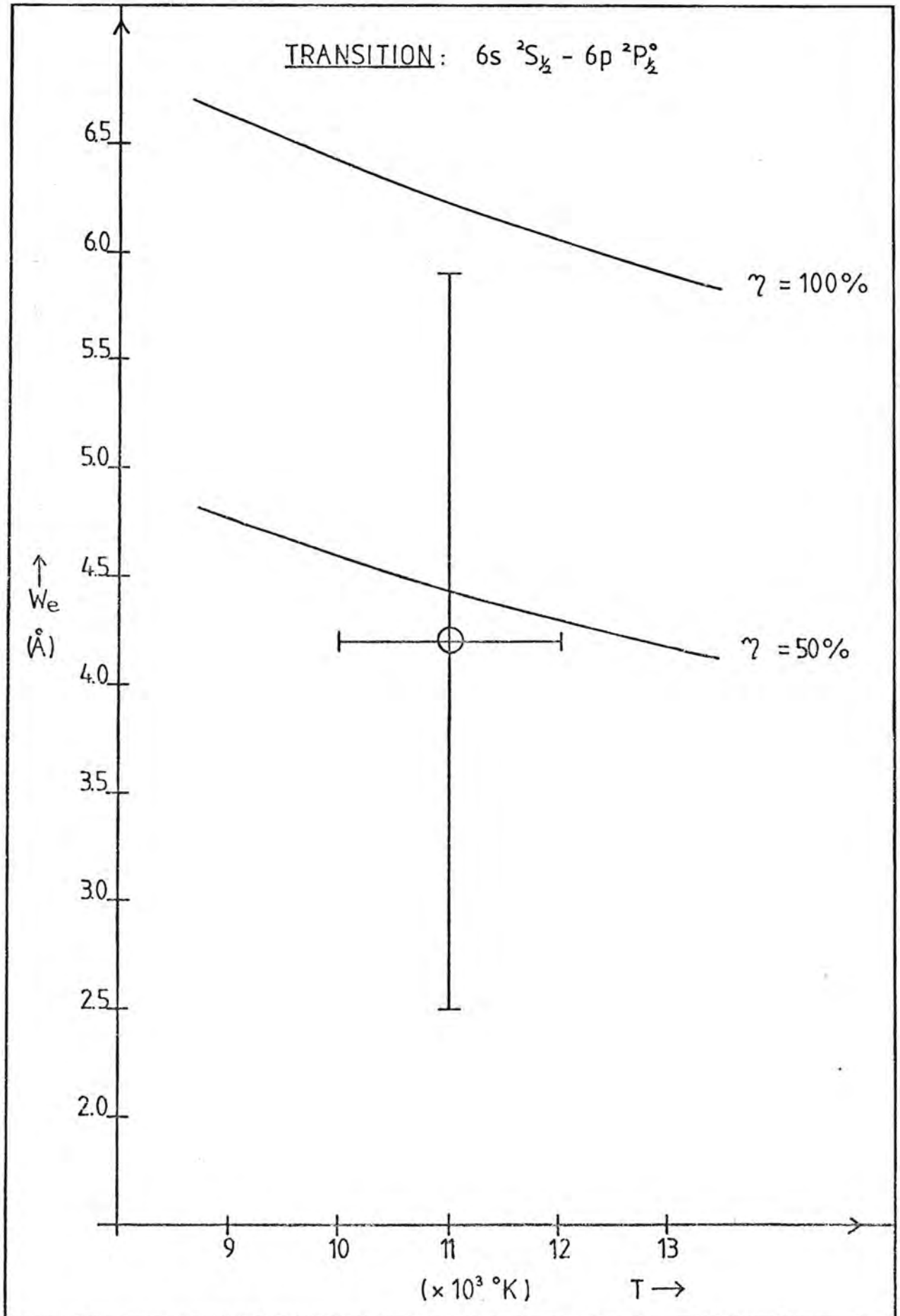
$\eta = 100 |\alpha_{11}|^2 = 100 |\alpha_{22}|^2$, thus showing the effect of no configuration mixing (pure configurations) and an extreme of 50% mixing, for which best agreement is obtained between measured and calculated line widths (see also fig. 5.2).

The percentage strong contribution to the line width (W_s/W_e) is given and is found to vary from about 20% up to ~50% for one multiplet. The estimated ion broadening (percentage W_i/W_e) tabulated has been calculated using the quadrupole estimate (eq. 4.32) and has been neglected in the total line width W_e . Since this neglect causes an error less than 10% (at most 5.6%), this procedure of assuming dominant electron impact broadening is well satisfied.

General agreement between calculated and measured line widths is good: for some multiplets it is even within 10% which is well within the estimated experimental uncertainties obtained by Miller et al. (1979) of over 12%. The worst agreement obtained must be seen in the context of the associated experimental uncertainties (table 5.5):

transition array	unshifted $\lambda(\text{\AA})$	$\frac{W_e}{W_m}$	exp. uncertainty
5s ² 6p - 5s ² 7s	6761.42	1.30	27%
5s ² 6p - 5s ² 7d	3575.27	1.79	33%
5s 5p ² - 5s ² 4f	3283.32	0.53	35%
	3352.20	0.50	32%

Table 5.5: Experimental uncertainties and agreement of theory with experiment

Fig. 5.2: Effect of configuration interaction

Apart from the criticism that the method employed neglects curvature corrections and does not question the constant threshold Gaunt factor assumed equal to 0.2 (van Regemorter: 1962), no reasons for the drastic deterioration of the method employed for the last mentioned multiplets can be forwarded.

Since the above criticism concerns the use of the effective Gaunt factor in particular, this investigation of lines of SnII can still be seen as significant with regard to the effects observed for the inclusion of radiator structure details.

As is seen in fig. 5.2, configuration interaction introduces a major change in predicted line widths (even greater than temperature variation effects of $\sim 20\%$), and the importance of this phenomenon needs to be reckoned with in line width calculation models. The sensitivity of the line width to this interaction depends clearly on the type of transition encountered. For transitions in which the lower level is perturbed, the sensitivity is less than for lines where the upper level is perturbed, since the latter form a greater contribution to the line width (compare, for example, the lines $\lambda = 6844 \text{ \AA}$ and 5561 \AA).

Another well illustrated effect is the variation within multiplets. The same trends between measured and calculated values is found throughout table 5.4. Given the good agreement for the $\lambda = 6844 \text{ \AA}$ line, the proposed $\lambda = 6453 \text{ \AA}$ line width can be considered as an accurate prediction. The large difference for the two members of the multiplet can be traced to (a) a different and larger set of perturbing levels

for $6p \ ^2P_{3/2}^{\circ}$ and (b) drastic differences in $\Delta E_{i',i}$ for the same perturbing level $|i'\rangle$. It is found that, despite (a), condition (b) is of overriding importance for the $5d \ ^2D_{3/2}$ perturber. This point can be aptly described by fig. 5.3, where the resultant contributions to the line width have been largely affected by this $\Delta E_{i',i}$ difference in the Gaunt factor \bar{g}_{Sn} as well as the difference in applicable 6-j symbols.

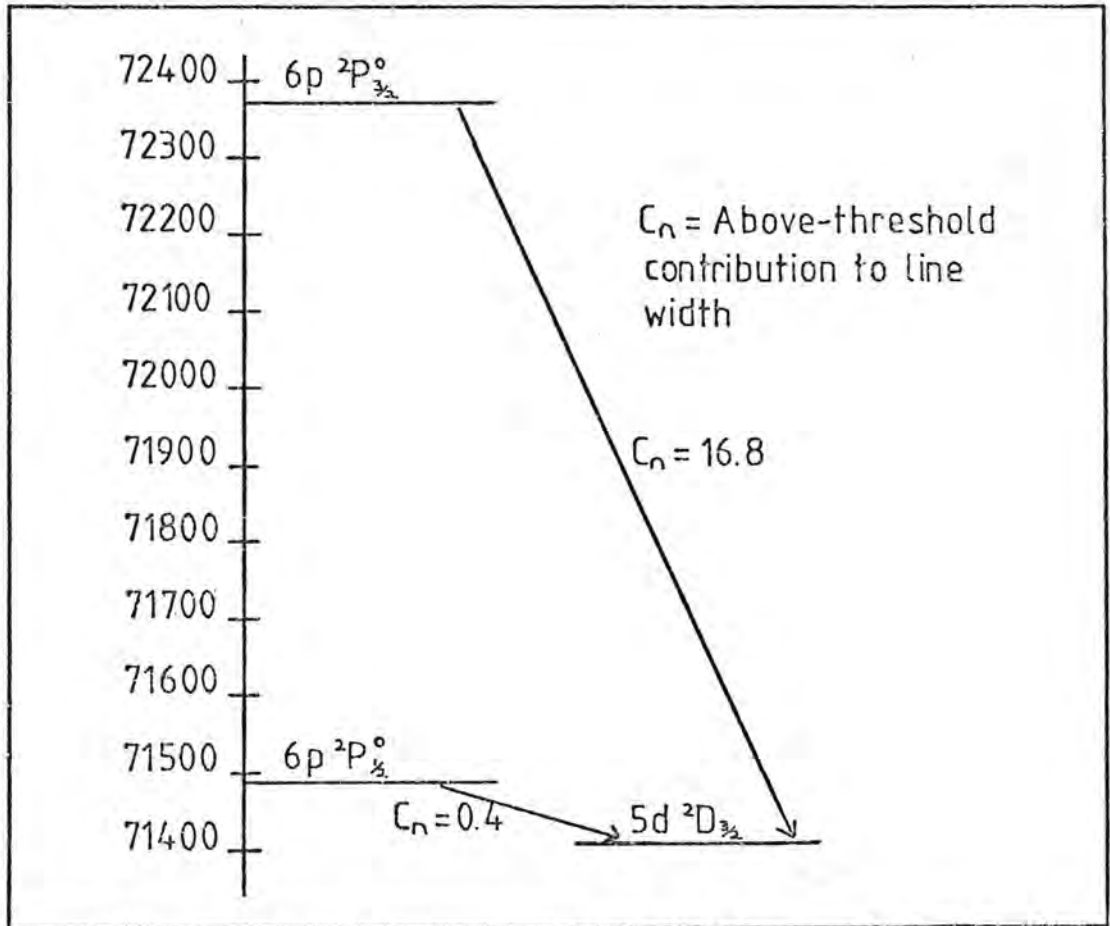


Fig. 5.3: Variations in contributions within multiplets

The effect of the different angular factors:

$$(2L+1)(2J'+1) \left\{ \begin{array}{ccc} L & L' & 1 \\ & J' & J & S \end{array} \right\}^2$$

is to vary the contributions by a factor of ~ 15 , thus attributing a variation of ~ 3 to the argument $x = \sqrt{\frac{3}{2} kT / \Delta E_{i',i}}$ used in the evaluation of \bar{g}_{Sn} . This latter important effect was pointed out by Hey (1978) and confirmed experimentally by Behringer and Thoma (1978) for the case of AII.

5.2 STARK WIDTHS OF ISOLATED OXYGEN ION LINES

As already discussed in the Introduction, the variation of Stark widths for homologous ions is to be investigated using the various ions tabulated in table O.1. Oxygen ions of ionisation stages $Z = 2, 3$ are members of this table as examples of the structure (ground level):



Despite the astrophysical importance of Stark broadening parameters for spectral lines from such low ionisation stage ions as OII and OIII (Griem: 1974; Mihalas: 1970), the only experimental data tabulated by Konjević and Wiese (1976) are from a low pressure pulsed arc source experiment by Platiša *et al.* (1975) which has remained the only reliable reference for Stark broadening data. Semi-classical calculations by Griem (1974)

were performed, and very satisfactory agreement was obtained for the OII lines measured:

$$\frac{W_m}{W_e} (\text{SC}) = 0.89 \pm 0.03$$

An earlier study by Hey and Bryan (1977), using a slightly modified form of Griem's semi-empirical method (1968), yielded less satisfactory agreement for thirteen lines from thirteen multiplets of OII:

$$\frac{W_m}{W_e} (\text{HB}) = 1.30 \pm 0.06$$

For OIII even worse agreement was obtained:

$$\frac{W_m}{W_e} (\text{HB}) = 1.89 \pm 0.10$$

particularly since the estimated experimental errors lay within $\sim \pm 16\%$. It was concluded that the underestimate resulted from an underestimate in the threshold Gaunt factor of 0.2, already suspected from earlier investigations by Blaha (1969) and Davis (1974), and improved \bar{g}_{th} values were suggested to improve the above results, namely:

$$\begin{aligned} \bar{g}_{\text{th}} &= 0.26 && \text{for OII} \\ \bar{g}_{\text{th}} &= 0.38 && \text{for OIII} \end{aligned}$$

In a recent study by Dimitrijević and Konjević (1980a) calculations based on Griem's semi-empirical and semi-

classical formulae (Griem: 1968 and Griem: 1974, eq. 526, respectively) were performed for OIII to yield for the four lines from two multiplets:

$$\frac{W_m}{W_e} \text{ (SC)} = 0.74 \pm 0.04 \quad \text{semi-classical (Griem: 1974)}$$

$$\frac{W_m}{W_e} \text{ (SEM)} = 1.05 \pm 0.05 \quad \text{modified semi-empirical}$$

$$\frac{W_m}{W_e} \text{ (SCM)} = 1.02 \pm 0.08 \quad \text{modified semi-classical}$$

Applying the method of calculation used for SnII to these two ions again proved unsatisfactory owing to the rather large dependence of this approach (MTD1 program - see section 5.1 and Part B) on the knowledge of the threshold effective Gaunt factor, as already mentioned in the previous investigation of SnII. Quite contrary to the case of SnII, the structural effects for oxygen ions at the temperature of ~ 2 eV are of lesser importance owing to the fact that on the whole $\Delta E > kT$. This places the line broadening calculations into the threshold regime of the Gaunt factors, where the theory applied is particularly stringently tested and a constancy in line width is observed. For example, applying \bar{g}_{Sn} as in MTD1 as for SnII results in the consistent use of below-threshold contributions and vanishing of above-threshold contributions (see eq. 5.2).

It was thus necessary to obtain a more rigorous form of the effective Gaunt factor taking curvature into account and being continuous below and above threshold, thus giving rise

to the developments as presented in detail in Chapter 3.

A quantum defect analysis of the two oxygen ions revealed no configuration interaction sufficient to warrant such an inclusion in the calculations, despite the occurrence of these in both ions (Condon and Shortley: 1935; Sobel'man: 1972), as well as a tendency towards LK coupling in the case of excited terms based on f orbital configurations. This can be justified by the observation made above that structural effects are minimised by the summation over small, near-threshold contributions, as indicated also by the constancy of line widths within multiplets. A problem that was encountered in OII and OIII were missing terms in the energy level tables by Moore (1971) which were found to be of importance due to the low completeness parameter $\Delta S_i/S_i$ (see Chapter 2.4) obtained. The terms for OII were located using simple quantum defect estimates and have been listed in table 5.21:

(³ P) 4p ² S _{1/2} ^o	244335 cm ⁻¹
4p ⁴ S _{3/2} ^o	247223 cm ⁻¹
4p ⁴ P _{3/2,1/2} ^o	245876 cm ⁻¹
4p ⁴ P _{5/2} ^o	245920 cm ⁻¹
(¹ D) 4p ² F ^o	266039 cm ⁻¹

Table 5.21: Estimated term energies of OII

In the case of OIII, the terms (²P^o) 4f ³D, ³F, ³G were determined using spectral line listings by Kelly and Palumbo

(1973). For these levels, LK coupling is more appropriate (Warner: 1968d) and simplified values were obtained by averaging of such an LK coupling scheme, justified by the large $\Delta E_{i,i}$ as compared with the K fine structure. The results are presented in table 5.22:

4f 3G_5	381403 cm ⁻¹
3G_4	381365 cm ⁻¹
3G_3	381177 cm ⁻¹
4f 3F_4	380685 cm ⁻¹
3F_3	380642 cm ⁻¹
3F_2	380622 cm ⁻¹
4f 3D_3	381457 cm ⁻¹
3D_2	381545 cm ⁻¹
3D_1	381623 cm ⁻¹

Table 5.22: Estimated term energies of OIII

Using thus the results from Chapters 1, 2 and 3 with \bar{g} evaluated for various estimates of $\bar{x} = \sqrt{\frac{\frac{1}{2} m v^2}{\Delta E}}$ yields the following (table 5.23) results for OII at the electron temperature of 25900 °K (MTD2 - see Part B). As is apparent from this calculation for estimates of the average kinetic energy of the electron perturbers using the root-mean-square, average and most probable electron velocities respectively, the Gaunt factor and thus line width is very sensitive to the choice of "average" made over the Maxwellian distribution. Furthermore, the procedure suggested by Griem (1968) of extrapolation of \bar{g} as a constant below threshold as employed in table 5.23 leads to setting almost all $\bar{g} = \bar{g}_{th}$ (5 out of 18

transition array	designation	$\lambda(\text{\AA})$	line width w_e (\AA) calculated for $\frac{1}{2} m \overline{v^2}$ averaged as		
			$\frac{3}{2} k T$	$\frac{4}{\pi} k T$	kT
$2p^2$ (3P) $3s - 3p$	$^4P_{5/2} - ^4D_{7/2}$	4649.1	0.374	0.352	0.348
	$^4P_{1/2} - ^4P_{3/2}$	4317.1	0.320	0.301	0.299
	$^4P_{1/2} - ^4S_{3/2}$	3712.8	0.255	0.239*	0.231

Table 5.23: Effect of type of velocity average on line widths

collision cross-sections for the result marked with an asterisk) for the average velocity estimate and all $\bar{g} = \bar{g}_{th}$ for estimation of $\langle \frac{1}{2} m v^2 \rangle = kT$. For OIII, all effective Gaunt factors were estimated by $\bar{g} = \bar{g}_{th}$ for the three approaches used above, thus indicating that a better form of averaging procedure needs to be applied for the Gaunt factors.

As a result of the above failure of the assumption that \bar{g} is a slowly varying function of electron energy, a rigorous averaging by integration of the Gaunt factor over a Maxwellian distribution was introduced as outlined in Chapter 3.4. The line widths are thus calculated using eq. 1.42 with eq. 2.8 and averages of eqs. 3.39 (3.41) given by eqs. 3.56 (3.57), a method which has been denoted as MTD2A. Details of this combination of the above-mentioned equations into one line width program are described in Part B (MTD2A) and also in the paper by Hey and Breger (1980b) given in Appendix II.

Results of the application of this refined version of

the line width calculation for OII and OIII are presented in tables 5.24 and 5.25 respectively. Because of the negligible variation within multiplets, as discussed above, one representative line has been chosen for each multiplet. Calculations were performed at a normalised electron density $N_e = 10^{17} \text{ cm}^{-3}$ and an electron temperature of 25900 °K. The two values tabulated for each line correspond to the type of below-threshold extrapolation chosen (see Chapter 3.5). Method I corresponds to the use of eqs. 3.39 and 3.41 of the effective Gaunt factor for all energies (including below threshold) for which $\bar{g} \geq 0$. Method II has been chosen in analogy to Griem (1968) and employs a constant $\bar{g} = \bar{g}_{\text{th}}$ for below-threshold energies. Furthermore, the percentage strong contributions (Chapter 4.1), percentage inelastic and elastic contributions (Chapter 3.5) as well as the neglected ion quadrupole broadening (Chapter 4.3) are given. χ denotes the completeness of choice of perturbing levels (see $\Delta S_i/S_i$ in Chapter 2.5) obtained. For comparison, the calculated line widths are tabulated (tables 5.26, 5.27) with theoretical values for OII lines obtained by Jones, Benett and Griem (JBG) (1971) as well as the previous results obtained by Hey and Bryan (1977) for OII and OIII lines.

In table 5.28, some of the threshold values obtained for OIII using eq. 3.39 (3.41) have been tabulated. It should be noted that these values do not contain "strong" contributions to the Gaunt factor, which are treated separately.

Table 5.24: Comparison between measured and calculated widths: OII

Key:

- W_m - measured FWHM
- W_e - calculated FWHM using method I
method II
- $\frac{W_s}{W_e}$ - percentage strong collision contribution
- $\frac{W_{in}}{W_e}$ - percentage inelastic collision contribution
- $\frac{W_{el}}{W_e}$ - percentage elastic collision contribution
- $\frac{W_{ion}}{W_e}$ - percentage ion perturber collision contribution (neglected)
- completeness of upper/lower perturbing level set in percent
- $\frac{W_m}{W_e}$ - per unit agreement

Transition Array	Designation	Unshifted λ (Å) (Air)	W_m (Å)	W_e (Å)	$\frac{W_s}{W_e}$ (%)	$\frac{W_{in}}{W_e}$ (%)	$\frac{W_{el}}{W_e}$ (%)	$\frac{W_{ion}}{W_e}$ (%)	χ (%)	$\frac{W_m}{W_e}$
$2p^2 (^3P) 3s - 3p$	$^4P_{5/2} - ^4D_{7/2}^0$	4649.1	0.229	0.285 0.366	36.2 28.2	41.1 31.9	22.7 39.9	1.2 1.0	95/95	0.80 0.63
$2p^2 (^3P) 3s - 3p$	$^4P_{1/2} - ^4P_{3/2}^0$	4317.1	0.219	0.242 0.314	34.5 26.6	41.9 32.3	23.6 41.1	1.5 1.2	96/95	0.91 0.70
$2p^2 (^3P) 3s - 3p$	$^4P_{3/2} - ^4S_{3/2}^0$	3712.8	0.204	0.189 0.242	32.3 25.1	44.2 34.3	23.5 40.6	2.1 1.7	94/95	1.08 0.84
$2p^2 (^3P) 3s - 3p$	$^2P_{3/2} - ^2D_{5/2}^0$	4414.9	0.267	0.283 0.360	35.4 27.8	42.3 33.3	22.2 38.9	1.5 1.2	94/95	0.94 0.74
$2p^2 (^3P) 3s - 3p$	$^2P_{3/2} - ^2P_{3/2}^0$	3973.3	0.227	0.233 0.297	33.5 26.2	43.7 34.3	22.8 39.5	2.0 1.6	94/95	0.97 0.76
$2p^2 (^3P) 3p - 3d$	$^2S_{1/2}^0 - ^2P_{1/2}$	3377.2	0.229	0.211 0.261	23.6 19.1	57.8 46.7	18.6 34.2	5.9 4.8	87/96	1.09 0.88
$2p^2 (^3P) 3p - 3d$	$^4D_{7/2}^0 - ^4F_{7/2}$	4092.9	0.235	0.299 0.371	27.6 22.3	53.4 43.2	18.9 34.5	4.2 3.4	83/95	0.79 0.63
$2p^2 (^3P) 3p - 4s$	$^4D_{5/2}^0 - ^4P_{3/2}$	3138.4	0.339	0.322 0.349	21.6 19.9	68.4 63.2	10.1 16.8	5.2 4.8	98/95	1.05 0.97
$2p^2 (^1D) 3s - 3p$	$^2D_{3/2} - ^2F_{5/2}^0$	4596.2	0.246	0.280 0.362	34.5 26.7	42.2 32.6	23.3 40.6	1.3 1.0	95/95	0.88 0.68
$2p^2 (^1D) 3s - 3p$	$^2D_{3/2} - ^2D_{3/2}^0$	4347.4	0.219	0.257 0.330	34.5 26.8	42.5 33.1	23.0 40.1	1.5 1.2	94/95	0.85 0.66
$2p^2 (^1D) 3s - 3p$	$^2D_{5/2} - ^2P_{3/2}^0$	3912.0	0.225	0.217 0.278	34.7 27.0	42.1 32.8	23.2 40.2	1.9 1.5	95/95	1.04 0.81
$2p^2 (^1D) 3p - 3d$	$^4P_{3/2}^0 - ^4P_{5/2}$	4153.3	0.256	0.315 0.391	23.9 19.3	56.5 45.5	19.5 35.2	4.3 3.4	86/96	0.81 0.65
$2p^2 (^1D) 3p - 3d$	$^2F_{5/2}^0 - ^2G_{7/2}$	4185.5	0.200	0.334 0.411	26.7 21.7	54.6 44.4	18.7 34.0	4.1 3.3	85/95	0.60 0.49

Table 5.25: Comparison between measured and calculated widths: OIII

Key: Same as for Table 5.24.

Transition Array	Designation	Unshifted $\lambda(\text{\AA})$	$W_m^{\circ}(\text{\AA})$	$W_e^{\circ}(\text{\AA})$	$\frac{W_s}{W_e}(\%)$	$\frac{W_{in}}{W_e}(\%)$	$\frac{W_{el}}{W_e}(\%)$	$\frac{W_{ion}}{W_e}(\%)$	$\chi(\%)$	$\frac{W_E}{W_e}$
$2p(^2P^{\circ})3s - 3p$	$^3P_1^{\circ} - ^3D_2$	3754.7	0.146	0.119 0.156	49.5 37.9	30.6 23.4	20.0 38.8	0.5 0.4	91/93	1.23 0.94
$2p(^2P^{\circ})3s - 3p$	$^3P_2^{\circ} - ^3P_2$	3047.1	0.108	0.074 0.098	43.6 32.7	34.3 25.7	22.1 41.6	1.0 0.7	90/93	1.46 1.10
$2p(^2P^{\circ})3p - 3d$	$^3D_2 - ^3F_3^{\circ}$	3261.0	0.127	0.098 0.125	45.5 35.6	39.2 30.7	15.2 33.7	1.4 1.1	81/91	1.30 1.02
$2p(^2P^{\circ})3p - 3d$	$^3P_2 - ^3D_3^{\circ}$	3715.1	0.142	0.133 0.170	43.3 33.8	40.8 31.9	15.9 34.3	1.2 0.9	83/90	1.07 0.84

Table 5.26: Comparison between various calculational methods: OII

Key: (I) - using method I of extrapolation below threshold

(II) - using method II of extrapolation below threshold

JBG - Jones, Benett and Griem (1971)

HB - Hey and Bryan (1977)

Transition Array	Designation	Unshifted λ (\AA) (Air)	W_e (\AA) (I)	W_e (\AA) (II)	W_e (\AA) (JBG)	W_e (\AA) (HB)	W_m (\AA)
$2p^2(^3P)3s - 3p$	$^4P_{5/2}^0 - ^4D_{7/2}^0$	4649.1	0.285	0.366	0.338	0.180	0.229
$2p^2(^3P)3s - 3p$	$^4P_{1/2}^0 - ^4P_{3/2}^0$	4317.1	0.242	0.314	0.238	0.158	0.219
$2p^2(^3P)3s - 3p$	$^4P_{1/2}^0 - ^4S_{3/2}^0$	3712.8	0.189	0.242	-	0.125	0.204
$2p^2(^3P)3s - 3p$	$^2P_{3/2}^0 - ^2D_{5/2}^0$	4414.9	0.283	0.360	0.291	0.193	0.267
$2p^2(^3P)3s - 3p$	$^2P_{3/2}^0 - ^2P_{3/2}^0$	3973.3	0.233	0.297	0.227	0.165	0.227
$2p^2(^3P)3p - 3d$	$^2S_{1/2}^0 - ^2P_{1/2}^0$	3377.2	0.211	0.261	0.196	0.165	0.229
$2p^2(^3P)3p - 3d$	$^4D_{7/2}^0 - ^4F_{7/2}^0$	4092.9	0.299	0.371	0.277	0.221	0.235
$2p^2(^3P)3p - 4s$	$^4D_{5/2}^0 - ^4P_{3/2}^0$	3138.4	0.322	0.349	0.445	0.290	0.339
$2p^2(^1D)3s - 3p$	$^2D_{3/2}^0 - ^2P_{5/2}^0$	4596.2	0.280	0.362	-	0.182	0.246
$2p^2(^1D)3s - 3p$	$^2D_{3/2}^0 - ^2D_{3/2}^0$	4347.4	0.257	0.330	-	0.166	0.219
$2p^2(^1D)3s - 3p$	$^2D_{5/2}^0 - ^2P_{3/2}^0$	3912.0	0.217	0.278	-	0.141	0.225
$2p^2(^1D)3p - 3d$	$^4P_{3/2}^0 - ^4P_{5/2}^0$	4153.3	0.315	0.391	0.283	0.246	0.256
$2p^2(^1D)3p - 3d$	$^2P_{5/2}^0 - ^2G_{7/2}^0$	4185.5	0.334	0.411	-	0.222	0.200

Table 5.27: Comparison between various calculational methods: OIII

- Key: (I) - using method I of extrapolation below threshold
 (II) - using method II of extrapolation below threshold
 (HB) - Hey and Bryan (1977)
 (SC) - Griem (1974)
 (SEM), (SCM) - Dimitrijević and Konjević (1980a)

Transition Array	Designation	Unshifted $\lambda(\text{\AA})$ (Air)	$w_e(\text{\AA})$ (I)	$w_e(\text{\AA})$ (II)	$w_e(\text{\AA})$ (HB)	$w_m(\text{\AA})$	$w_e(\text{\AA})$ (SC)	$w_e(\text{\AA})$ (SEM)	$w_e(\text{\AA})$ (SCM)
$2p(^2P^0)3s - 3p$	$^3P_1^0 - ^3D_2$	3754.7	0.119	0.156	0.076	0.146	0.187	0.142	0.130
$2p(^2P^0)3s - 3p$	$^3P_2^0 - ^3P_2$	3047.1	0.074	0.098	0.053	0.108	0.132	0.099	0.092
$2p(^2P^0)3p - 3d$	$^3D_2 - ^3F_3^0$	3261.0	0.098	0.125	0.064	0.127	0.167	0.110	0.131
$2p(^2P^0)3p - 3d$	$^3P_2 - ^3D_3^0$	3715.1	0.133	0.170	0.090	0.142	0.229	0.153	0.178

Table 5.28: Threshold effective Gaunt factors: OIII

Transition	\bar{g}		
	3s - 3p	3s - 4p	4s - 3p
ns $^3P^0$ - np 3S	0.236	0.402	
- np 3P	0.235	0.444	0.335
- np 3D	0.238	0.389	0.350
	3p - 3d	3p - 4d	4p - 3d
np 3P - nd $^3P^0$	0.248		
- nd $^3D^0$	0.250	0.363	0.335
np 3D - nd $^3D^0$	0.252		0.320
- nd $^3F^0$	0.253	0.366	0.328

From tables 5.24 and 5.25, the average ratio of measured to calculated (FWHM) widths is, for OII:

$$\frac{W_m}{W_e} \text{ (I)} = 0.91 \pm 0.04 \quad (\text{method I})$$

$$\frac{W_m}{W_e} \text{ (II)} = 0.73 \pm 0.04 \quad (\text{method II})$$

while, for OIII:

$$\frac{W_m}{W_e} \text{ (I)} = 1.27 \pm 0.08 \quad (\text{method I})$$

$$\frac{W_m}{W_e} \text{ (II)} = 0.98 \pm 0.06 \quad (\text{method II})$$

According to Platiša et al., the experimental accuracy is ~16%, and it is thus apparent that excellent agreement is obtained for OII results by method I, whereas for OIII the results by method II are favoured. With the exception of the last OII line, the agreement between this theory and experiment is thus good and from table 5.26 yields better agreement than other theories for 8 of the 13 tabulated lines.

For OIII, the agreement obtained by method II is comparable with that of Dimitrijević and Konjević (1980a), as their standard deviation is larger.

Why the two ions should differ with respect to inclusion of elastic contributions to the broadening, is not clear, but there seems to be a trend according to which the importance of elastic contributions increases for higher ionisation stages. The vital importance of elastic contributions to

the broadening as discussed by Griem (1968) is clearly confirmed. However, the simple estimate of Griem (1968) appears to lead to an underestimate of the elastic contributions. This is apparent on comparing his factor $[1 - \exp(-\Delta E/kT)]$ with the more detailed calculation performed here (c.f. methods MTD2, MTD2A in part B).

Comparing the strong contributions to the line width with those obtained by Griem (1974), it is clear that a rather different demarcation for the regimes of strong and weak contributions is employed in the present method. Griem's estimates assign a rather larger fraction of the broadening to strong collisions, but the consistency in cut-off of the impact parameter seems an important point in favour of the method employed here.

From the rather small contributions of ion perturbers to the line width (for OII less than 6%, for OIII less than 2%), the neglect of these in the calculation is justified, since no accurate means of inclusion of these as an integral part of the present calculation is available.

It can thus be concluded that the present theory has been successful in the derivation of:

- (a) an analytical Gaunt factor incorporating curvature effects independent of semi-empirical corrections at lower energies;
- (b) a model suitable for various ionisation stages even higher than $Z = 2$;
- (c) an explicit allowance of radiator structural effects

which predict variations within multiplets correctly;
and

- (d) a strong collision estimate which assumes the negative elastic "interference" terms to cancel the strong contributions from the lower transition level fully.

Accepting the arguments that lead to the formulation of the present method (MTD2A) as valid for all ions, this method is employed for all ions considered in the following sections, where in particular the above conclusions (a)-(d) are confirmed.

5.3 STARK WIDTHS OF ISOLATED SULPHUR ION LINES

The recent experimental study by Platiša et al. (1979) is of interest here as it provides comparison of theoretical and measured line widths for ions homologous to the previously considered ion OIII and also NIII (see table 0.1 in the Introduction). The ground state structure is of the form:

$$\begin{array}{ll} ns^2 np^2 \ ^3p & \text{for SIII} \\ ns^2 np \ ^2p^0 & \text{for SIV} \end{array} .$$

Furthermore, comparison with several calculated line widths is possible. The semi-empirical method (SE) (Griem: 1968) and semi-classical method (SC) (Griem: 1974, eq. 526) have yielded far inferior agreement with experiment than is reported for singly-ionised ion spectra. Calculations by Platiša et al. (1979) yield for these methods for sixteen lines from eight multiplets of SIII:

$$\frac{W_m}{W_e} \text{ (SE)} = 1.67 \pm 0.05$$

$$\frac{W_m}{W_e} \text{ (SC)} = 0.74 \pm 0.04$$

Slightly modified versions of these two methods have been used by Dimitrijević and Konjević (1980a) to yield for SIII:

$$\frac{W_m}{W_e} \text{ (SEM)} = 1.16 \pm 0.12$$

$$\frac{W_m}{W_e} \text{ (SCM)} = 0.96 \pm 0.04$$

for eight lines from three multiplets.

A calculation by Sahal-Bréchet (1969b) yields for two multiplets (four lines) of SIII, after appropriate wavelength scaling and correction for temperature:

$$\frac{W_m}{W_e} \text{ (SB)} = 0.90 \pm 0.03$$

With this excellent agreement obtained in other calculations, this ion offers a particularly stringent comparison of the presented method (Hey: 1979) and the other reported models.

The ionisation energies used for SIII and SIV were taken from Kelly and Palumbo (1973) and after correction for the appropriate ground state of the next ionisation stage, the values used were:

$$\text{SIII} : E_{\infty} = 281533 \text{ cm}^{-1}$$

$$\text{SIV} : E_{\infty} = 381541 \text{ cm}^{-1}$$

Again, problems associated with the absence of term energies from the energy tables (Moore: 1971a) were encountered. Using a study of lines observed in a SIII spectrum (Dynefors and Martinson: 1978), a number of the missing terms could be located:

$$3d \ ^3F_4^{\circ} \quad E_{n^*} = 122801.9 \text{ cm}^{-1}$$

$$3d \ ^3F_3^{\circ} \quad E_{n^*} = 122403.3 \text{ cm}^{-1}$$

$$4d \ ^3P_2^{\circ} \quad E_{n^*} = 205811 \text{ cm}^{-1}$$

In the last case, the remaining numbers of the multiplet were taken to have the same energy as discussed by Condon and Shortley (1935, p. 200). The following term values were obtained by simple quantum defect estimates (Condon and Shortley: 1935):

$$5p \ ^3S \quad E_{n^*} = 221022 \text{ cm}^{-1}$$

$$5p \ ^3P \quad E_{n^*} = 220419 \text{ cm}^{-1}$$

$$5p \ ^3D \quad E_{n^*} = 219184 \text{ cm}^{-1}$$

$$4f \ ^3D \quad E_{n^*} = 218233 \text{ cm}^{-1}$$

$$4f \ ^3F \quad E_{n^*} = 218233 \text{ cm}^{-1}$$

$$4f \ ^3G \quad E_{n^*} = 218233 \text{ cm}^{-1}$$

In the case of SIV, the level $5p \ ^2P_{3/2}$ was obtained from the study by Dynefors and Martinson (1978) and the remaining

member of the multiplet was derived by scaling of the spin-orbit coupling parameter with effective quantum number (Condon and Shortley: 1951):

$$\begin{array}{ll} 5p \ ^2P_{3/2} & E_{n^*} = 283585.1 \text{ cm}^{-1} \\ 5p \ ^2P_{1/2} & E_{n^*} = 283491.1 \text{ cm}^{-1} \end{array}$$

Following the same arguments as for OIII, the configuration interaction in the term system of SIII was neglected, since again the level separations $\Delta E_{i,i}$ were comparable with kT , thus minimising structural effects. That configuration interaction is present, can be seen from the term splitting of the $3p \ 3d$ configuration, for which the ratio:

$$\frac{(P - F)}{(F - D)} = 7.66$$

instead of the theoretical value derived for pure LS coupling of 0.55 (Condon and Shortley: 1951). Perturbation by the $3s \ 3p^3$ configuration is thus indicated. For OIII this interaction was less significant - the corresponding value for the term splitting of the $2p \ 3d$ configuration is 1.30.

Since SIV is homologous to SnII, the neglect of configuration interaction for the former ion needs to be justified by considering an essential difference between these two ions. For SnII, configuration interaction occurs between the terms denoted by $5p^2 \ ^2D$ and $5d \ ^2D$ which correspond structurally to the terms $3p^2 \ ^2D$ and $3d \ ^2D$ in SIV. Transitions to $6p \ ^2P^0$ and $4p \ ^2P^0$ for SnII and SIV respectively

should both be corrected for configuration interaction when calculating the corresponding excitation rates. However, quantitative differences in importance of configuration interaction for the two ions may be illustrated by the following ratios, in SIV:

$$\frac{(4p^2P^{\circ} - 3p^2\ ^2D)}{(4p^2P^{\circ} - 3d\ ^2D)} = 1.943$$

as compared with SnII, where:

$$\frac{(6p^2P^{\circ} - 5p^2\ ^2D)}{(6p^2P^{\circ} - 5d\ ^2D)} = 44.07 ,$$

suggesting that this perturbation may be neglected for SIV. The importance of such structural differences between ions is emphasised further in Chapter 6.

As discussed in Chapter 2.2, corrections need to be made to the oscillator strengths of $3p\ 3d \rightarrow 3p^2$ transitions. The correction factor is given (for levels) by eq. 2.20 as:

$$N \left| G_{S,L_i}^{SL} \right|^2 = 2$$

Using the same calculational method as for oxygen, the results obtained at an electron temperature of $T = 28500\ ^{\circ}\text{K}$ and normalised electron density $N_e = 10^{17}\ \text{cm}^{-3}$ are presented in table 5.31. The symbols and format used in table 5.31 are the same as for the previous ion (table 5.24).

In the calculated line widths, ion perturber widths have been neglected and from the estimate (eq. 4.32) this

Table 5.31: Comparison between measured and calculated widths: SIII, SIV

Key: W_m - measured FWHM
 W_e - calculated FWHM
 W_s - strong collision contribution
 W_{in} - inelastic collision contribution
 W_{el} - elastic collision contribution
 W_{ion} - ion perturber width (neglected)
 - completeness of upper/lower set of perturbing levels

Ion	Transition Array	Designation	Unshifted λ (Å) (Air)	W_m^0 (Å)	W_e (Å)	$\frac{W_s}{W_e} \%$	$\frac{W_{in}}{W_e} \%$	$\frac{W_{el}}{W_e} \%$	$\frac{W_{ion}}{W_e} \%$	$\chi \%$	$\frac{W_m}{W_e}$
		$^1P_1^o - ^1P_1$	3387.1	0.151	0.134 0.166	42.6 34.4	42.8 34.6	14.6 31.0	1.5 1.2	99/58	1.13 0.91
		$^3D_1^o - ^3P_2$	3928.6	0.173	0.187 0.232	40.9 33.1	44.3 35.8	14.8 31.1	1.1 0.9	98/76	0.93 0.75
		$^3D_2^o - ^3P_1$	3983.8	0.169	0.193 0.239	41.1 33.3	44.3 35.8	14.7 30.9	1.1 0.9	59/76	0.88 0.71
	3p($^2P^o$)4s - 3p 4p	$^3P_2^o - ^3D_1$	4332.7	0.245	0.238 0.301	37.7 29.8	43.3 34.2	19.1 36.0	0.8 0.6	92/94	1.03 0.81
		$^3P_1^o - ^3D_2$	4361.5	0.247	0.239 0.303	37.2 29.3	43.5 34.3	19.3 36.4	0.8 0.7	92/94	1.03 0.82
		$^3P_0^o - ^3P_1$	3832.0	0.198	0.203 0.254	36.1 28.9	45.8 36.7	18.1 34.4	1.0 0.8	99/94	0.98 0.78
		$^3P_2^o - ^3P_1$	3899.1	0.192	0.211 0.263	36.1 28.9	45.8 36.6	18.1 34.5	1.0 0.8	99/94	0.91 0.73
		$^3P_1^o - ^3S_1$	3662.0	0.182	0.186 0.233	37.0 29.6	44.4 35.5	18.5 34.9	1.1 0.9	98/94	0.98 0.78
	3p($^2P^o$)4p - 3p 4d	$^3D_2 - ^3F_3^o$	2856.0	0.206	0.192 0.221	34.7 30.2	53.5 46.5	11.8 23.3	3.2 2.8	89/92	1.07 0.93
		$^3D_1 - ^3F_3^o$	2863.5	0.202	0.199 0.228	35.3 30.9	53.3 46.6	11.4 22.5	3.1 2.7	88/91	1.02 0.99
		$^3D_1 - ^3F_2^o$	2872.0	0.200	0.188 0.217	33.8 29.2	53.9 46.7	12.3 24.1	3.2 2.8	89/92	1.06 0.92
		$^3D_1 - ^3D_1^o$	2718.9	0.202	0.171 0.196	30.1 26.2	58.1 50.7	11.8 23.1	3.7 3.2	87/92	1.18 1.03
		$^3D_1 - ^3D_1^o$	2756.9	0.206	0.184 0.209	31.9 28.0	56.9 49.9	11.2 22.1	3.5 3.1	87/91	1.12 0.99
		$^3P_1 - ^3D_2^o$	2950.2	0.210	0.213 0.244	29.8 26.1	58.8 51.5	11.4 22.5	3.1 2.7	87/99	0.99 0.86
		$^3P_1 - ^3D_1^o$	2964.8	0.212	0.221 0.251	30.7 26.9	58.2 51.1	11.1 22.0	3.1 2.7	87/98	0.96 0.84
S(IV)	3s(1S)4s - 3s 2 4p	$^3S_1 - ^3P_{1/2}^o$	3097.5	0.116	0.102 0.130	51.4 40.3	31.4 24.6	17.2 35.0	0.7 0.5	97/96	1.14 0.89

Table 5.32: Comparison between various calculated line widths: SIII, SIV

Key: (I) - using method I
 (II) - using method II
 (SE) - Griem (1968)
 (SC) - Griem (1974)
 (SB) - Sahal-Bréchet (1969b)
 (SEM), (SCM) - Dimitrijević and Konjević (1980a)

Ion	Transition Array	Designation	Unshifted $\lambda(\text{\AA})$ (Air)	$w_e(\text{\AA})$ (I)	$w_e(\text{\AA})$ (II)	$w_e(\text{\AA})$ (SE)	$w_e(\text{\AA})$ (SC)	$w_e(\text{\AA})$ (SB)	$w_m(\text{\AA})$	$w_e(\text{\AA})$ (SEM)	$w_e(\text{\AA})$ (SCM)	
S(III)	3p(² P ^o); 3d - 3p 4p	³ P ₂ ^o - ³ P ₁	3370.4	0.131	0.162	0.080	0.147		0.149	0.129	0.150	
		³ P ₁ ^o - ³ P ₀	3367.1	0.132	0.163	0.080	0.147		0.151	0.129	0.150	
		³ D ₃ ^o - ³ P ₂	3928.6	0.182	0.226	0.114	0.206		0.173	0.178	0.205	
		³ D ₂ ^o - ³ P ₁	3983.8	0.188	0.233	0.114	0.206		0.169	0.178	0.205	
	3p(² P ^o); 4s - 3p 4p	³ P ₀ ^o - ³ D ₁	4332.7	0.237	0.300	0.165	0.416	0.259	0.245	0.273	0.273	
		³ P ₂ ^o - ³ D ₂	4361.5	0.238	0.302	0.165	0.416	0.263	0.247	0.279	0.273	
		³ P ₀ ^o - ³ P ₁	3832.0	0.202	0.253	0.135	0.345	0.222	0.198	0.226	0.222	
		³ P ₂ ^o - ³ P ₁	3899.1	0.209	0.262	0.135	0.345	0.229	0.192	0.226	0.222	
		³ P ₁ ^o - ³ S ₁	3662.0	0.185	0.232	0.127	0.325		0.182	0.217	0.212	
	3p(² P ^o); 4p - 3p 4d	³ D ₂ - ³ F ₃ ^o	2856.0	0.192	0.221	0.112	0.273		0.206	0.130	0.130	
		³ D ₃ - ³ F ₄ ^o	2863.5	0.199	0.228	0.112	0.273		0.202	0.130	0.186	
		³ D ₁ - ³ F ₂ ^o	2872.0	0.188	0.217	0.112	0.273		0.200	0.130	0.186	
		³ D ₁ - ³ D ₁ ^o	2718.9	0.171	0.196	0.106	0.257		0.202	0.125	0.181	
		³ D ₃ - ³ D ₁ ^o	2756.9	0.184	0.202	0.106	0.257		0.206	0.125	0.181	
		³ P ₁ - ³ D ₂ ^o	2950.2	0.213	0.245	0.125	0.304		0.210	0.147	0.211	
		³ P ₂ - ³ D ₃ ^o	2964.8	0.221	0.251	0.125	0.304		0.212	0.147	0.211	
	S(IV)	3s ² (¹ S); 4s-3s ² 4p	² S _{1/2} - ² P _{1/2} ^o	3077.5	0.102	0.130	0.071	0.196		0.116	0.145	0.109

contribution is less than 4% and the neglect is thus satisfactorily justified. Agreement of calculated and measured widths for SIII using Method I of extrapolation below threshold is excellent - for twelve of the sixteen lines calculated the difference is below 10%, and for the remaining four lines it is well below 20%. For SIV, only one comparison is possible and an agreement of 14% and less has been achieved by both methods I and II. From the results obtained for both SIII and SIV, the agreement between measured and calculated widths seems to indicate, as already suspected for the oxygen ions, that the extrapolation below threshold lies somewhere between method I and II. It appears, however, that using the derived expression of \bar{g} below threshold instead of a constant \bar{g}_{th} yields better results for SIII and still satisfactory results for SIV.

The present results are compared in table 5.32 with the values computed by various other authors as quoted above, and agreement between theory and experiment can be summarised as follows (table 5.33) for SIII:

Method	Author and reference	$\frac{W_m}{W_e}$
method I	Hey (1979)	1.02 ± 0.02
method II	Hey (1979)	0.85 ± 0.02
semi-empirical	Griem (1968)	1.67 ± 0.05
semi-classical	Griem (1974)	0.74 ± 0.04
semi-classical	Sahal-Bréchet (1969)	0.90 ± 0.03
semi-empirical	(Dimitrijević and	1.16 ± 0.12
semi-classical	(Konjević (1980)	0.96 ± 0.04

Table 5.33: Comparison of various computational methods for SIII line widths

The best results obtained by other methods are by Dimitrijević and Konjević (1980) and are marginally less accurate than the results obtained by Hey and Breger (1980c). However, their modified versions of Griem's semi-classical method (1968) fail to show differences between members of multiplets and the present results can thus be seen as significantly superior, as they provide the correct variations within multiplets as well. It should be noted also that rather different estimates for the ion broadening have been obtained by Sahal-Bréchet (1969), which indicates that a more careful consideration may be required as to the proper method of inclusion of these contributions.

An important observation made in the calculation of the line widths for oxygen and sulphur ions is that the preference of method I is highly dependent on the choice of perturbing levels. As is apparent from table 5.31, the best agreement using method I is obtained for fairly complete sets of perturbing levels. The rather inferior agreement for SIII lines $3d\ ^3P - 4d\ ^3P$ can thus be attributed to the low completeness of 58% obtained for the lower transition levels. This may also indicate that selection rules other than those for allowed electric dipole transitions may be more important than is usually supposed. This point is discussed in further detail for the case of CIII (Section 5.8) where the question of allowance of spin-flip becomes pertinent.

As for oxygen, rather smaller "strong" collision contributions have been obtained for the present estimate than those calculated by Griem (1974) and Sahal-Bréchet (1969b),

Table 5.34: Threshold effective Gaunt factors: SIII

Transition	\bar{g}		
	4s - 4p	4s - 5p	5s - 4p
ns ³ P - np ³ S	0.211	0.418	0.297
- np ³ P	0.212	0.417	0.300
- np ³ D	0.214	0.387	0.310
	4p - 3d	4p - 4d	5p - 4d
np ³ S - nd ³ P	0.299	0.218	
np ³ P - nd ³ P	0.297	0.219	
- nd ³ D	0.286	0.220	0.233
np ³ D - nd ³ P	0.291	0.222	
- nd ³ D	0.280	0.223	0.228
- nd ³ F	0.336	0.221	0.235

Table 5.35: Threshold effective Gaunt factors: SIII

Transition	\bar{g}	
	3d - 4f	4d - 4f
nd ³ P - nf ³ D	0.285	
nd ³ D - nf ³ D	0.276	0.206
- nf ³ F	0.276	0.206
nd ³ F - nf ³ D		0.208
- nf ³ F		0.208
- nf ³ G		0.208
	3p ² - 3d	3p ² - 4s
np ² ³ P - nd ³ P	0.293	
- nd ³ D	0.293	
- ns ³ P		0.419

but the differences in demarcation as discussed for oxygen may be the reason for this difference.

As far as the proposed effective Gaunt factor model (Chapter 3) is concerned, poor agreement with values by Griem (1974) is again obtained. In particular, his proposed trends regarding $\Delta n = 0$ and $\Delta n \neq 0$ transitions have not been confirmed. For comparison, a selection of the threshold Gaunt factors employed in the SIII calculations are tabulated in tables 5.34 and 5.35.

In conclusion, therefore, the assessment of the present theory (Hey: 1979), as made for oxygen, is seen to be accurate.

5.4 STARK WIDTHS OF ISOLATED ARGON LINES

The measurements of AIII and AIV ion lines as part of a programme of measurement of Stark widths from multiply ionised ions by Platiša *et al.* (1975) is of interest not only because it forms part of the list of homologous ions (table 0.1), but also because of a reported discrepancy between measured temperature effects on line broadening and predicted temperature dependence (Hey: 1977b). The experimental data at two measured temperatures provide thus an excellent opportunity of testing the proposed theory (Hey: 1979, private communication) for their temperature behaviour. The importance of the temperature dependence of the thermally averaged Gaunt factor has been discussed by Dimitrijević and Konjević (1978).

Using the semi-empirical method of Griem (1968), Hey (1977b) obtained the following agreement between measured and calculated line widths for AIII and AIV:

$$\begin{aligned} \frac{W_m}{W_e} \text{ (SE)} &= 1.57 \pm 0.08 && \text{A III @ 21 100}^\circ\text{K} \\ \frac{W_m}{W_e} \text{ (SE)} &= 1.16 \pm 0.04 && \text{A III @ 23 080}^\circ\text{K} \\ \frac{W_m}{W_e} \text{ (SE)} &= 1.24 \pm 0.01 && \text{A IV @ 20 750}^\circ\text{K} \\ \frac{W_m}{W_e} \text{ (SE)} &= 1.27 \pm 0.03 && \text{A IV @ 22 200}^\circ\text{K} \end{aligned}$$

Very promising agreement has been reported recently by Dimitrijević and Konjević (1980a) for their modified forms of Griem's original semi-empirical (1968) and semi-classical methods (1974, eq. 526). Including their calculated results of Griem's semi-classical method, the following agreement has been reported:

$$\begin{aligned} \frac{W_m}{W_e} \text{ (SC)} &= 0.71 \pm 0.04 && \text{A III @ 21 100}^\circ\text{K} \\ \frac{W_m}{W_e} \text{ (SCM)} &= 0.99 \pm 0.05 && \text{A III @ 21 100}^\circ\text{K} \\ \frac{W_m}{W_e} \text{ (SEM)} &= 0.99 \pm 0.08 && \text{A III @ 21 100}^\circ\text{K} \\ \frac{W_m}{W_e} \text{ (SC)} &= 0.59 \pm 0.01 && \text{A IV @ 20 750}^\circ\text{K} \\ \frac{W_m}{W_e} \text{ (SC)} &= 0.60 \pm 0.01 && \text{A IV @ 22 200}^\circ\text{K} \\ \frac{W_m}{W_e} \text{ (SCM)} &= 0.92 \pm 0.01 && \text{A IV @ 20 750}^\circ\text{K} \\ \frac{W_m}{W_e} \text{ (SCM)} &= 0.93 \pm 0.02 && \text{A IV @ 22 200}^\circ\text{K} \\ \frac{W_m}{W_e} \text{ (SEM)} &= 0.75 \pm 0.01 && \text{A IV @ 20 750}^\circ\text{K} \\ \frac{W_m}{W_e} \text{ (SEM)} &= 0.77 \pm 0.02 && \text{A IV @ 22 200}^\circ\text{K} \end{aligned}$$

for four lines from two multiplets for AIV and five lines from four multiplets for AIII.

For the present calculations, the ionisation energy for AIII was taken from Kelly and Palumbo (1973) and when corrected for the correct ionisation limit the following values were obtained:

(² P ⁰) parent	$E_{\infty} = 363575 \text{ cm}^{-1}$
(⁴ S ⁰) parent	$E_{\infty} = 328600 \text{ cm}^{-1}$
(² D ⁰) parent	$E_{\infty} = 349767 \text{ cm}^{-1}$

The problem of important levels missing from the energy level tables (Moore: 1971a) was even greater than for the previous investigations. Intensive search using the bibliographies by Fuhr, Miller and Martin (1978), Hagan (1977) and Hagan and Martin (1972) for references suggesting measured energy level values proved futile and a quantum defect analysis had to be relied on to give the approximate positions of the missing terms, tabulated below (table 5.41).

For AIV, the corrected ionisation energy (series limit) for levels of (³P) parentage is:

$$E_{\infty} = 483784 \text{ cm}^{-1}$$

The published data on positions of important energy levels were found to be even more scarce and estimated term positions using a quantum defect analysis are also listed in table 5.41.

Using these input data, the results of calculations of

	term	energy (cm ⁻¹)
AIII:	(² P ^o) 4f ³ D	296900
	(⁴ S ^o) 5p ⁵ P	261969
	(² D ^o) 5p ³ P	284834
	(² D ^o) 5p ³ D	282086
	(² D ^o) 5p ³ F	282438
	(² D ^o) 3d ³ P ₂	188517
	(² D ^o) 3d ³ G	186000
AIV:	(³ P) 5s ⁴ P	358928
	5p ⁴ S ^o	374000
	3d ⁴ P	220794.4
	4d ⁴ P	348000
	5d ⁴ P	401000
	3d ⁴ D	224000

Table 5.41: Estimated term energies of Argon

the line width (FWHM) at electron density $N_e = 10^{17} \text{ cm}^{-3}$ (using method MTD2A as for O, S ions) are listed in tables 5.42 and 5.43 for the various electron temperatures. The ion quadrupole width has again been neglected and since the resultant error is estimated to be less than 1% (tables 5.42, 5.43) this is justified.

Table 5.44 summarises the various published agreements obtained between measured and calculated line widths.

From tables 5.42 and 5.43 it is clear that the present theory does not provide the correct temperature behaviour for AIII, which, as is seen from table 5.44, is not achieved by any author. It is furthermore of interest to note that the

Table 5.42: Comparison between measured and calculated widths: AIII

Transition array	Designation	Wavelength	W_m	W_e	$\frac{W_s}{W_e} \%$	$\frac{W_{in}}{W_e} \%$	$\frac{W_{el}}{W_e} \%$	$\frac{W_i}{W_e} \%$	$\chi \%$	$\frac{W_m}{W_e}$
T = 21100 °K $N_e = 10^{17} \text{ cm}^{-3}$										
$3s^2 3p^3 ({}^2P^0) 3d'' - 4p''$	${}^3P_2^0 - {}^3P_2$	3391.8	0.132	0.111 0.149	52.0 38.5	31.7 23.5	16.3 37.9	1.2 0.9	96/58	1.19 0.89
$3s^2 3p^3 ({}^4S^0) 4s - 4p$	${}^5S_2^0 - {}^5P_3$	3285.8	0.145	0.108 0.155	47.1 32.7	28.7 20.0	24.2 47.3	1.1 0.8	98/93	1.34 0.94
$3s^2 3p^3 ({}^4S^0) 4s - 4p$	${}^5S_2^0 - {}^5P_2$	3301.9	0.139	0.109 0.157	47.1 32.7	28.8 20.0	24.2 47.3	1.1 0.8	98/93	1.28 0.89
$3s^2 3p^3 ({}^2D^0) 4s' - 4p'$	${}^3D_3^0 - {}^3D_3$	3480.6	0.132	0.128 0.181	45.6 32.3	32.0 22.6	22.4 45.1	1.0 0.7	100/94	1.03 0.73
$3s^2 3p^3 ({}^2D^0) 4s' - 4p'$	${}^3D_3^0 - {}^3F_4$	3336.1	0.143	0.119 0.168	45.9 32.4	31.3 22.1	22.9 45.6	1.0 0.7	100/94	1.20 0.85
T = 23080 °K $N_e = 10^{17} \text{ cm}^{-3}$										
$3s^2 3p^3 ({}^4S^0) 4s - 4p$	${}^5S_2^0 - {}^5P_3$	3285.8	0.103	0.106 0.150	45.8 32.5	30.3 21.5	23.8 45.9	1.1 0.8	98/93	0.97 0.69
$3s^2 3p^3 ({}^4S^0) 4s - 4p$	${}^5S_2^0 - {}^5P_2$	3301.9	0.096	0.107 0.151	45.8 32.5	30.4 21.6	23.8 45.9	1.1 0.8	98/93	0.90 0.64
$3s^2 3p^3 ({}^2D^0) 4s' - 4p'$	${}^3D_3^0 - {}^3D_3$	3480.6	0.101	0.126 0.175	44.4 32.1	33.5 24.2	22.1 43.7	1.0 0.7	100/94	0.80 0.58
$3s^2 3p^3 ({}^2D^0) 4s' - 4p'$	${}^3D_3^0 - {}^3F_4$	3336.1	0.104	0.117 0.162	44.6 32.2	32.8 23.6	22.6 44.2	1.1 0.8	100/94	0.89 0.64

Table 5.43: Comparison between measured and calculated widths: AIV

Transition array	Designation	Wavelength	W_m	W_e	$\frac{W_s}{W_e} \%$	$\frac{W_{in}}{W_e} \%$	$\frac{W_{el}}{W_e} \%$	$\frac{W_i}{W_e} \%$	$x \%$	$\frac{W_m}{W_e}$
T = 20750 °K $N_e = 10^{17} \text{ cm}^{-3}$										
3s ² 3p ² (³ P)4s - 4p	⁴ P _{5/2} - ⁴ D _{7/2} ⁰	2809.4	0.061	0.068 0.094	59.7 43.0	23.7 17.1	16.6 39.9	0.6 0.4	95/94	0.90 0.65
3s ² 3p ² (³ P)4s - 4p	⁴ P _{5/2} - ⁴ P _{5/2} ⁰	2640.3	0.055	0.061 0.085	60.0 43.7	22.7 16.4	16.7 39.9	0.6 0.5	95/94	0.90 0.65
T = 22200 °K $N_e = 10^{17} \text{ cm}^{-3}$										
3s ² 3p ² (³ P)4s - 4p	⁴ P _{5/2} - ⁴ D _{7/2} ⁰	2809.4	0.059	0.066 0.091	58.9 42.9	24.3 17.7	16.8 39.4	0.6 0.4	95/94	0.89 0.65
3s ² 3p ² (³ P)4s - 4p	⁴ P _{5/2} - ⁴ P _{5/2} ⁰	2640.3	0.055	0.060 0.082	59.7 43.6	23.4 17.0	16.9 39.4	0.7 0.5	95/94	0.92 0.67

method	author and reference	$\frac{W_m}{W_e}(T_1)$	$\frac{W_m}{W_e}(T_2)$
AIII		$T = 21100 \text{ } ^\circ\text{K}$	$T = 23080 \text{ } ^\circ\text{K}$
method I	MTD2A (Hey 1979)	1.21 ± 0.05	0.89 ± 0.03
method II	MTD2A (Hey 1979)	0.86 ± 0.04	0.64 ± 0.02
semi-empirical	Hey (1977b)	1.57 ± 0.08	1.16 ± 0.04
semi-classical	} Dimitrijević and Konjević (1980a)	0.71 ± 0.04	-
SEM		0.99 ± 0.08	-
SCM		0.99 ± 0.05	-
AIV		$T = 20750 \text{ } ^\circ\text{K}$	$T = 22200 \text{ } ^\circ\text{K}$
method I	MTD2A	0.91 ± 0.01	0.91 ± 0.01
method II	MTD2A	0.65 ± 0.01	0.66 ± 0.01
semi-empirical	Hey (1977b)	1.24 ± 0.01	1.27 ± 0.03
semi-classical	} Dimitrijević and Konjević (1980a)	0.59 ± 0.01	0.60 ± 0.01
SEM		0.75 ± 0.01	0.77 ± 0.02
SCM		0.92 ± 0.01	0.93 ± 0.02

Table 5.44: Comparison of calculational methods for AIII and AIV

often assumed temperature scaling as $\frac{1}{\sqrt{T}}$ is not strictly applicable, as is borne out by the consideration of the following parameter (Hey: 1977b) at normalised electron density $N_e = 10^{17} \text{ cm}^{-3}$:

$$C(1, 2) = \frac{W_m(T_2)}{W_m(T_1)} \left(\frac{kT_2}{kT_1} \right)^{1/2}$$

which for the two Argon ions becomes:

AIII	$\lambda 3285.8 \text{ \AA}$	$C(1,2) = 0.94$
	$\lambda 3301.9 \text{ \AA}$	$C(1,2) = 0.72$
	$\lambda 3480.6 \text{ \AA}$	$C(1,2) = 0.80$
	$\lambda 3336.1 \text{ \AA}$	$C(1,2) = 0.72$
AIV	$\lambda 2809.4 \text{ \AA}$	$C(1,2) = 1.00$
	$\lambda 2640.3 \text{ \AA}$	$C(1,2) = 1.03$

For AIV, $C(1,2)$ is of the order of unity and indeed good agreement has been obtained (for the temperature scaling) by all authors.

If one accepts the previous observation that extrapolation below threshold should be accomplished using elastic contributions lying between method I and method II for AIII, then it appears from table 5.44 that comparable agreement with the experiment as obtained by Dimitrijević and Konjević (1980a) should be obtained as is indeed the case for AIV. In order to ascertain the success by Dimitrijević and Konjević (1980a) in the calculation of the AIII line widths, results of their methods (SCM, SEM) at a temperature of 23080 °K are required, as the correct scaling cannot be deduced from their success for AIV. Their good agreement may thus be fortuitous at the temperature of 21100 °K.

A subsequent investigation of the apparent discrepancies in AIII line widths by Konjević (1980, private communication) has revealed that some of the earlier data of Platiša et al. (1975) obtained for the lower plasma temperature, are faulty, owing to possible experimental problems related to the plasma source, but that their higher temperature data may be regarded as reliable. This may be taken as a confirmation of the

contention by Hey (1977b).

On the whole, the AIII and AIV lines seem to confirm thus the conclusions made already for the oxygen ions.

5.5 STARK WIDTHS OF ISOLATED NITROGEN ION LINES

Apart from providing a means for investigation of homologous and multiply ionised ions (table 0.1), the ions NIII and NIV exemplify the already encountered difficulty of scaling of line widths with temperature and density. A recent study by Källne et al. (1979) raised several controversial questions, as inconsistencies with published experimental data (Popović et al.: 1975) and also theoretical line widths were reported.

Semi-empirical (Griem: 1968) calculations performed by Hey (1976b; see also Hey and Bryan: 1977) of line widths from NIII measurements by Popović et al. (1975) at the temperature of ~ 2 eV and electron density $N_e = 5.5 \times 10^{16} \text{ cm}^{-3}$ yielded the rather unsatisfactory agreement of:

$$\frac{W_m}{W_e} (H) = 1.67 \pm 0.22$$

Theoretical line widths have also been published for these three lines by Dimitrijević and Konjević (1980a) yielding the following agreement:

$$\frac{W_m}{W_e} \text{ (SC)} = 0.67 \pm 0.11 \quad (\text{Griem: 1974, eq. 526})$$

$$\frac{W_m}{W_e} \text{ (SEM)} = 0.92 \pm 0.13$$

$$\frac{W_m}{W_e} \text{ (SCM)} = 0.95 \pm 0.17$$

The subsequent experimental study by Källne et al. (1979) at electron density $N_e = 1.4 \times 10^{18} \text{ cm}^{-3}$ and electron temperature of $T = 5 \text{ eV}$ reported for NIII:

$$\frac{W_m}{W_e} \text{ (SC)} = 1.43 \pm 0.22$$

and for a single NIV line:

$$\frac{W_m}{W_e} \text{ (SC)} = 5.28$$

Furthermore, the reported experimental line widths, when scaled down to the conditions of Popović et al. (1975) were found to exceed the earlier measured widths. Defining (Hey: 1977b):

$$C(1,2) = \frac{W_m(T_2, N_{e2}) \left(\frac{k T_2}{k T_1} \right)^{1/2} N_{e1}}{W_m(T_1, N_{e1}) N_{e2}}$$

the above disagreement between experiment can be expressed as follows:

$$\text{N III } 3s \ ^2S_{1/2} - 3p \ ^2P_{3/2}^o \quad \lambda = 4097.3 \text{ \AA} \quad C(1,2) = 0.2$$

(compare with ~ 0.76 for AIII (Hey: 1977b)).

It is thus of particular interest to examine how the present theory (Hey: 1979) copes with this anomaly. Recently compiled data on the atomic structure of Nitrogen (Moore: 1971b, 1975) minimised the problems of missing term values. Nevertheless, the following NIII term values had to be estimated from quantum defect analysis:

(³ P ⁰) 4s 2P ⁰	E = 370267 cm ⁻¹
5s 2P ⁰	E = 401421 cm ⁻¹
5d 2D	E = 409669 cm ⁻¹
5f 2D, 2F, 2G	E = 410471 cm ⁻¹

Correcting the ionisation energies of NIII and NIV given by Moore (1971b, 1975) for the appropriate series limit from the higher ionisation stage yields:

NIII	(¹ S) parent	E _∞ = 382703.8 cm ⁻¹
	(³ P ⁰) parent	E _∞ = 450049.1 cm ⁻¹
NIV	(² S) parent	E _∞ = 624866 cm ⁻¹

In the case of NIII, transitions to the ground state 2p² need to be corrected for equivalent electrons, and using eq. 2.20 one obtains:

$$f(2p3s \rightarrow 2p^2) = \frac{5}{6} f(3s \rightarrow 2p) \quad , \quad N |G_{s,l}^{s,l}|^2 = 2$$

Similarly, for NIV transitions to the state 2s² need to be included and one obtains as above:

$$f(2s3p \rightarrow 2s^2) = \frac{1}{2} f(3p \rightarrow 2s) \quad , \quad N |G_{s,l}^{s,l}|^2 = 2$$

As for the previous ions, the method MTD2A was employed for calculations, but with the inclusion of estimates of the disentanglement parameter and average collision time obtained for typical collisions (see Chapter 4).

The results obtained for calculations at temperatures of 2 eV and 5 eV have been tabulated in table 5.51 for a normalised electron density of $N_e = 10^{17} \text{ cm}^{-3}$. The same notation as for the previous tables has been used. The additional columns DP and CP refer to the estimates of the disentanglement parameter and also the collision time parameter $W_e \bar{\tau}$, which are both required to be much less than unity for validity of the impact approximation. The two values quoted in the table refer to estimates for method I only and correspond to evaluation for the upper and lower transition level respectively. For method II similar values have been obtained and these have thus been omitted from the table. It should be noted that only the NIII line (1S) $3s - 3p \lambda = 4097.3$ is common to both experiments. The notation, e.g. 2-06 for 2×10^{-6} , is employed for these two parameters.

Ion broadening contributions to the line width have been neglected and since estimates of the quadrupole ion width remain below 1% this neglect is sufficiently justified.

The general agreement of theoretical line widths with experimental data at the high electron temperature of 5 eV (Källne et al.: 1979) for NIII of:

Transition array	Designation	λ (Å)	W_m	W_e	$\frac{W_s}{W_e} \%$	$\frac{W_{in}}{W_e} \%$	$\frac{W_{el}}{W_e} \%$	$\frac{W_i}{W_e} \%$	$x \%$	$\frac{W_m}{W_e}$	DP	CP ($W_e \tau$)
NIII T = 2 eV W_m from Popović <u>et al.</u> (1975) $N_e = 10^{17} \text{ cm}^{-3}$												
$2s^2 ({}^1S) 3s - 3p$	${}^2S_{1/2} - {}^2P_{3/2}^0$	4097.3	0.174	0.163 0.212	41.4 31.9	38.3 29.5	20.3 38.6	0.6 0.4	92/94	1.07 0.82	8-05 2-06	7-04 9-05
$2s^2 ({}^1S) 3p - 3d$	${}^2P_{1/2}^0 - {}^2D_{3/2}$	4634.2	0.204	0.218 0.280	37.9 29.6	46.5 36.3	15.6 34.1	0.8 0.6	82/92	0.94 0.73	6-05 8-05	7-04 7-04
$2s^2 ({}^1S) 3p - 3d$	${}^2P_{3/2}^0 - {}^2D_{5/2}$	4640.6	0.209	0.230 0.292	40.7 32.1	44.4 35.0	14.9 32.9	0.8 0.6	82/92	0.91 0.72	6-05 8-05	7-04 7-04
$2s^2 ({}^3P^0) 3s - 3p$	${}^4P_{5/2}^0 - {}^4P_{5/2}$	3367.3	0.178	0.101 0.134	33.0 24.9	45.3 34.2	21.8 40.9	0.9 0.7	89/94	1.76 1.33	5-06 3-06	2-04 9-05
NIII T = 5 eV W_m from Källne <u>et al.</u> (1979) $N_e = 10^{17} \text{ cm}^{-3}$												
$2s^2 ({}^1S) 3s - 3p$	${}^2S_{1/2} - {}^2P_{3/2}^0$	4097.3	0.54	0.152 0.170	30.0 26.9	59.7 53.5	10.4 19.5	0.6 0.5	92/94	3.55 3.18	5-06	1-04
$2s^2 ({}^1S) 3s - 3p$	${}^2S_{1/2} - {}^2P_{1/2}^0$	4103.3	0.41	0.154 0.171	30.6 27.5	59.1 53.1	10.3 19.4	0.6 0.5	92/94	2.66 2.40	5-06	1-04
$2s^2 ({}^3P^0) 3s - 3p$	${}^2P_{1/2}^0 - {}^2D_{3/2}$	4195.7	0.59	0.194 0.213	26.6 24.1	64.4 58.6	9.0 17.3	0.6 0.5	92/100	3.04 2.77	5-06 9-06	2-04 2-04
$2s^2 ({}^3P^0) 3s - 3p$	${}^2P_{3/2}^0 - {}^2D_{5/2}$	4200.0	0.53	0.193 0.213	26.1 23.8	64.8 58.9	9.0 17.4	0.6 0.5	92/100	2.75 2.49	5-06 9-06	2-04 2-04
NIV T = 5 eV W_m from Källne <u>et al.</u> (1979) $N_e = 10^{17} \text{ cm}^{-3}$												
$2s ({}^2S) 3p - 3d$	${}^1P_1^0 - {}^1D_2$	4057.8	0.53	0.104 0.118	38.1 33.7	53.3 47.1	8.6 19.2	0.4 0.4	81/92	5.10 4.49		

Table 5.51: Comparison between measured and calculated widths: NIII, NIV

$$\frac{W_m}{W_e} \text{ (I)} = 3.00 \pm 0.20 \text{ method I}$$

$$\frac{W_m}{W_e} \text{ (II)} = 2.71 \pm 0.18 \text{ method II}$$

is highly unsatisfactory. This is surprising, as in this high temperature regime the major contributions are from weak inelastic contributions to the line width, for which the present theory is expected to hold best. For NIV, the agreement is of the same inferior magnitude as obtained by the semi-classical method (Griem: 1974, eq. 526):

$$\frac{W_m}{W_e} \text{ (SC)} = 5$$

With the exception of the last NIII line $\lambda 3367.3 \text{ \AA}$, agreement between calculated and measured values at 2 eV (Popović et al.: 1975) is better than 10%. This is a marked improvement on the agreement obtained previously by Hey (1976b; Hey and Bryan: 1977) and is comparable with the results obtained by Dimitrijević and Konjević (1980a).

Calculation of the disentanglement condition and the collision time restrictions indicate that the impact approximation is well satisfied by the present demarcation of weak and strong collisions. The high completeness (χ) obtained excludes the possibility of major contributions to the line width by "forbidden" transitions. Calculations of the Doppler width (FWHM):

$$W_D = 2\lambda \sqrt{\frac{2kT \ln 2}{M c^2}}$$

for the NIV line at experimental conditions of $N_e = 1.4 \times 10^{18} \text{ cm}^{-3}$ and $T = 5 \text{ eV}$ confirm the assertion by Källne et al. (1979) that this mechanism is negligible compared with the Stark broadening process. The complete failure by all of the listed methods to predict the NIII and NIV line widths correctly at such high temperatures seems to indicate the presence of either an experimental error in the line width quoted by Källne et al. (1979), or a temperature dependence of line widths so far unexplained. To test the latter possibility, an investigation of line widths published for the homologous ion CIII at the temperature of $\sim 5 \text{ eV}$ has been included in this chapter, and good agreement between theory and experiment (Bogen: 1972) has been obtained. In a private communication from Dimitrijević and Konjević (1980b), strong evidence has been suggested to show that important optical depth corrections were ignored in the data analysis by Källne et al. (1979), which consequently invalidates many of their published line widths.

Despite the deterioration of the present theory for the NIII $\lambda 3367.3$ line, a still acceptable agreement between theory and experiment (Popović et al.: 1975) by the present method is obtained:

$$\frac{W_m}{W_e} \text{ (I)} = 1.17 \pm 0.20$$

$$\frac{W_m}{W_e} \text{ (II)} = 0.90 \pm 0.14$$

thus supporting the conclusions already made for the oxygen ions for the present theory.

5.6 STARK BROADENING FROM ISOLATED ClIII AND FII ION LINES

FII and ClIII are homologous to AIII and AIV respectively. Measurements from a low pressure pulsed arc were obtained by Platiša et al. (1977) for both ions in a regime of plasma conditions ($N_e = 5.8 \times 10^{16} \text{ cm}^{-3}$, $T = 24200 \text{ }^\circ\text{K}$) where the previously stated anomaly of temperature and density scaling does not arise. Experimental line widths of five FII lines from three multiplets and of fifteen ClIII lines from seven multiplets as well as predicted line widths by a wide range of authors are available and the reported agreements have been tabulated below:

F II:	$\frac{W_m}{W_e}$ (G)	= 1.04 ± 0.01	2 lines	1 multiplet	Jones et.al. (1971)
	$\frac{W_m}{W_e}$ (B)	= 0.64 ± 0.02	5 l.	3 m.	Baranger (1962)
	$\frac{W_m}{W_e}$ (CO)	= 1.13 ± 0.05	5 l.	3 m.	Cooper+Oertel (1967,1969)
	$\frac{W_m}{W_e}$ (SE)	= 0.80 ± 0.04	5 l.	3 m.	Griem (1968)
	$\frac{W_m}{W_e}$ (H)	= 1.54 ± 0.13	3 l.	3 m.	Hey (1977d)
Cl III:	$\frac{W_m}{W_e}$ (B)	= 1.10 ± 0.03	15 l.	7 m.	
	$\frac{W_m}{W_e}$ (CO)	= 1.83 ± 0.07	15 l.	7 m.	
	$\frac{W_m}{W_e}$ (SE)	= 0.86 ± 0.02	15 l.	7 m.	
	$\frac{W_m}{W_e}$ (H)	= 1.70 ± 0.06	7 l.	7 m.	
	$\frac{W_m}{W_e}$ (SC)	= 0.74 ± 0.02	7 l.	7 m.	Griem (1974)
	$\frac{W_m}{W_e}$ (SEM)	= 1.01 ± 0.03	7 l.	7 m.	} Dimitrijević + Konjević (1980a)
	$\frac{W_m}{W_e}$ (SCM)	= 1.04 ± 0.04	7 l.	7 m.	

For both FII and ClIII, the measured variations within multiplets are very small, and this can be attributed to the fact that ΔE is comparable with kT , thus minimising structure effects at these plasma conditions. It is thus sufficient to calculate line widths for one representative member of each multiplet only, as done by Hey (1977d) and Dimitrijević and Konjević (1980a).

Using the atomic data by Kelly and Palumbo (1973), the ionisation energies for these ions were:

FII	$(^4S^0)$ parent	$E_\infty = 282058.6 \text{ cm}^{-1}$
	$(^2D^0)$ parent	$E_\infty = 316157 \text{ cm}^{-1}$
ClIII	(^3P) parent	$E_\infty = 320408.67 \text{ cm}^{-1}$
	(^1D) parent	$E_\infty = 333266 \text{ cm}^{-1}$

Several term energies missing from the energy level tables for ClIII (Moore: 1971a) had to be estimated using quantum defect analysis, as they were found to contribute substantially to the completeness of the perturbing level set. The following values were used (in cm^{-1}):

(^3P)	5p $^4S^0$	256800
	5p $^4P^0$	255800
	5p $^4D^0$	254800
	4f 4D	256800
(^3P)	5s 2P	245900
	4d 2P	248200
	4p 2S	207000
	5p 2S	257100
(^1D)	3d 2G	197800
	4d 2G	252600
	5p $^2P, ^2D$	271500

Since the equivalent electron level of ClIII, $3s^2 3p^3 4s^0$, was found to contribute sufficiently to be incorporated, the atomic oscillator strength for transitions to this level had to be corrected using eq. 2.20, thus yielding for ClIII:

$$f(3p^2(^3P)nl LSJ \rightarrow 3p^3 ^4S_{3/2}^0) = 3.0 f(nl LSJ \rightarrow 3p ^4S_{3/2}^0)$$

$$f(3p^2(^3P)nl LSJ \rightarrow 3p^3 ^2P_{3/2}) = 1.5 f(nl LSJ \rightarrow 3p ^2P_{3/2})$$

$$f(3p^2(^3P)nl LSJ \rightarrow 3p^3 ^2D_{3/2}) = 1.5 f(nl LSJ \rightarrow 3p ^2D_{3/2})$$

$$f(3p^2(^1D)nl LSJ \rightarrow 3p^3 ^2D_{3/2}) = 1.5 f(nl LSJ \rightarrow 3p ^2D_{3/2})$$

$$f(3p^2(^1D)nl LSJ \rightarrow 3p^3 ^2P_{3/2}) = 0.833f(nl LSJ \rightarrow 3p ^2P_{3/2})$$

The fractional parentage coefficients were obtained from Sobel'man (1972, p. 105). Similarly, in the case of FII, the inclusion of the equivalent electron level $2p^4$ required the use of:

$$f(2p^3(^2D^0)nl LSJ \rightarrow 2p^4 ^3P_{3/2}) = 1.66 f(nl LSJ \rightarrow 2p ^3P_{3/2})$$

$$f(2p^3(^2D^0)nl LSJ \rightarrow 2p^4 ^1S_{3/2}) = 0 f(nl LSJ \rightarrow 2p ^1S_{3/2})$$

$$f(2p^3(^2D^0)nl LSJ \rightarrow 2p^4 ^1D_{3/2}) = 3.0 f(nl LSJ \rightarrow 2p ^1D_{3/2})$$

Using the above details for the atomic structure, the results obtained for calculations (MTD2A) at the plasma conditions

of electron density $N_e = 10^{17} \text{ cm}^{-3}$ and temperature $T = 24200 \text{ }^\circ\text{K}$, are presented in tables 5.61, 5.62. Ion broadening contributions to the line width were neglected and the quadrupole ion broadening estimate (eq. 4.32) indicates an associated error of about 1%.

For both ions, the weak collisions remain within the impact approximation as formulated by Baranger (1958b). Excellent completeness (χ) is obtained for FII and most lines of ClIII, where a 59% complete set of perturbers only was achieved for the lower level of one transition.

For FII, the agreement between calculated and measured line widths:

$$\frac{W_m}{W_e} \text{ (I)} = 1.04 \pm 0.09 \text{ method I}$$

$$\frac{W_m}{W_e} \text{ (II)} = 0.77 \pm 0.06 \text{ method II}$$

is comparable for method I with the best agreement obtained by Jones et al. (1971) and for method II lies within the range of obtained results. Comparing the completeness obtained with the result from Platiša et al. (1977) indicates that similar perturber sets were employed. The ion contributions obtained here are similar to the ones calculated by Platiša et al. (1977) giving the ion broadening parameter α as formulated by Griem (1964). From the comparison of results from method I and method II it would appear as if the correct extrapolation procedure below threshold for the inclusion of the elastic terms is slightly underestimated by

Table 5.61: Comparison between measured and calculated widths: FII

Transition array	Designation	λ (Å)	W_m	W_e	$\frac{W_s}{W_e} \%$	$\frac{W_{in}}{W_e} \%$	$\frac{W_{el}}{W_e} \%$	$\frac{W_i}{W_e} \%$	$x \%$	$\frac{W_m}{W_e}$	DP	CP
T = 24200 °K $N_e = 10^{17} \text{ cm}^{-3}$												
$2p^3 3s - 2p^3 ({}^4S^0) 3p$	${}^5S_2^0 - {}^5P_3$	3847.1	0.203	0.168 0.228	38.9 28.7	35.2 26.0	25.8 45.3	1.7 1.2	96/95	1.21 0.89	4-05 1-06	5-04 7-05
$2p^3 3s - 2p^3 ({}^2D^0) 3p$	${}^3D_3^0 - {}^3D_3$	4109.17	0.193	0.192 0.260	38.6 28.5	35.8 26.4	25.7 45.1	1.5 1.1	96/95	1.01 0.74	4-05 8-07	6-04 6-05
$2p^3 3s - 2p^3 ({}^2D^0) 3p$	${}^1D_2^0 - {}^1F_3$	4299.17	0.203	0.224 0.299	37.7 28.2	37.3 27.9	25.0 44.0	1.4 1.1	96/94	0.91 0.68	4-05 2-06	4-04 1-04

Table 5.62: Comparison between measured and calculated widths: ClIII

Transition array	Designation	λ (Å)	W_m	W_e	$\frac{W_s}{W_e} \%$	$\frac{W_{in}}{W_e} \%$	$\frac{W_{el}}{W_e} \%$	$\frac{W_i}{W_e} \%$	$x \%$	$\frac{W_m}{W_e}$	DP	$\frac{CP}{(W_e \tau)}$
T = 24200 °K $N_e = 10^{17} \text{ cm}^{-3}$												
$3p^2 (^3P) 3d - 4d$	$^4P_{3/2} - ^4P_{5/2}^o$	4018.5	0.191	0.161 0.211	46.9 36.0	36.7 28.1	16.3 35.9	1.0 0.8	90/59	1.19 0.91	3-05 9-07	6-04 9-05
$3p^2 (^3P) 4s - 4p$	$^4P_{5/2} - ^4D_{7/2}^o$	3602.1	0.183	0.130 0.178	42.5 31.1	34.7 25.4	22.8 43.5	1.1 0.8	88/93	1.41 1.03	3-05 2-06	7-04 7-05
$3p^2 (^3P) 4s - 4p$	$^4P_{3/2} - ^4P_{5/2}^o$	3283.41	0.167	0.119 0.161	42.5 31.4	35.5 26.3	22.0 42.3	1.3 1.0	90/93	1.40 1.04	3-05 2-06	6-04 6-05
$3p^2 (^3P) 4s - 4p$	$^4P_{5/2} - ^4S_{3/2}^o$	3191.45	0.166	0.125 0.165	41.4 31.3	38.3 28.9	20.3 39.7	1.3 1.0	97/94	1.33 1.01	2-05 2-06	7-04 7-05
$3p^2 (^3P) 4s - 4p$	$^2P_{1/2} - ^2D_{3/2}^o$	3748.81	0.186	0.179 0.230	37.7 28.9	43.2 33.1	19.2 38.1	0.9 0.7	98/94	1.04 0.80	1-04 2-06	7-04 7-05
$3p^2 (^1D) 4s - 4p$	$^2D_{5/2} - ^2F_{7/2}^o$	3530.03	0.181	0.161 0.212	39.2 29.9	41.0 31.2	19.7 38.9	1.0 0.7	100/93	1.12 0.85	3-05 2-06	8-04 8-05
$3p^2 (^1D) 4s - 4p$	$^2D_{3/2} - ^2D_{5/2}^o$	3392.89	0.147	0.139 0.180	38.9 29.7	41.5 31.6	19.6 38.7	1.1 0.9	96/93	1.06 0.80	3-05 2-06	8-04 7-05

method I and should lie in between this method and the constant extrapolation at \bar{g}_{th} suggested by Griem (1968).

For ClIII, the following agreement has been obtained between calculated and measured values:

$$\frac{W_m}{W_e} \text{ (I)} = 1.22 \pm 0.06 \quad \text{method I}$$

$$\frac{W_m}{W_e} \text{ (II)} = 0.92 \pm 0.04 \quad \text{method II}$$

Method I is thus seen to be inferior to previously applied calculations, whereas method II yields comparable results to the successful predictions by Dimitrijević and Konjević. The question of a definite choice of extrapolation procedures thus remains to be solved. It is furthermore of interest to note that the ion broadening estimates made are similar to those by Platiša *et al.* (1977) and the problem experienced in achieving completeness of perturbing levels for the $\lambda 4018.5$ line was also encountered by Platiša *et al.* (1977), who obtained a similar low value of completeness.

Similar ratios of measured to calculated widths as for ClIII were obtained for OIII, thus leading to the conclusion that elastic contributions might be of greater importance for higher ionisation stages - this and the remaining conclusions made for oxygen are substantiated by the agreement of experiment and theory obtained for FII and ClIII.

5.7 STARK WIDTHS OF ISOLATED CIII ION LINES

Comparison of theoretical line widths with measured widths is of particular interest for this ion, as CIII is isoelectronic to NIV, for which unsatisfactory agreement was obtained between theory and experiment (see Chapter 5.5). Furthermore, measurements of seven CIII lines (Bogen: 1972) were performed at the comparatively high plasma temperature of 56000 °K, thus placing calculations into a regime where the effective Gaunt factor approximation for the calculation of collision cross-sections is expected to hold best (Bethe approximation). An additional point of interest is the reported discrepancy between theory and experiment for the $\lambda = 4326 \text{ \AA}$ line reported in the literature (Bogen: 1972; Griem: 1974). It has been suggested by Bogen (1972) that this discrepancy could be owing to the neglect of collisions causing transitions between the two CIII term systems with ionisation limits CIV 2S and 2P . This case was also discussed by Hey (1977b), who argued that a more plausible explanation might be the neglect of "semi-forbidden" collision-induced transitions of the type $3p \ ^1D \rightarrow 3d \ ^3F$, $3p \ ^1D \rightarrow 3d \ ^3D^0$. This possibility of spin-flip has already been mentioned in the case of SIII (see Chapter 5.3).

The following agreement between theoretical Stark widths and the measurements from a theta pinch experiment (Bogen: 1972) at electron temperature $T = 56000 \text{ }^\circ\text{K}$ and electron density $N_e = 4 \times 10^{17} \text{ cm}^{-3}$ has been reported (Bogen: 1972; Griem: 1974; Dimitrijević and Konjević: 1980a):

$\frac{W_m}{W_e}$ (SE)	= 1.66 ± 0.37	semi-empirical method by Griem (1968)
$\frac{W_m}{W_e}$ (SEM)	= 1.29 ± 0.17	modified semi-empirical method by Dimitrijević and Konjević (1980a)
$\frac{W_m}{W_e}$ (SC)	= 0.93 ± 0.12	semi-classical method by Griem (1974, eq. 526)
$\frac{W_m}{W_e}$ (SCM)	= 0.97 ± 0.17	modified semi-classical method by Dimitrijević and Konjević (1980a)
$\frac{W_m}{W_e}$ (SCP)	= 1.32 ± 0.22	straight classical path method by Griem (1962)

The success obtained by the straight classical path method has been attributed to the small inherent level splitting ($\Delta E \ll kT$) occurring in CIII (Griem: 1974).

Using the energy level tables by Moore (1970) to compile the required input data for MTD2A, the ionisation energy was corrected for the appropriate series limit to yield:

$$\begin{array}{ll}
 {}^2S \text{ parent} & E_{\infty} = 386241 \text{ cm}^{-1} \\
 {}^2P \text{ parent} & E_{\infty} = 450797 \text{ cm}^{-1}
 \end{array}$$

The results thus obtained by the present theory (MTD2A) have been listed in table 5.71 using the same notation as for the previous sections of this chapter. An estimate of the

Table 5.71: Comparison between measured and calculated widths: CIII

T = 56000 °K N _e = 10 ¹⁷ cm ⁻³												
Transition array	Designation	λ (Å)	W _m	W _e	$\frac{W_s}{W_e}$ %	$\frac{W_{in}}{W_e}$ %	$\frac{W_{el}}{W_e}$ %	$\frac{W_i}{W_e}$ %	χ %	$\frac{W_m}{W_e}$	DP	$\frac{CP}{(W_e \tau)}$
2s(²S)3p - 3d	¹P ₁ ^o - ¹D ₂	5695.9	0.475	0.345 0.382	17.3 15.6	73.4 66.2	9.2 18.1	0.7 0.6	90/92	1.38 1.24	2-05 3-05	3-04 3-04
2s(²S)3s - 3p	³S ₁ - ³P ₂ ^o	4647.4	0.238	0.247 0.271	24.0 21.9	67.5 61.6	8.5 16.4	0.5 0.5	90/95	0.96 0.88	3-05 6-06	4-04 1-04
2s(²S)4f - 5g	¹F ₃ ^o - ¹G ₄	4186.9	1.02	1.04 1.07	12.5 12.1	84.4 81.9	3.1 6.0	6.7 6.5	86/90	0.98 0.95	3-05 2-05	6-03 9-03
2s(²S)3d - 4f	¹D ₂ - ¹F ₃ ^o	2162.9	0.115	0.114 0.121	17.2 16.2	77.6 73.3	5.2 10.4	8.0 7.5	90/90	1.01 0.95	2-05 2-05	3-03 8-04
2s(²S)3p - 4d	¹P ₁ ^o - ¹D ₂	1531.8	0.107	0.108 0.111	8.7 8.6	89.2 87.2	2.1 4.2	6.6 6.4	79/92	0.99 0.96	3-05 3-05	7-03 2-03
2s(²P ^o)3s - 3p	¹P ₁ ^o - ¹D ₂	4325.5	0.525	0.257 0.278	21.4 19.7	71.3 65.9	7.3 14.3	0.6 0.6	91/93	2.04 1.89	7-06 1-05	2-03 4-04

neglected ion broadening has been made. Calculations have been performed at $T = 56000$ °K and $N_e = 10^{17}$ cm⁻³.

Comparing the results obtained in table 5.71 with the typical values obtained for the ions dealt with in the previous sections, it is immediately apparent that a much smaller proportion of the line width is made up by strong contributions and elastic collision contributions. This predominance of the inelastic contributions to the line width is expected, because of the much higher electron temperature encountered here. This high value of temperature is also responsible for the increased importance of the ion broadening mechanism. Agreement for the first six isolated lines (thus excluding the controversial $\lambda = 4325.56$ Å line) between the present theory and experiments is indeed excellent:

$$\frac{W_m}{W_e} \text{ (I)} = 1.06 \pm 0.08$$

$$\frac{W_m}{W_e} \text{ (II)} = 1.00 \pm 0.06$$

Recalculation of the $\lambda = 4325.56$ Å line width including the normally forbidden energy levels $3d \text{ } ^3F_{2,3}^0$ and $3d \text{ } ^3D_{1,2,3}^0$ in the set of perturbing levels yields the following improvement:

$$\frac{W_m}{W_e} \text{ (I)} = 1.54$$

$$\frac{W_m}{W_e} \text{ (II)} = 1.45$$

This 50% improvement of agreement seems to verify the remark

by Hey (1977b) regarding the possibility of spin flip as an additional effect of importance in the calculation of Stark widths. It should be pointed out, however, that a distorted-wave calculation by Blaha (1978, private communication) yielded collision strengths $\Omega(3p\ ^1D - 3d\ ^3D, ^3F)$ which were much smaller than $\Omega(3p\ ^1D - 3d\ ^1D)$, suggesting the need for an additional mechanism to explain this discrepancy. A proposal by Griem (1980, private communication) that a breakdown of LS coupling for these particular closely situated terms might be responsible, would probably also not help matters much. The inclusion of coupling correction factors (Hey: 1977b) would clearly increase the "most optimistic" ratios W_m/W_e given above. Furthermore, the n - and l -values involved for the outer (bound) electron are rather small, thus minimising LS coupling deviations (Cowan and Andrew: 1965). Further work to explain this discrepancy in the line width calculation is thus indicated.

The overall agreement obtained by the present theory is seen to lie well within the accuracy achieved by other authors:

$$\frac{W_m}{W_e} \text{ (I)} = 1.23 \pm 0.17$$

$$\frac{W_m}{W_e} \text{ (II)} = 1.14 \pm 0.16$$

and when considering the first six isolated lines only, the success achieved by the present method (MTD2A) remains unsurpassed.

It is thus apparent that the conclusions (a - d) made for

oxygen (section 5.2) remain valid for the type of electron structure exhibited by CIII and NIV, thus substantiating the contention made by Dimitrijević and Konjević (1980b, private communication) regarding the possible error in the measurement of the NIV line width by Källne et al. (1979).

CHAPTER 6CONCLUSION : TRENDS AND REGULARITIES

As already discussed, the ions investigated in the previous chapter can be grouped according to the outer electron structure (table 6.1) of their ground term. It has been pointed out repeatedly (Purić *et al.*: 1974, 1978, 1979a, b, 1980; Konjević and Dimitrijević: 1980) that the Stark width parameter exhibits regularities with respect to this ground term structure.

ground term	ion
$ns^2 \ ^1S$	CIII, NIV
$ns^2 np \ ^2P^0$	NIII, SIV, SnII
$ns^2 np^2 \ ^3P$	OIII, SIII
$ns^2 np^3 \ ^4S^0$	OII, ClIII, AIV
$ns^2 np^4 \ ^3P$	FII, AIII

Table 6.1: Homologous ions

Tabulation of the agreement obtained between the present theory (MTD2A, method I and II) and experimental data together with the experimental uncertainties for ions of various outer electron structure confirms this behaviour, insofar that the calculations yielded satisfactory consistency for the various groups of homologous ions (see tables 6.2 to 6.5). The unsatisfactory results obtained for NIV and NIII from the high temperature theta pinch experiment by Källne

Table 6.2: Transitions within homologous ions: ground term: $ns^2 np^2 p^0$

Ion	Transition	$\lambda (\text{\AA})$	$\frac{W_m}{W_e}$	Error (experiment)
NI ^{III}	$2s^2 3s - 2s^2 3p$	4097.3	$\begin{cases} 1.07 \\ 0.82 \end{cases}$	30%
SI ^{IV}	$3s^2 4s - 3s^2 4p$	3097.5	$\begin{cases} 1.14 \\ 0.89 \end{cases}$	18%

Table 6.3: Transitions within homologous ions: ground term: $ns^2 np^2 {}^3P$

Ion	Transition	$\lambda (\text{\AA})$	$\frac{W_m}{W_e}$	Error (experiment)
OI ^{III}	$2p3s {}^3P^0 - 2p3p {}^3D$	3754.7	$\begin{cases} 1.23 \\ 0.94 \end{cases}$	16%
SI ^{III}	$3p4s {}^3P^0 - 3p4p {}^3D$	4332.7	$\begin{cases} 1.03 \\ 0.81 \end{cases}$	18%
OI ^{III}	$2p3s {}^3P^0 - 2p3p {}^3P$	3047.1	$\begin{cases} 1.46 \\ 1.10 \end{cases}$	16%
SI ^{III}	$3p4s {}^3P^0 - 3p4p {}^3P$	3832.0	$\begin{cases} 0.98 \\ 0.78 \end{cases}$	18%
OI ^{III}	$2p3p {}^3D - 2p3d {}^3F^0$	3261.0	$\begin{cases} 1.30 \\ 1.02 \end{cases}$	16%
SI ^{III}	$3p4p {}^3D - 3p4d {}^3F^0$	2856.0	$\begin{cases} 1.07 \\ 0.93 \end{cases}$	18%
OI ^{III}	$2p3p {}^3P - 2p3d {}^3D^0$	3715.1	$\begin{cases} 1.07 \\ 0.84 \end{cases}$	16%
SI ^{III}	$3p4p {}^3P - 3p4d {}^3D^0$	2964.8	$\begin{cases} 0.96 \\ 0.84 \end{cases}$	18%

Table 6.4: Transitions within homologous ions: ground term: $ns^2 np^3 \ ^4S^0$

Ion	Transition	λ (Å)	$\frac{W_m}{W_e}$	Error (experiment)
OII	$2p^2(^3P)3s \ ^4P - 3p \ ^4D^0$	4649.1	$\left\{ \begin{array}{l} 0.80 \\ 0.63 \end{array} \right.$	16%
ClIII	$3p^2(^3P)4s \ ^4P - 4p \ ^4D^0$	3602.10	$\left\{ \begin{array}{l} 1.41 \\ 1.03 \end{array} \right.$	15%
AIV	$3p^2(^3P)4s \ ^4P - 4p \ ^4D^0$	2809.4	$\left\{ \begin{array}{l} 0.90 \\ 0.65 \end{array} \right.$	50%
		2809.4	$\left\{ \begin{array}{l} 0.89 \\ 0.65 \end{array} \right.$	50%
OII	$2p^2(^3P)3s \ ^4P - 3p \ ^4P^0$	4317.1	$\left\{ \begin{array}{l} 0.91 \\ 0.70 \end{array} \right.$	16%
ClIII	$3p^2(^3P)4s \ ^4P - 4p \ ^4P^0$	3283.4	$\left\{ \begin{array}{l} 1.40 \\ 1.04 \end{array} \right.$	15%
AIV	$3p^2(^3P)4s \ ^4P - 4p \ ^4P^0$	2640.3	$\left\{ \begin{array}{l} 0.90 \\ 0.65 \end{array} \right.$	50%
		2640.3	$\left\{ \begin{array}{l} 0.92 \\ 0.67 \end{array} \right.$	50%
OII	$2p^2(^3P)3s \ ^4P - 3p \ ^4S^0$	3712.8	$\left\{ \begin{array}{l} 1.08 \\ 0.84 \end{array} \right.$	16%
ClIII	$3p^2(^3P)4s \ ^4P - 4p \ ^4S^0$	3191.5	$\left\{ \begin{array}{l} 1.33 \\ 1.01 \end{array} \right.$	15%
OII	$2p^2(^3P)3s \ ^2P - 3p \ ^2D^0$	4414.9	$\left\{ \begin{array}{l} 0.94 \\ 0.74 \end{array} \right.$	16%
ClIII	$2p^2(^3P)4s \ ^2P - 4p \ ^2D^0$	3748.8	$\left\{ \begin{array}{l} 1.04 \\ 0.80 \end{array} \right.$	15%
OII	$2p^2(^1D)3s \ ^2D - 3p \ ^2F^0$	4596.2	$\left\{ \begin{array}{l} 0.88 \\ 0.68 \end{array} \right.$	16%
ClIII	$3p^2(^1D)4s \ ^2D - 4p \ ^2F^0$	3530.0	$\left\{ \begin{array}{l} 1.12 \\ 0.85 \end{array} \right.$	15%
OII	$2p^2(^1D)3s \ ^2D - 3p \ ^2D^0$	4347.4	$\left\{ \begin{array}{l} 0.85 \\ 0.66 \end{array} \right.$	16%
ClIII	$3p^2(^1D)4s \ ^2D - 4p \ ^2D^0$	3392.9	$\left\{ \begin{array}{l} 1.06 \\ 0.80 \end{array} \right.$	15%

Table 6.5: Transitions within homologous ions: ground term: $ns^2 np^4 \ ^3P$

Ion	Transition	$\lambda (\text{\AA})$	$\frac{W_m}{W_e}$	Error (experiment)
FII	$2p^3 (^4S^0) 3s \ ^5S^0 - 3p \ ^5P$	3847.10	$\left\{ \begin{array}{l} 1.21 \\ 0.89 \end{array} \right.$	17%
AIII	$3p^3 (^4S^0) 4s \ ^5S^0 - 4p \ ^5P$	3285.8	$\left\{ \begin{array}{l} 1.34 \\ 0.94 \end{array} \right.$	30%
		3285.8	$\left\{ \begin{array}{l} 0.97 \\ 0.69 \end{array} \right.$	
		3301.9	$\left\{ \begin{array}{l} 1.28 \\ 0.89 \end{array} \right.$	
		3301.9	$\left\{ \begin{array}{l} 0.90 \\ 0.64 \end{array} \right.$	
FII	$2p^3 (^2D^0) 3s \ ^3D^0 - 3p \ ^3D$	4109.2	$\left\{ \begin{array}{l} 1.01 \\ 0.74 \end{array} \right.$	17%
AIII	$3p^3 (^2D^0) 4s \ ^3D^0 - 4p \ ^3D$	3480.6	$\left\{ \begin{array}{l} 1.03 \\ 0.73 \end{array} \right.$	30%
		3480.6	$\left\{ \begin{array}{l} 0.80 \\ 0.58 \end{array} \right.$	

et al.: (1979) are thus an exception to the rule (see the excellent agreement for five CIII lines, Chapter 5.7) and the contention by Dimitrijević and Konjević (1980, private communication) regarding the erroneous analysis of the experimental data seems thus confirmed. Excluding these measurements from the sample of ion lines investigated, the results obtained by the present theory have been listed in table 6.6 together with the experimental plasma conditions. Together with these data, the best theoretical (semi-classical) method of calculation available from the literature has been presented in each case. From this presentation it is apparent that the modified semi-classical and semi-empirical methods of Dimitrijević and Konjević (1980a) form the only competitive (practical) means of predicting reliable Stark widths in large numbers apart from the method presented in this investigation. It seems clear, therefore, that the extension of the impact approximation by the classical path method and evaluation of collision cross-sections by the effective Gaunt factor method, as discussed in Chapter 1, is valid for practical computational purposes for the ionisation stages $Z = 2$ to 4 considered in this thesis.

Since the modified semi-classical and semi-empirical methods are based on the original formulation by Griem (semi-empirical: 1968; semi-classical: 1974), the two methods, as usually employed, fail to predict variations of line widths within multiplets (Hey: 1978) and they also exclude radiator structure effects such as equivalent electron configurations and configuration interaction. The present method, however,

Ground Term	Ion	$\frac{W_m}{W_e}$		Number of Lines	$(\frac{N_e}{10^{17}} \text{ (cm}^{-3}\text{)}, T(\text{eV}))$	Best Method
		Method I	Method II			
$ns^2 \ ^1S$	CIII	1.06 ± 0.08	<u>1.00 ± 0.06</u>	5	(4, 5)	MTD2A
$ns^2np \ ^2P$	NIII	1.17 ± 0.20	<u>0.89 ± 0.14</u>	4	(0.5, 2)	SCM
	SIV	1.14	<u>0.89</u>	1	(0.5, 2.5)	SCM
	SnII		<u>1.10 ± 0.15</u>	10	(1, 1)	MTD1
$ns^2np^2 \ ^3P$	OIII	1.27 ± 0.08	<u>0.98 ± 0.06</u>	4	(0.5, 2)	MTD2A
	SIII	<u>1.02 ± 0.02</u>	0.85 ± 0.02	16	(0.5, 2.5)	MTD2A
$ns^2np^3 \ ^4S^0$	OII	<u>0.91 ± 0.04</u>	0.73 ± 0.04	13	(0.5, 2)	MTD2A
	ClIII	1.22 ± 0.06	<u>0.92 ± 0.04</u>	6	(0.5, 2)	SEM
	AIV	<u>0.91 ± 0.01</u>	0.66 ± 0.01	4	(0.5, 2)	SCM
$ns^2np^4 \ ^3P$	FII	<u>1.04 ± 0.09</u>	0.77 ± 0.06	3	(0.5, 2)	CP
	AIII	<u>0.89 ± 0.03</u>	0.64 ± 0.02	4	(0.5, 2)	MTD2A

Key: MTD1, MTD2A - present investigation;
 SCM - modified semi-classical method by Dimitrijević and Konjević (1980a);
 SEM - modified semi-empirical method by Dimitrijević and Konjević (1980a);
 CP - classical path method by Jones et al. (1971).

Underlined result gives W_m/W_e ratio closer to unity.

Table 6.6: Comparison between theory and measurement

takes these details carefully into account (Chapter 2), as has been demonstrated in the case of SnII.

A further important difference between the present method and the previously derived semi-empirical and semi-classical method by Griem (1968, 1974) is the reformulation of the effective Gaunt factor approximation. The derived Gaunt factor (Chapter 3) has been found to yield improved theoretical

predictions of line widths owing to a better treatment of the upper and lower limits of the allowed impact parameter. This was seen to lead to several improvements on the previously developed Gaunt factor obtained by Griem (1968, 1974):

- (a) the correction for curvature of the electron orbit enabled the higher Z regime of ions to be dealt with successfully;
- (b) the correct limiting behaviour as well as continuity with energy has been ensured (Chapter 3.3);
- (c) rigorous averaging of the \bar{g} factor over a Maxwellian velocity distribution eliminated the need of a Gaunt factor varying slowly with respect to energy;
- (d) the artificial threshold value obtained on empirical grounds (van Regemorter: 1962) could be dispensed with;
- (e) the approach used lends itself readily to investigation of the method of inclusion of elastic cross-sections by extrapolation below threshold (Chapter 3.5).

From table 6.6 it is apparent that the method of extrapolation below threshold of the effective Gaunt factor forms a critical part in determining the success obtained by the line width calculations. Method I and method II correspond to two extreme means of extrapolation and both were found to yield successful predictions of line widths. Method II corresponds to extrapolation of $\bar{g} = \bar{g}_{th}$ below threshold (Griem: 1968) and is seen to result in many cases in an

overestimate of the elastic terms. Conversely, the continuous use of the derived Gaunt factor function in both the below- and above-threshold regimes of energy is seen to lead to an underestimate in some cases where method II of extrapolation was employed with greater success. From table 6.6 it would appear that the importance of the dipole elastic terms is related to the number of electrons in the outer orbitals of the ground configuration, since method I seems to be more successful for ions of the type $ns^2 np^i$ ($i \geq 3$) and method II for ions of the type $ns^2 np^i$ ($i < 3$). However, the determination of a single extrapolation procedure has to remain unsolved and further work in this respect is clearly required.

The effective Gaunt factor derived in this investigation is found to differ drastically from the simple constant value assumed by Purić et al. (1974, 1978, 1979a, b, 1980) in the prediction of trends and regularities of Stark widths based only on the regularities in the atomic oscillator strength (Wiese: 1968, 1969). As already discussed in Chapter 3.6, the effective Gaunt factor (expressions 3.39 and 3.41) differs significantly in its dependence on the radiator structure. Closer investigation of the variables entering into eqs. 3.39 and 3.41 shows that the threshold Gaunt factor:

$$\bar{g}_{th} \equiv \bar{g}_{th} (n_{l_s}^*, \Delta n^*, l_{n_c}, Z, l_s)$$

or

$$g_{th} \equiv g_{th} (n_{l_s}^*, E_\infty, \Delta E, Z, l_s)$$

- where
- $n_{l>}^*$ = effective principal quantum number of the higher angular momentum state;
 - Δn^* = level separation ΔE expressed as the difference in effective principal quantum number;
 - $l_{n<}$ = orbital angular momentum of the lower level;
 - Z = ionisation stage of radiator;
 - $l_{>}$ = maximum of $l_i, l_{i'}$.

One thus obtains for an ion of particular Z undergoing collisional excitation from $n\ell \rightarrow n'\ell'$ that:

$$\bar{g}_{th} \equiv \bar{g}_{th} (n_{l>}^*, \Delta n^*)$$

This unique behaviour is illustrated by the following graphs for an ion of ionisation stage Z (figs. 6.1, 6.2, 6.3). The dependence of the threshold Gaunt factor on the ionisation stage is found to be of the approximate form:

$$\bar{g}_{th} = a_0 + a_1 Z^{-1}$$

for the ions investigated in Chapter 5. This behaviour is apparent when plotting (\bar{g}_{th}) versus Z^{-1} as is shown for the example of the transition $(3.0)s \rightarrow (4.0)p$ in fig. 6.4.

This unique behaviour makes deductions of simple trends for the investigated non-resonance ion lines in an analogous

Fig. 6.1: Dependence of threshold Gaunt factor on change in effective principal quantum number: s-p transitions

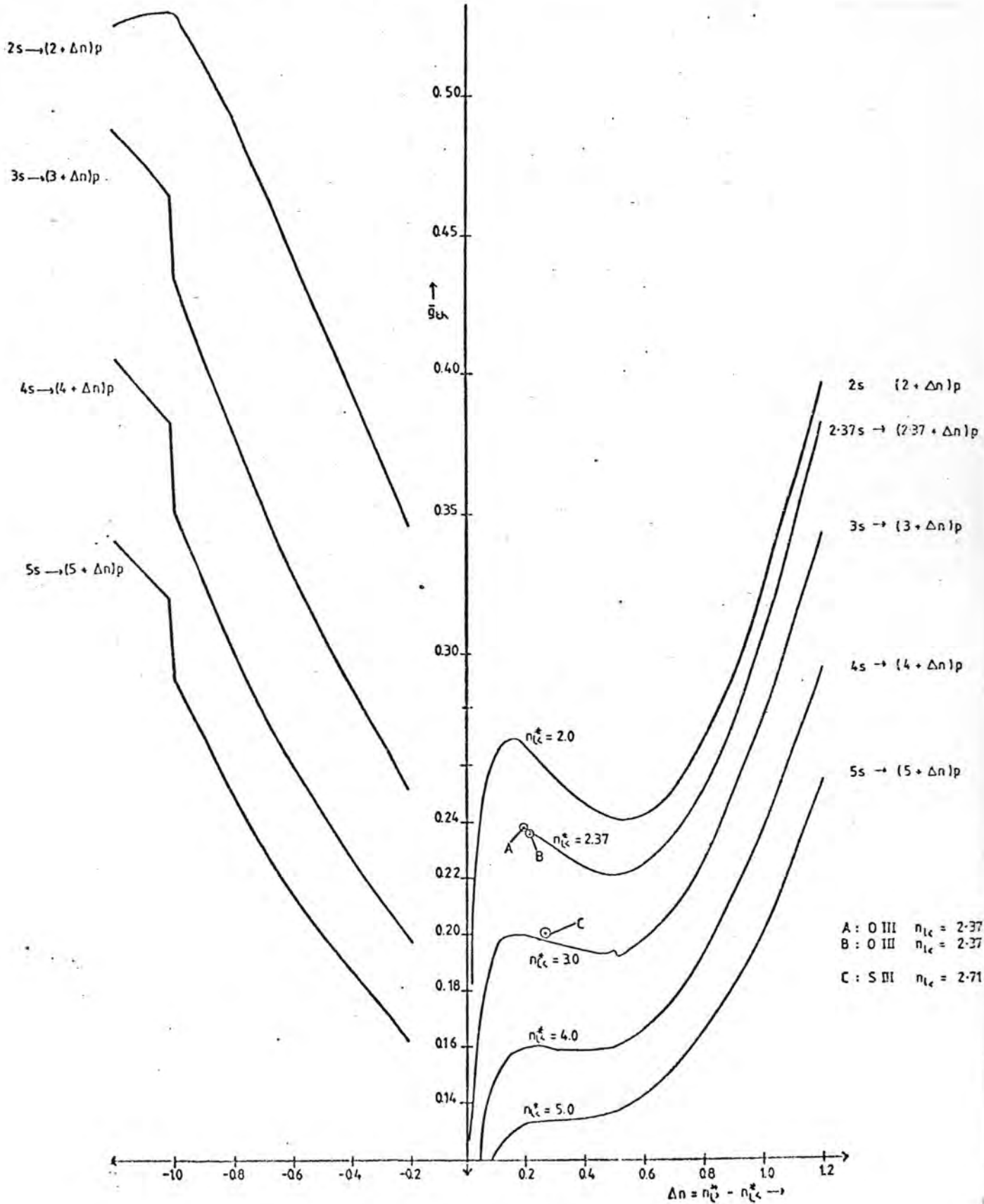


Fig. 6.2: Dependence of threshold Gaunt factor on change in effective principal quantum number: p-d transitions

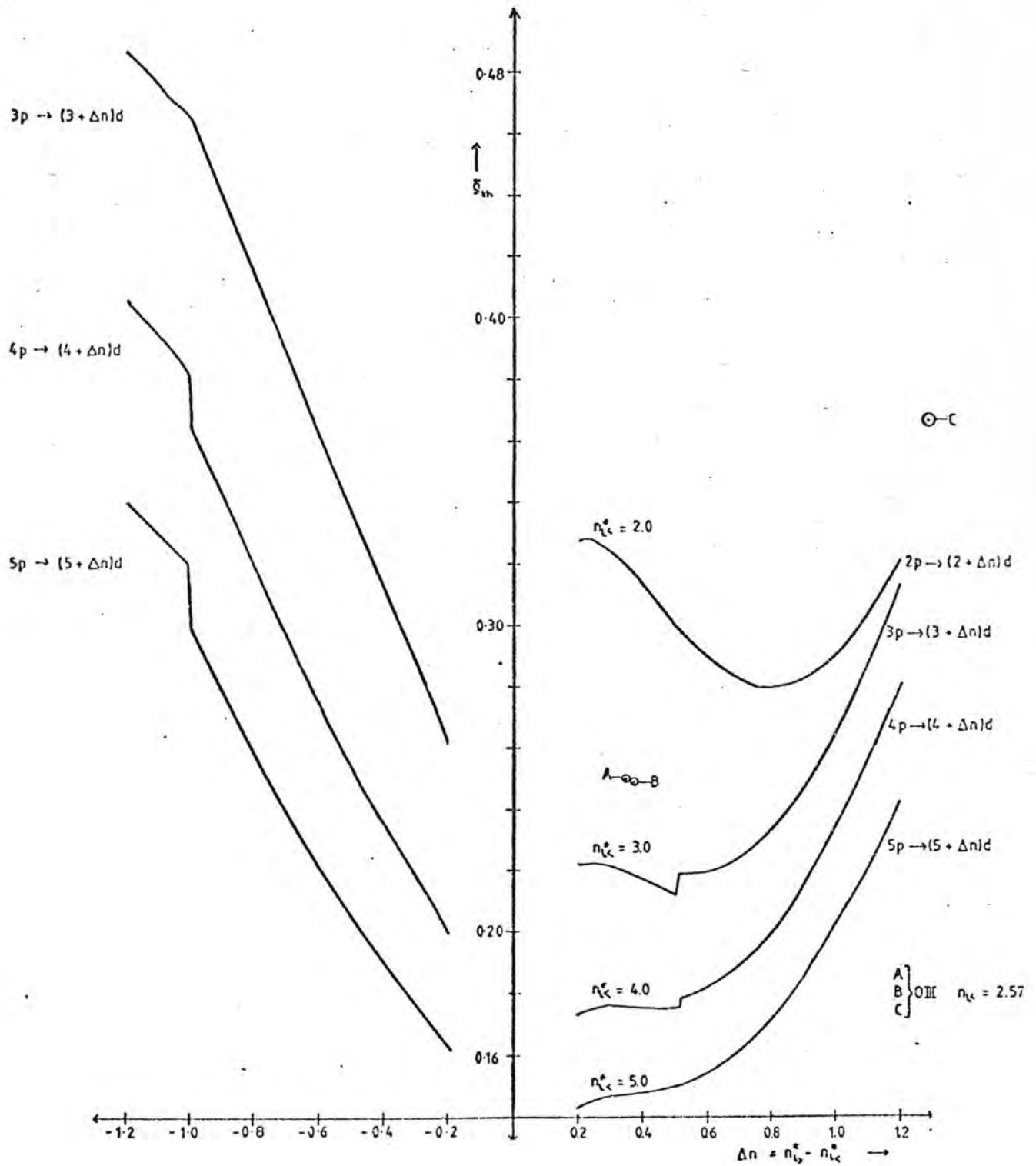


Fig. 6.3: Dependence of threshold Gaunt factor on change in effective principal quantum number: d-f transitions

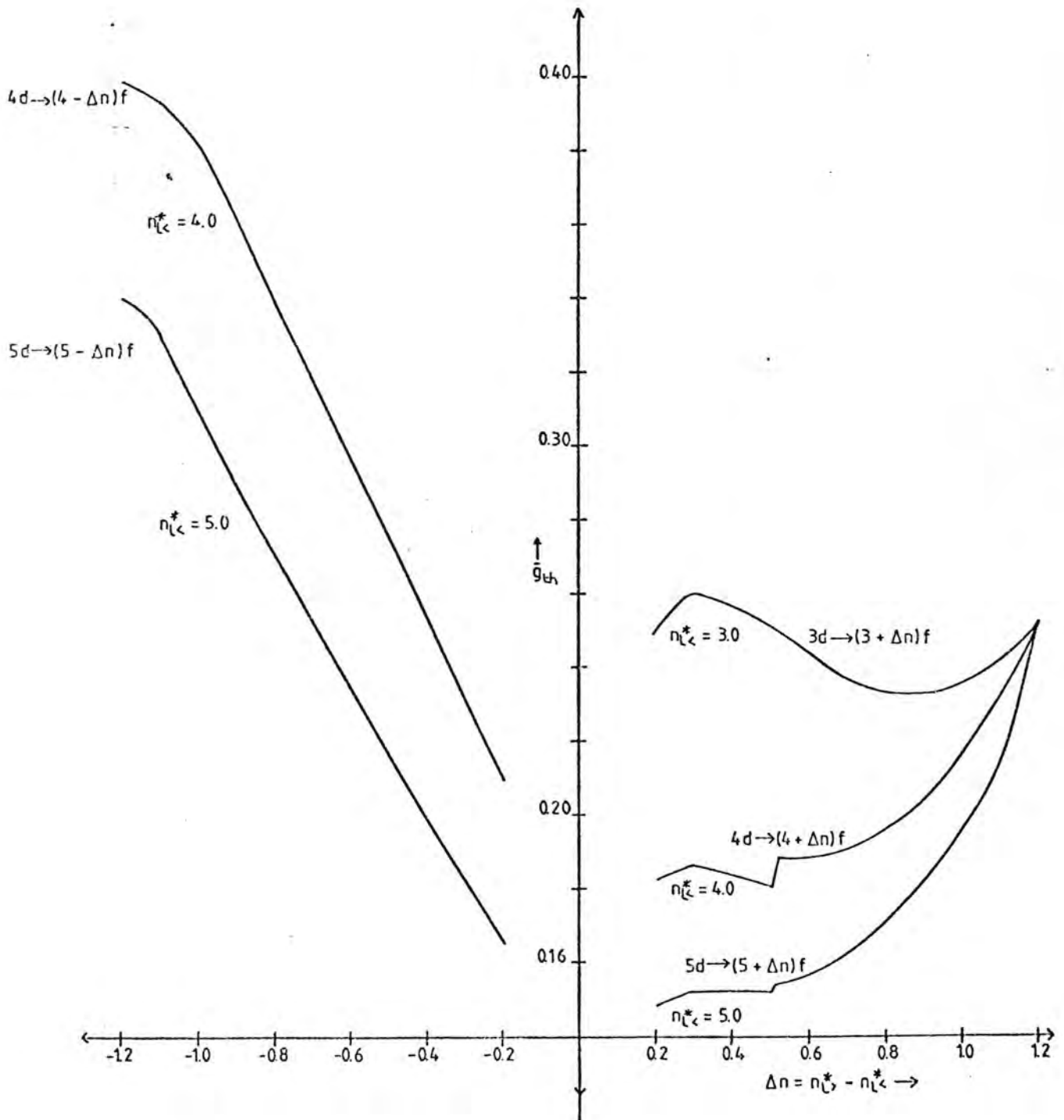
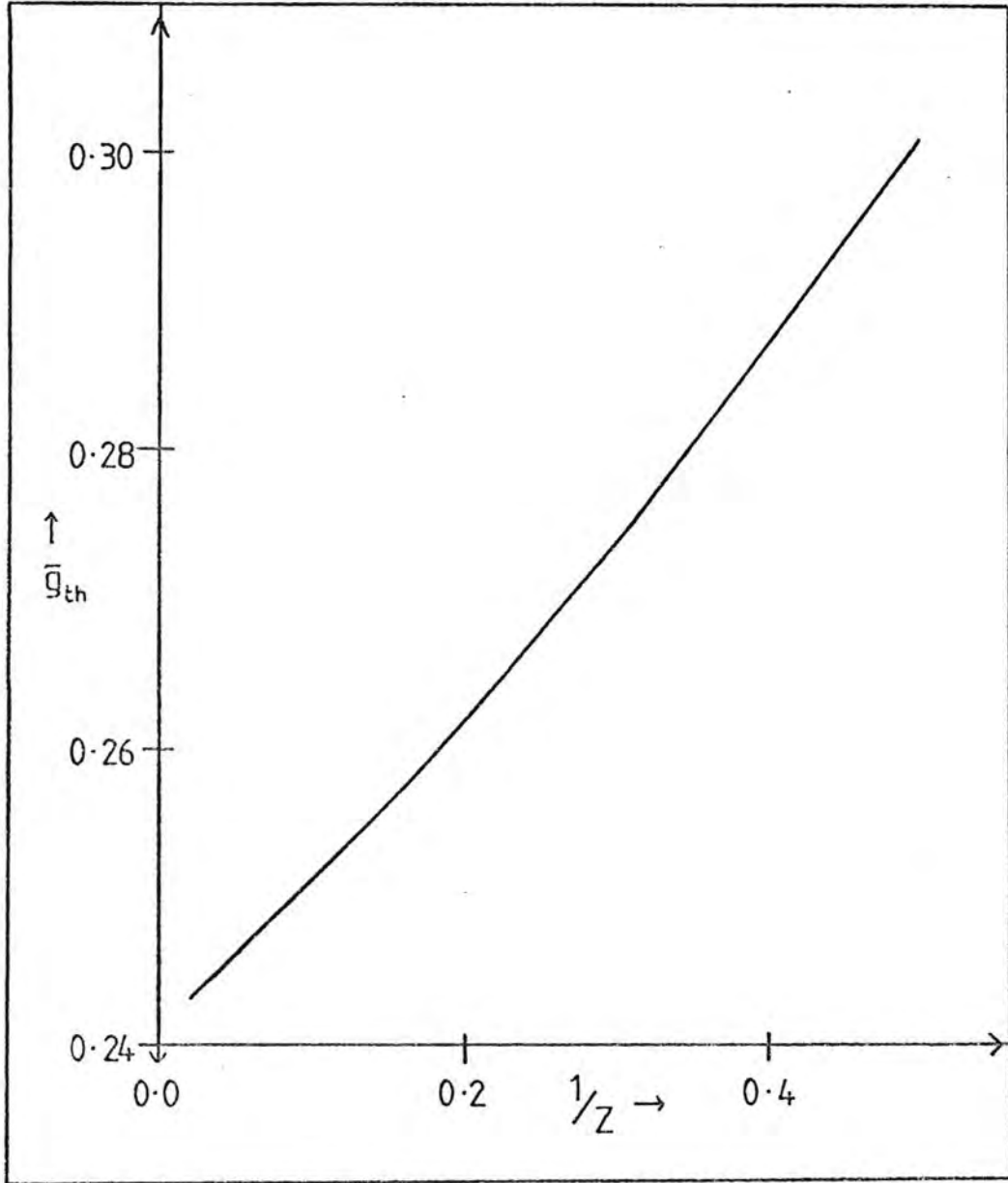


Fig. 6.4: Plot of threshold Gaunt factor versus $\frac{1}{Z}$



way to the reported regularities in resonance line widths (Purić et al.: 1974, 1978, 1979a, b, 1980) impossible (Konjević and Dimitrijević: 1980).

As has been indicated already at the conclusion of Chapter 3, comparisons of the derived effective Gaunt factor with expressions advanced by other authors are not readily viable, owing to the rather different approach taken in definition of this quantity. Comparisons are thus better restricted to the calculated line widths only.

A further difference in the present formulation of the effective Gaunt factor has been the exclusion of strong collisions from this term, which are included in the line width by the derivation of a separate expression (Chapter 4.1). The demarcation between "strong" and "weak" collisions proposed may not be entirely satisfactory, but errors arising therefrom are minimised by the consistency between the evaluation of the "weak" and "strong" contributions of the line width. Furthermore, it has been assumed that the negative elastic interference terms arising in the formulation of the contribution of "strong" collisions cancel the strong contributions from the lower transition level exactly. The good agreement obtained between calculated and measured line widths seems to support this simplification.

Finally, it has been confirmed that ion broadening contributions remain negligible and that electron impact broadening is the major broadening mechanism at the plasma conditions under consideration. Evaluation of typical values of collision times used in the line width calculations confirm

that the criteria employed in the present theory are consistent with the impact approximation as formulated originally by Baranger (1958a, b, c).

It can thus be concluded that the present method of calculation of Stark widths is successful in extending the semi-classical method of Griem (1974) for singly-ionised radiators for ions of higher ionisation stages and greater structural complexities. It thus forms an important part in the derivation of a reliable and practical method for diagnosis of experimental plasma conditions, as discussed in the Preface.

Since the present derivation depends on the exclusion of higher order terms in the Dyson series, further improvement (Griem: 1980, private communication) to the present calculation would require the inclusion of these terms.

PART B : SECTION 1IMPLEMENTATION OF COMPUTER CODESPROGRAM 1: MTD1

This method of calculation of line widths has been employed to investigate in particular the effect of configuration interaction on the Stark width, and has been applied to several isolated SnII lines (Chapter 5.1; see also Hey and Breger: 1980a in Appendix I).

The full formula for the Stark width (FWHM) has been discussed already in Chapter 5.1, and the result obtained is (eqs. 5.1 to 5.7):

$$W_e = \frac{\alpha \lambda^2 a_0^2}{\sqrt{\pi}} N_e \left(\frac{E_H}{kT} \right)^{1/2} \left[\left\{ \sum_{j=i,f} \sum_{j',i',f'} \frac{\langle \Omega(j,j') \rangle}{2J_j + 1} \right\} + 2 \left\{ 1 + \frac{n_i^{*4}}{Z^2} \left(1 + \frac{kT}{E_H} \right) \right\} \right]$$

where the subscript j denotes the level i or f of the transition, j' denotes the perturbing levels. The average collision strength is obtained from:

$$\sum_j \frac{\langle \Omega(j,j') \rangle}{2J_j + 1} = \frac{8\pi}{3\sqrt{3}} \left[\frac{n_j^{*2}}{2Z^2} (5n_j^{*2} + 1 - 3l(l+1)) \bar{g}_{th} + \sum_{j'} (\langle \bar{g}(j;j) \rangle - \bar{g}_{th}) \frac{1}{2J_j + 1} \frac{S(j,j')}{a_0^2 e^2} \right]$$

where

$$S(J, J') = (2J+1)(2J'+1)(2L+1)(2L'+1) l_{\nu} a_0^2 e^2 \left(R_{n'l'}^{nl} \right)^2 \\ \times \left\{ \begin{matrix} l & L & L_1 \\ L' & l' & 1 \end{matrix} \right\}^2 \left\{ \begin{matrix} J & L & S \\ L' & J' & 1 \end{matrix} \right\}^2$$

Collecting all the terms, one obtains for W_e in Å units:

$$W_e = 5.5723 \times 10^{-11} N_e \left(\frac{E_H}{kT} \right)^{1/2} \lambda^2 \\ \times \left[\sum_{j=i,f} \left[n_j^{*2} (5n_j^{*2} + 1 - 3l^2 - 3l) \frac{\bar{g}_{th}}{2Z^2} \right. \right. \\ \left. \left. + \sum_{j'} (\bar{g}_{j'j} - \bar{g}_{th}) \frac{\bar{\Phi}^2}{Z^2} (2L+1)(2J'+1) \left\{ \begin{matrix} J & L & S \\ L' & J' & 1 \end{matrix} \right\}^2 \right. \right. \\ \left. \left. \times 2.25 n_{l_{\nu}}^{*2} (n_{l_{\nu}}^{*2} - (l_{\nu}+1)^2) \frac{l_{\nu}+1}{2l_{\nu}+1} (2l_{\nu}+1)(2L'+1) \right. \right. \\ \left. \left. \times \left\{ \begin{matrix} l & L & L_1 \\ L & l & 1 \end{matrix} \right\}^2 \right] \right] \\ \left. + 0.413497 \left[1 + \frac{n_i^{*4}}{Z^2} \left[1 + \frac{kT}{E_H} \right] \right] \right] \quad (B1.1)$$

This expression is evaluated by combining the main program MTDLM with the following sub-programs:

GBAR (VERSION 1)
 RACAHL
 RCAH2
 COLUMN
 INTERP
 STRONG (VERSION 1)
 RAO (VERSION 1)

all of which are listed together with short descriptions and explanatory comments in Section 2. The sub-programs RACAH1, RACAH2 evaluate the 6-j symbols; the Gaunt factor \bar{g}_{Sn} at the root-mean-square velocity is evaluated by GBAR (VERSION 1); the sub-programs COLUMN and INTERP interpolate the appropriate Bates-Damgaard factor from a table supplied to the program as input data; and the strong collision term:

$$0.413497 \left[1 + \frac{n_i^{*4}}{Z^2} \left[1 + \frac{kT}{E_H} \right] \right]$$

is evaluated by STRONG (VERSION 1).

The main program MTD1M follows essentially the structure depicted in flowchart 1, where both cases of configuration mixing of the transition levels $i(f)$ and perturbing levels $i'(f')$ have been allowed for (see Chapter 2.4). According to this structure, the following input data are therefore required by the calculation MTD1 (the quantities underlined are in integer format (ASCII FORTRAN), the remaining variables are in real format, and the corresponding variable names occurring in the computer codes are given in brackets):

YES or NO (detailed or abbreviated printout respectively)

input of data file BATES. (see Appendix IV)

Z(Z)

T(T), N_e (D)

λ (W1)

upper level:

$$\underline{\ell(L0), L(L), L(L1), J(J), S(S), E_n^*(E), E(E1), |\alpha_{mn}|^2(WT1),}$$

(CONS)

(J1) no. of perturbing levels

$$\left. \begin{array}{l} \underline{\ell'(M0), L'(M), J'(K), E_n^*(F), |\alpha'_{mn}|^2(WT2)} \\ \cdot \\ \cdot \\ \cdot \end{array} \right\} \text{J1 times}$$

lower level:

repeat as for upper level.

The variable CONS is the matrix element of the upper/lower level corresponding to the ℓ'' character and is given by:

$$\frac{n^{*2}}{2Z^2} [5n^{*2} + 1 - 3(l'' + 1)]$$

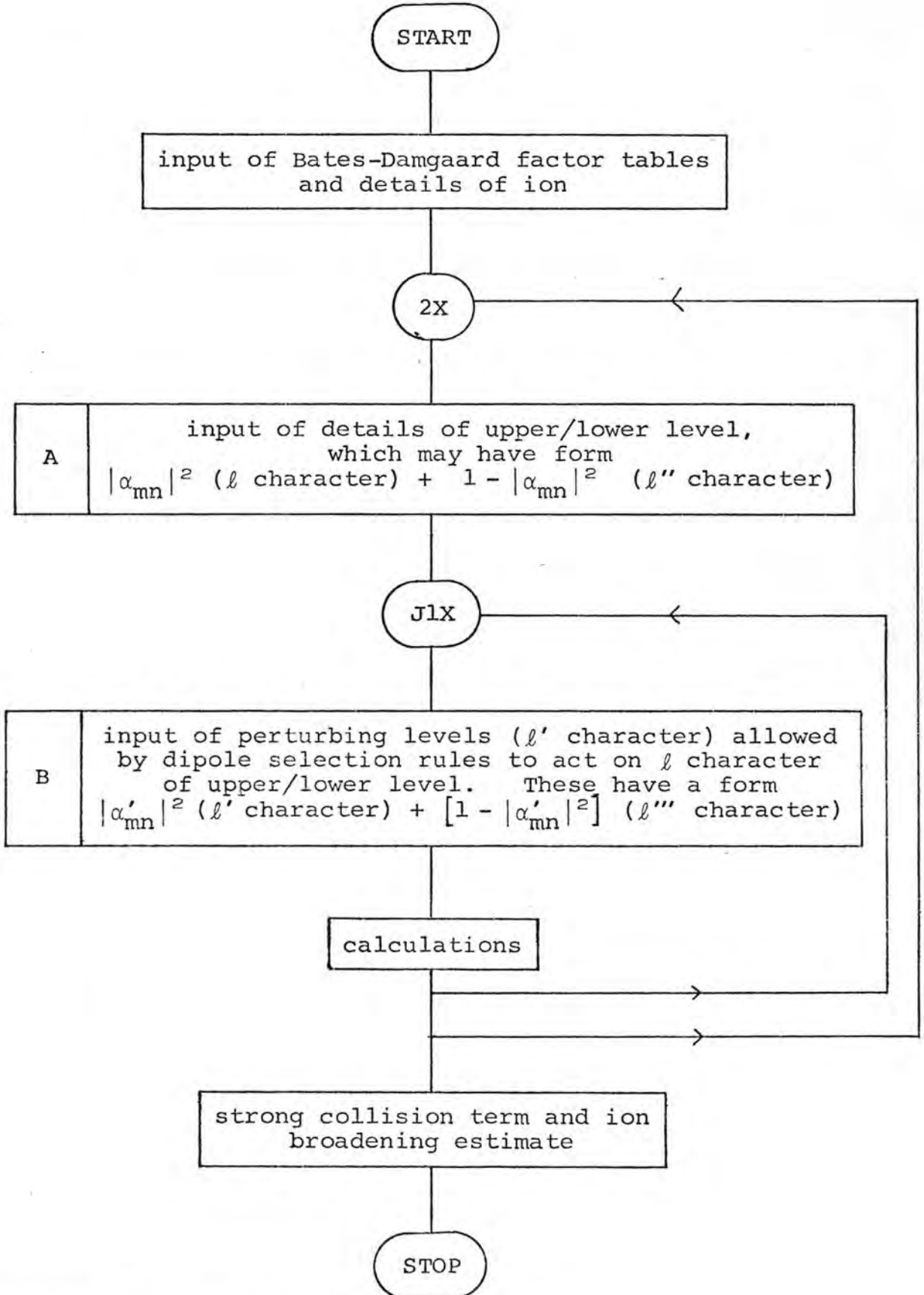
The calculations following the block B in flowchart 1 are depicted in flowchart 2, to make the correspondence between the computer codes and eq. B1.1 clear.

The calculation and output of the variable C2 in the program has been done in order to supply information about the completeness of the set of perturbing levels included in the calculation. Since one has the sum rules:

$$\sum_{L'} (2L+1)(2L'+1) \left\{ \begin{array}{ccc} L & L & L_i \\ L' & l' & 1 \end{array} \right\}^2 = 1$$

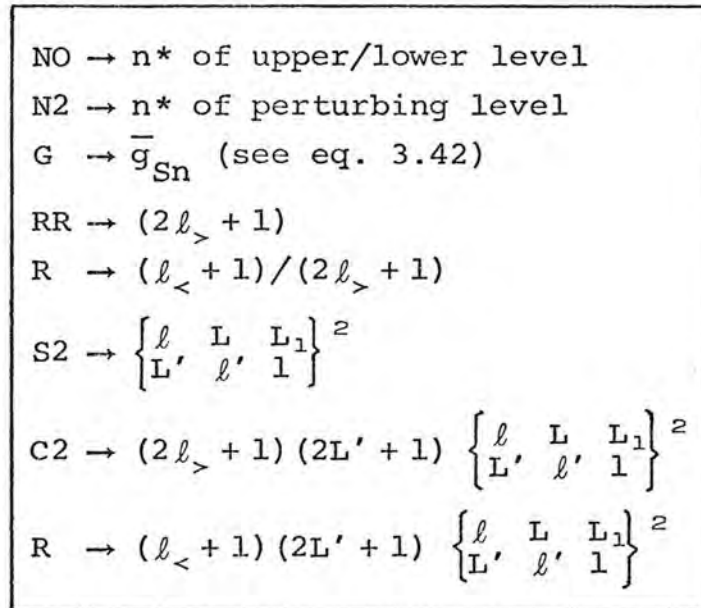
and

$$\sum_{J'} (2L+1)(2J'+1) \left\{ \begin{array}{ccc} L & J & S \\ J & L & 1 \end{array} \right\}^2 = 1$$

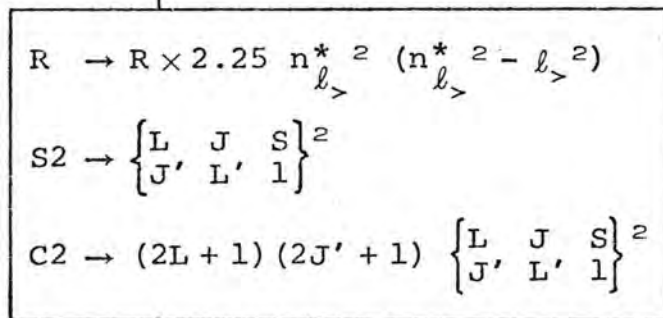


Flowchart 1: Flow of main program MTD1M

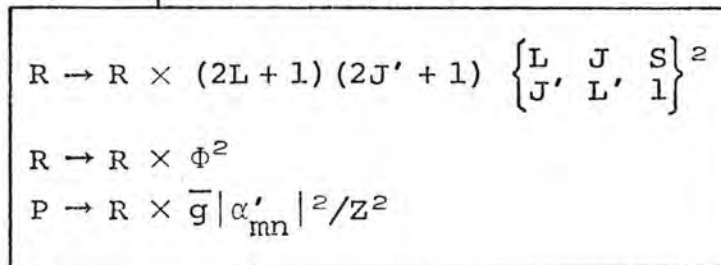
Flowchart 2: Structure of calculations



output S2, C2



output S2, C2



the completeness of inclusion of perturbing levels can be easily checked by addition of the C2 printed on the resultant output sheet.

As an example, the input data for the calculation of the SnII line $\lambda = 6844.2 \text{ \AA}$ ($6s \text{ } ^2S_{1/2} - 6p \text{ } ^2P_{1/2}^0$) at 9000 °K with 50% mixing is given below, together with extracts from the resultant computer output.

INPUT

```
>@XQT STARKB.MTD1
  DO YOU WANT A DETAILED PRINTOUT ? (YES OR NO)
>YES
>@ADD BATES.
  2
  6250.9,1.E+17
  14608.4
  1,1,0,0.5,0.5,71494.3,118017.,1.0,0.
  3
  2,2,1.5,71405.6,.50
  2,2,1.5,58843.8,0.50
  0,0,0.5,56885.9,1.0
  0,0,0,0.5,0.5,56885.9,118017.,1.0,0.
  2
  1,1,1.5,72377.3,1.0
  1, 1,0.5,71494.3,1.
```


PROGRAM 2: MTD2

This calculation makes use of the derived effective Gaunt factor expressions (eqs. 3.39, 3.41) to evaluate the weak cross-sections required. Instead of performing an integration over the Maxwellian distribution to perform the average over the electron velocities, the Gaunt factor is evaluated at the root-mean-square velocity. The full formula for the Stark width (FWHM) is thus obtained by collecting eqs. 1.42, 2.8, 2.9, 2.10, 3.39, 3.41, 4.11 to yield:

$$\begin{aligned}
 W_e = & 5.5723 \times 10^{-11} N_e \left(\frac{E_H}{kT} \right)^{1/2} \lambda^2 \\
 & \times \left[\left[\sum_{j=i,f} \sum_{j'=i',f'} l_{j'} (2L+1)(2L'+1)(2J'+1) \begin{Bmatrix} l & L & L_1 \\ L' & l' & 1 \end{Bmatrix}^2 \begin{Bmatrix} L & J & S \\ J & L & 1 \end{Bmatrix}^2 \right. \right. \\
 & \times \left. \left. \left(\frac{3 n_{l_j}^*}{2Z} \right)^2 (n_{l_j}^{*2} - l_{j'}^2) \overline{Q}^2 \right. \right. \\
 & \times \left. \left. \langle \overline{g}(j',j) \rangle \right] \right. \\
 & \left. + 0.413497 \left[1 + \overline{d_{ji}^2} \left[1 + \frac{kT}{E_H} \right] + 2(Z-1) \overline{d_{ji}} \right] \right] \quad (B1.2)
 \end{aligned}$$

where $\overline{d_{i',i}^2}$ and $\overline{d_{i',i}}$ are defined in Chapter 4.1 by eqs. 4.7, 4.8. Furthermore, the following additions are made to the line width calculation.

To ensure completeness of the perturbing levels, the sum of the Coulomb integrals is compared with the hydrogenic sum and the percentage difference is added to the line width, making use of an average \overline{g}_{th} for the upper/lower transition level. The completeness obtained by expression 2.41 is also

printed in the output.

An estimate of the inelastic contribution to the line width is made by using:

$$\% \text{ inelastic} = 100 \exp \left[- \frac{\Delta E}{kT} \right].$$

An investigation into the \bar{g}_{th} obtained is facilitated by compiling a table of all the \bar{g}_{th} for the transitions occurring in the program.

The calculation MTD2 is obtained by combining the main program MTD2M with the following sub-programs:

RACAH1
 RACAH2
 BATESD (VERSION 1)
 COLUMN
 INTERP
 RAO (VERSION 2)
 GBAR (VERSION 2)
 GAV
 STRONG (VERSION 2)
 TABLE
 CUBIC

The sub-program BATESD (VERSION 1) selects the appropriate Bates-Damgaard factor by interpolation using COLUMN and INTERP. The radial integral is evaluated in the Coulomb approximation using the Bates-Damgaard method implemented in

RAO (VERSION 2). The Gaunt factor (eq. 3.39 and 3.41) is calculated using GBAR (VERSION 2) and the cubic (eq. 3.21) arising in the curvature correction is solved by CUBIC. The subroutine GAV calculates the threshold Gaunt factor and TABLE tabulates these according to transitions. The strong contribution to the line width is calculated using STRONG (VERSION 2).

Flowchart 1 describes the structure of the main program MTD2M, but configuration interaction has not been included in the computations. The calculations following block B in flowchart 1 are depicted in flowchart 3, to make the correspondence between the computer codes and eq. B1.2 clear.

The required input data are summarised below using the same notation as for MTD1.

YES or NO (detailed or abbreviated printout respectively)

input of data file BATES, (see Appendix IV)

Z(Z)

T(T), N_e (D)

λ (W1)

upper level:

l (LO), L(L), L_1 (L1), J(J), S(S), E_{n^*} (E), E (E1), 1.00, 0.00

principal quantum no. n(JN1)

(J1) no. of perturbing levels

l' (MO), L' (M), J' (K), E'_{n^*} (F), 1.00, n' (JN2)

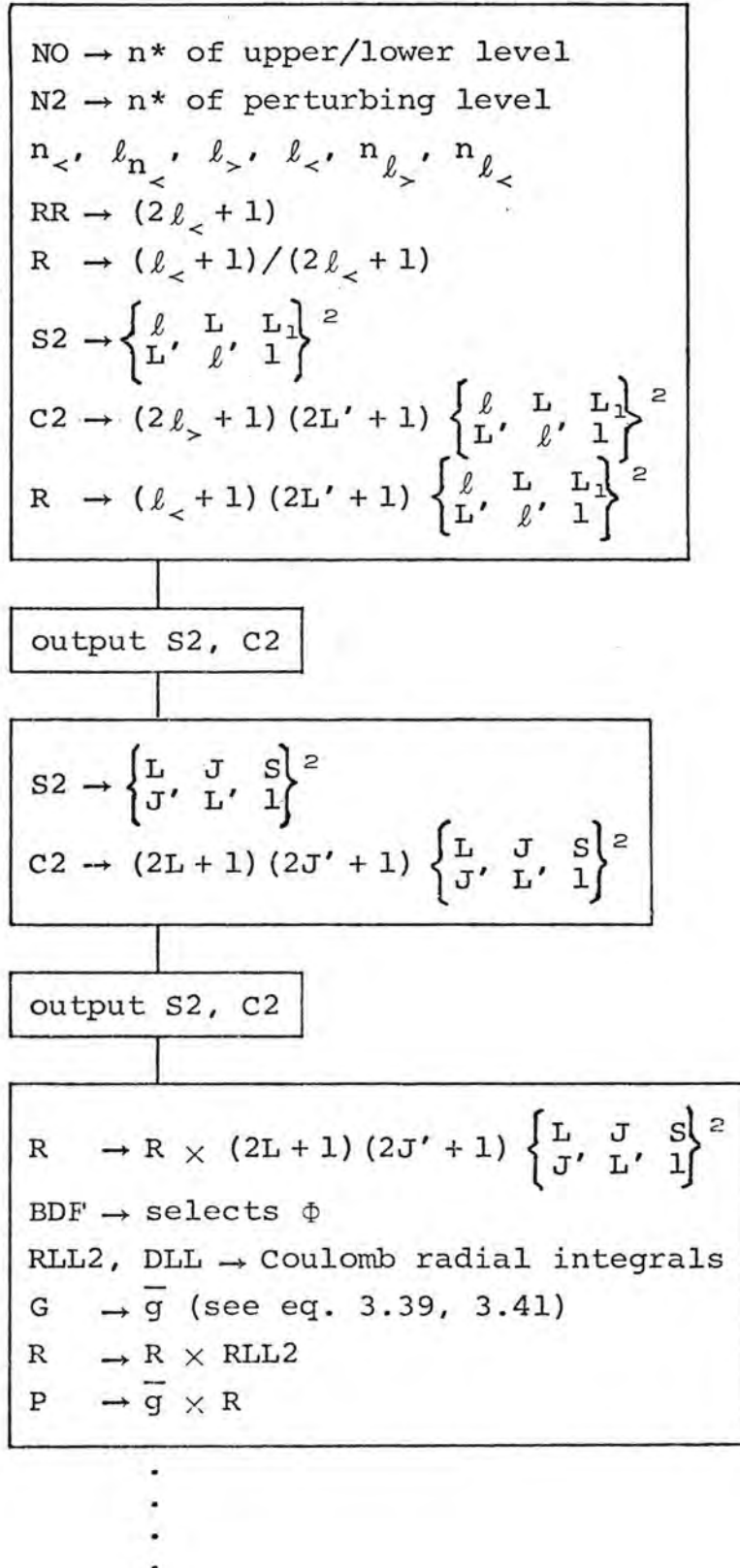
.
.

.

.

.

Flowchart 3: Structure of calculations



lower level:

repeat as for upper level.

(Note: the configuration mixing parameters have been set to 1.00 and 0.00 to exclude this effect.)

Some of the more important variable names in the computer codes are as follows:

$n_{<}^*$	- NS	$n_{l_{>}}$	- NLG
$l_{n_{<}^*}$	- LNS	$n_{l_{<}}$	- NLS
$l_{>}$	- LG	ϕ	- BDF
$l_{<}$	- LS	$d_{i,i}$	- DLL
$(R_{n'L}^{nl})^2$	- RLL2	solution of cubic	- PHI

As an example, the input data for the calculation of the OII line $\lambda = 4318.4 \text{ \AA}$ ($[^3P]3p \ ^4P_{3/2}^0 - 3s \ ^4P_{1/2}$) at 2 eV are given below.

INPUT

```

>@XQT STARKB.MTD2
  DO YOU WANT A DETAILED PRINTOUT ? (YES OR NO)
>YES
>@ADD BATES.
  2
  18005.,1E+17
  23156.91
  1,1,1,1.5,1.5,208392.27,283448.,1.00,0.00,3
  12
  0,1,0.5,185235.36,1.00,3
  0,1,1.5,185340.68,1.00,3
  0,1,2.5,185499.2,1.00,3
  0,1,0.5,238626.32,1.00,4
  0,1,1.5,238731.54,1.00,4
  0,1,2.5,238892.96,1.00,4
  2,1,0.5,232602.57,1.00,3
  2,1,1.5,232536.06,1.00,3
  2,1,2.5,232462.83,1.00,3
  2,2,0.5,232711.7,1.00,3
  2,2,1.5,232745.98,1.00,3
  2,2,2.5,232747.51,1.00,3
  0,1,1,0.5,1.5,185235.36,283448.,1.00,0.00,3
  10
  1,0,1.5,212161.94,1.00,3
  1,1,0.5,208346.17,1.00,3
  1,1,1.5,208392.27,1.00,3
  1,1,0.5,245876.,1.00,4
  1,1,1.5,245876.,1.00,4
  1,2,0.5,206730.8,1.00,3
  1,2,1.5,206786.34,1.00,3
  1,2,0.5,245767.8,1.00,4
  1,2,1.5,245816.29,1.00,4
  1,0,1.5,247223.,1.00,4

```

PROGRAM 3: MTD2A

This method of calculation of line widths has been employed with great success to all the ion lines with the exception of SnII (see Chapter 5) for which MTD1 was used. It is based on MTD2, but makes use of an integrated average of the effective Gaunt factor, as discussed in Chapter 1 and Chapter 3:

The full formula for the Stark width (FWHM) is thus obtained collecting eqs. 1.42, 2.8, 2.9, 2.10, 3.39, 3.41, 4.11 to yield, as for MTD2:

$$\begin{aligned}
 W_e = & 5.5723 \times 10^{-11} N_e \left(\frac{E_H}{kT} \right)^{1/2} \lambda^2 \\
 & \times \left[\left[\sum_{j=i,f} \sum_{j'=i',f'} l_{\nu} (2L+1)(2L'+1)(2J'+1) \begin{Bmatrix} l & L & L_1 \\ L' & l' & 1 \end{Bmatrix}^2 \begin{Bmatrix} L & J & S \\ J & L & 1 \end{Bmatrix}^2 \right. \right. \\
 & \times \left. \left. \left(\frac{3n_{l_{\nu}}^*}{2Z} \right)^2 (n_{l_{\nu}}^{*2} - l_{\nu}^2) \bar{Q}^2 \right. \right. \\
 & \times \left. \left. \langle \bar{g}(j',j) \rangle \right] \right. \\
 & \left. + 0.413497 \left[1 + \bar{d}_{i,i}^{-2} \left[1 + \frac{kT}{E_H} \right] + 2(Z-1)\bar{d}_{i,i} \right] \right] \quad (B1.3)
 \end{aligned}$$

where $\bar{d}_{i,i}^2$ and $\bar{d}_{i,i}$ are defined in Chapter 4.1 by eqs. 4.7, 4.8. The average effective Gaunt factor is evaluated from eqs. 3.56, 3.57:

$$\begin{aligned}
 \langle \bar{g}(j',j) \rangle &= \int_0^{\infty} \bar{g}(z) \exp(-z) dz && \text{for excitation} \\
 \langle \bar{g}(j',j) \rangle &= \int_0^{\infty} g\left(z + \frac{\Delta E}{kT}\right) \exp(-z) dz && \text{for de-excitation}
 \end{aligned}$$

The argument of the integrals (Gaunt factor \bar{g}) is given by eqs. 3.39 and 3.41. In the case of excitation processes, the integration is split up into two parts - above- and below-threshold integrals. This allows a direct computation of the dipole elastic contributions to the line width and thus dispenses with the estimate used in MTD2.

The introduction of the above integration procedure for the evaluation of the effective Gaunt factor average makes the crude inclusion of an extra contribution to ensure completeness meaningless. The completeness parameter $\Delta S_i/S_i$ (see eq. 2.41) indicates thus the degree of incompleteness of the line width calculation with respect to the set of perturbing levels employed. A table of threshold Gaunt factors for all transitions occurring in the computation is compiled in the same way as in MTD2. These threshold Gaunt factors are, however, not immediately relevant to the line width calculation, but have been included for comparison with computations employing this simplified quantity.

A further extension to the line width calculation has been made, namely the inclusion of the correction of the oscillator strengths for equivalent electron configurations (see Chapter 2.2). This correction factor was determined to be $N |G_{S_1 L_1}^{SL}|$ and is denoted by WT3 in the computer code.

A further addition to the computation is the evaluation of the disentanglement parameter as well as an average collision time, which has been discussed in Chapter 4 (Sections 4 and 5).

With the exception of configuration interaction inclusion,

flowcharts 1 and 3 depict the overall structure of the main program MTD2AM. The line width calculation MTD2A is obtained by combining the main program MTD2AM with the following sub-programs:

RACAH1

RACAH2

BATESD (VERSION 2)

COLUMN

INTERP

RAO (VERSION 2)

GBARAV

GTRY

FINT

SIM1NI

GBAV

CUBIC

GAV

GBAR (VERSION 2)

DISENT

FINTDA

FINTDB

COLTIM

ROMINS

FINTC

STRONG (VERSION 2)

TABLE

As before, in MTD1, MTD2, the sub-programs RACAHI and RACAH2 evaluate the 6-j symbols. BATESD (VERSION 2) differs from BATESD (VERSION 1) insofar as it includes Bates-Damgaard factors for $f \rightarrow g$ and $g \rightarrow h$ transitions (see Appendix IV). Interpolation between the tabulated Bates-Damgaard factors is done by COLUMN, INTERP. RAO (VERSION 2) evaluates the radial integral by the Bates-Damgaard method.

In order to evaluate the Maxwellian average over the velocity distribution, sub-programs GBARAV, GTRY, FINT, SIM1NI, GBAV and CUBIC are called upon. SIM1NI is the MATH-PACK version of the Simpson $\frac{1}{3}$ Rule for the evaluation of the integrals (MATH PACK PROGRAMMERS REF. SPERRY UNIVAC UP-7542 REV11).

In order to evaluate the threshold Gaunt factors, GAV and GBAR (VERSION 2), CUBIC are required, and the results are tabulated using TABLE.

The disentanglement parameter and collision time parameter are estimated using DISENT, FINTDA, FINTDB, COLTIM, ROMINS, FINTC. The numerical integration is again performed using SIM1NI.

Strong collision contributions are evaluated using the sub-program STRONG (VERSION 2).

Flowchart 4 depicts the program flow for the evaluation of the Maxwellian average of the effective Gaunt factor. The upper limit "infinity" was chosen in the calculations to be at $10^4 \times$ threshold velocity (i.e. $x = 100$).

The input data required for MTD2A are thus given as follows, where the notation is the same as previously:

YES or NO (detailed or abbreviated printout respectively)

(MAXIT), " ∞ " (ZZZ) (usually 1000, 100. suffices)

input of data file BATES2. (see Appendix IV)

Z(Z)

T(T), N_e (D)

λ (W1)

upper level:

l (LO), L(L), L_1 (L1), J(J), S(S), E_{n^*} (E), E_∞ (E1), 1.00, 0.00,

principal quantum no. n(JN1)

(J1) no. of perturbing levels

(EMIN) energy of level for which disentanglement and

collision time is to be evaluated

l' (MO), L' (M), J' (K), E'_{n^*} (F), 1.00, n' (JN2), $N |G_{S_1 L_1}^{SL}|^2$ (WT3)

.
.
.
.

lower level:

repeat as for upper level.

For a compilation of some of the more important variable names, see method MTD2.

As an example, the input data for the calculation of the NIV line $\lambda = 4058.9 \text{ \AA}$ ($3p \ ^1P^0 - 3d \ ^1D$) at 5 eV are given below.

INPUT

```

ELAM*DATA(1).NIUC1
  1      4
  2      40332.3,1E+17
  3      24637.2
  4      2,2,0,2.,0.0,429159.6,624866.,1.00,0.00,3
  5      4
  6      130693.9
  7      1,1,1.,130693.9,1.00,2,1.0
  8      1,1,1.,507027.9,1.00,4,1.0
  9      1,1,1.,404522.4,1.00,3,1.0
 10      3,3,3.,521862.8,1.00,4,1.0
 11      1,1,0,1.0,0.0,404522.4,624866.,1.00,0.00,4
 12      5
 13      0.9
 14      0,0,0.0,388854.6,1.00,3,1.0
 15      0,0,0.0,495057.7,1.00,4,1.0
 16      2,2,2.0,429159.6,1.00,3,1.0
 17      2,2,2.0,514647.7,1.00,4,1.0
 18      0,0,0.0,0.0,1.00,2,2.00
>@XQT STARKB.MTD2A
DEBUG UNIT      -1
  DO YOU WANT A DETAILED PRINTOUT ? (YES OR NO)
>YES
>1000,100.
      1000  100.00000
>@ADD BATES2.
>@ADD DATA.NIUC1

```

PART B : SECTION 2COMPUTER CODES

The various main programs and sub-programs are arranged in order in which they are discussed in the previous section.

To summarise, the three programs presented in section 1 are obtained by combining the various elements as follows:

MTD1: pp. 218-225

ELAN*STARKB(1).MAP1

```

1      IN STARKB.MTD1M
2      IN STARKB.RACAH1,.RACAH2,.STRONG,.RAO1,.COLUMN,.INTERP,.OURG
3      LIB SYS$*FTNLIB$.

```

MTD2: pp. 226-235

ELAN*STARKB(1).MAP2

```

1      IN STARKB.MTD2M
2      IN STARKB.RACAH1,.RACAH2,.BATESD1,.COLUMN,.INTERP,.RAO2,.OURG2,.GAV
3      IN STARKB.STRONG2,.TABLE,.CUBIC2
4      LIB SYS$*FTNLIB$.

```

MTD2A: pp. 235-246

ELAN*STARKB(1).MAP2A

```

1      IN STARKB.MTD2AM
2      IN STARKB.RACAH1,.RACAH2,.BATESD2,.COLUMN,.INTERP,.RAO2,.GBARAV,.GTRY
3      IN STARKB.GBAV,.CUBIC2,.GAV,.OURG2,.DISENT,.COLTIM,.STRONG2,.TABLE
4      LIB ASCII*RMATHSTAT.
5      LIB SYS$*FTNLIB$.

```

ELAN*STARKB(1).MTD1M

```

1      C ***** 3/8/79 *****
2      C THIS PROGRAM EVALUATES THE SPECTRAL LINE BROADENING CAUSED BY
3      C ELECTRON COLLISIONS .CONFIGURATION MIXING AS WELL AS STRONG
4      C CONTRIBUTIONS TO THE BROADENING ARE INCLUDED,AND AN ESTIMATE OF
5      C THE (NEGLECTED) ION BROADENING IS MADE.
6      C THE INPUT REQUIRES BATES DAMGAARD FACTORS FOR THE EVALUATION OF
7      C RADIAL INTEGRALS.THEN .DETAILS OF THE ATOM NEED TO BE
8      C SPECIFIED FOR CORRECT OPERATION (FORMAT()):
9      C
10     C      IONIZATION STAGE
11     C      TEMPERATURE (CM-1),DENSITY(CM-3)
12     C      WAVELENGTH (CM-1)
13     C
14     C      UPPER LEVEL :
15     C          SMALL L,CAPITAL L,PARENTAGE,J,SPIN,ENERGY,IONIZATION
16     C          ENERGY,WEIGHT,MX.ELT. FOR SECONDARY ANG.
17     C          NON.CHARACTER
18     C          NO. OF PERTURBING LEVELS
19     C          SMALL L,CAPITAL L,J,ENERGY,WEIGHT
20     C
21     C      LOWER LEVEL :
22     C          SAME AS FOR UPPER LEVEL.
23     C
24     C      THE CONTRIBUTION FROM PERTURBING LEVELS IS SPLIT INTO TWO
25     C PARTS,A BELOW THRESHOLD SUM AND AN ABOVE THRESHOLD CONTRIBUTION OF
26     C SPECIFIC PERTURBING LEVELS.
27     C THE GAUNT FACTOR IS OBTAINED USING GBAR (VERSION 1).
28     C *****
29     C THE FOLLOWING SUBROUTINES ARE CALLED FROM THIS MAIN PROGRAM:
30     C
31     C          GBAR (VERSION 1)
32     C          RACAH1
33     C          RACAH2
34     C          COLUMN
35     C          INTERP
36     C          STRONG (VERSION 1)
37     C *****
38     C      DIMENSION JJ(3,25),KK(3,25),LL(3,25),O(25),PP(20),QN(2)
39     C      REAL JJ,KK,LL,NO,N2,J,N1,N3,L2,N2,M3,M4,K,NLG
40     C      INTEGER Z,H,Q
41     C      CHARACTER DETAIL*4
42     C      Q=5
43     C      PRINT 901
44     C 901  FORMAT(3X,'DO YOU WANT A DETAILED PRINTOUT ? (YES OR NO)')
45     C      READ 902,DETAIL
46     C 902  FORMAT(A3)
47     C *** THRESHOLD GAUNT FACTOR
48     C      GO=0.2
49     C *** READ IN THE BATES DAMGAARD FACTORS FROM FILE BATES.
50     C      DO 500 N=1,3
51     C      DO 501 NN=1,25
52     C      READ 100,JJ(N,NN)
53     C 501  CONTINUE
54     C 500  CONTINUE

```

```

55         DO 600 N=1,3
56         DO 601 NN=1,25
57         READ 100, KK(N, NN)
58     601   CONTINUE
59     600   CONTINUE
60         DO 700 N=1,3
61         DO 701 NN=1,25
62         READ 100, LL(N, NN)
63     701   CONTINUE
64     700   CONTINUE
65     C *** READ IN ION SPECIFICATIONS
66         READ 100, Z
67         READ 100, T, D
68         READ 100, W1
69         WRITE(Q, 100) Z
70         WRITE(Q, 100) W1
71         WRITE(Q, 100) T, D
72     C START OF COMPUTATIONS
73         WRITE(Q, 103)
74         RP4=0.
75     C *** START OF UPPER/LOWER LEVEL CALCULATION
76         DO 3 H=1,2
77         P1=0.
78         WRITE(Q, 102) H
79     C *** READ IN TRANSITION LEVEL, NO. OF PERTURBING LEVELS
80         READ 100, LO, L, L1, J, S, E, E1, WT1, CONS
81         READ 100, J1
82         IF(J1.EQ.0) GO TO 30
83     C *** START OF PERTURBATION
84         DO 4 I=1, J1
85     C *** READ IN PERTURBING LEVEL SPECS.
86         READ 100, MO, M, K, F, WT2
87         ZZ=FLOAT(Z)
88         N0=SQRT(109737.*ZZ**2/(E1-E))
89         N2=SQRT(109737.*ZZ**2/(E1-F))
90         QN(H)=N0
91         CALL GBAR(F, E, X, T, G, GO, Z, N0)
92     C *** EVALUATE ARGUMENTS OF THE RACAH COEFF. OF L-MOMENTA
93         IF(MO.LT.LO) GO TO 5
94         RR=FLOAT(2*LO+1)
95         R=(FLOAT(LO+1))/RR
96         L2=FLOAT(LO)
97         N1=N2
98         N3=N0
99         N2=FLOAT(L)
100        N3=FLOAT(H)
101        M4=FLOAT(L1)
102        GO TO 6
103     5    L2=FLOAT(MO)
104         RR=FLOAT(2*LO+1)
105         R=(FLOAT(MO+1))/RR
106         N1=N0
107         N3=N2
108         M2=FLOAT(M)
109         M3=FLOAT(L)
110         M4=FLOAT(L1)
111     6    CALL RACAH1(L2, M2, M4, N3, S2)

```

```

112 C *** CHECK COMPLETENESS OF L-SPLITTING
113     C2=RR*(FLOAT(2*M+1))*S2
114 C *** LINE STRENGTH COLLECTION
115     R=R*C2
116     MM=1
117     IF(DETAIL.EQ.3HNO )GO TO 800
118     WRITE(Q,101)N0,N2
119     WRITE(Q,104)
120     WRITE(Q,100)L0,N0,L,M,MM,L1
121     WRITE(Q,105)S2,C2
122 C *** EVALUATION OF RADIAL INTEGRAL (BATES-DAMGAARD)
123 800     R=R*2.25*N1**2.*(N1**2-(L2+1.))**2)
124 C *** EVALUATE ARGUMENTS OF RACAH COEFF. OF J-MOMENTA
125     IF(M-L)7,8,9
126 8     IF(K-J)10,11,12
127 12     L2=J
128     M2=FLOAT(L)
129     M3=FLOAT(M)
130     M4=S
131     GO TO 13
132 10     L2=K
133     M2=FLOAT(M)
134     M3=FLOAT(L)
135     M4=S
136     GO TO 13
137 9     L2=FLOAT(L)
138     M2=J
139     M3=K
140     M4=S
141     GO TO 13
142 7     L2=FLOAT(M)
143     M2=K
144     M3=J
145     M4=S
146 13     CALL RACAH1(L2,M2,M4,M3,S2)
147     GO TO 14
148 11     CALL RACAH2(L,J,S,S2)
149 C *** CHECK COMPLETENESS OF J-SPLITTING
150 14     C2=FLOAT(2*L+1)
151     C2=C2*(2.*K+1.)*S2
152     IF(DETAIL.EQ.3HNO )GO TO 801
153     WRITE(Q,106)
154     WRITE(Q,100)L,M,J,K,MM,S
155     WRITE(Q,105)S2,C2
156 C *** LINE STRENGTH COLLECTION
157 801     R=R*C2
158 C *** EXTRAPOLATE BATES-DAMGAARD FACTOR FROM TABLE SUPPLIED
159     IF(N0.LT.L0)GO TO 15
160     L2=L0
161     GO TO 16
162 15     L2=N0
163 16     X2=N3-N1
164     IF(X2.GT.1.)GO TO 33
165     X2=ABS(X2)

```

```

166          IF(X2.GT.1.3)GO TO 33
167          IF(L2.EQ.0.)GO TO 17
168          IF(L2.EQ.1.)GO TO 18
169          IF(L2.EQ.3.)GO TO 31
170          NLG=N1-1.
171          CALL COLUMN(KL,NLG)
172          DO 19 N=1,25
173      19          O(N)=LL(KL,N)
174          GO TO 20
175      17          NLG=N1
176          CALL COLUMN(KL,NLG)
177          DO 21 N=1,25
178      21          O(N)=JJ(KL,N)
179          GO TO 20
180      18          NLG=N1
181          CALL COLUMN(KL,NLG)
182          DO 22 N=1,25
183      22          O(N)=KK(KL,N)
184      20          CALL INTERP(N3,N1,O,F4)
185          GO TO 32
186      33          F4=0.
187          GO TO 32
188      31          F4=0.6203
189      32          O0=SQRT(F4)
190          X2=N3-N1
191      C *** LINE STRENGTH COLLECTION
192          R=R*F4
193          ZZ=FLOAT(Z)
194      C *** ABOVE THRESHOLD CONTRIBUTION
195          P=WT2*(G-GO)*R/ZZ**2
196          P1=P1+P
197          IF(DETAIL.EQ.3HNO )GO TO 4
198          PRINT 115,X2,O0
199          WRITE(Q,107)H,I
200          WRITE(Q,108)P
201      4          CONTINUE
202      C *** THRESHOLD CONTRIBUTION
203      30          NO=SQRT(109737.*ZZ**2/(E1-E))
204          QN(H)=NO
205          RLO=FLOAT(LO)
206          P2=NO**2*(5.*NO**2+1.-3.*RLO**2-3.*RLO)/2.
207          P2=(P2*GO/ZZ**2)*WT1+(1.-WT1)*CONS*2.*GO
208      C *** STRONG COLLISIONS (VERSION 1)
209          WRITE(Q,109)H,P2
210          CALL STRONG(T,ZZ,P4,NO,LO,H)
211          PP(H)=P2+P1+P4
212          WRITE(Q,112)P1
213          WRITE(Q,111)P4
214          RP4=P4+PP4
215      C *** ADD UPPER AND LOWER LEVEL CONTRIBUTIONS AND LINE WIDTH
216      3          CONTINUE
217          P3=PP(1)+PP(2)
218          W1=1.0/W1
219      C *** ION WIDTH
220          W=0.5576E-10*D*P3*W1**2*SQRT(109737./T)
221          WION=4.08682E-11*W1**2/Z**2
222          WION=WION*D*(QN(1)**2-QN(2)**2)**2

```

```

223 C *** % STRONG
224     PIE=WION/U*100.
225     RP4=RP4/P3*100.
226     WRITE(Q,110)U1,U
227     WRITE(Q,113)WION,PIE
228     WRITE(Q,114)RP4
229     100  FORMAT( )
230     101  FORMAT(///,8X,' N* UPPER (LOWER) STATE = ',F13.6,9X,' N* PERTURB
231           &ING LEVEL      = ',F13.6)
232     102  FORMAT(///,30X,'ENERGY LEVEL NUMBER ',I1,///)
233     103  FORMAT(1H1,/,18X,'*', ' SPECTRAL LINE BROADENING ',*',///)
234     104  FORMAT( )
235     105  FORMAT(/,9X,'S2',21X,'=',3X,F13.6,10X,'C2'22X,'=',3X,F13.6)
236     106  FORMAT( )
237     107  FORMAT(9X,'H',22X,'=',13X,I3,10X,'I',23X,'=',13X,I3)
238     108  FORMAT(9X,'CONTRIBUTION',11X,'=',3X,F13.6,///)
239     109  FORMAT(///,9X,'H',22X,'=',13X,I3,10X,'THRESHOLD',14X,'=',3X,F13.
240           &6)
241     110  FORMAT(9X,'LAMBDA',17X,'=',2X,1PE11.5,13X,'FWHM',19X,'=',2X,1PE1
242           &1.5)
243     111  FORMAT(59X,'STRONG CONTRIBUTION',4X,'=',F13.6)
244     112  FORMAT(59X,'ABOVE THRESHOLD',8X,'=',F13.6)
245     113  FORMAT(59X,'ION WIDTH (%)',10X,'=',2X,1PE11.5,1X,'(',,0PF4.1,')')
246     114  FORMAT(59X,'STRONG WIDTH (%)',7X,'=',3X,F4.1)
247     115  FORMAT(9X,'DELTA N*',15X,'=',3X,F13.6,10X,'PHI',21X,'=',3X,F13.
248           &6)
249     STOP
250     END

```

ELAN#STARKB(1).OURG

```

1 C ***** 3/8/79 *****
2 C ** VERSION 1 **
3 C THIS SUBROUTINE CALCULATES A PROPOSED SEMICLASSICAL FORM
4 C OF THE SAUNT FACTOR, NOT TAKING THE CURVATURE OF THE ORBIT
5 C INTO ACCOUNT.
6 C *****
7     SUBROUTINE GBAR(F,E,X,T,G,GO,Z,NO)
8     REAL NO
9     INTEGER U,Z
10    Y=ABS(F-E)
11    X=SQRT(1.5*T/Y)
12    ZZ=FLOAT(Z)
13    CP=2.0*(1.5*T)**1.5/((ZZ-1.)*SQRT(109737.))*Y)
14    EMIN = 1.5*T/(109737.*(ZZ-1.))**2)
15    EMIN=(1.0+(NO**4/ZZ**2))*(1.0+1.5*T/109737.))*EMIN
16    EMIN=1.0*EMIN
17    G=(CP**2+1.)/EMIN
18    G=SQRT(3.)/(2.0*3.14159)*ALOG(G)
19    IF(G.GE.0.2)GO TO 1
20    G=GO
21    GO TO 5
22    1  F4=2.0*NO**2/ZZ
23    PRINT 201,F4
24    201 FORMAT(/,9X,'GRIENS DIPOLE MOMENT',3X,'=',3X,F13.6)
25    5  PRINT 202,X,G
26    202 FORMAT(/,9X,'X',22X,'=',3X,F13.6,10X,'G',23X,'=',3X,F13.6)
27    RETURN
28    END

```

ELAM*STARKB(1).RACAH1

```

1 C ***** 3/8/79 *****
2 C THIS SUBROUTINE CALCULATES THE RACAH COEFFICIENT USING AN
3 C EXPANSION GIVEN BY BRINK FOR THE 6-J SYMBOL:
4 C
5 C / \
6 C [ A A+1 1 ]
7 C [ C C ]
8 C [ M3 C 0 ]
9 C \ /
10 C
11 C WHERE M3 = C-1,B,B+1 .
12 C
13 C *****
14 C SUBROUTINE RACAH1(A,B,C,M3,S2)
15 C REAL M3
16 C IF(M3.EQ.B)GO TO 1
17 C IF(M3.EQ.(B-1.0))GO TO 2
18 C S2=(A+B+C+3.)*(A+B+C+2.)*(A+B-C+2.)*(A+B-C+1.0)
19 C D1=(2.0*A+3.0)*(2.0*A+2.)*(2.*A+1.)
20 C D1=D1*(2.*B+3.)*(2.*B+2.)*(2.*B+1.)
21 C S2=S2/D1
22 C GO TO 3
23 C 1 S2=(A+B+C+2.0)*(A-B+C+1.)*(A+B-C+1.)*(C-A+B)
24 C D1=(2.0*A+3.0)*(2.*A+2.)*(2.*A+1.)*B*(2.*B+2.)*(2.*B+1.)
25 C S2=S2/D1
26 C GO TO 3
27 C 2 S2=(C-A+B)*(C-A+B-1.)*(A-B+C+2.)*(A-B+C+1.)
28 C D1=(2.*A+3.)*(2.*A+2.)*(2.*A+1.)*(2.*B-1.)*2.*B*(2.*B+1.)
29 C S2=S2/D1
30 C 3 RETURN
31 C END

```

ELAM*STARKB(1).RACAH2

```

1 C ***** 3/8/79 *****
2 C THIS SUBROUTINE CALCULATES THE RACAH COEFFICIENT USING AN
3 C EXPANSION FORMULA GIVEN BY BRINK FOR THE 6-J SYMBOL:
4 C
5 C / \
6 C [ A A 1 ]
7 C [ C C ]
8 C [ B B C ]
9 C \ /
10 C
11 C *****
12 C SUBROUTINE RACAH2(LL,J,S,S2)
13 C REAL J,L
14 C L=FLOAT(LL)
15 C S2=(L*(L+1.)+J*(J+1.))-S*(S+1.))**2
16 C D1=(2.*L+2.)*(2.*L+1.)*2.*L*(2.*J+1.)*(J+1.)*J
17 C S2=S2/D1
18 C RETURN
19 C END

```

ELAM*STARKB(1).COLUMN

```

1      C ***** 3/8/79 *****
2      C THIS SUBROUTINE SELECTS THE RELEVANT CLOLUMN OF BATES DAM-
3      C GAARD FACTORS FROM A TABLE IN MEMORY.THE TYPE OF PROCESS IS
4      C ESTABLISHED AND DETERMINES THE COLUMN NUMBER.
5      C *****
6          SUBROUTINE COLUMN(K,A)
7          IF(A.LT.3.5)GO TO 1
8          IF(A.LT.4.5)GO TO 2
9          K=3
10         GO TO 3
11         1    K=1
12         GO TO 3
13         2    K=2
14         3    RETURN
15        END

```

ELAM*STARKB(1).INTERP

```

1      C ***** 7/8/79 *****
2      C THIS SUBROUTINE INTERPOLATES BETWEEN THE VARIOUS VALUES
3      C READ IN FROM A TABLE OF BATES DAMGAARD FACTORS.
4      C *****
5          SUBROUTINE INTERP(N3,N1,0,F4)
6          DIMENSION O(25)
7          INTEGER V
8          REAL NN,N1,N3
9          DO 1 N=2,25
10         X1=N3-N1
11         NN=FLOAT(N)
12         X3=-1.5+0.1*NN
13         IF(X1.LT.X3)GO TO 2
14         1    CONTINUE
15         2    VV=NN
16         V=IFIX(VV)
17         A=0.5*(O(V+1)-2.*O(V)+O(V-1))
18         B=0.5*(O(V+1)-O(V-1))-2.*A*VV
19         C=O(V)-A*VV**2-B*VV
20         X1=(X1+1.5)*10.
21         OO=A*(X1)**2+B*(X1)+C
22         F4=OO**2
23         RETURN
24        END

```

ELAN*STARKB(1).STRONG

```

1      C ***** 3/8/79 *****
2      C ** VERSION 1 **
3      C THIS SUBROUTINE EVALUATES THE STRONG COLLISION CONTRIBUTION
4      C IN ELECTRON COLLISION BROADENING.
5      C *****
6      C SUBROUTINES CALLED :
7      C           RAD (VERSION 1)
8      C *****
9      SUBROUTINE STRONG(T,ZZ,P4,NO,LO,H)
10     REAL NO
11     INTEGER H
12     P4=1.0+(T/109737.)
13     LZ=IFIX(ZZ)
14     CALL RAD(NO,LZ,LO,RAAD)
15     P4=P4*RAAD
16     P4=(P4+1.0)*0.413497
17     XX=FLOAT(H)
18     P4=P4*(2.0-XX)
19     RETURN
20     END

```

ELAN*STARKB(1).RAD1

```

1      C ***** 3/8/79 *****
2      C ** VERSION 1 **
3      C THIS SUBROUTINE CALCULATES THE DISTANCE DLL IN THE DENOMINATOR
4      C OF THE GBAR FACTOR AS  $N^{**4}/Z^{**2}$ .
5      C *****
6      SUBROUTINE RAD(N,Z,L,R)
7      REAL N
8      INTEGER Z
9      R=N**4/Z**2
10     RETURN
11     END

```

ELAM*STARKB(1).MTD2M

```

1      C ***** 21/8/79 *****
2      C THIS PROGRAM EVALUATES THE SPECTRAL LINE BROADENING CAUSED BY
3      C ELECTRON PERTURBERS.STRONG CONTRIBUTIONS FOR THE UPPER LEVEL
4      C ARE INCLUDED,AND AN ESTIMATE OF THE ION BROADENING IS MADE.TO
5      C ENSURE COMPLETENESS OF THE PERTURBERS,THE SUM OF THE USED MATRIX
6      C ELEMENTS IS COMPARED TO THE HYDROGENIC ESTIMATE.
7      C *****
8      C SUBROUTINES CALLED FROM HAIN PROGRAM :
9      C
10     C      RACAHI
11     C      RACAHI2
12     C      BATESD
13     C      RAD (VERSION 2)
14     C      GBAR (VERSION 2)
15     C      GAV
16     C      STRONG (VERSION 2)
17     C      TABLE
18     C *****
19     DIMENSION JJ(3,25),KK(3,25),LL(3,25),PP(2),QH(2),GT(2)
20     DIMENSION TG(30),JLS(30),JNLS(30),JNLG(30),JLLS(30),JLLG(30)
21     DIMENSION JJLS(30),JJLG(30)
22     DIMENSION P1IN(2)
23     REAL JJ,KK,LL,NO,N2,J,N1,N3,L2,M2,M3,M4,K,NLG,NLS
24     CHARACTER DETAIL*4
25     INTEGER Z,H,Q
26     Q=5
27     PRINT 901
28     901  FORMAT(3X,'DO YOU WANT A DETAILED PRINTOUT ? (YES OR NO)')
29     READ 902,DETAIL
30     902  FORMAT(A3)
31     C *** READ IN THE BATES DANGAARD FACTORS FROM FILE BATES.
32     DO 500 N=1,3
33     DO 501 NN=1,25
34     READ 100,JJ(N,NN)
35     501  CONTINUE
36     500  CONTINUE
37     DO 600 N=1,3
38     DO 601 NN=1,25
39     READ 100,KK(N,NN)
40     601  CONTINUE
41     600  CONTINUE
42     DO 700 N=1,3
43     DO 701 NN=1,25
44     READ 100,LL(N,NN)
45     701  CONTINUE
46     700  CONTINUE
47     C *** READ IN ION SPECIFICATIONS
48     READ 100,Z
49     READ 100,T,D
50     READ 100,W1
51     WRITE(Q,100)Z
52     WRITE(Q,100)W1
53     WRITE(Q,100)T,D
54     C *** START OF COMPUTATIONS
55     WRITE(Q,103)

```

```

56      RP4=0.
57      C *** START OF UPPER/LOWER LEVEL CALCULATIONS
58          DO 3 H=1,2
59              STOR=0.
60              STOR2=0.
61              SUMG=0.
62              P1=0.
63              PP1=0.0
64              P1IN(H)=0.0
65              WRITE(Q,102)H
66      C *** READ IN TRANSITION LEVEL,NO. OF PERTURBING LEVELS
67          READ 100,LO,L,L1,J,S,E,E1,WT1,CONS,JN1
68          READ 100,J1
69          IF(J1.EQ.0)GO TO 30
70      C *** START OF EACH PERTURBATION
71          DO 4 I=1,J1
72      C *** READ IN PERTURBING LEVEL
73          READ 100,MO,M,K,F,WT2,JN2
74          ZZ=FLOAT(Z)
75          NO=SQRT(109737.*ZZ**2/(E1-E))
76          N2=SQRT(109737.*ZZ**2/(E1-F))
77          WRITE(Q,101)NO,N2
78          QN(H)=NO
79      C *** ORDER PRINCIPAL Q.NO. AND ANGULAR MOMENTA BY SIZE
80      C *** ALL J***(**) ARE COLLECTED FOR TABULATION OF THE
81      C *** THRESHOLD GAUNT FACTORS AT THE END.
82          NS=AMIN1(NO,N2)
83          IF(NO.LT.#2)GO TO 401
84          LNS=MO
85          GO TO 402
86      401      LNS=LO
87      402      LG=AMAX1(LO,MO)
88          LS=AMIN1(LO,MO)
89          IF(H.EQ.1)II=I
90          IF(H.EQ.2)II=I+JSJ
91          IF(LO.GT.MO)GO TO 403
92          NLG=N2
93          JNLG(II)=JN2
94          NLS=NO
95          JNLS(II)=JN1
96          JLLS(II)=L+1
97          JLLG(II)=M+1
98          JJLS(II)=J
99          JJLG(II)=K
100         GO TO 404
101      403      NLG=NO
102             JNLG(II)=JN1
103             NLS=N2
104             JNLS(II)=JN2
105             JLLS(II)=M+1
106             JLLG(II)=L+1
107             JJLS(II)=K
108             JJLG(II)=J
109      404      WRITE(Q,121)NLG,LNS
110             WRITE(Q,122)LG,LS

```

```

111 C *** EVALUATE ARGUMENTS OF RACAH COEFFICIENTS OF THE L-MOMENTA
112     IF(NO.LT.L0)GO TO 5
113     RR=FLOAT(2*L0+1)
114 C *** START OF LINE STRENGTH COLLECTION
115     R=(FLOAT(L0+1))/RR
116     L2=FLOAT(L0)
117     N1=N2
118     N3=NO
119     M2=FLOAT(L)
120     M3=FLOAT(M)
121     M4=FLOAT(L1)
122     GO TO 6
123 5     L2=FLOAT(NO)
124     RR=FLOAT(2*L0+1)
125     R=(FLOAT(NO+1))/RR
126     N1=NO
127     N3=N2
128     M2=FLOAT(M)
129     M3=FLOAT(L)
130     M4=FLOAT(L1)
131 6     CALL RACAH1(L2,M2,M4,M3,S2)
132 C *** CHECK COMPLETENESS OF L-SPLITTING
133     C2=RR*(FLOAT(2*N+1))*S2
134 C *** LINE STRENGTH COLLECTION
135     R=R*C2
136     MM=1
137     IF(DETAIL.EQ.3HNO )GO TO 800
138     WRITE(Q,104)
139     WRITE(Q,100)L0,NO,L,M,MM,L1
140     WRITE(Q,105)S2,C2
141 C *** EVALUATE ARGUMENTS OF RACAH COEFF. OF J-MOMENTA
142 800    IF(M-L)7,8,9
143 8     IF(K-J)10,11,12
144 12    L2=J
145     M2=FLOAT(L)
146     M3=FLOAT(M)
147     M4=S
148     GO TO 13
149 10    L2=K
150     M2=FLOAT(M)
151     M3=FLOAT(L)
152     M4=S
153     GO TO 13
154 9     L2=FLOAT(L)
155     M2=J
156     M3=K
157     M4=S
158     GO TO 13
159 7     L2=FLOAT(M)
160     M2=K
161     M3=J
162     M4=S
163 13    CALL RACAH1(L2,M2,M4,M3,S2)
164     GO TO 14
165 11    CALL RACAH2(L,J,S,S2)

```

```

166 C *** CHECK COMPLETENESS OF J-SPLITTING
167 14 C2=FLOAT(2*L+1)
168 C2=C2*(2.*K+1.)*S2
169 IF(DETAIL.EQ.3HNO )GO TO 801
170 WRITE(Q,106)
171 WRITE(Q,100)L,M,J,K,MM,S
172 WRITE(Q,105)S2,C2
173 C *** LINE STRENGTH COLLECTION
174 801 R=R*C2
175 X2=N3-N1
176 DE=ABS(F-E)
177 CALL BATESD(JJ,KK,LL,MLG,NLS,LS,BDF)
178 CALL RAO(NLG,LNS,LG,Z,BDF,RLL2,DLL)
179 C *** STORE SUM OF DIPOLE MOMENTS FOR AVERAGE
180 STOR=STOR+DLL
181 STOR2=STOR2+DLL**2
182 WRITE(Q,109)RLL2,BDF
183 C *** CALCULATE GAUNT FACTOR
184 CALL GBAR(Z,DE,T,DLL,PHI,G)
185 WRITE(Q,116)DLL,PHI
186 C *** LINE STRENGTH COLLECTION
187 R=R*RLL2
188 P=WT2*(G)*R
189 C *** INELASTIC CONTRIBUTION
190 IF(F-E)15,15,16
191 16 PIN=P*EXP(-DE/T)
192 P1IN(H)=P1IN(H)+PIN
193 C *** HYDROGENIC MATRIX ELEMENT
194 15 RLO=FLOAT(L0)
195 P2=NO**2*(5.*NO**2+1.-3.*RLO**2-3.*RLO)/2./Z**2
196 C *** SUM MATRIX ELEMENTS
197 PP1=PP1+R
198 P1=P1+P
199 C *** THRESHOLD GAUNT FACTOR
200 CALL GAV(Z,DE,DLL,GAVT)
201 SUMG=SUMG+GAVT
202 TG(II)=GAVT
203 JLS(II)=LS+1
204 IF(DETAIL.EQ.3HNO )GO TO 4
205 WRITE(Q,123)X2,BDF
206 WRITE(Q,107)H,I
207 WRITE(Q,108)P
208 4 CONTINUE
209 30 NO=SQRT(109737.*ZZ**2/(E1-E))
210 ON(H)=NO
211 C *** AVERAGE DIPOLE MOMENT
212 AVR=STOR/FLOAT(J1)
213 AVR2=STOR2/FLOAT(J1)
214 GT(H)=SUMG/FLOAT(J1)
215 SG=SUMG+SG
216 JSJ=JSJ+J1
217 CALL STRONG(Z,T,AVR,AVR2,P4,H)
218 C *** COMPLETENESS AND EXTRA CONTRIBUTION
219 PP2=PP1/P2*100.
220 P3=(P2-PP1)*GT(H)

```

```

221 C *** SUM WEAK,STRONG AND EXTRA CONTRIBUTIONS
222     PP(H)=P1+P4+P3
223     WRITE(Q,112)P1
224     WRITE(Q,111)P4
225     WRITE(Q,118)P3
226     WRITE(Q,119)P1IN(H)
227     WRITE(Q,115)P2,PP2
228     RP4=P4+RP4
229     3     CONTINUE
230 C *** ADD UPPER AND LOWER LEVEL CONTRIBUTIONS AND FIND WIDTH
231     P3=PP(1)+PP(2)
232     W1=1.0/W1
233     W=0.5576E-10*D*W1**2*SQRT(109737./T)
234     WW=W*P3
235 C *** CALCULATE (NEGLECTED) ION WIDTH
236     WION=4.08682E-11*W1**2/Z**2
237     WION=WION*D*(QN(1)**2-QN(2)**2)**2
238     PIE=WION/WW*100.
239 C *** % STRONG WIDTH
240     PRP4=RP4/P3*100.
241     GAVT=SG/JSJ
242 C *** % INELASTIC CONTRIBUTIONS
243     P1INP=(P1IN(1)+P1IN(2))/P3*100.
244     PSUM=P1IN(1)+P1IN(2)
245     WRP4=W*RP4
246     WPSUM=W*PSUM
247     WRITE(Q,110)W1,WW
248     WRITE(Q,114)WRP4,PRP4
249     WRITE(Q,113)WION,PIE
250     WRITE(Q,120)WPSUM,P1INP
251     WRITE(Q,117)GAVT
252 C *** COMPILE TABLE OF ALL THRESHOLD GAUNT FACTORS IN PROGRAM
253     CALL TABLE(TG,JLS,JNLS,JNLG,JLLS,JLLG,JJLS,JJLG,JSJ,Z)
254     100     FORMAT(
255     101     FORMAT(///,8X,' N* UPPER (LOWER) STATE = ',F13.6,9X,' N* PERTURB
256     &ING LEVEL      = ',F13.6)
257     102     FORMAT(///,30X,'ENERGY LEVEL NUMBER ',I1,/)
258     103     FORMAT(1H1,/,28X,'*', ' SPECTRAL LINE BROADENING ', '*',///)
259     104     FORMAT(/)
260     105     FORMAT(/,9X,'S2',21X,'=',3X,F13.6,10X,'C2'22X,'=',3X,F13.6)
261     106     FORMAT(/)
262     107     FORMAT(9X,'H',22X,'=',13X,I3,10X,'I',23X,'=',13X,I3)
263     108     FORMAT(9X,'CONTRIBUTION',11X,'=',3X,F13.6,///)
264     109     FORMAT(9X,'RLL2',19X,'=',3X,F13.6,10X,'BDF',21X,'=',3X,F13.6)
265     110     FORMAT(/,9X,'LAMBDA',17X,'=',2X,1PE11.5,13X,'FWHM',20X,'=',2X,1PE1
266     &1.5)
267     111     FORMAT(59X,'STRONG CONTRIBUTION',5X,'=',3X,F13.6)
268     112     FORMAT(59X,'TOTAL CONTRIBUTION',5X,'=',3X,F13.6)
269     113     FORMAT(59X,'ION WIDTH (%)',11X,'=',2X,1PE11.5,1X,'(', 'OPF4.1,')')
270     114     FORMAT(59X,'STRONG WIDTH (%)',8X,'=',2X,1PE11.5,1X,'(', 'OPF4.1,')')
271     115     FORMAT(59X,'CHECK ON COMPLETENESS(%)',2X,1PE11.5,'(', 'OPF4.1,')')
272     116     FORMAT(9X,'DLL',20X,'=',3X,F13.6,10X,'PHI',21X,'=',3X,F13.6)
273     117     FORMAT(59X,'AVERAGE THRESHOLD G      =',3X,F13.6)
274     118     FORMAT(59X,'EXTRA CONTRIBUTION',5X,'=',3X,F13.6)
275     119     FORMAT(59X,'INELASTIC CONTRIBUTION',2X,'=',3X,F13.6)
276     120     FORMAT(59X,'INELASTIC WIDTH (%)',5X,'=',2X,1PE11.5,' ( ', 'OPF4.1,')'
277     &)
278     121     FORMAT(9X,'NLG',20X,'=',3X,F13.6,10X,'LNS',21X,'=',13X,I3)
279     122     FORMAT(9X,'LG',21X,'=',13X,I3,10X,'LS',22X,'=',13X,I3)
280     123     FORMAT(9X,'DELTA N*',15X,'=',3X,F13.6,10X,'BDF',21X,'=',3X,F13.6)
281     STOP
282     END

```

ELAN*STARKB(1).BATESD1

```

1      C ***** 21/8/79 *****
2      C ** VERSION 1 **
3      C THIS SUBROUTINE DETERMINES THE APPROPRIATE BATES DANGAARD FACTOR
4      C FROM THE TABLES GIVEN BY FILE BATES.
5      C *****
6      C SUBROUTINES CALLED :
7      C         COLUMN
8      C         INTERP
9      C *****
10     SUBROUTINE BATESD(JJ, KK, LL, NLG, NLS, LS, BDF)
11     DIMENSION JJ(3,25), KK(3,25), LL(3,25), O(25)
12     REAL JJ, KK, LL, NLS, NLG, NL
13     X2=NLS-NLG
14     IF(X2.GT.1.)GO TO 33
15     X2=ABS(X2)
16     IF(X2.GT.1.3)GO TO 33
17     IF(LS.EQ.0.)GO TO 17
18     IF(LS.EQ.1.)GO TO 18
19     IF(LS.EQ.3.)GO TO 31
20     NL=NLG-1.
21     CALL COLUMN(KL, NL)
22     DO 19 N=1,25
23     19  O(N)=LL(KL, N)
24     GO TO 20
25     17  NLG=NLG
26     CALL COLUMN(KL, NLG)
27     DO 21 N=1,25
28     21  O(N)=JJ(KL, N)
29     GO TO 20
30     18  NLG=NLG
31     CALL COLUMN(KL, NLG)
32     DO 22 N=1,25
33     22  O(N)=KK(KL, N)
34     20  CALL INTERP(NLS, NLG, O, F4)
35     GO TO 32
36     33  F4=0.
37     GO TO 32
38     31  F4=0.6203
39     32  BDF=SQRT(F4)
40     RETURN
41     END

```

ELAN*STARKB(1).RA02

```

1      C ***** 23/11/79 *****
2      C ** VERSION 2 **
3      C THIS PROGRAM EVALUATES THE RADIAL INTEGRAL AS WELL AS THE
4      C DIPOLE MOMENT OPERATOR IN THE COULOMB APPROXIMATION.
5      C *****
6      SUBROUTINE RAO(NLG, LNS, LG, Z, BDF, R, D)
7      REAL NLG
8      INTEGER Z
9      R=(NLG**2-FLOAT(LG)**2)*2.25*(NLG/Z)**2*BDF**2
10     D=R*FLOAT(LG)/FLOAT(2*LNS+1)/3.
11     D=SQRT(D)
12     RETURN
13     END

```

ELAM*STARKB(1).OURG2

```

1 C ***** 21/8/79 *****
2 C ** VERSION 2 **
3 C THIS SUBROUTINE CALCULATES THE EFFECTIVE GAUNT FACTOR TAKING
4 C THE CURVATURE OF THE CLASSICAL HYPERBOLIC ORBIT INTO ACCOUNT.
5 C THE UPPER LIMIT OF THE IMPACT PARAMETER AS GIVEN BY THE
6 C MINIMUM OF THE REQUIRED ELECTRON ENERGY AND THE LOWER LIMIT
7 C IS DETERMINED IN ACCORDANCE TO THE LIMIT OF STRONG COLLISIONS.
8 C *****
9 C SUBROUTINES CALLED:
10 C CUBIC
11 C *****
12 SUBROUTINE GBAR(Z,DE,T,R,PHI,G)
13 INTEGER Z
14 X=SQRT(1.5*T/DE)
15 Y=SQRT(109737./DE)
16 ZZ=FLOAT(Z)
17 CALL CUBIC(ZZ,X,Y,PHI)
18 CP=(ZZ-1.0)*Y/(2.0*X**3)
19 G=1.0+PHI**4/CP**2
20 TT=((ZZ-1.)*Y/X)**2
21 TEST=1*R**2-TT
22 IF(TEST.LT.0.0)GO TO 2
23 DEN=1.+R**2*(1.0+(X/Y)**2+2.*(ZZ-1.)/R)-TT
24 GO TO 3
25 2 DEN=1.+R**2*((X/Y)**2+2.0*(ZZ-1.)/R)
26 3 DEN=1.0+DEN*(X/Y)**2/(ZZ-1.0)**2
27 F=SQRT(3)/3.14159
28 G=F/2.0*ALOG(G/DEN)
29 IF(G.GT.0.0)GO TO 1
30 G=0.0
31 1 PRINT 101,X,G
32 101 FORMAT(/,9X,'X',22X,'=',3X,F13.6,10X,'G',23X,'=',3X,F13.6)
33 RETURN
34 END

```

ELAM*STARKB(1).GAV

```

1 C ***** 27/8/79 *****
2 C THIS SUBROUTINE CALCULATES THE EFFECTIVE GAUNT FACTOR OF THE
3 C PARTICULAR LINE OBSERVED.
4 C *****
5 C SUBROUTINES CALLED :
6 C GBAR (VERSION 2)
7 C *****
8 SUBROUTINE GAV(Z,DE,RLL,GA)
9 INTEGER Z
10 T=DE/1.5
11 CALL GBAR(Z,DE,T,RLL,PHI,GA)
12 RETURN
13 END

```

ELAM*STARKB(1).STRONG2

```

1      C ***** 21/8/79 *****
2      C ** VERSION 2 **
3      C THIS STRONG COLLISION TERM MAKES USE OF CURVATURE CORRECTIONS AND
4      C THE AVERAGED RADIAL INTEGRAL COMPUTED.
5      C *****
6      SUBROUTINE STRONG(Z,T,AVR,AVR2,P4,H)
7      INTEGER Z,H
8      P4=(1.0+T/109737.)*AVR2
9      P4=2.0*(Z-1)*AVR+P4+1.
10     XX=FLOAT(H)
11     P4=P4*(2.0-XX)*0.413497
12     RETURN
13     END

```

ELAM*STARKB(1).TABLE

```

1      C ***** 14/9/79 *****
2      C A TABLE OF THE PROCESSES IN THIS LINE WIDTH CALCULATION IS
3      C PRINTED WITH THE RELEVANT THRESHOLD GAUNT FACTOR OF EACH.
4      C *****
5      SUBROUTINE TABLE(TG,LS,NLS,NLG,CLS,CLG,JLS,JLG,JSJ,Z)
6      DIMENSION TG(50),LS(50),NLS(50),NLG(50),CLS(50),CLG(50)
7      DIMENSION JLS(50),JLG(50)
8      CHARACTER A1*1,A2*1,A3*1,A4*1
9      INTEGER Z,CLS,CLG
10     PRINT 100,Z
11     100 FORMAT(1H1,/,20X,'IONISATION STAGE ',I2,/)
12     PRINT 101
13     101 FORMAT(9X,'N L CL J ',10X,'N L CL J ',10X,'G EFF.',/,10('*
14     &*****'),/)
15     DO 1 K=1,JSJ
16     CALL TRANSL(LS(K),A1)
17     CALL TRANSL(CLS(K),A2)
18     LG=LS(K)+1
19     CALL TRANSL(LG,A3)
20     CALL TRANSL(CLK(K),A4)
21     PRINT 102,NLS(K),A1,A2,JLS(K),NLG(K),A3,A4,JLG(K),TG(K)
22     102 FORMAT(9X,2(I1,2X,A1,2X,A2,2X,I2,10X),F5.3)
23     1 CONTINUE
24     RETURN
25     SUBROUTINE TRANSL(I,A)
26     CHARACTER A*1
27     IF(I.EQ.1)A=1HS
28     IF(I.EQ.2)A=1HP
29     IF(I.EQ.3)A=1HD
30     IF(I.EQ.4)A=1HF
31     IF(I.EQ.5)A=1HG
32     RETURN
33     END

```

ELAM*STARKB(1).CUBIC2

```

1      C ***** 14/9/79 *****
2      C THIS SUBROUTINE SOLVES THE CUBIC ARISING IN THE GBAR
3      C CALCULATION USING AN EXACT METHOD AND NOT AN ITERATION.
4      C *****
5          SUBROUTINE CUBIC(Z,X,Y,PHI)
6          CP=(Z-1.)*Y/(X**3*2.)
7          SCP=CP**2
8          TCP=1./27.
9          IF(SCP-TCP)1,2,2
10         1      T=(TCP/SCP)-1.
11             T=SQRT(T)
12             T=ATAN(T)
13             T=T/3.
14             PHI=2./SQRT(3.)*COS(T)
15             GO TO 3
16         2      T=SQRT(SCP-TCP)
17             T1=CP+T
18             T2=CP-T
19             PHI=T1**0.33333+T2**0.33333
20         3      RETURN
21         END

```

ELAM*STARKB(1).CUBIC1

```

1      C ***** 3/8/79 *****
2      C THIS SUBROUTINE SOLVES THE CUBIC ARISING DUE TO THE CURVATURE
3      C EFFECT FOR ITS POSITIVE ROOTS BY MEANS OF A HILL-CLIMBING METHOD.
4      C *****
5          SUBROUTINE CUBIC(Z,X,Y,PHI)
6          PHI=0.0
7          ASSIGN 10 TO J
8          ASSIGN 1 TO K
9          6      CUB=PHI**3-PHI-(Z-1.)*Y/X**3
10             IF(CUB.EQ.0.0)GO TO 5
11             IF(CUB.GT.0.0)GO TO K,(1,3,4,5)
12             GO TO J,(10,11,12,13)
13         10     PHI=PHI+0.1
14             GO TO 6
15         1      PHI=PHI-0.1+0.01
16             ASSIGN 11 TO J
17             ASSIGN 3 TO K
18             GO TO 6
19         11     PHI=PHI+0.01
20             GO TO 6
21         3      PHI=PHI-0.01+0.001
22             ASSIGN 12 TO J
23             ASSIGN 4 TO K
24             GO TO 6
25         12     PHI=PHI+0.001
26             GO TO 6
27         4      PHI=PHI-0.001+0.0001
28             ASSIGN 13 TO J
29             ASSIGN 5 TO K
30             GO TO 6
31         13     PHI=PHI+0.0001
32             GO TO 6
33         5      RETURN
34         END

```

ELAM*STARKB(1).MTD2AM

```

1   C ***** 21/8/79 *****
2   C THIS PROGRAM EVALUATES THE SPECTRAL LINE BROADENING CAUSED BY
3   C ELECTRON PERTURBERS.STRONG CONTRIBUTIONS FOR THE UPPER LEVEL
4   C ARE INCLUDED,AND AN ESTIMATE OF THE (NEGLECTED) ION BROADENING IS
5   C MADE.TO ESTIMATE COMPLETENESS OF THE PERTURBERS,THE SUM OF THE
6   C USED RADIAL INTEGRALS IS COMPARED TO THE HYDROGENIC ESTIMATE.
7   C THE GAUNT FACTOR IS CALCULATED USING A RIGOROUS AVERAGING OVER THE
8   C MAXWELLIAN VELOCITY DISTRIBUTION.TO DO THIS AN ADDITIONAL INPUT IS
9   C REQUIRED AFTER ENTERING THE 'DETAIL',NAMELY THE MAXIMUM NO.OF ITER-
10  C RATIONS AND THE UPPER LIMIT OF INTEGRATION:
11  C
12  C           MAXIT,ZZZ
13  C
14  C THE FINAL WIDTH IS NOT CORRECTED FOR COMPLETENESS.
15  C *****
16  C LIST OF SUBROUTINES CALLED FROM MAIN PROGRAM:
17  C           RACAH1
18  C           RACAH2
19  C           BATESD(VERSION 2)
20  C           RAO (VERSION 2)
21  C           GBARAV
22  C           DISENT
23  C           GAV
24  C           STRONG (VERSION 2)
25  C           TABLE
26  C *****
27  C           DIMENSION JJ(3,25),KK(3,25),LL(3,25),PP(2),QN(2),GT(2)
28  C           DIMENSION MM(3,25),MNN(3,25)
29  C           DIMENSION TG(50),JLS(50),JNLS(50),JNLG(50),JLLS(50),JLLG(50)
30  C           DIMENSION JJLS(50),JJLG(50)
31  C           DIMENSION SPEL(2)
32  C           COMMON/AA/Z,DE,T,DLL,PHI,G,GIN,SEL,FK,MAXIT,AAA,ZZZ
33  C           REAL JJ,KK,LL,NO,N2,J,N1,N3,L2,M2,M3,M4,K,NLG,NLS
34  C           REAL MM,MNN
35  C           CHARACTER DETAIL*4
36  C           INTEGER Z,H,Q
37  C           Q=5
38  C           PRINT 901
39  C           901  FORMAT(3X,'DO YOU WANT A DETAILED PRINTOUT ? (YES OR NO)')
40  C           READ 902,DETAIL
41  C           C *** READ IN INTEGRATION DETAILS
42  C           READ 100,MAXIT,ZZZ
43  C           PRINT 100,MAXIT,ZZZ
44  C           902  FORMAT(A3)
45  C           C *** READ IN THE BATES DAMGAARD FACTORS FROM FILE BATES2.
46  C           DO 500 N=1,3
47  C           DO 501 NN=1,25
48  C           READ 100,JJ(N,NN)
49  C           501  CONTINUE
50  C           500  CONTINUE
51  C           DO 600 N=1,3
52  C           DO 601 NN=1,25
53  C           READ 100,KK(N,NN)
54  C           601  CONTINUE
55  C           600  CONTINUE

```

```

56         DO 700 N=1,3
57         DO 701 NN=1,25
58         READ 100,LL(N,NN)
59         701 CONTINUE
60         700 CONTINUE
61         DO 8000 N=1,3
62         DO 8001 NN=1,25
63         READ 100,MM(N,NN)
64         8001 CONTINUE
65         8000 CONTINUE
66         DO 9000 N=1,3
67         DO 9001 NN=1,25
68         READ 100,MNN(N,NN)
69         9001 CONTINUE
70         9000 CONTINUE
71         C *** READ IN ION SPECIFICATIONS
72         READ 100,Z
73         READ 100,T,D
74         READ 100,W1
75         WRITE(Q,100)Z
76         WRITE(Q,100)W1
77         WRITE(Q,100)T,D
78         C *** START OF COMPUTATIONS
79         WRITE(Q,103)
80         RP4=0.
81         C *** START OF UPPER/LOWER LEVEL CALCULATION
82         DO 3 H=1,2
83         STOR=0.
84         STOR2=0.
85         SUMG=0.
86         P1=0.
87         PP1=0.0
88         SPEL(H)=0.0
89         WRITE(Q,102)H
90         C *** READ IN TRANSITION LEVEL,NO. OF PERTURBING LEVELS
91         READ 100,LO,L,L1,J,S,E,E1,WT1,CONS,JN1
92         READ 100,J1
93         READ 100,EMIN
94         IF(J1.EQ.0)GO TO 30
95         C *** START OF EACH PERTURBATION
96         DO 4 I=1,J1
97         C *** READ IN PERTURBING LEVEL
98         READ 100,HO,M,K,F,WT2,JN2,WT3
99         ZZ=FLOAT(Z)
100        NO=SQRT(109737.*ZZ**2/(E1-E))
101        N2=SQRT(109737.*ZZ**2/(E1-F))
102        WRITE(Q,101)NO,N2
103        QN(H)=NO
104        C *** ORDER PRINCIPAL Q.NO. AND ANGULAR MOM. BY SIZE
105        C *** ALL J***(**) ARE COLLECTED FOR TABULATION OF THE
106        C *** THRESHOLD GAUNT FACTOR AT THE END.
107        NS=AMIN1(NO,N2)
108        IF(NO.LT.N2)GO TO 401
109        LNS=MO
110        GO TO 402

```

```

111      401      LNS=L0
112      402      LG=AMAX1(LO,MO)
113              LS=AMIN1(LO,MO)
114              IF(H.EQ.1)II=I
115              IF(H.EQ.2)II=I+JSJ
116              IF(LO.GT.MO)GO TO 403
117              NLG=N2
118              JNLG(II)=JN2
119              NLS=NO
120              JNLS(II)=JN1
121              JLLS(II)=L+1
122              JLLG(II)=M+1
123              JJLS(II)=J
124              JJLG(II)=K
125              GO TO 404
126      403      NLG=NO
127              JNLG(II)=JN1
128              NLS=N2
129              JNLS(II)=JN2
130              JLLS(II)=M+1
131              JLLG(II)=L+1
132              JJLS(II)=K
133              JJLG(II)=J
134      404      WRITE(Q,121)NLG,LNS
135              WRITE(Q,122)LG,LS
136      C *** EVALUATE ARGUMENTS OF RACAH COEFFICIENTS S2(L2,M2,M4,M3;1,0)
137      C *** OF THE L-MOMENTA
138              IF(MO.LT.L0)GO TO 5
139              RR=FLOAT(2*L0+1)
140      C *** START OF LINE STRENGTH COLLECTION
141              R=(FLOAT(L0+1))/RR
142              L2=FLOAT(L0)
143              N1=N2
144              N3=NO
145              M2=FLOAT(L)
146              M3=FLOAT(M)
147              M4=FLOAT(L1)
148              GO TO 6
149      5        L2=FLOAT(M0)
150              RR=FLOAT(2*L0+1)
151              R=(FLOAT(M0+1))/RR
152              N1=NO
153              N3=N2
154              M2=FLOAT(M)
155              M3=FLOAT(L)
156              M4=FLOAT(L1)
157      6        CALL RACAH1(L2,M2,M4,M3,S2)
158      C *** CHECK COMPLETENESS OF L-SPLITTING
159              C2=RR*(FLOAT(2*M+1))*S2
160      C *** LINE STRENGTH COLLECTION
161              R=R*C2
162              MMH=1
163              IF(DETAIL.EQ.3HND )GO TO 800
164              WRITE(Q,104)
165              WRITE(Q,100)LO,MO,L,M,MMH,L1

```

```

166          WRITE(Q,105)S2,C2
167  C *** EVALUATE ARGUMENTS OF RACAH COEFF. OF J-MOMENTA
168  800      IF(M-L)7,8,9
169  B        IF(K-J)10,11,12
170  12      L2=J
171          M2=FLOAT(L)
172          M3=FLOAT(M)
173          M4=S
174          GO TO 13
175  10      L2=K
176          M2=FLOAT(M)
177          M3=FLOAT(L)
178          M4=S
179          GO TO 13
180  9        L2=FLOAT(L)
181          M2=J
182          M3=K
183          M4=S
184          GO TO 13
185  7        L2=FLOAT(M)
186          M2=K
187          M3=J
188          M4=S
189  13      CALL RACAH1(L2,M2,M4,M3,S2)
190          GO TO 14
191  11      CALL RACAH2(L,J,S,S2)
192  C *** CHECK COMPLETENESS OF J-SPLITTING
193  14      C2=FLOAT(2*L+1)
194          C2=C2*(2.*K+1.)*S2
195          IF(DETAIL.EQ.3HND )GO TO 801
196          WRITE(Q,106)
197          WRITE(Q,100)L,M,J,K,MMM,S
198          WRITE(Q,105)S2,C2
199  C *** LINE STRENGTH COLLECTION
200  801      R=R*C2
201          X2=N3-N1
202          DE=ABS(F-E)
203          CALL BATESD(JJ,KK,LL,MM,MNN,NLG,NLS,LS,BDF)
204          CALL RAD(NLG,LNS,LG,Z,BDF,RLL2,DLL)
205  C *** STORE SUM OF DIPOLE MOMENTS FOR AVERAGE
206          STOR=STOR+DLL
207          STOR2=STOR2+DLL**2
208          WRITE(Q,109)RLL2,BDF
209  C *** EXCITATION OR DE-EXCITATION ?
210          IF(F-E)17,17,18
211  17      FK=1.0
212          GO TO 19
213  18      FK=2.0
214  19      CALL GBARAV
215          WRITE(Q,116)DLL,PHI
216  C *** FOR WORST CASE CALL DISENTANGLEMENT TEST
217          IF(F-EMIN)51,50,51
218  50      CALL DISENT(D,W1)
219  51      CONTINUE
220  C *** LINE STRENGTH COLLECTION

```

```

221          R=R*RLL2*WT3
222          P=WT2*(G)*R
223 C *** ELASTIC CONTRIBUTION AND %
224          IF(F-E)15,15,16
225          16          PEL=P*GEL/G
226          SPEL(H)=SPEL(H)+PEL
227 C *** HYDROGENIC MATRIX ELEMENT
228          15          RLO=FLOAT(L0)
229          P2=NO**2*(5.*NO**2+1.-3.*RLO**2-3.*RLO)/2./Z**2
230 C *** SUM MATRIX ELEMENTS
231          PP1=PP1+R
232          P1=P1+P
233 C *** THRESHOLD GAUNT FACTOR
234          CALL GAV(Z,DE,DLL,GAVT)
235          SUNG=SUNG+GAVT
236          TG(II)=GAVT
237          JLS(II)=LS+1
238          IF(DETAIL.EQ.3HNO )GO TO 4
239          WRITE(Q,123)X2,BDF
240          WRITE(Q,107)H,I
241          WRITE(Q,108)P
242          4          CONTINUE
243          30          NO=SQRT(109737.*ZZ**2/(E1-E))
244          QN(H)=NO
245 C *** AVERAGE DIPOLE MOMENT
246          AVR=STOR/FLOAT(J1)
247          AVR2=STOR2/FLOAT(J1)
248          GT(H)=SUNG/FLOAT(J1)
249          SG=SUNG+SG
250          JSJ=JSJ+J1
251          CALL STRONG(Z,T,AVR,AVR2,P4,H)
252 C *** COMPLETENESS AND (NEGLECTED) EXTRA CONTRIBUTION
253          PP2=PP1/P2*100.
254          P3=(P2-PP1)*GT(H)
255 C *** ADD WEAK AND STRONG
256          PP(H)=P1+P4
257          WRITE(Q,112)P1
258          WRITE(Q,111)P4
259          WRITE(Q,118)P3
260          WRITE(Q,119)SPEL(H)
261          WRITE(Q,115)P2,PP2
262          RP4=P4+RP4
263          3          CONTINUE
264 C *** ADD UPPER AND LOWER LEVEL CONTRIBUTIONS AND COMPUTE
265 C *** LINE WIDTH
266          P3=PP(1)+PP(2)
267          W1=1.0/W1
268          W=0.5576E-10*D*W1**2*SQRT(109737./T)
269          UW=W*P3
270 C *** ION WIDTH AND %
271          WION=4.08682E-11*W1**2/Z**2
272          WION=WION*D*(QN(1)**2-QN(2)**2)**2
273          PIE=WION/UW*100.
274 C *** % STRONG,AVERAGE G-THRESHOLD,% ELASTIC AND STRONG WIDTH
275          PRP4=RP4/P3*100.

```

```

276      GAVT=SG/JSJ
277      PELP=(SPEL(1)+SPEL(2))/P3*100.
278      PSUM=SPEL(1)+SPEL(2)
279      WRP4=W*RP4
280      WPSUM=W*PSUM
281  C *** % INELASTIC AND INEL. WIDTH
282      PINL=100.-PELP-PRP4
283      WINL=PINL/100.*W
284      WRITE(Q,110)W1,W
285      WRITE(Q,114)WRP4,PRP4
286      WRITE(Q,113)WION,PIE
287      WRITE(Q,120)WPSUM,PELP
288      WRITE(Q,124)WINL,PINL
289      WRITE(Q,117)GAVT
290  C *** COMPILE TABLE OF ALL THRESHOLD GAUNT FACTORS IN PROGRAM
291      CALL TABLE(TG,JLS,JNLS,JNLG,JLLS,JLLG,JJLS,JJLG,JSJ,Z)
292      100  FORMAT( )
293      101  FORMAT(///,8X,' N# UPPER (LOWER) STATE = ',F13.6,9X,' N# PERTURB
294      &ING LEVEL      = ',F13.6)
295      102  FORMAT(///,30X,'ENERGY LEVEL NUMBER ',I1,/)
296      103  FORMAT(1H1,/,28X,'*', ' SPECTRAL LINE BROADENING ',*,///)
297      104  FORMAT( )
298      105  FORMAT(/,9X,'S2',21X,'=',3X,F13.6,10X,'C2'22X,'=',3X,F13.6)
299      106  FORHAT( )
300      107  FORMAT(9X,'H',22X,'=',13X,I3,10X,'I',23X,'=',13X,I3)
301      108  FORHAT(9X,'CONTRIBUTION',11X,'=',3X,F13.6,///)
302      109  FORMAT(9X,'RLL2',19X,'=',3X,F13.6,10X,'BDF',21X,'=',3X,F13.6)
303      110  FORHAT(/,9X,'LAHBDA',17X,'=',2X,1PE11.5,13X,'FWHM',20X,'=',2X,1PE1
304      &1.5)
305      111  FORMAT(59X,'STRONG CONTRIBUTION',5X,'=',3X,F13.6)
306      112  FORHAT(59X,'TOTAL CONTRIBUTION',5X,'=',3X,F13.6)
307      113  FORHAT(59X,'ION WIDTH (%)',11X,'=',2X,1PE11.5,1X,'(',,OPF4.1,')')
308      114  FORMAT(59X,'STRONG WIDTH (%)',8X,'=',2X,1PE11.5,1X,'(',,OPF4.1,')')
309      115  FORHAT(59X,'CHECK ON COMPLETENESS(%)',2X,1PE11.5,'(',,OPF4.1,')')
310      116  FORHAT(9X,'DLL',20X,'=',3X,F13.6,10X,'PHI',21X,'=',3X,F13.6)
311      117  FORMAT(59X,'AVERAGE THRESHOLD G      =',3X,F13.6)
312      118  FORHAT(59X,'EXTRA CONTRIBUTION',5X,'=',3X,F13.6)
313      119  FORHAT(59X,'ELASTIC CONTRIBUTION',4X,'=',3X,F 13.6)
314      120  FORHAT(59X,'ELASTIC WIDTH (%)',7X,'=',2X,1PE11.5,' (',,OPF4.1,')'
315      &)
316      121  FORMAT(9X,'NLG',20X,'=',3X,F13.6,10X,'LNS',21X,'=',13X,I3)
317      122  FORMAT(9X,'LG',21X,'=',13X,I3,10X,'LS',22X,'=',13X,I3)
318      123  FORHAT(9X,'DELTA N#',15X,'=',3X,F13.6,10X,'BDF',21X,'=',3X,F13.6)
319      124  FORMAT(59X,'INELASTIC WIDTH (%)',5X,'=',2X,1PE11.5,' (',,OPF4.1,')'
320      &)
321      STOP
322      DEBUG SUBTRACE
323      END

```

ELAM*STARKB(1).BATESD2

```

1      C ***** 21/8/79 *****
2      C ** VERSION 2 **
3      C THIS SUBROUTINE DETERMINES THE APPROPRIATE BATES DAMGAARD FACTOR
4      C FROM THE TABLES GIVEN BY FILE BATES2.
5      C *****
6      C SUBROUTINES CALLED :
7      C           COLUMN
8      C           INTERP
9      C *****
10     SUBROUTINE BATESD(JJ, KK, LL, MM, NN, NLG, NLS, LS, BDF)
11     DIMENSION JJ(3,25), KK(3,25), LL(3,25), O(25)
12     DIMENSION MM(3,25), NN(3,25)
13     REAL JJ, KK, LL, MM, NN, NLS, NLG, NL
14     X2=NLS-NLG
15     IF(X2.GT.1.)GO TO 1
16     X2=ABS(X2)
17     IF(X2.GT.1.3)GO TO 1
18     IF(LS.EQ.0.)GO TO 2
19     IF(LS.EQ.1.)GO TO 3
20     IF(LS.EQ.3.)GO TO 4
21     IF(LS.EQ.4.)GO TO 6
22     NL=NLG-1.
23     CALL COLUMN(KL, NL)
24     DO 19 N=1,25
25     19  O(N)=LL(KL, N)
26     GO TO 20
27     2  NLG=NLG
28     CALL COLUMN(KL, NLG)
29     DO 21 N=1,25
30     21  O(N)=JJ(KL, N)
31     GO TO 20
32     3  NLG=NLG
33     CALL COLUMN(KL, NLG)
34     DO 22 N=1,25
35     22  O(N)=KK(KL, N)
36     20  CALL INTERP(NLS, NLG, O, F4)
37     GO TO 32
38     1  F4=0.
39     GO TO 32
40     4  NL=NLG-2.
41     CALL COLUMN(KL, NL)
42     DO 5 N=1,25
43     5  O(N)=MM(KL, N)
44     GO TO 20
45     6  NL=NLG-3.
46     CALL COLUMN(KL, NL)
47     DO 7 N=1,25
48     7  O(N)=NN(KL, N)
49     GO TO 20
50     32  BDF=SQRT(F4)
51     RETURN
52     END

```

ELAM*STARKB(1).GBARAV

```

1      C ***** 12/12/79 *****
2      C THIS ELEMENT CONTAINS ALL THE BITS AND PIECES REQUIRED TO USE
3      C THE MATHPACK VERSION OF THE SIMPSONS 1/3 METHOD TO EVALUATE THE
4      C MAXWELL AVERAGE OF THE GBAR AS FORMULATED IN OURG(VERSION 2).
5      C *****
6      C SUBROUTINES CALLED :
7      C      GTRY
8      C      FINT (FUNCTION )
9      C      SIMINI (MATHPACK FUNCTION)
10     C *****
11     SUBROUTINE GBARAV
12     COMMON/AA/Z,DE,T,DLL,PHI,G,GIN,GEL,FK,MAXIT,AAA,ZZZ
13     EXTERNAL FINT
14     DIMENSION A(2)
15     INTEGER Z
16     LOGICAL REL
17     REL =.TRUE.
18     IF(FK.EQ.1.0)GO TO 1
19     CALL GTRY
20     A(1)=AAA
21     A(2)=DE/T
22     E=0.0001
23     GEL=SIMINI(FINT,A,E,REL,MAXIT,FK,$555)
24     PRINT 101,FK,GEL
25     101  FORMAT(9X,'FK',21X,'=',3X,F13.6,10X,'GEL',21X,'=',3X,F13.6)
26     GO TO 8
27     1    GEL=0.0
28     8    A(1)=DE/T
29     A(2)=ZZZ*DE/T
30     E=0.0001
31     GIN=SIMINI(FINT,A,E,REL,MAXIT,FK,$555)
32     PRINT 103,FK,GIN
33     103  FORMAT(9X,'FK',21X,'=',3X,F13.6,10X,'GIN',21X,'=',3X,F13.6)
34     G=GEL+GIN
35     PRINT 104,G
36     104  FORMAT(59X,'G',23X,'=',3X,F13.6)
37     RETURN
38     555  PRINT 102,MAXIT
39     102  FORMAT(3X,'***WARNING*** MAXIT =',2X,I5,2X,' IS NOT SUFFICIENT')
40     RETURN
41     END
42     C *****
43     C INTEGRAND REQUIRED BY THE GAUNT FACTOR INTEGRAL.
44     C *****
45     C SUBROUTINES CALLED :
46     C      GBAV
47     C *****
48     FUNCTION FINT(ZZ,FK)
49     COMMON/AA/Z,DE,T,DLL,PHI,G,GIN,GEL,FFK,MAXIT,AAA,ZZZ
50     INTEGER Z
51     X=SQRT(ZZ*T/DE)
52     CALL GBAV(X)
53     K=IF1X(FK+0.1)
54     GO TO(1,2),K
55     1    FINT=G*EXP(-ZZ)*EXP(DE/T)
56     RETURN
57     2    FINT=G*EXP(-ZZ)
58     RETURN
59     END

```

ELAM*STARKB(1).GTRY

```

1 C ***** 26/5/80 *****
2 C THIS SUBROUTINE ESTABLISHES WHERE THE GAUNT FACTOR TURNS ZERO
3 C AND THUS OBTAINS THE LOWER LIMIT FOR MAXWELLIAN INTEGRATION.
4 C *****
5 C SUBROUTINES CALLED:
6 C   GBAV
7 C *****
8   SUBROUTINE GTRY
9   COMMON/AA/Z,DE,T,DLL,PHI,G,GIN,GEL,FKK,MAXIT,AAA,ZZZ
10  INTEGER Z
11  DO 1 J=1,20
12  ZZ=(0.05*J)**2*DE/T
13  X=SQRT(ZZ*T/DE)
14  CALL GBAV(X)
15  IF(G.GT.0.0)GO TO 2
16  1 CONTINUE
17  2 AAA=ZZ
18  RETURN
19  END

```

ELAM*STARKB(1).GBAV

```

1 C ***** 12/12/79 *****
2 C THIS SUBROUTINE IS USED FOR MAXWELL AVERAGING.
3 C THIS SUBROUTINE CALCULATES THE EFFECTIVE GAUNT FACTOR TAKING
4 C THE CURVATURE OF THE CLASSICAL HYPERBOLIC ORBIT INTO ACCOUNT.
5 C THE UPPER LIMIT OF THE IMPACT PARAMETER AS GIVEN BY THE
6 C MINIMUM OF THE REQUIRED ELECTRON ENERGY AND THE LOWER LIMIT
7 C IS DETERMINED IN ACCORDANCE TO THE LIMIT OF STRONG COLLISIONS.
8 C *****
9 C SUBROUTINES CALLED :
10 C   CUBIC
11 C *****
12   SUBROUTINE GBAV(X)
13   COMMON/AA/Z,DE,T,R,PHI,G,GIN,GEL,FK,MAXIT,AAA
14   INTEGER Z
15   IF(X.GE.1.0)GO TO 55
16   X=1.0
17   55 CONTINUE
18   Y=SQRT(109737./DE)
19   ZZ=FLOAT(Z)
20   CALL CUBIC(ZZ,X,Y,PHI)
21   CP=(ZZ-1.0)*Y/(2.0*X**3)
22   G=1.0+PHI**4/CP**2
23   TT=((ZZ-1.0)*Y/X)**2
24   TEST=1.*R**2-TT
25   IF(TEST.LT.0.0)GO TO 2
26   DEN=1.+R**2*(1.0+(X/Y)**2+2.*(ZZ-1.0)/R)-TT
27   GO TO 3
28   2 DEN=1.+R**2*((X/Y)**2+2.0*(ZZ-1.0)/R)
29   3 DEN=1.0+DEN*(X/Y)**2/(ZZ-1.0)**2
30   F=SQRT(3)/3.14159
31   G=F/2.0*ALOG(G/DEN)
32   IF(G.GT.0.0)GO TO 1
33   G=0.0
34   1 CONTINUE
35   101 FORMAT(/,9X,'X',22X,'=',3X,F13.6,10X,'G',23X,'=',3X,F13.6)
36   RETURN
37   END

```

ELAM*STARKB(1).DISENT

```

1      C ***** 26/5/80 *****
2      C THIS SUBROUTINE TESTS THE VALIDITY OF THE BARANGER FORMULATION
3      C OF THE DISENTANGLEMENT OF THE STRONG COLLISIONS IN TIME.IT ALSO
4      C FACILITATES THE COMPARISON OF THE AVERAGE COLLISION TIME WITH THE
5      C FINAL ANSWER OBTAINED FOR THE LINE WIDTH.
6      C *****
7      C SUBROUTINES CALLED :
8      C     GTRY
9      C     SIMINI (MATHPACK FUNCTION)
10     C     FINTDA (FUNCTION)
11     C     FINTDB (FUNCTION)
12     C     COLTIM
13     C *****
14     SUBROUTINE DISENT(D,W1)
15     COMMON/AA/Z,DE,T,DLL,PHI,G,GIN,GEL,FK,MAXIT,AAA,ZZZ
16     EXTERNAL FINTDA
17     EXTERNAL FINTDB
18     DIMENSION A(2)
19     LOGICAL REL
20     INTEGER Z
21     REL=.TRUE.
22     C *** ESTABLISH LOWER AND UPPER LIMITS OF INTEGRATION
23     IF(FK.EQ.2.)GO TO 1
24     GCORCT=0
25     CALL GTRY
26     G=GCORCT
27     A(1)=AAA
28     GO TO 2
29     1  A(1)=DE/T
30     2  A(2)=ZZZ*DE/T
31     E=0.001
32     C *** EVALUATE INTEGRALS
33     DISPA=SIMINI(FINTDA,A,E,REL,MAXIT,FK,$555)
34     DISPB=SIMINI(FINTDB,A,E,REL,MAXIT,FK,$555)
35     DISP=8.0*D*DISPA*DISPB
36     CALL COLTIM(A,W1)
37     PRINT 101,DISP
38     101 FORMAT(59X,'DISENTANGLEMENT',9X,'=',3X,1PE11.5)
39     RETURN
40     555 PRINT 102
41     102 FORMAT(3X,'*** WARNING ***MAXIT IS NOT SUFFICIENT IN DISENT.')
42     RETURN
43     END
44     C *****
45     C FUNCTION FOR FIRST INTEGRATION OF ROMINIUM.
46     C *****
47     C SUBROUTINE CALLED :
48     C     ROMINS
49     C *****
50     FUNCTION FINTDA(ZZ,FK)
51     COMMON/AA/Z,DE,T,DLL,PHI,G,GIN,GEL,FKK,MAXIT,AAA,ZZZ
52     INTEGER Z
53     CALL ROMINS(ZZ,ROMIN)
54     FINTDA=ROMIN*EXP(-ZZ)
55     RETURN
56     END

```

```

57 C *****
58 C FUNCTION FOR SECOND INTEGRATION OF ROMINIMUM SQUARED.
59 C *****
60 C SUBROUTINE CALLED :
61 C   ROMINS
62 C *****
63   FUNCTION FINTDB(ZZ,FK)
64     COMMON/AA/Z,DE,T,DLL,PHI,G,GIN,GEL,FKK,MAXIT,AAA,ZZZ
65     INTEGER Z
66     CALL ROMINS(ZZ,ROMIN)
67     FINTDB=ROMIN**2*EXP(-ZZ)*ZZ
68     RETURN
69     END
70 C *****
71 C THIS SUBROUTINE CALCULATES ROMINIMUM OF THE INCOMING ELECTRON
72 C PERTURBER ALLOWED FOR WEAK COLLISIONS.
73 C *****
74   SUBROUTINE ROMINS(ZZ,ROMIN)
75     COMMON/AA/Z,DE,T,DLL,PHI,G,GIN,GEL,FK,MAXIT,AAA,ZZZ
76     INTEGER Z
77     DLL2=DLL**2
78     ZD=(Z-1)**2*109737./DLL2/T
79     CA=DLL2*(0.529172)**2*1E-16
80     CB=109737.*CA/DLL2/T
81     CB=CB*(1.+DLL2+2.*(Z-1)*DLL)
82     CC=(Z-1)*109737./T
83     CC=CC**2*CA/DLL2
84     CE=CB-CC/ZD
85     IF (ZZ.LT.ZD)GO TO 20
86     ROMIN=SQRT(CA+CB/ZZ-CC/(ZZ**2))
87     RETURN
88 20  ROMIN=SQRT(CA+CE/ZZ)
89     RETURN
90     END

```

ELAM*STARKB(1).COLTIM

```

1      C ***** 26/45/80 *****
2      C THIS SUBROUTINE CALCULATES THE AVERAGE COLLISION TIME
3      C TO MAKE COMPARISON WITH THE LINE WIDTH POSSIBLE.
4      C *****
5      C SUBROUTINES CALLED :
6      C     FINTC (FUNCTION)
7      C     SIM1NI (MATHPACK FUNCTION)
8      C *****
9      SUBROUTINE COLTIM(A,W1)
10     COMMON/AA/Z,DE,T,DLL,PHI,G,GIN,GEL,FK,MAXIT,AAA,ZZZ
11     EXTERNAL FINTC
12     DIMENSION A(2)
13     LOGICAL REL
14     INTEGER Z
15     REL=.TRUE.
16     ZR=FLOAT(Z)
17     COLT=4.482346*1E-16/DE
18     E=0.001
19     CINT=SIM1NI(FINTC,A,E,REL,MAXIT,FK,$555)
20     COLT=COLT*CINT*W1**2
21     PRINT 101,COLT
22     101  FORMAT(59X,'COLLISION TIME',10X,'=',3X,1PE11.5)
23     RETURN
24     555  PRINT 102
25     102  FORMAT(3X,'*** WARNING *** MAXIT NOT SUFFICIENT IN COLTIM.')
26     RETURN
27     END
28     C *****
29     C INTEGRAND OF COLLISION TIME INTEGRAL
30     C *****
31     C SUBROUTINES CALLED :
32     C     CUBIC
33     C *****
34     FUNCTION FINTC(ZZ,FK)
35     COMMON/AA/Z,DE,T,DLL,PHI,G,GIN,GEL,FKK,MAXIT,AAA,ZZZ
36     INTEGER Z
37     ZR=FLOAT(Z)
38     X=SQRT(ZZ*T/DE)
39     Y=SQRT(109737./DE)
40     CALL CUBIC(ZR,X,Y,PHI)
41     FINTC=SQRT(ZZ)*PHI**2*EXP(-ZZ)
42     RETURN
43     END

```

Appendix I: Hey and Breger (1980a)

J. Quant. Spectrosc. Radiat. Transfer Vol. 23, pp. 311-321
 © Pergamon Press Ltd., 1980. Printed in Great Britain

0022-4073/80/0301-0311\$02.00/0

STARK BROADENING OF ISOLATED LINES EMITTED BY SINGLY-IONIZED TIN

JOHN D. HEY and PETER BREGER

Department of Physics, University of Cape Town, Rondebosch 7700, Cape, South Africa

(Received 8 August 1979)

Abstract—Calculations have been performed on the electron impact broadening of isolated lines from singly-ionized tin from a cool plasma. These have been compared with results of measurements recently performed by Miller, Roig, and Bengtson on a plasma produced by a conventional shock tube, and satisfactory overall agreement has been obtained. Our method is similar in procedure to that of the semi-empirical approximation of Griem, but we take into account the details of the radiator structure, including configuration interaction for two of the terms. We propose a new expression from which the relevant effective Gaunt factors for singly-charged ions can be calculated for incident energies above threshold. In some cases, a significant variation of line width within multiplets is noted. Some difficulties have been experienced with transitions to states involving equivalent electrons.

INTRODUCTION

The practical importance of the Stark broadening mechanism for the purposes of plasma diagnostics is well known, and considerable success has been achieved with the calculation of reliable Stark-broadening parameters for overlapping lines from the simpler (one- and two-electron) atoms and ions, applicable over a wide range of plasma conditions.¹⁻⁴ At the same time, theoretical predictions for the spectral line widths from the narrower isolated ion lines have been tested in a number of experiments,⁵⁻⁷ from which generally very favourable conclusions have been drawn regarding the accuracy of the available computational techniques,^{1,8,10} particularly for lines from singly-ionized species, while the situation appears far less certain for the spectra of multiply-ionized radiators.^{6,7,11,12} For theoretical reasons,¹ these lines from multiply-ionized species should form the subject of a separate study, to which the present authors hope to return in the future.

In this paper, we are concerned with a singly-ionized species (tin), and now refer more specifically to some results obtained recently, where comparison between experiment and established theory has yielded notable discrepancies and led to a number of interesting conclusions.

Firstly, discrepancies have been traced to the neglect, in calculations based upon the original theory of broadening by electron impact,¹³⁻¹⁵ of competing mechanisms. One such effect important at high densities is the interference between line and continuum (perturber) radiation,^{1,16} which produces an asymmetry in the line wings and measurable^{17,18} deviations from the Lorentzian impact-broadened profile. Since the percentage asymmetry is itself independent of electron density for given $\Delta\omega$, the overall effect is enhanced by increasing N_e .^{1,16}

Second, and of primary importance for present purposes, are discrepancies due to oversimplifications, not warranted in some cases, of the electronic structure of the radiator. For example, *LS* coupling is conventionally^{19,10,14,15} used to describe the (internal) radiator states; while the summation rules for line strengths¹⁹⁻²³ may eliminate some errors in individual inelastic cross sections resulting from failure to allow for the breakdown of *LS* coupling, some residual errors may remain which affect the calculated line width in a systematic way. A notable case in point concerns lines which arise from states of high orbital angular momentum in ionized nitrogen, where an incorrect choice of coupling scheme for the description of the bound electrons yields systematic errors in the line widths, which may very well be demonstrated in the future by a suitably designed experiment.^{24,25}

However, even within the *LS* coupling scheme, one has the problem of accounting satisfactorily for interactions occurring between different (bound) electronic configurations,^{19,23} which are manifested in the perturbation of individual members of Rydberg series from their relative positions predicted on the basis of simple quantum defect analysis.^{19,21,26,27} Situations

may therefore arise for complex atomic structures in which the upper (lower) level of the line in question is situated very close ($|\Delta E_{ij}| \ll kT$) to one or more perturbing levels. The corresponding inelastic collision-induced transitions would then predominate in the line-broadening process. If in addition this applies only to certain members of the multiplet in question (i.e. in other cases, the perturbing levels remain well separated), then appreciable variations of line width may be produced within certain Stark-broadened multiplets under suitable plasma conditions. Although this possibility is implied by the original formulation of the impact approximation,¹³⁻¹⁵ it was first pointed out explicitly only rather recently²⁸ as a consequence of established theory, and the effect has been clearly demonstrated by some measurements by Behringer and Thoma²⁹ on an ionized argon plasma.

While very satisfactory agreement has been obtained between recent calculations^{28,29} and the measured Ar(II) line widths,²⁹ the same cannot be said of ionized silicon, which has also been the subject of recent study in this field.³⁰⁻³³ This ion, whose spectrum is of considerable interest from the point of view of both laboratory and stellar plasma studies, has a term structure which exhibits considerable configuration interaction (notably between the terms denoted by $3s3p^2\ ^2D$ and $3s^23d\ ^2D$). While there is clearly a need to allow for configuration interaction in the calculation of oscillator strengths for this ion,³⁴ the (apparently) paradoxical situation has arisen that worse agreement has been obtained between the most recent measurements^{31,33} and calculations³¹⁻³³ which attempt to allow for the mixing of pure-configuration, *LS* coupled wave functions, than with classical-path calculations^{1,9} which ignore such mixing effects. This situation is not well understood, and an investigation of the Stark-broadened spectrum of an ion with similar structure to that of Si(II) would therefore be of great interest.

Such an ion is Sn(II), for which experimental data on the Stark-broadening parameters have become available recently.³⁵ For this ion, the major configuration interaction occurs between the terms denoted by $5s5p^2\ ^2D$ and $5s^25d\ ^2D$, giving rise to a number of fairly strong lines from "forbidden (two-electron)" transitions in the spectrum.^{35,36} Simple semi-empirical¹⁵ estimates of some of the line widths have already been made,³⁵ which provide encouragement for a more detailed theoretical study.

Our aim in the present paper is to make use of a more refined version^{24,25,32} of the semi-empirical impact approximation due to Griem,¹⁵ in order to make a detailed comparison with the recent measurements, and to elucidate if possible the structure of the ion through a study of the Stark-broadening of the spectrum. Thereby, it is hoped that such a study will assist in improving our understanding of the Stark-broadening process in similar ions.

OUTLINE OF THEORY

Since most of the aspects of the theory involved in this work appear in a number of earlier papers,^{15,24,25,28,32} we shall confine the present discussion to a synopsis of the salient features. The lines of interest, corresponding to transitions $|i\rangle \rightarrow |f\rangle$ between states of definite parity, are broadened primarily by electron impact, while the contribution to the broadening from quasi-static ion perturbers is small, entering in second-order dipole and first-order quadrupole terms.¹ Neglecting the broadening by ions, one obtains an expression for the width (W_e^{if}) of the resulting Lorentzian line profile in terms of the cross sections for the collision-induced transitions $|i\rangle \rightarrow |i'\rangle$, $|f\rangle \rightarrow |f'\rangle$ from the upper and lower states to perturbing levels.¹³ When these cross sections are written in terms of the corresponding collision strengths (Ω), the line width may be re-expressed (in wavelength units) as

$$W_e^{if} = \frac{\alpha\lambda^2 a_0^2}{\sqrt{\pi}} N_e \left(\frac{E_H}{kT} \right)^{1/2} \left\{ \sum_{i'} \frac{\langle \Omega(i, i') \rangle}{\bar{\omega}_i} + \sum_{f'} \frac{\langle \Omega(f, f') \rangle}{\bar{\omega}_f} \right\} \quad (1)$$

(full width at half maximum = FWHM). Here $\bar{\omega}_i$ denotes the statistical weight of level i , E_H the ionization energy of hydrogen, α the fine-structure constant, and other symbols have their usual meaning.

The above equation is derived from the original expression of Baranger¹³ by simplifying the elastic contributions to the broadening. This is done by retaining only the dipole elastic terms which involve the presence of other states, and by allowing for these through extrapolation of

the inelastic cross sections below threshold. This procedure, due to Griem,¹⁵ greatly facilitates the calculation of the spectral line widths; its justification lies in a quantum mechanical consideration of the scattering process.^{17,38}

We now make a further simplification, viz. that of retaining only the direct collision (i.e. non-exchange) terms which contribute to Eq. (1), and of treating these as collisions inducing (allowed) inelastic dipole transitions in the radiator. In that case, each $\Omega(i, i')$ may be written in terms of the corresponding atomic line strength $S(J, J')$ and effective Gaunt³⁹ factor \bar{g} as

$$\Omega(i, i') = \frac{8\pi}{3^{3/2}\bar{g}(i, i')} \frac{S(J, J')}{a_0^2 e^2}. \quad (2)$$

It may be pointed out here that each factor in Eq. (2) is entirely symmetrical in the labels (i, i'), and that the expression therefore holds whether the perturbing level i' lies below or above i in energy. With the assumption that the LS coupling scheme is appropriate for the description of the radiator states, the line strength $S(J, J')$ may be written

$$\frac{1}{(2J+1)} \frac{S(J, J')}{a_0^2 e^2} = l_>(2L+1)(2L'+1)(2J'+1) \left\{ \begin{matrix} l & l' & 1 \\ L' & L & L_1 \end{matrix} \right\}^2 \left\{ \begin{matrix} L & L' & 1 \\ J' & J & S \end{matrix} \right\}^2 (R_{nl}^{n'l'})^2. \quad (3)$$

In this expression, it is assumed that a single bound electron (situated outside the shells or subshells which contain the rest) participates in the transition. We therefore ignore for the moment possible complications arising in connection with configuration mixing (see below). The designations $l(l')$ refer to the orbital angular momentum of the outer electron, $l_>$ being the greater of these; $L(L')$ denotes the total orbital angular momentum, L_1 being that of the core electrons, and $J(J')$ denotes the total angular momentum of the state $|i\rangle(|i'\rangle)$. The square of the radial integral ($R_{nl}^{n'l'}$) is here evaluated in the Coulomb approximation,⁴⁰ which for reasons given below is of sufficient accuracy for the calculation of most of the major individual contributions to the line widths.

The procedure which we have chosen to adopt for the calculation of \bar{g} is quasi-classical in nature, along the lines proposed by Griem.¹⁵ Its justification lies in the success of the classical-path approximation as applied to both neutral and singly-ionized radiators.^{1,14,15,42} In terms of the eccentricity (ϵ) of the incoming electron trajectory,

$$\bar{g} = \frac{\sqrt{3}}{\pi} \ln \frac{\epsilon_{\max}}{\epsilon_{\min}}. \quad (4)$$

The necessity for making upper and lower cutoffs to ϵ , is explained in Refs. 1, 15, 41–43, in which a number of approaches to this problem are suggested.

We proceed from the basic expression for ϵ in terms of impact parameter (ρ) and incident (asymptotic) electron speed (v):

$$\epsilon = \left\{ 1 + \frac{m^2 \rho^2 v^4}{(Z-1)^2 e^4} \right\}^{1/2}$$

with ϵ_{\max} obtained by choosing, as on p. 270 of Ref. 1,

$$\rho_{\max} = (\hbar v / \Delta E_{fi}).$$

Consistency with the strong collision contribution to the line width (see the following section) requires one to choose the ϵ_{\min} which corresponds to the ρ_{\min} in Eq. (7). In terms of the mean thermal energy of the electron perturbers, we therefore obtain

$$\bar{g} \approx \frac{\sqrt{3}}{2\pi} \ln \left[\frac{1 + (\xi_{nl}^{n'l'})^{-2}}{1 + \frac{3kT}{2(Z-1)^2 E_{fi}} \left[1 + \frac{n^{*4}}{Z^2} \left(1 + \frac{3kT}{2E_{fi}} \right) \right]} \right] \quad (5)$$

for the collision-induced transition $|i(nl)\rangle \rightarrow |i'(n'l')\rangle$, where n^* is the effective principal quantum number of level i , and Z (here equal to 2) the ionization stage of the radiator. The (averaged) Coulomb parameter $(\xi_{nl}^{n'})^{-1}$ is determined from the level separation $\Delta E_{ri} = E_{r'} - E_i$ by

$$(\xi_{nl}^{n'})^{-1} = \frac{2\left(\frac{3}{2}kT\right)^{3/2}}{(Z-1)E_H^{1/2}|\Delta E_{ri}|}, \quad (6)$$

always assuming that the level separation exceeds the plasmon energy $\hbar\omega_p$ for the above relation to be valid.¹

The threshold value of the Gaunt factor, \bar{g}_{th} (here chosen equal to 0.2 as in Refs. 1, 15) is adopted as appropriate wherever the latter value exceeds the calculated value from Eq. (5).

The importance of summing in Eq. (1) over a complete set of perturbing levels (within the allowed electric-dipole scheme) has been discussed in the literature.^{8,9,14} In our case, completeness has been ensured by noting that in the present approximation, individual contributions to the line width are of two kinds. The total threshold contribution [see Eq. (2)], which includes contributions from all distant ($|\Delta E_{ri}| \geq kT$) perturbing levels and the small contribution to the width from continuum states, is determined by the reduced matrix element

$$\frac{8\pi}{3^{3/2}} \left\langle i \left| \frac{r^2}{a_0^2} \right| i \right\rangle \bar{g}_{th}.$$

Each nearby perturbing level contributes in addition to the width a value determined by

$$\frac{8\pi}{3^{3/2}} [\bar{g}(i, i') - \bar{g}_{th}] \frac{1}{2J+1} \frac{S(J, J')}{a_0^2 e^2}.$$

The advantage of such a separation of contributions is clear, since only those radial integrals are specifically evaluated for which the simple hydrogenic estimates are rather close to those obtained by the standard Coulomb approximation (i.e. $n_i^* \approx n_i^*$). The latter approximation is thus only employed in cases where reasonably high accuracy may be expected.⁴⁰

ADDITIONAL CONTRIBUTIONS TO BROADENING

Consistent with the introduction above of a lower cutoff for the eccentricity (impact parameter) in the quasi-classical expression for \bar{g} , would be the addition of an extra term to the broadening to account for strong (disruptive and higher multipole) collisions.¹ On examining the various expressions for

$$W_s = 2\pi N_e v \rho_{min}^2, \quad (7)$$

where ρ_{min} is the lower cutoff to the impact parameters for monopole-dipole terms in the classical path approximation) as proposed by Griem *et al.*^{1,14,15,41-43} we have concluded that, although strong collisions are of some importance for lines such as those under consideration, no completely satisfactory expressions exist in the literature for present purposes. The difficulties inherent in the problem become apparent when one refers to pp. 46-81 and pp. 270-271 of Ref. 1.

We have found that the apparent tendency is to overestimate the strong collision contribution to the widths in question when simply adding independent contributions in the form of Eq. (7) above for both the upper and lower states of the line, with no account of negative ("interference") contributions that are clearly important, e.g. for hydrogenic ions [see Eqs. (111) and (128) and a remark on p. 79 of Ref. 1].

In the absence of plausible estimates for the negative contribution to the upper-lower state interference term, we propose to account only for strong upper-state contributions, and to ignore the lower state of the line for these purposes.

There are three basic requirements for ρ_{min} in monopole-dipole interactions: it should exceed the de Broglie wavelength of the electron perturber (ρ_1); the electron perturber should

remain outside the orbit of the bound electron (ρ_2); it should be large enough to preserve unitarity in the scattering process and to justify truncation of the multipole series in the interaction (ρ_3).¹ With the corresponding substitutions for the various cutoffs without curvature correction (see below):

$$\rho_1 = (\hbar/mv), \quad \rho_2 = (n^{*2}a_0/Z), \quad \rho_3 = (\alpha c/v)(n^{*2}a_0/Z)$$

(α is the fine-structure constant), one can summarily account for the strong collision (mainly higher multipole) contribution by writing

$$\rho_{\min} = [\rho_1^2 + \rho_2^2 + \rho_3^2]^{1/2}$$

from which the thermal average of Eq. (7), converted to wavelength units, yields (FWHM)

$$W_s = \frac{2}{\sqrt{\pi}} \alpha \lambda^2 a_0^2 N_e \left(\frac{E_{II}}{kT} \right)^{1/2} \left[1 + \frac{n^{*4}}{Z^2} \left(1 + \frac{kT}{E_{II}} \right) \right]. \quad (8)$$

It remains to verify that the contribution to the broadening from ion perturbers is indeed small, as already indicated in the previous section. Here again a number of different estimates can be made, depending upon the degree of validity of the quasi-static or impact approximations for ion-ion interactions as discussed by Sahal-Bréchet.^{10,31,44} For quadrupole interactions, the quasi-static and impact approximations yield very similar results which in wavelength units may be estimated by (FWHM)¹

$$W_i^q = \frac{2\alpha\lambda^2 a_0^2}{Z^2} \sum_p N_p Z_p (n_i^{*2} - n_f^{*2})^2, \quad (9)$$

where N_p and $Z_p e$ are the perturber concentration and charge, respectively. The condition of quasi-neutrality in the plasma enables one to substitute above

$$N_e = \sum_p N_p Z_p. \quad (10)$$

The second-order dipole (quadratic) contribution to the line width is, however, appreciably different when calculated in the impact and quasi-static approximations.¹ In the latter case, the contribution to the broadening is usually insignificant compared with that produced by electron perturbers; in the former case the calculation is more involved than for the quadrupole case (see pp. 275–277 of Ref. 1). Provided that the ions may indeed be treated within or near to the regime of validity of the quasi-static approximation, we may consider that

$$W_i^q \ll W_e$$

provides a sufficient guarantee that the electron broadening completely predominates.

For the electron perturbers, the validity of the impact approximation over the major portion of the measurable profile is guaranteed by¹

$$v/\rho \gg \frac{1}{2} W_e$$

and, with $\rho_{\max} = (\hbar v/|\Delta E_{Fi}|)$ as above, the criterion for the isolated line approximation therefore ensures the validity of the impact approximation provided that inelastic collisions predominate in the broadening; greater care might be required for plasmas whose temperature is so low that inelastic processes are unimportant.

For the validity of the quasi-static approximation for ion perturbers throughout the (electron-broadened) profile, Griem¹ obtains a relation equivalent to

$$\frac{kT}{E_{II}} < 6 \left(\frac{m_p}{m} \right)^{1/2} \frac{n_i^{*4} N_e a_0^2}{Z^2 N_p^{1/3}}, \quad (11)$$

assuming equal ion and electron temperatures, where N_p and m_p are the perturber concentration and mass, respectively. For proton perturbers, one finds that the above inequality is not properly fulfilled under the plasma conditions relevant to this investigation. This indicates that neither of the conventional approximations is valid for ion perturbers throughout the line profile.^{31,44} We shall assume, however, in view of the remarks preceding Eq. (9), that the smallness of W_i^q relative to W_e is a sufficient guarantee of the predominance of electron impact broadening throughout the line core.

RADIATOR STRUCTURE

Earlier investigations by one of us have shown that in certain cases careful attention should be paid to the details of the radiator structure when calculating the Stark widths.^{24,25,28,29} Certain features of the level structure of ionized tin should therefore be noted.

Most of the terms of interest are derived from configurations with a single electron added to a 1S parent. The question of the possible breakdown of LS coupling²²⁻²⁵ therefore does not arise in the present case. Furthermore, the structure^{35,45} of these terms is extremely regular with a single exception, indicating the general absence of appreciable configuration interaction. The quantum defects $\Delta = n - n^*$ for the various Rydberg series may be accurately listed as follows:

$$\begin{aligned}\Delta(np^2P^0) &= 2.88 - 0.01(n-7), \quad (n > 6); \\ \Delta(nd^2D) &= 2.02, \quad (n > 5); \\ \Delta(nf^2F^0) &= 0.11, \quad (n > 4); \\ \Delta(ng^2G) &= 0.023, \quad (n > 5).\end{aligned}$$

One missing term ($5g^2G$) in the tabulations of Moore⁴⁵ could therefore be reliably located, in confirmation of a more recent listing of terms.⁴⁶

In one case ($5d^2D$), the quantum defect (1.918) deviates significantly from that of the remaining members of its series, indicating substantial perturbation (producing an upward shift of some 3000 cm^{-1} on the term diagram) as a result of interaction with the term designated as $5s5p^2D$. One therefore expects the corresponding unperturbed (pure configuration) wave functions to be appreciably mixed; this is confirmed by the existence of fairly strong "two-electron" transitions, some of which have been studied by Miller *et al.*³⁵ The mixed wave functions corresponding to these two terms designated as $5d^2D$ and $5p^2D$ may then be written as

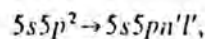
$$\psi_I(^2D) = \alpha_{11}\psi(5s^25d) + \alpha_{12}\psi(5s5p^2), \quad (12)$$

$$\psi_{II}(^2D) = \alpha_{21}\psi(5s^25d) + \alpha_{22}\psi(5s5p^2). \quad (13)$$

Originally, it was hoped that the values of the coefficients α could be deduced from a comparison between calculated and measured³⁵ probabilities for transitions to these states. In this endeavour we were, however, only partially successful, owing to the rather large estimated uncertainties³⁵ for certain key A -values, and the omission of certain other transitions of this type which could confirm such an assignment. The indications are, however, that a value for $|\alpha_{11}|^2 = |\alpha_{22}|^2$ of between 0.5 and 0.75 should be fairly reliable.

In the calculation of the line strengths for transitions involving these states and others with parentage 1S , the value obtained from Eq. (3) above should therefore be multiplied by $|\alpha_{11}|^2$ or $|\alpha_{21}|^2$ as appropriate.

A final complication in connection with the wave functions in Eqs. (12) and (13) should be mentioned; this was not appreciated in the corresponding case for Si(II), as treated in Ref. 32, and its omission is probably in part responsible for the systematically small value for the line widths of the first multiplet in that paper. In the calculation of line widths for transitions from states which may be represented by Eqs. (12) or (13), one has to consider the summation over collision-induced transitions of the type



where $l' = 2$ or 0 . In the former case, one has from Sobel'man²¹ the relation for the oscillator strengths

$$\begin{aligned} f(5s5p^2 \rightarrow 5s5pn'd) &= \frac{1}{3} \frac{|E_i - E_f|}{E_H} \frac{Nl}{(2l+1)} (R_{5l}^{nl'})^2 \\ &= 2f(5p \rightarrow n'd) \end{aligned} \quad (14)$$

with $N = 2$, $l = 1$. In the latter case, with $n' > 5$, one finds similarly

$$f(5s5p^2 \rightarrow 5s5pn's) = 2f(5p \rightarrow n's). \quad (15)$$

The case of transitions to the ground term is more involved. Analogously to the treatment on p. 318 of Ref. 21, one obtains

$$f(l'^{N-1}l^p \rightarrow l'^N l^{p-1}) = \frac{p}{2} \left(\frac{4l' + 3 - N}{2l' + 1} \right) f(nl \rightarrow n'l'), \quad (16)$$

from which it readily follows that

$$f(5s5p^2 \rightarrow 5s^25p) = f(5p \rightarrow 5s). \quad (17)$$

Simple estimates show that, this single term [Eq. (17)] is probably only a minor contribution ($\sim 10\%$) to the total sum of the type

$$\bar{g}_{th} \sum_{n'l'} \left\langle \left\langle \psi(5s5pn'l') \left| \frac{r}{a_0} \right| \psi(5s5p^2) \right\rangle \right\rangle^2 = 2\bar{g}_{th} \left[\left\langle 5p'' \left| \frac{r^2}{a_0^2} \right| 5p'' \right\rangle - \frac{1}{6} (R_{5p}^{5p''})^2 \right], \quad (18)$$

where the primes are inserted as a reminder that the single-electron radial integrals should be calculated properly for a $5p$ or $5s$ electron moving in a potential which generates the series of eigen-energies with limit terminating on the excited terms $5s5p^3P^0$ of Sn(III) rather than the ground term $5s^2^1S$.

Consistent with the relatively crude Coulombic or hydrogenic estimates of radial integrals used in this paper, it is probably satisfactory to omit the last term in Eq. (18) and to multiply the conventionally used formula for the reduced matrix element^{19,20}

$$\left\langle nl \left| \frac{r^2}{a_0^2} \right| nl \right\rangle = \frac{n^*2}{2Z^2} [5n^{*2} + 1 - 3l(l+1)] \quad (19)$$

by $N = 2$ when dealing with the situation of equivalent electrons. In a rough way, one could say that the summation procedure probably reduces the inaccuracy inherent in the results for individual transitions of this type, and that this correction factor $N = 2$ therefore represents a reasonable estimate for the procedure used here.

RESULTS AND DISCUSSION

We have applied the theory outlined in the previous sections to the measurements performed on isolated lines of ionized tin by Miller *et al.*³⁵ Results of the present calculations for electron density $N_e = 10^{17} \text{ cm}^{-3}$ and temperature $11,000^\circ\text{K}$ are presented in Table 1; in addition to the measured lines (width W_m), we have included an extra member of each of the multiplets $5s^26s^2S - 5s^26p^2P^0$ and $5s5p^2^2D - 5s^24f^2F^0$ for interest. All widths given in the table are FWHM, the unshifted wavelengths being given for air.⁴⁷

The parameter $\eta = 100|\alpha_{11}|^2 = 100|\alpha_{22}|^2$ in Eqs. (12) and (13) denotes the degree to which the interacting configurations are treated as pure. Best agreement between the measured widths and calculated widths from electron impact broadening is obtained for a 50% mixture of configurations, which is the same as that chosen in Ref. 32 for a similar study of isolated lines from ionized silicon. In some cases (notably where configuration mixing affects only lower-state

Table I. Comparison between measured (W_m) and calculated (W_c) widths (FWHM) of isolated lines from the indicated transitions, for electron density $N_e = 10^{17} \text{ cm}^{-3}$ and temperature $T = 11,000^\circ\text{K}$. The measurements were performed by Miller, Roig, and Bengtson.¹⁵ The parameter η denotes percentage purity of two interacting configurations (see text). The last three columns, for 50% configuration mixture, give respectively the ratio of calculated to measured width, the fractional contribution from strong collisions, and an estimate of the importance of the neglected contribution to the broadening from ion perturbers.

Transition Array	Designation	Unshifted λ (Å)	W_m (Å)	$\frac{W_c(R)}{\eta = 100\%}$	$\frac{W_c(R)}{\eta = 50\%}$	$\eta = 50\%$		
						$\frac{W_c}{W_m}$	$\frac{W_s}{W_c}$	$\frac{W_i}{W_c}$
$5s^2 6s - 5s^2 6p$	$^2S_{1/2} - ^2P_{1/2}^0$	6843.49	4.2 ± 1.7	6.21	4.44	1.06	0.23	0.005
	$^2S_{1/2} - ^2P_{3/2}^0$	6453.41	-	4.32	3.38	-	0.22	0.007
$5s^2 6p - 5s^2 6d$	$^2P_{1/2}^1 - ^2D_{1/2}$	5561.37	5.1 ± 0.7	6.11	5.41	1.06	0.34	0.021
	$^2P_{3/2}^1 - ^2D_{3/2}$	5332.48	5.3 ± 0.7	6.66	5.58	1.05	0.30	0.021
$5s^2 5d - 5s^2 4f$	$^2D_{3/2} - ^2F_{7/2}^0$	5799.33	4.2 ± 1.2	4.95	4.32	1.03	0.43	0.026
	$^2D_{5/2} - ^2F_{9/2}^0$	5589.29	3.8 ± 1.0	5.02	4.27	1.12	0.40	0.026
$5s^2 6p - 5s^2 7s$	$^2P_{1/2}^1 - ^2S_{1/2}$	6761.42	5.5 ± 1.5	8.86	7.13	1.30	0.29	0.013
$5s^2 6p - 5s^2 7d$	$^2P_{3/2}^1 - ^2D_{3/2}$	3575.27	3.0 ± 1.0	5.64	5.36	1.79	0.35	0.055
$5s 5p^2 - 5s^2 4f$	$^2D_{3/2} - ^2F_{7/2}^0$	3283.32	2.3 ± 0.8	1.19	1.21	0.53	0.49	0.056
	$^2D_{5/2} - ^2F_{9/2}^0$	3352.20	2.5 ± 0.8	1.25	1.26	0.50	0.49	0.055
	$^2D_{3/2} - ^2F_{7/2}^0$	3351.53	-	1.25	1.26	-	0.49	0.055
$5s 5p^2 - 5s^2 6p$	$^4P_{1/2} - ^2P_{1/2}^0$	4618.22	1.6 ± 0.5	1.97	1.48	0.93	0.32	0.055

contributions to the broadening which in turn are minor components of the total width), sensitivity to η is small; in other cases, particularly $\lambda 6844 \text{ \AA}$, the calculated width (W_c) shows a significant dependence upon η . This case is illustrated in Fig. 1, in which the calculated width is plotted against temperature for the two values of η relevant to the Table. The measured result is also shown, with corresponding error bars^{35,46} for both width and estimated reliability of the temperature measurement. It can be seen that inclusion of configuration interaction has in this case a far more significant effect on the line width than would a correction of even $\sim 20\%$ to the estimated plasma temperature.

The strong collision contribution (W_s) to the width [see Eq. (7)] is given as a fraction of the total electron impact width (W_c). We note that this exceeds 20% in all cases and may even approach 50% for one multiplet. The ion contribution W_i has been estimated from Eq. (9), and we see that the effect of ion perturbers on the width would be to produce at most an increase of $\sim 10\%$.

Apart from three lines, the agreement between calculation and measurement is very satisfactory, and for some multiplets excellent (within 10%), well within the estimated error limits given in Ref. 35. In view of the success of the present method in predicting correctly the width of the line $\lambda 6844 \text{ \AA}$, we may safely assume that the other tabulated member ($\lambda 6453 \text{ \AA}$) of the multiplet $5s^2 6s \ ^2S - 5s^2 6p \ ^2P^0$ has been correctly calculated as well. In that case, a substantial variation of line width within this multiplet is predicted, which could also form the subject of a future experimental study to test an effect discussed recently.^{28,29}

Other than a general criticism of the present method, applicable to all of the lines under consideration, we cannot provide at this stage specific reasons for the significant discrepancy between calculation and measurement for the multiplet $5s 5p^2 \ ^2D - 5s^2 4f \ ^2F^0$. It is interesting to note that a similar discrepancy was obtained in Ref. 32 for the $3s 3p^2 \ ^2D - 3s^2 4p \ ^2P^0$ multiplet of Si(II).

Probably the most serious shortcomings of the present theory can be traced to two factors: the reliability of the formula for \bar{g} in Eq. (5) and the estimated strong collision contribution. With regard to the first of these, a notable omission in our formula is a correction^{41,43} to the upper impact parameter cutoff for the effect of curvature of the perturber trajectory; such a correction, it should be noted, has also been omitted in the corresponding estimates in Eq. (526) of Ref. 1. This correction is most important for perturber energies in the vicinity of threshold; for higher energies it can be shown to tend rapidly to unity. Its inclusion would probably obviate the need for introducing a cutoff to the argument of the logarithm in Eq. (5) corresponding to

Stark broadening of isolated lines of Sn(II)

319

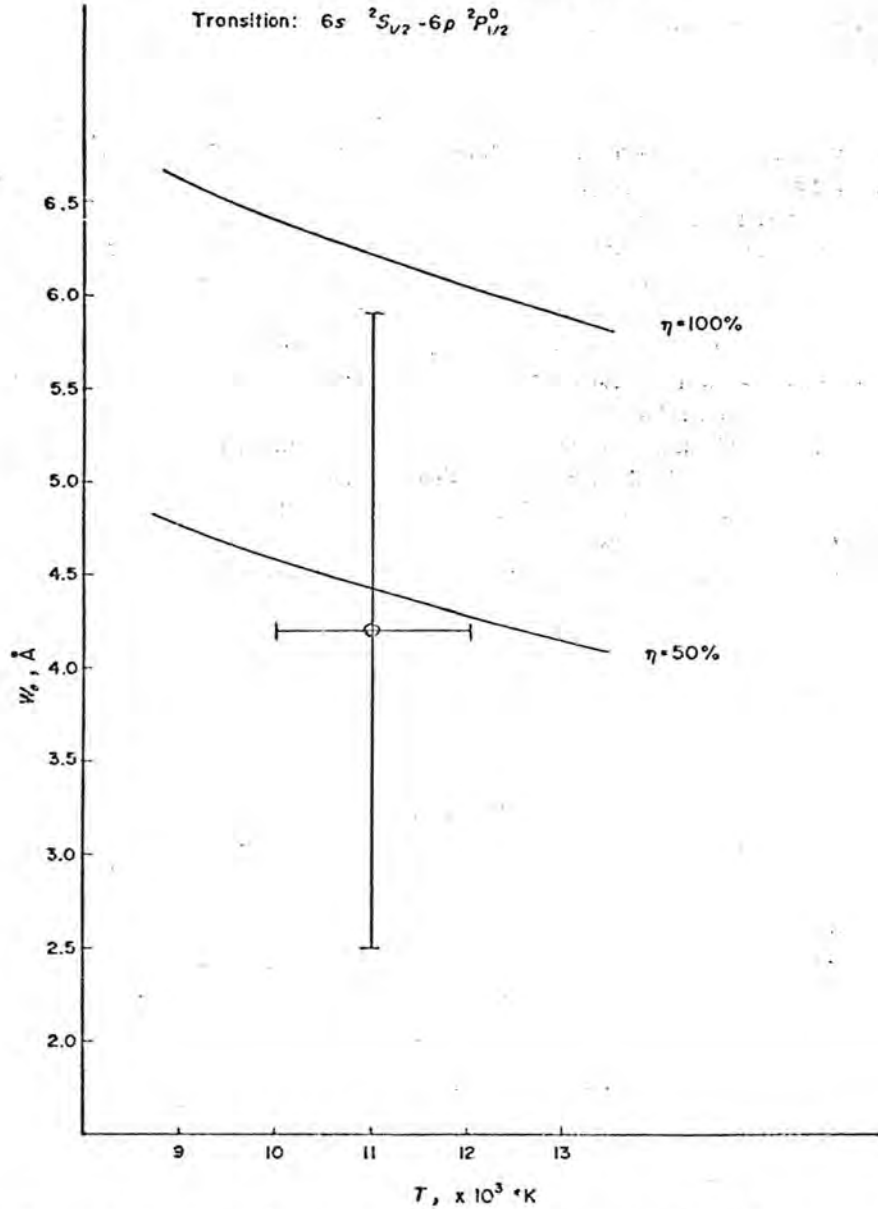


Fig. 1. Calculated width of λ 6844 Å line as a function of temperature, for $N_e = 10^{17} \text{ cm}^{-3}$. The parameter η indicates assumed purity of the interacting configurations. The measured point with associated error bars is taken from Ref. 35.

the value of \bar{g}_{th} , which must then be specified separately. Our chosen value $\bar{g}_{th} = 0.20$ seems to be suitable for most cases considered here, but may perhaps be a significant underestimate for the multiplet under discussion.

On the other hand, the chosen value for the lower impact parameter cutoff is attractive in that it is completely consistent with the calculation of W_s . This is not in fact the case with the proposed formulae in Section IV.6 of Ref. 1, as one sees from Eqs. (500), (509) and (526) in that work. However, the calculation of W_s itself is certainly open to criticism for the following reasons:

- (i) lower-state and upper-lower-state interference contributions have been omitted;
- (ii) the values employed for ρ_2 and ρ_3 can at best be regarded as crude estimates.

In view of the many theoretical difficulties¹ involved in the calculation of W_s , it is clear that any significant and plausible improvement to the approximate expression (8) used here would require a detailed and fundamental study of the problem. It should be pointed out that a notable omission above is a correction to the ρ values for curvature of the perturber orbit. This

correction could lead to either an increase (ϵ large) or decrease⁴⁸ ($\epsilon \approx 1$) in W_j , as one sees from Fig. 8 of Ref. 1.

CONCLUSIONS

On the basis of recent experimental data for the Stark broadening of isolated lines of singly-ionized tin,³⁵ we are able to draw the following conclusions.

Firstly, the present method, which involves a detailed account of radiator structure and the use of quasi-classical Gaunt factors, appears to yield satisfactory values for the electron impact widths of this ion, with the notable exception of one multiplet involving a "forbidden (two-electron)" transition. Secondly, the effect of strong collisions is important for the isolated ion lines¹ and, in view of the approximate nature of several of the formulae that have hitherto been proposed to account for these contributions to the broadening, further theoretical work on this subject is clearly indicated.

Thirdly, the importance has been shown of accounting for configuration interaction whenever it plays a significant role in the displacement of terms from their unperturbed positions. Some further work is needed, however, in order to clarify the difficulties hitherto experienced (in particular for ions such as Sn(II) and Si(II)) in accounting for the broadening of lines from transitions involving configurations with equivalent electrons.

Acknowledgements—The authors are indebted to Dr. M. H. Miller for making available the results in Ref. 35 prior to publication. The calculations were performed at the Computer Science Centre of the University of Cape Town. We wish to thank Prof. H. R. Griem for helpful comments on the manuscript.

REFERENCES

1. H. R. Griem, *Spectral Line Broadening by Plasmas*. Academic Press, New York (1974).
2. H. R. Griem, *Adv. Atomic and Molec. Phys.* 11, 331 (1975).
3. H. R. Griem, *Phys. Rev.* A17, 214 (1978).
4. R. W. Lee, *J. Phys. B:Atom. Molec. Phys.* 11, L167 (1978).
5. N. Konjević and W. L. Wiese, *J. Phys. Chem. Ref. Data* 5, 259 (1976).
6. M. Platiša, M. Dimitrijević, M. Popović, and N. Konjević, *Astron. Astrophys.* 54, 837 (1977).
7. M. Platiša, M. Dimitrijević, M. Popović, and N. Konjević, *J. Phys. B:Atom. Molec. Phys.* 10, 2997 (1977).
8. W. W. Jones, *Phys. Rev.* A7, 1826 (1973).
9. W. W. Jones, S. M. Bennett, and H. R. Griem, *University of Maryland Tech. Rep.* No. 71-128 (1971), College Park, Maryland, U.S.A.
10. S. Sahal-Bréchet, *Astron. Astrophys.* 1, 91: 2, 322 (1969).
11. M. Platiša, M. Popović, M. Dimitrijević, and N. Konjević, *Z. Naturforsch.* 36a, 212 (1975).
12. J. D. Hey, *JQSRT* 18, 649 (1977).
13. M. Baranger, *Phys. Rev.* 112, 855 (1958).
14. H. R. Griem, *Phys. Rev.* 128, 515 (1962).
15. H. R. Griem, *Phys. Rev.* 165, 258 (1968).
16. D. D. Burgess, *Phys. Rev.* 176, 150 (1968).
17. E. A. M. Baker and D. D. Burgess, *J. Phys. B:Atom. Molec. Phys.* 10, L177 (1977).
18. W. T. Chiang and H. R. Griem, *J. Phys. B:Atom. Molec. Phys.* 11, L761 (1978).
19. E. U. Condon and G. H. Shortley, *The Theory of Atomic Spectra*. Cambridge University Press (1951).
20. H. A. Bethe and E. E. Salpeter, *Quantum Mechanics of One- and Two-Electron Atoms*. Springer-Verlag, Berlin (1957).
21. I. I. Sobel'man, *Introduction to the Theory of Atomic Spectra*. Pergamon Press, Oxford (1972).
22. R. D. Cowan and K. L. Andrew, *J. Opt. Soc. Am.* 55, 502 (1965).
23. B. Warner, *Mon. Not. Roy. Astr. Soc.* 139, 273 (1963).
24. J. D. Hey, *JQSRT* 17, 721 (1977).
25. J. D. Hey and M. Blaha, *JQSRT* 20, 557 (1978).
26. A. W. Weiss, *Phys. Rev.* 178, 82 (1969).
27. A. W. Weiss, *Phys. Rev.* A9, 1524 (1974).
28. J. D. Hey, *JQSRT* 20, 403 (1978).
29. K. Behringer and P. Thoma, *JQSRT* 20, 615 (1978).
30. J. Purić, S. Djenžić, J. Labat, and L. Čirković, *Z. Physik* 267, 71 (1974).
31. A. Lesage, S. Sahal-Bréchet, and M. H. Miller, *Phys. Rev.* A16, 1617 (1977).
32. J. D. Hey, *JQSRT* 18, 425 (1977).
33. W. T. Chiang and H. R. Griem, *Phys. Rev.* A18, 1169 (1978).
34. C. F. Fischer, *Astrophys. J.* 151, 759 (1968).
35. M. H. Miller, R. A. Roig, and R. D. Bengtson, *Phys. Rev.* A20, 499 (1979).
36. T. Wujec and J. Musielok, *Astron. Astrophys.* 50, 405 (1976).
37. M. Gailitis, *Sov. Phys. JETP* 17, 1328 (1963).
38. O. Bely, *Phys. Rev.* 185, 79 (1969).
39. H. Van Regemorter, *Astrophys. J.* 136, 908 (1962).

40. D. R. Bates and A. Damgaard, *Phil. Trans. Roy. Soc. London (Ser. A)* **242**, 101 (1949).
41. H. R. Griem and K. Y. Shen, *Phys. Rev.* **122**, 1490 (1961).
42. H. R. Griem, M. Baranger, A. C. Kolb, and G. Oertel, *Phys. Rev.* **125**, 177 (1962).
43. H. R. Griem, *Phys. Rev. Lett.* **17**, 509 (1966).
44. C. Fleurier, S. Sahal-Bréchet, and J. Chapelle, *J. Phys. B: Atom. Molec. Phys.* **10**, 3435 (1977).
45. C. E. Moore, *Atomic Energy Levels*, Vol. III. NBS Circular No. 467, Washington, D.C. (1958).
46. M. H. Miller, Private communication.
47. C. de Witt Coleman, W. R. Bozman, and W. F. Meggers, *Table of Wavenumbers*, Vol. I. NBS Monograph 3, Washington, D.C. (1960).
48. M. Baranger, *Atomic and Molecular Processes* (Edited by D. R. Bates), Chap. 13. Academic Press, New York (1962).

Appendix II: Hey and Breger (1980b)

CALCULATED STARK WIDTHS OF
OXYGEN ION LINES

JOHN D. HEY and PETER BREGER
Department of Physics
University of Cape Town
Rondebosch 7700, Cape
South Africa

Calculations have been performed on the electron impact broadening of isolated lines from singly-ionized and doubly-ionized oxygen emitted from a plasma of electron density 10^{17} cm^{-3} and temperature about 2 eV. These have been compared with results of measurements performed by Platiša, Popović and Konjević on a plasma produced by a low pressure pulsed arc. Good overall agreement has been obtained for both ionization stages, which we interpret as strong support for a recently derived expression for the effective Gaunt factor in line broadening calculations. This in turn indicates the important role that the curvature of the perturber trajectory plays in the broadening process, and that by proper allowance for this effect, classical path calculations of the isolated ion line widths can be extended to spectra of the multiply-charged ions. Some ambiguity still remains, however, as to the proper method of extrapolation of the effective Gaunt factors below threshold energies in the classical path calculation of the elastic contribution to the broadening. The present comparison appears to indicate that for the higher ionization stages, extrapolation of \bar{g} as a constant equal to its threshold value, is satisfactory.

INTRODUCTION

Notwithstanding the astrophysical importance¹ of Stark broadening parameters for spectral lines from neutral, singly- and multiply-ionized atoms of the common elements, the amount of available experimental information on the spectral line widths for the oxygen ion lines continues to be rather scarce.^{2,3} The comprehensive experimental study by Platiša et al.⁴ therefore remains of great interest. In this paper, the average ratio of measured widths (\bar{w}_m) to the corresponding values (\bar{w}_e) calculated by the classical-path approximation,^{1,5} was found to be:

$$\frac{\bar{w}_m}{\bar{w}_e} = 0.89 \pm 0.03$$

for thirteen lines from seven multiplets of O(II), while no theoretical values were available at the time for the O(III) line widths. Subsequently, Hey and Bryan⁶ undertook a comparison between the measured widths and the corresponding values obtained from the semi-empirical approximation derived by Griem⁷ (with slight modifications). For the O(II) lines, rather poorer agreement was obtained than with the previously published theoretical widths^{1,5}:

$$\frac{\bar{w}_m}{\bar{w}_e} = 1.30 \pm 0.06$$

for thirteen lines from thirteen multiplets. For O(III),

$$\frac{W_m}{W_e} = 1.89 \pm 0.10$$

for four lines from four multiplets. Estimated experimental errors⁴ for the lines lay within $\sim \pm 16\%$.

Possible reasons for these discrepancies were examined,⁶ and it was concluded that the most plausible explanation lay in the consistent underestimation of the threshold values of the effective Gaunt factor \bar{g} used in these calculations,⁶⁻⁸ particularly for O(III). Similar disagreements with the older threshold value^{7,9} $\bar{g} = 0.20$ had already been reported in the literature.^{9,10} Indeed, although the initial impression gained from the first systematic comparisons between theory and experiment for the semi-empirical method was rather good⁷ (typical agreement within a factor ~ 1.5 and in many cases much better^{1,7}), the semi-empirical procedure has been found to deteriorate markedly in accuracy when applied to multiply-charged ion lines.^{11,12} While such comparisons can still be useful for indicating trends in ion excitation cross sections,^{12,13} there can be no doubt that the predictive ability of the theory as originally formulated by Griem⁷ is rather less than was originally expected,^{14,15} in spite of the rather impressive success of this model which is still reported for certain singly-charged ions.

In the recent past, attention has been devoted to this problem mainly from the viewpoint of improving the treatment of radiator structure (i.e. attempting to take a more careful

account of the eigenstates of the bound electrons than in several classical-path calculations applied to the isolated lines^{1,5,16}). In certain cases like lines of N(II)¹⁷ and Ar(II)¹⁸ this refinement^{19,20} of the theory has led to better agreement with experiment and has explained unusual features^{18,21} of the broadening, while in other cases like Si(II)^{22,23} and Sn(II)²⁴ significant discrepancies remain unexplained.^{25,26} As long as such significant uncertainties¹² still exist in the \bar{g} -values, it is clear that the additional improvement that may be derived from these modifications to the original theory,⁷ is severely limited.

In his monograph, Griem¹ has proposed formulae for the effective Gaunt factors, applicable to the multiply-charged ions. He distinguishes between cases for which the principal quantum number changes and those where it remains the same in the collisional excitation process (see pp. 272-274 of Ref. 1).
While there are already clear indications^{1,27} that these represent an improvement upon the expression in Ref. 7, at least for ionization stage $Z > 2$, the new expressions contain a number of unsatisfactory features in common with the old formula.⁷ The most notable of these is the prescription of a fixed threshold value of \bar{g} for the ion in question, which is imposed on separate grounds such as experimental evidence or quantum mechanical calculations.^{1,7,28} Examples of these are:

$$\bar{g}_{th} = 0.2 \quad (\text{Refs. 1, 8, for } \Delta n \neq 0)$$

$$\bar{g}_{th} = 0.9 - \frac{1.1}{Z} \quad (\text{Ref. 1, for } \Delta n = 0 \text{ and } Z \geq 2)$$

$$\bar{g}_{th} = 0.26 + 0.09(Z-2) \quad (\text{Ref. 12, for } Z = 2, 3).$$

Such a prescribed value can at best be viewed as a rough interpolation between the various values actually applicable to the many different types of transitions (s-p, p-d, etc.) taking place within the ion. The success of this procedure in fact rests upon the smoothing out of the individual variations in the summation over the complete set of perturbing levels.

The need for such an independent prescription of \bar{g}_{th} must therefore be seen as an indication that the quasi-classical model whereby the \bar{g} -values are calculated,^{1,7} is defective to some extent. Difficulties with the quasi-classical model arise for values of the (incident) perturber energy comparable to the threshold energy, and are manifested when the argument of a logarithm turns negative.⁷ This is particularly serious, since many of the experimental data (notably for $Z > 2$) apply to plasma conditions where the broadening arises primarily by elastic collisions, i.e. where reliable \bar{g} values are mainly required for electron energies in the range in which the quasi-classical formula is least accurate.

Although in a formal sense, the principle of extrapolation as introduced by Griem⁷ (whereby elastic contributions to the broadening are derived by extrapolation of the inelastic cross sections below threshold) has been justified on quantum mechanical grounds,²⁹⁻³² the actual procedure for accurate computation over the various resonances below threshold is far from straight-forward theoretically, or for that matter even unique.³³⁻³⁷ With these difficulties in mind, the initial

success achieved by a simple model such as that of Griem⁷ is remarkable indeed: according to the data available at the time, no significant deterioration in agreement with his model was detected as the relative importance of the elastic contributions to the broadening increased.

The problems to which we have alluded in the previous paragraphs (in particular the threshold values of \bar{g}), are closely related to the manner in which the initial choice of minimum and maximum impact parameters in the classical-path calculation, is corrected to allow for the effect of curvature of the perturber trajectory.^{38,39} In the revised formulae on pp. 272-274 of Ref. 1, no such correction factors were incorporated (hence the need to introduce an interpolated \bar{g}_{th}), while in Ref. 7 their incorporation was not sufficient to guarantee that the expression for \bar{g} remained analytical for all perturber energies above threshold.

Subsequently to the completion of the work reported in Ref. 26, a new derivation of \bar{g} was undertaken⁴⁰ in an endeavour to overcome the difficulties outlined above. The success of the new formula in predicting the widths of the Stark-broadened lines of ionized oxygen, is the subject of the present paper. The ingredients of the new formula are discussed in the following sections; its most notable feature is the manner in which a suitable choice of impact parameter cut-offs, together with proper allowance for curvature effects, has ensured the analytical behaviour of the function for all perturber energies above threshold.

FORMULATION OF THEORY

For the isolated ion lines of interest, the predominant contribution to the broadening is derived from the action of the free electron perturbers operating in the impact régime. The contribution to the broadening from quasi-static ion perturbers is small, entering in second-order dipole and first-order quadrupole terms.¹ In this section, broadening by ions is therefore neglected. In the impact approximation, the Baranger^{7,29} expression for the full width of the line ($|i\rangle \rightarrow |f\rangle$) at half maximum (FWHM) may be written:

$$W_e^{if} = N_e \left\{ v \left(\sum_{i' \neq i} \sigma_{i',i} + \sum_{f' \neq f} \sigma_{f',f} + \int |\phi_i - \phi_f|^2 d\Omega \right) \right\}_{AV} \quad (1)$$

Here ϕ_i and ϕ_f are elastic scattering amplitudes for the two states of the perturbed system, the integral being performed over the scattering angles (Ω). The average is performed over directions and the Maxwellian velocity distribution of the electron perturbers. Ignoring for the moment the elastic terms in eqn. (1), and substituting for the cross section $\sigma_{i',i}$ in terms of the corresponding collision strengths

$$\sigma_{i',i} = \pi a_0^2 \frac{E_H}{\frac{1}{2} m v^2} \frac{\Omega(i,i')}{\tilde{\omega}_i} \quad (2)$$

one obtains in wavelength units:

$$W_e^{if} = \frac{\alpha \lambda^2 a_0^2}{\sqrt{\pi}} N_e \left(\frac{E_H}{kT} \right)^{\frac{1}{2}} \left\{ \sum_{i'} \frac{\langle \Omega(i,i') \rangle}{\tilde{\omega}_i} + \sum_{f'} \frac{\langle \Omega(f,f') \rangle}{\tilde{\omega}_f} \right\} \quad (3)$$

The average indicated in parentheses denotes:

$$\langle \Omega(i,i') \rangle = \int_{z_{i',i}}^{\infty} \Omega(i,i') \exp(-z) dz \quad (4a)$$

in the case of inelastic collisions, and:

$$\langle \Omega(i,i') \rangle = \int_0^{\infty} \Omega(i,i') \exp(-z) dz \quad (4b)$$

in the case of superelastic collisions, where:

$$z = \frac{mv^2}{2kT} \quad \text{and} \quad z_{i',i} = \frac{\Delta E_{i',i}}{kT}, \quad \text{with} \quad \Delta E_{i',i} = |E_{i'} - E_i|.$$

The elastic contributions to the broadening are now simply incorporated by extrapolating the inelastic terms in eqn. (3) below threshold, i.e. by replacing $z_{i',i}$ in (4a) by 0. For a discussion of this procedure and its quantum mechanical justification, the reader is referred to Refs. (30) - (37).

We now make a further simplification, viz. that of retaining only the direct collision (i.e. non-exchange) terms which contribute to (3), and of treating these as collisions inducing (allowed) inelastic dipole transitions in the radiator. In that case, each $\Omega(i,i')$ may be written in terms of the corresponding atomic line strength $S(J,J')$ and effective Gaunt factor \bar{g} as:

$$\Omega(i,i') = \frac{8\pi}{3^{3/2}} \bar{g}(i,i') \frac{S(J,J')}{a_0^2 e^2} \quad (5)$$

Each factor in (5) is entirely symmetrical in the labels (i,i').

and the expression therefore holds whether the perturbing level i' lies below or above i in energy.

THE EFFECTIVE GAUNT FACTOR

The expression for \bar{g} given below has been derived⁴⁰ by a quasi-classical calculation, in several respects following the earlier method of Griem^{1,7,38,39} but with some significant modifications to the approach adopted by the latter. The argument given on p. 75 of Ref. (1) against the symmetrization procedure in line broadening calculations has been accepted, and accordingly the entire derivation has been performed in terms of parameters relevant to the trajectory of the incoming electron. From perturbation theory applied to the classical path approximation,⁷ one has:

$$\bar{g} = \frac{\sqrt{3}}{\pi} \ln \frac{\epsilon_{\max}}{\epsilon_{\min}} \quad (6)$$

in terms of upper and lower cutoff values for the eccentricity of the perturber orbit. The eccentricity may be written in terms of impact parameter (ρ) and incident (asymptotic) electron speed (v) as:

$$\epsilon = \left\{ 1 + \frac{m^2 \rho^2 v^4}{(Z-1)^2 e^4} \right\}^{1/2} \quad (7)$$

A crucial question that now arises is the truncation of ρ for small and large values. One easily shows that the choice of cutoff values vitally affects the range of energies over

which the expression derived for \bar{g} remains analytical⁴⁰. For the upper cutoff, the validity criterion of the impact approximation^{1,7,38,39,41} requires that:

$$\rho_{\max} = \frac{\hbar v}{\Delta E_{i'i}} \quad (8)$$

for a rectilinear trajectory. For our purposes, it was found to be very important to correct this expression for curvature of the perturber trajectory⁴⁰. Invoking the conditions of conservation of energy and angular momentum for the unperturbed trajectory, one obtains instead of (8):

$$\rho_{\max} = \frac{\hbar v}{\Delta E_{i'i}} \phi^2 \quad (9)$$

where the curvature factor ϕ obeys the cubic equation:

$$\phi^3 - \phi - 2\xi_{n\ell}^{n'\ell'} = 0 \quad (10)$$

in terms of the parameter:

$$\xi_{n\ell}^{n'\ell'} = \frac{(Z-1)e^2}{\hbar v} \frac{\Delta E_{i'i}}{mv^2} \quad (11)$$

This cubic equation has the following explicit solutions:

$$\phi = \frac{2}{\sqrt{3}} \cos \left[\frac{1}{3} \arccos (\sqrt{27} \xi) \right] \quad (12)$$

$$\phi = \left[\xi + \sqrt{\xi^2 - \frac{1}{27}} \right]^{1/3} + \left[\xi - \sqrt{\xi^2 - \frac{1}{27}} \right]^{1/3} \quad (13)$$

(for $\xi \geq \frac{1}{\sqrt{27}}$)

For small ρ , three conditions must be fulfilled. Firstly, ρ should exceed the (reduced) de Broglie wavelength of the electron perturber in order to ensure validity of the classical path treatment. From the requirement of conservation of angular momentum, the curvature correction is trivial in this case, and we may put:

$$\rho \geq \rho_1 = \frac{\hbar}{mv} \quad (14)$$

Secondly, the perturbing electron should remain sufficiently far removed from the radiator system in order for the dipole approximation as employed here to remain valid. A suitable criterion for these purposes is that the perihelion of the perturber orbit should be distant enough for the dipole moment of the perturber-nucleus always to exceed that of the bound (optical) electron-nucleus. In terms of impact parameter, this condition may be written⁴⁰:

$$\rho \geq \rho_2 = \left(\frac{\hbar}{mv}\right) d_{i,i} \left[\frac{\frac{1}{2} m v^2}{E_H} + \frac{2(Z-1)}{d_{i,i}} \right]^{\frac{1}{2}} \quad (15)$$

It is probably always sufficient for these purposes to employ the square of the dipole moment of the atomic system averaged over angular momentum states, i.e.:

$$d_{i,i}^2 = \left[\frac{1}{3} \frac{\ell}{2\ell+1} R_{i,i}^2 \right]^{\frac{1}{2}} \quad (16)$$

in terms of the square of the radial integral $(R_{i,i})$.

Lastly, the condition of unitarity (flux conservation)

should also be fulfilled. For rectilinear trajectories, the condition:

$$\rho \geq \rho_3 = \left(\frac{\hbar}{mv}\right) d_{i,i} \quad (17)$$

can be reduced with further simplification to the (unnecessarily stringent - see below) condition given on p.271 of Ref. (1). It may be argued that in the general (hyperbolic) case, one should replace ρ_{\min}^2 in the square of the Weisskopf radius (employed in the "strong collision" term^{1,7,41-43}) by⁴⁰:

$$\rho_{\min}^2 + \frac{(Z-1)^2 e^4}{m^2 v^4}$$

(see below) when calculating the contribution to the broadening from strong ($\rho < \rho_{\min}$) collisions. In that case one writes:

$$\rho \geq \rho_3 = \left[\left(\frac{\hbar}{mv}\right)^2 d_{i,i}^2 - \frac{(Z-1)^2 e^4}{m^2 v^4} \right]^{\frac{1}{2}} \quad (18)$$

provided that the expression in parentheses remains positive. Thus a plausible justification may be provided for the corresponding eqn. (194) of Ref. (1).

All three of the conditions may conveniently be incorporated into the single cutoff

$$\rho \geq \rho_{\min} = \left[\rho_1^2 + \rho_2^2 + \rho_3^2 \right]^{\frac{1}{2}} \quad (19)$$

For perturber energies such that

$$\frac{1}{2} m v^2 \leq (Z-1)^2 E_H / d_{i,i}^2 \quad (20)$$

ρ_3 should be equated to zero in eqn. (18), since negative values of this quantity are meaningless⁴³.

With:

$$x = \sqrt{\frac{\frac{1}{2} m v^2}{\Delta E_{i,i}}} \quad , \quad y = \sqrt{\frac{E_H}{\Delta E_{i,i}}} \quad ,$$

the calculation of \bar{g} may thus be conveniently parameterized

by the following two expressions:

$$\bar{g} = \frac{\sqrt{3}}{2\pi} \ln \left[\frac{1 + \frac{4x^6}{(Z-1)^2 y^2} \phi^4}{1 + \frac{x^2}{(Z-1)^2 y^2} \left[1 + d_{i',i}^2 \left(1 + \frac{x^2}{y^2} + \frac{2(Z-1)}{d_{i',i}} \right) - \frac{(Z-1)^2 y^2}{x^2} \right]} \right] \quad (21)$$

$$\bar{g} = \frac{\sqrt{3}}{2\pi} \ln \left[\frac{1 + \frac{4x^6}{(Z-1)^2 y^2} \phi^4}{1 + \frac{x^2}{(Z-1)^2 y^2} \left[1 + d_{i',i}^2 \left(\frac{x^2}{y^2} + \frac{2(Z-1)}{d_{i',i}} \right) \right]} \right] \quad (22)$$

where the second expression replaces the first in the low energy region:

$$x^2 \leq (Z-1)^2 y^2 / d_{i',i}^2 \quad (23)$$

and ϕ obeys the relation:

$$\phi^3 - \phi - (Z-1)y/x^3 = 0 \quad (24)$$

As regards the general validity of the formula for \bar{g} given above, it may be pointed out here that in the high-energy limit, our expression is identical with the (corrected) form of the quantum mechanical Bethe approximation as given by Seaton.¹⁵ An important aspect of this work was to ensure that the formula for \bar{g} remains analytical for all $x \geq 1$, thereby enabling extrapolation to be made into the range of below-threshold energies where necessary. With analyticity as one of the criteria for the validity of eqns. (21) and (22), it could easily be shown⁴⁰ that the three cut-offs employed

in P_{\min} are better choices than the simpler forms given on pp. 79, 270 and 271 of Ref. (1). A useful inequality for these purposes, $d_{i',i} \leq y$, follows directly from the observation that⁴⁴:

$$d_{i',i}^2 \frac{1}{y^2} = \frac{1}{3} \left(\frac{\ell_{\gamma}}{2\ell+1} \right) R_{i',i}^2 \frac{\Delta E_{i',i}}{E_H} = f_{i',i} \quad (25)$$

which in fact shows why the simpler¹ $d_{i',i} \sim \frac{n^*2}{Z}$ leads to breakdown of the corresponding expressions in Ref. (1) (when not supplemented as on pp. 272, 273 by artificial threshold values), since the cutoffs imposed should naturally be relaxed for those transitions $|i\rangle \rightarrow |i'\rangle$ which are intrinsically less probable.

In summary, it could be rigorously shown⁴⁰ that expressions (21) and (22) remain well behaved for all x and y , with $\Delta E_{i',i}$ larger than $\sim 200 \text{ cm}^{-1}$ in the case of singly-charged radiators. A direct numerical check on the computer extended the range to level separations as small as $\sim 150 \text{ cm}^{-1}$. For $Z > 2$, a breakdown of the above formulae can be regarded as highly unlikely.

ADDITIONAL CONTRIBUTIONS TO BROADENING

Consistent with the introduction in the previous section of a lower cutoff for the eccentricity (impact parameter) in the quasi-classical expression for \bar{g} , would be the addition of an extra term to the broadening to account for strong (disruptive and higher multipole) collisions.¹ The expression

conventionally adopted for the Lorentz-Weisskopf term^{1,7,18, 39, 39, 42, 43}:

$$W_s = 2\pi N_e \left\{ v \rho_{\min}^2 \right\}_{AV} \quad (26)$$

(where the average is carried out over both the electron velocity distribution and the relevant minimum impact parameters for those collision-induced transitions $|i\rangle \rightarrow |i'\rangle$ which contribute to the line width), is in fact strictly applicable to rectilinear perturber trajectories only. What is needed for present purposes, is the appropriate generalization for hyperbolic paths. This is readily achieved by the introduction of the semi-major axis $a = \frac{(Z-1)e^2}{mv^2}$ of the hyperbola, and the new expression for W_s becomes⁴⁰:

$$W_s = 2\pi N_e \left\{ v \left[\rho_{\min}^2 + \frac{(Z-1)^2 e^4}{m^2 v^4} \right] \right\}_{AV} \quad (27)$$

On substituting from above and performing the double average, one obtains (FWHM, in wavelength units):

$$W_s = \frac{2}{\sqrt{\pi}} \alpha \lambda^2 a_0^3 N_e \left(\frac{E_H}{kT} \right)^{\frac{1}{2}} \left[1 + 2(Z-1) \bar{d}_{i,i} + \left(1 + \frac{kT}{E_H} \right) \bar{d}_{i,i}^2 \right] \quad (28)$$

In view of the difficulties associated with the calculation of the negative contribution to the upper-lower state interference term from strong collisions,¹ we have adopted in all cases the simplifying assumption that these "strong" interference terms fully cancel the strong

contribution from the lower-state terms alone.²⁸ Hence in eqn. (28) we ignore all but those collision-induced transitions associated with the upper state of the line. This useful simplification we shall regard as justified for the ions in question by the agreement between theory and measurement.

It remains to verify that the contribution to the broadening from ion perturbers is indeed small, as already indicated above. Here again a number of different estimates can be made, depending upon the degree of validity of the quasi-static or impact approximations for ion-ion interactions as discussed by Sahal-Bréchet.^{22, 37, 45} For quadrupole interactions, the quasi-static and impact approximations yield very similar results which in wavelength units may be estimated by (FWHM)¹:

$$W_i^Q = \frac{2 \alpha \lambda^2 a_0^2}{Z^2} \sum_p N_p Z_p \left(n_i^{*2} - n_f^{*2} \right)^2 \quad (29)$$

where N_p and $Z_p e$ are the perturber concentration and charge respectively. The condition of quasi-neutrality in the plasma enables one to substitute above:

$$N_e = \sum_p N_p Z_p \quad (30)$$

The second-order dipole (quadratic) contribution to the line width is, however, appreciably different when calculated in the impact and quasi-static approximations.¹ In the latter case, the contribution to the broadening is usually insignificant compared with that produced by electron

perturbers; in the former case the calculation is more involved than for the quadrupole case (see pp. 275-277 of Ref. (1)). Provided that the ions may indeed be treated within or near to the regime of validity of the quasi-static approximation, we may consider that

$$W_1^q \ll W_e$$

provides a sufficient guarantee that the electron broadening completely predominates.

For the electron perturbers, the validity of the impact approximation over the major portion of the measurable profile is guaranteed by

$$v/p \gg \frac{1}{2} W_e$$

and with $\rho_{\max} \sim \frac{\pi v}{|\Delta E_{i,i}|}$ as above, the criterion for the isolated line approximation therefore ensures the validity of the impact approximation provided that inelastic collisions predominate in the broadening. (Greater care might be required for plasmas whose temperature is so low that inelastic processes are unimportant.)

For the validity of the quasi-static approximation for ion perturbers throughout the (electron-broadened) profile, Griem¹ obtains a relation equivalent to

$$\frac{kT}{E_H} < \frac{3\pi^2}{4} \left(\frac{m_p}{m}\right)^{1/2} \frac{n_i^{*4}}{Z^2} \frac{N_e a_0^2}{N_p^{1/3}} \quad (31)$$

assuming equal ion and electron temperatures, where N_p and m_p are the perturber concentration and mass, respectively. For

proton perturbers, one finds that the above inequality is not properly fulfilled under the plasma conditions relevant to this investigation. This indicates that neither of the conventional approximations is valid for ion perturbers throughout the line profile.^{22,37} We shall assume, however, in view of the remarks preceding eq. (29) above that the smallness of W_1^q relative to W_e is a sufficient guarantee of the predominance of electron impact broadening throughout the line core.

Lastly, it should be mentioned that perturber correlations (Debye shielding) play an insignificant role in the line broadening. This is because $\Delta E_{i,i} \gg \pi\omega_p$ (the plasmon energy) in all cases under consideration, justifying the approximation of isolated lines broadened by impact of unshielded perturbers.^{1,6,20,41}

RADIATOR STRUCTURE

Two aspects of atomic structure which could complicate this type of calculation, have been noted for the ions in question.^{19,20,25,26} Configuration interaction has long been known^{44,45} to occur to some extent in both O(II) and O(III), both of which also show a tendency towards LK coupling in the case of excited terms corresponding to motion of the outer electron in an f orbital.^{46,47} In the present calculation, both of these radiator effects have been ignored. The justification²¹ for this considerable simplification in the present case lies in the fact that for all perturbing levels i' within the allowed electric-dipole scheme, the energy gap

$\Delta E_{i',i} = |E_{i'} - E_i|$ is larger than kT (usually far larger). Therefore in the summation over perturbing levels, the relevant Gaunt factors remain typically near their threshold value, and the sum rules for the atomic line strengths tend to minimize the importance of such structural effects. This is borne out by the practical constancy of the measured line widths within multiplets.⁴ A rather different state of affairs could, however, be expected if the same lines were observed in the high-temperature regime.^{10,21}

A corollary to the discussion in the previous paragraph, is that the calculated Gaunt factors are here subjected to a particularly stringent test, since numerical values are required for perturber energies largely in a domain (near threshold) where the present theory might be supposed to be least accurate. It was encouraging, however, to note that in earlier studies^{6,7} no significant dependence of agreement between measurement and calculation upon $kT/\Delta E_{i',i}$ could be found. This important question is discussed more fully in the following section.

We have therefore assumed that the simple LS coupling scheme is appropriate for the description of the radiator states. The line strength $S(J,J')$ in eqn. (5) may accordingly be written as

$$\frac{1}{2J+1} \frac{S(J,J')}{a_0^2 e^2} = \ell_{>} (2L+1) (2L'+1) (2J'+1) \left\{ \begin{matrix} \ell & \ell' & 1 \\ L' & L & L_1 \end{matrix} \right\}^2 \times \left\{ \begin{matrix} L & L' & 1 \\ J' & J & S \end{matrix} \right\}^2 \left(R_n^{n' \ell \ell'} \right)^2 \quad (32)$$

In all cases considered here, a single electron (situated outside the shells or subshells which contain the rest)

participates in the transition. The designations $\ell(\ell')$ refer to the orbital angular momentum of the outer electron, ℓ , being the greater of these; $L(L')$ denotes the total orbital angular momentum, L , being that of the core electrons, and $J(J')$ denotes the total angular momentum of the state $|i\rangle (|i'\rangle)$. The square of the radial integral $\left(R_n^{n' \ell \ell'} \right)$ is here evaluated in the Coulomb approximation, which should be of sufficient accuracy for the calculation of most of the major individual contributions to the width, particularly since transitions involving equivalent electrons are not considered in this study.^{4,9,50}

RESULTS

The theory described in the previous sections has been applied to the measurements performed on isolated lines of singly- and doubly-ionized oxygen by Platiša et al,⁶ referred to an electron density $N_e = 10^{17} \text{ cm}^{-3}$ and temperature $T = 25900^\circ\text{K}$. (The actual value of $N_e = (5.2 \pm 0.4) \times 10^{16} \text{ cm}^{-3}$.) The results are presented in Tables I-IV. In view of the close agreement between the various measured widths for lines from the same multiplet,⁶ we have selected one representative line in each case where a choice exists. In Tables I and II, after each representative transition are listed in order: two values of the electron impact width (W_e) calculated by the present theory applied in two ways (see below); the fractional contribution to the line width from strong collisions (W_s/W_e) expressed as a percentage; the fractional contribution to the line width from the inelastic part of the weak (i.e. non-strong)

interactions (\bar{W}_{in}/W_e) expressed as a percentage; the fractional contribution from the elastic part of the weak interactions (\bar{W}_{el}/W_e) expressed as a percentage. These three percentages should thus in all cases add up to unity.

The next column gives an estimate of the importance of the neglected contribution to the broadening from ion perturbers (\bar{W}_i/W_e) also in percent, as calculated from eqn. (29). Next we give the completeness parameter (χ) reduced to percent, which indicates the degree of completeness of the subset of perturbing levels actually employed in the calculation. [In Refs. (1) and (2), χ is denoted by $\Delta S/S$.] This parameter is calculated (also in the Coulomb approximation^{43,50}) from the reduced matrix elements^{44,45}

$$\chi = \frac{1}{2J+1} \frac{\sum_{i'} |\langle i' || \frac{r}{a_0} || i \rangle|^2}{(R_{n\ell})^2} \quad (33)$$

where $R_{n\ell}$ is given in terms of the effective principal quantum number (n^*) and orbital angular momentum (ℓ) of the radiating electron (coordinate r) by⁵¹

$$(R_{n\ell})^2 = \frac{n^{*2}}{2Z^2} [5n^{*2} + 1 - 3\ell(\ell+1)] \quad (34)$$

for an ion of charge ($Z-1$). The first value of χ in each row applies to the perturbing levels for the upper state, the second to perturbing levels for the lower state.

In the case of O(II), the following terms of some importance in the calculation were found to be missing from the tables,⁴⁵ and their positions were chosen by simple quantum defect⁴⁵ estimates: (³P) 4p ²S⁰, 4p ⁴S⁰, 4p ⁴P⁰, (¹D) 4p ²F⁰. In the

case of O(III), the terms (²P⁰) 4f ³D, ³F, ³G which strictly speaking should not be classified by LS coupling, were determined from the spectral lines listed in Ref. (47), with the simplification of averaging over the structure related to the more appropriate JK coupling scheme.⁴⁸ [This approximation is justified by the small energy differences between the various K sublevels as compared with $\Delta E_{i,i}$].

The major theoretical difficulty encountered in the present calculations, was related to the elastic contribution to the broadening, which is in theory obtainable by extrapolation of the Gaunt factors for below-threshold energies.²³⁻³² The proper choice of analytical continuation of the function employed here (eqns. (21) and (22)) into the domain of below-threshold energies is not directly obtainable from our semi-classical derivation, which does not account explicitly for the existence of resonances below threshold. The correct analytical continuation clearly depends upon the nature of these resonances (their spacing and size), and would require a quantum mechanical study of the problem.

We therefore chose two simple methods of approaching this problem, which are both natural extensions of the present theory. In the first, eqns. (21) and (22) are simply employed as they stand for below-threshold energies, the Maxwellian average in eqn. (4a) being simply cut off at the value of $z = \frac{mv^2}{2kT}$ such that $\bar{g} = 0$, this point being solved for numerically (Method I). In the second method, the threshold value \bar{g}_{th} is employed for all $0 \leq z \leq z_{i,i}$, the approximation first proposed by Griem⁷ (Method II).

The inelastic contribution to the broadening (W_{in}) thus consists of the sum of (4a) and (4b) for all inelastic plus superelastic collision-induced transitions. The elastic contribution is obtained from the sum of all integrals of the type

$$\int_{z_{min}}^{z_{i,i}} \Omega(i, i') \exp(-z) dz ,$$

using either Method I or Method II.

In the past in calculations of this kind the simplification has often been adopted of dispensing with the Maxwellian averaging, and of employing merely \bar{g} calculated at the thermal average electron energy.^{5,7,11,12,26,52} We have found this procedure to be inapplicable in the present case, since in eqns. (21) and (22), the values of \bar{g} do not vary sufficiently slowly with energy. A simple test of the validity of such an approximation is to compare \bar{g} for the following particle speeds: root-mean-square, most probable and mean. An appreciable change in \bar{g} was obtained, and this indicated the need for careful averaging to be performed.

Some of the threshold values of \bar{g} for O(III), obtained from the present theory, are listed in Table V. These values contain no contribution from strong collisions.

DISCUSSION

The average ratio of measured to calculated (FWHM) widths in the present study, is for O(II):

$$\frac{W_m}{W_e} = 0.91 \pm 0.04 \quad (\text{Method I})$$

$$\frac{W_m}{W_e} = 0.73 \pm 0.04 \quad (\text{Method II})$$

while for O(III):

$$\frac{W_m}{W_e} = 1.27 \pm 0.08 \quad (\text{Method I})$$

$$\frac{W_m}{W_e} = 0.98 \pm 0.06 \quad (\text{Method II}) .$$

The present results are compared in Tables III and IV with the earlier values for O(II) obtained by Jones, Benett and Griem^{1,5} (here denoted by JBG) and the later values for both O(II) and O(III) published by Hey and Bryan⁶ (here denoted by HB). For O(II), the results by Method I compare very favourably with those from Refs. (1) and (5), while for O(III) the results yielded by Method II are in excellent agreement with the experiment.⁴ Noting that the experimental accuracy is estimated to be $\sim \pm 16\%$ in Ref. (4) for each line width, it appears that the experiment (with the exception of the last O(II) line) is in overall good agreement with the present theory, and appears to favour the extrapolation procedure by

Method I for O(II) while showing strong preference for Method II in the case of O(III). Why the two ions should differ in this respect with regard to the elastic contribution to the broadening is not clear, but perhaps this observation indicates that while the "correct" extrapolation procedure lies between the two approximations, the tendency is towards $\bar{g} = \bar{g}_{th}$ (for energies $0 < z < z_{i,1}$) for the higher ionization stages. In any case, the vital importance of the elastic contribution to the broadening as discussed by Griem,⁷ is clearly shown in Tables I and II.

As far as the strong collision contribution is concerned, it appears from comparison with W_s/W_e in Refs. (1) and (5) that our cutoff separating strong from weak collisions is rather different from that of Griem et al.¹ Our strong collision term is far less important than theirs, perhaps in part because of a different demarcation of the two regimes. However, an important point in favour of the present theory is that the lower impact parameter cut-offs (eqns. (14) - (19)) are completely consistent with the corresponding expression for W_s in eqn. (28).

It appears from the ratios W_m/W_e that we are entirely justified in neglecting the contribution to the broadening from ion perturbers, as is also indicated in Table I. Furthermore, we have not found evidence for the possible importance of (optically) forbidden, or semi-forbidden, collision-induced transitions in accounting in part for earlier discrepancies between measurement and calculation for the multiply-ionized species.^{6,11,13} In fact, the major reason

for the great improvement in the present results over those in Ref. (6) appears to be due mainly to the proper incorporation of effects associated with curvature of the perturber trajectory, as already discussed in Ref. (26).

There has been a certain amount of speculation in the literature^{1,12} on suitable \bar{g} values for the calculation of line widths of multiply charged ions. Accordingly, we have listed in Table V the threshold values calculated from the present theory applied to O(III), for the given collision-induced transitions. The dependence on J, J' is small and has been ignored. We see that the present values are not in accord with the suggested ones in p.273 of Ref. (1). The mean value of $\bar{g} = 0.31 \pm 0.02$ is in fair agreement with that proposed in Ref. (12). It is important to note that our values apply to dipole interactions only, and do not contain contributions from the strong collision term (as in Ref. (7)), which is here added separately to the line width (eqn. (28)).

CONCLUSIONS

Although a great deal of further investigation is clearly required in testing the present model against other experimental data, the following conclusions may be advanced from the present study:

- (1) By suitable incorporation of curvature effects, an analytical Gaunt factor has been derived⁶ which does not require semi-empirical correction at lower energies.

- (ii) The present model appears to be suitable for dealing with ionization stages $Z = 2$ and 3 , and we hope in future to study larger values of Z . For these values of Z , extrapolation of \bar{g} below threshold as a constant is an adequate procedure.
- (iii) Our model represents an improvement in the proposed formula (526) of Ref. (1), also in the sense that explicit allowance can be made for radiator structure effects where necessary, and therefore possible variations within multiplets can be studied.^{18,21}
- (iv) The negative "interference" terms which contribute to the strong collision term¹ appear to be adequately accounted for by assuming that these cancel fully the term corresponding to eqn. (28) for the lower state. The good agreement shown in Tables I and II would not be possible unless this were a good approximation.

We regard conclusions (i) - (iv) as tentative so far, subject to further studies of this kind.

REFERENCES

1. H.R. GRIEM, *Spectral Line Broadening by Plasmas*. Academic Press, New York (1974).
2. N. KONJEVIĆ and W.L. WIESE, *J. Phys. Chem. Ref. Data* 5, 259 (1976).
3. J.R. FUHR, B.J. MILLER and G.A. MARTIN, *Bibliography on Atomic Line Shapes and Shifts (June 1975-June 1978)*, NBS Special Publication 366 Supplement 3. Washington, D.C. (1978).
4. M. PLATIŠA, M.V. POPOVIĆ, and N. KONJEVIĆ, *Astron. Astrophys.* 45, 325 (1975).
5. W.W. JONES, S.M. BENETT and H.R. GRIEM, *University of Maryland Technical Report No. 71-128* (1971).
6. J.D. HEY and R.J. BRYAN, *JQSRT* 17, 221 (1977).
7. H.R. GRIEM, *Phys. Rev.* 165, 258 (1968).
8. H. VAN REGEMORTER, *Astrophys. J.* 136, 906 (1962).
9. M. BLAHA, *Astrophys. J.* 157, 473 (1969).
10. J. DAVIS, *JQSRT* 14, 549 (1974).
11. J.D. HEY, *JQSRT* 17, 729 (1977).
12. J.D. HEY, *JQSRT* 18, 649 (1977).

13. M. DIMITRIJEVIĆ and N. KONJEVIĆ, *JQSRT* 20, 223 (1978).
14. H.R. GRIEM, *Proceedings of the Eighth International Summer School on the Physics of Ionized Gases* (Ed. B. Navinsek, Dubrovnik, 1976) p.699.
15. M.J. SEATON, *Advances Atom. Molec. Phys.* 11, 83 (1975).
16. H.R. GRIEM, *Phys. Rev.* 128, 515 (1962).
17. M.V. POPOVIĆ, M. PLATIŠA and N. KONJEVIĆ, *Astron. Astrophys.* 41, 463 (1975).
18. K. BEHRINGER and P. THOMA, *JQSRT* 20, 615 (1978).
19. J.D. HEY, *JQSRT* 17, 721 (1977).
20. J.D. HEY and M. BLAHA, *JQSRT* 20, 557 (1978).
21. J.D. HEY, *JQSRT* 20, 403 (1978).
22. A. LESAGE, S. SAHAL-BRÉCHOT and M.H. MILLER, *Phys. Rev.* A16, 1617 (1977).
23. W.T. CHIANG and H.R. GRIEM, *Phys. Rev.* A18, 1169 (1978).
24. M.H. MILLER, R.A. ROIG and R.D. BENGTON, *Phys. Rev.* A20, 499 (1979).
25. J.D. HEY, *JQSRT* 18, 425 (1977).
26. J.D. HEY and P. BREGER, *JQSRT* (in press).
27. E. KÄLLNE, L.A. JONES and A.J. BARNARD, *JQSRT* 22, 589 (1979).

28. O. BELY and D. PETRINI, *Astron. Astrophys.* 6, 318 (1970).
29. M. BARANGER, *Phys. Rev.* 112, 855 (1958).
30. M. GAILITIS, *Sov. Phys. JETP* 17, 1328 (1963).
31. M.J. SEATON, *J. Phys. B. : Atom. Molec. Phys.* 2, 5 (1969).
32. O. BELY, *Phys. Rev.* 185, 79 (1969).
33. K.S. BARNES and G. PEACH, *J. Phys. B. : Atom. Molec. Phys.* 3, 350 (1970).
34. O. BELY and H.R. GRIEM, *Phys. Rev.* A1, 97 (1970).
35. D.E. ROBERTS, *Astron. Astrophys.* 6, 1 (1970).
36. D. PETRINI, *Astron. Astrophys.* 9, 392 (1970).
37. C. FLEURIER, S. SAHAL-BRÉCHOT and J. CHAPELLE, *JQSRT* 17, 595 (1977).
38. H.R. GRIEM and K.Y. SHEN, *Phys. Rev.* 122, 1490 (1961).
39. H.R. GRIEM, *Phys. Rev. Lett.* 17, 509 (1966).
40. J.D. HEY, unpublished report, University of Cape Town (1979).
41. M. BARANGER, Ch.12 of *Atomic & Molecular Processes* (Ed. D.R. Bates), Academic Press, New York (1962).
42. H.R. GRIEM, M. BARANGER, A.C. KOLB and G. OERTEL, *Phys. Rev.* 125, 177 (1962).
43. J. COOPER and G.K. OERTEL, *Phys. Rev.* 180, 286 (1969).

44. I.I. SOBEL'MAN, *Introduction to the Theory of Atomic Spectra*. Pergamon Press, Oxford (1972).
45. E.U. CONDON and G.H. SHORTLEY, *The Theory of Atomic Spectra*. Cambridge University Press (1951).
46. C.E. MOORE, *Atomic Energy Levels, Vol.I*. NSRDS-NBS 35, Washington, D.C. (1971).
47. R.L. KELLY and L.J. PALUMBO, *Atomic and Ionic Emission Lines Below 2000 Angstroms*. Naval Research Laboratory, Washington, D.C. (1973).
48. B. WARNER, *Mon. Not. Roy. Astr. Soc.* 139, 273 (1968).
49. D.R. BATES and A. DAMGAARD, *Phil. Trans. Roy. Soc. London (Ser. A)* 242, 101 (1949).
50. G.K. CERTEL and L.P. SHOMO, *Astrophys. J. Suppl.* 16, 175 (1968).
51. H.A. BETHE and E.E. SALPETER, *Quantum Mechanics of One- and Two-Electron Atoms*. Springer-Verlag, Berlin (1957).
52. V.A. ALEKSEEV and E.A. YUKOV, *Opt. Spectrosc. (USSR)* 25, 363 (1968).

Transition Array	Designation	Unshifted λ (\AA) (Air)	W_m (\AA)	W_e (\AA)	$\frac{W_s}{W_e}$ (%)	$\frac{W_{in}}{W_e}$ (%)	$\frac{W_{el}}{W_e}$ (%)	$\frac{W_{ion}}{W_e}$ (%)	χ (%)
$2p^2(^3P)3s-3p$	$^4P_{3/2}^0 - ^4D_{7/2}^0$	4649.1	0.229	0.285 0.366	36.2 28.2	41.1 31.9	22.7 39.9	1.2 1.0	95/95
$2p^2(^3P)3s-3p$	$^4P_{1/2}^0 - ^4P_{3/2}^0$	4317.1	0.219	0.242 0.314	34.5 26.6	41.9 32.3	23.6 41.1	1.5 1.2	96/95
$2p^2(^3P)3s-3p$	$^4P_{1/2}^0 - ^4S_{3/2}^0$	3712.8	0.204	0.189 0.242	32.3 25.1	44.2 34.3	23.5 40.6	2.1 1.7	94/95
$2p^2(^3P)3s-3p$	$^2P_{3/2}^0 - ^2D_{5/2}^0$	4414.9	0.267	0.283 0.360	35.4 27.8	42.3 33.3	22.2 38.9	1.5 1.2	94/95
$2p^2(^3P)3s-3p$	$^2P_{3/2}^0 - ^2P_{3/2}^0$	3973.3	0.227	0.233 0.297	33.5 26.2	43.7 34.3	22.8 39.5	2.0 1.6	94/95
$2p^2(^3P)3p-3d$	$^2S_{1/2}^0 - ^2P_{1/2}^0$	3377.2	0.229	0.211 0.261	23.6 19.1	57.8 46.7	18.6 34.2	5.9 4.8	87/96
$2p^2(^3P)3p-3d$	$^4D_{7/2}^0 - ^4F_{7/2}^0$	4092.9	0.235	0.299 0.371	27.6 22.3	53.4 43.2	18.9 34.5	4.2 3.4	83/95
$2p^2(^3P)3p-4s$	$^4D_{5/2}^0 - ^4P_{3/2}^0$	3138.4	0.339	0.322 0.349	21.6 19.9	68.4 63.2	10.1 16.8	5.2 4.8	93/95
$2p^2(^1D)3s-3p$	$^2D_{3/2}^0 - ^2F_{5/2}^0$	4596.2	0.246	0.260 0.352	34.5 26.7	42.2 32.6	23.3 40.6	1.3 1.0	95/95
$2p^2(^1D)3s-3p$	$^2D_{3/2}^0 - ^2D_{3/2}^0$	4347.4	0.219	0.257 0.330	34.5 26.8	42.5 33.1	23.0 40.1	1.5 1.2	94/95
$2p^2(^1D)3s-3p$	$^2D_{5/2}^0 - ^2P_{3/2}^0$	3912.0	0.225	0.217 0.278	34.7 27.0	42.1 32.8	23.2 40.2	1.9 1.5	95/95
$2p^2(^1D)3p-3d$	$^4P_{3/2}^0 - ^4F_{5/2}^0$	4153.3	0.256	0.315 0.391	23.9 19.3	56.5 45.5	19.5 35.2	4.3 3.4	86/96
$2p^2(^1D)3p-3d$	$^2F_{5/2}^0 - ^2G_{7/2}^0$	4185.5	0.200	0.334 0.411	26.7 21.7	54.6 44.4	12.7 34.0	4.1 3.3	85/95

TABLE I

Comparison between measured (W_m) and calculated (W_e) widths (FWHM) of isolated lines of O(II) from the indicated transition for electron density $N_e = 10^{17} \text{ cm}^{-3}$ and temperature $T = 25900 \text{ }^\circ\text{K}$. The measurements have been taken from Ref. (4). The strong (W_s), inelastic (W_{in}) and elastic (W_{el}) contributions to the width are listed as percentages. The importance of neglected contribution to the broadening from ion perturbers is estimated by W_{ion} . The completeness parameter is denoted by χ . For each case, two sets of results are given: the first obtained by Method I and the second by Method II (see

Transition Array	Designation	Unshifted λ (Å)	W_m (Å)	W_e (Å)	$\frac{W_s}{W_e}$ (%)	$\frac{W_{in}}{W_e}$ (%)	$\frac{W_{el}}{W_e}$ (%)	$\frac{W_{ion}}{W_e}$ (%)	χ (%)	$\frac{W_m}{W_e}$
$2p(^2P^0)3s - 3p$	$^3P_1^0 - ^3D_2$	3754.7	0.146	0.119 0.156	49.5 37.9	30.6 23.4	20.0 38.8	0.5 0.4	91/93	1.23 0.94
$2p(^2P^0)3s - 3p$	$^3P_2^0 - ^3P_2$	3047.1	0.108	0.074 0.098	43.6 32.7	34.3 25.7	22.1 41.6	1.0 0.7	90/93	1.46 1.10
$2p(^2P^0)3p - 3d$	$^3D_2 - ^3F_3^0$	3261.0	0.127	0.098 0.125	45.5 35.6	39.2 30.7	15.2 33.7	1.4 1.1	81/91	1.30 1.02
$2p(^2P^0)3p - 3d$	$^3P_2 - ^3D_3^0$	3715.1	0.142	0.133 0.170	43.3 33.8	40.8 31.9	15.9 34.3	1.2 0.9	83/90	1.07 0.84

TABLE II'

Comparison between measured (W_m) and calculated (W_e) widths (FWHM) of isolated lines of O(III) from the indicated transitions, for electron density $N_e = 10^{17} \text{ cm}^{-3}$ and temperature $T = 25900 \text{ }^\circ\text{K}$. The measured values have been obtained from Ref. (4). The strong (W_s), inelastic (W_{in}) and elastic (W_{el}) contributions to the width are listed as percentages. The importance of the neglected contribution to the broadening from ion perturbers is estimated by W_{ion} . The completeness parameter is denoted by χ . For each case, two sets of results are given: the first obtained by Method I and the second by Method II (see text).

Transition Array	Designation	Unshifted λ (Å) (Air)	W_e (Å) (I)	W_e (Å) (II)	W_e (Å) (JBG)	W_e (Å) (HB)	W_m (Å)
$2p^2 ({}^3P) 3s - 3p$	${}^4F_{5/2} - {}^4D_{7/2}^0$	4649.1	0.285	0.366	0.338	0.180	0.22
$2p^2 ({}^3P) 3s - 3p$	${}^4P_{1/2} - {}^4F_{3/2}^0$	4317.1	0.242	0.314	0.238	0.158	0.21
$2p^2 ({}^3P) 3s - 3p$	${}^4P_{1/2} - {}^4S_{3/2}^0$	3712.8	0.189	0.242	-	0.125	0.20
$2p^2 ({}^3P) 3s - 3p$	${}^2P_{3/2} - {}^2D_{5/2}^0$	4414.9	0.283	0.360	0.291	0.193	0.26
$2p^2 ({}^3P) 3s - 3p$	${}^2P_{3/2} - {}^2P_{3/2}^0$	3973.3	0.233	0.297	0.227	0.165	0.22
$2p^2 ({}^3P) 3p - 3d$	${}^2S_{1/2}^0 - {}^2P_{1/2}$	3377.2	0.211	0.261	0.196	0.165	0.22
$2p^2 ({}^3P) 3p - 3d$	${}^4D_{7/2}^0 - {}^4F_{7/2}$	4092.9	0.299	0.371	0.277	0.221	0.23
$2p^2 ({}^3P) 3p - 4s$	${}^4D_{5/2}^0 - {}^4P_{3/2}$	3138.4	0.322	0.349	0.445	0.290	0.33
$2p^2 ({}^1D) 3s - 3p$	${}^2D_{3/2} - {}^2P_{5/2}^0$	4596.2	0.280	0.362	-	0.182	0.24
$2p^2 ({}^1D) 3s - 3p$	${}^2D_{3/2} - {}^2D_{3/2}^0$	4347.4	0.257	0.330	-	0.166	0.21
$2p^2 ({}^1D) 3s - 3p$	${}^2D_{5/2} - {}^2P_{3/2}^0$	3912.0	0.217	0.278	-	0.141	0.22
$2p^2 ({}^1D) 3p - 3d$	${}^4P_{3/2}^0 - {}^4P_{5/2}$	4153.3	0.315	0.391	0.283	0.246	0.25
$2p^2 ({}^1D) 3p - 3d$	${}^2F_{5/2}^0 - {}^2G_{7/2}$	4185.5	0.334	0.411	-	0.222	0.20

TABLE III

Comparison between the electron impact widths calculated by Methods I and II (see text) for the indicated O(II) line with the corresponding values (where given) calculated by Jones, Benett and Griem (JBG) in Refs. (1), (5) and by Hey and Bryan (HB) in Ref. (6). The measured widths (W_m) from Ref. (4) are also given. The plasma conditions are as in Table I and Table II.

Transition Array	Designation	Unshifted λ (Å) (Air)	W_e (Å) (I)	W_e (Å) (II)	W_e (Å) (HB)	W_m (Å)
$2p(^2P^0)3s - 3p$	$^3P_1^0 - ^3D_2$	3754.7	0.119	0.156	0.076	0.146
$2p(^2P^0)3s - 3p$	$^3P_2^0 - ^3P_2$	3047.1	0.074	0.098	0.053	0.108
$2p(^2P^0)3p - 3d$	$^3D_2 - ^3F_3^0$	3261.0	0.098	0.125	0.064	0.127
$2p(^2P^0)3p - 3d$	$^3P_2 - ^3D_3^0$	3715.1	0.133	0.170	0.090	0.142

278

TABLE IV

Comparison between the electron impact widths calculated by Methods I and II (see text) for the indicated O(III) lines, with the corresponding values calculated by Hey and Bryan (HB) in Ref. (6). The measured widths (W_m) from Ref. (4) are also given. The plasma conditions are as in Table I and Table II.

Transition	\bar{g}		
	3s - 3p	3s - 4p	4s - 3p
ns $^3P^0$ - np 3S	0.236	0.402	
- np 3P	0.235	0.444	0.335
- np 3D	0.238	0.389	0.350
	3p - 3d	3p - 4d	4p - 3d
np 3P - nd $^3P^0$	0.248		
- nd $^3D^0$	0.250	0.363	0.335
np 3D - nd $^3D^0$	0.252		0.320
- nd $^3F^0$	0.253	0.366	0.328

TABLE V

Effective Gaunt factors for several collision-induced transitions in O(III). The values of \bar{g}_{th} apply to electron perturbers incident at threshold energy.

Appendix III: Hey and Breger (1980c)

CALCULATED STARK WIDTHS OF ISOLATED
S(III) AND S(IV) LINES

JOHN D. HEY and PETER BREGER

Department of Physics
University of Cape Town
Rondebosch 7700, Cape
South Africa

ABSTRACT

Calculations have been performed on the electron impact broadening of isolated lines from doubly-ionized and triply-ionized sulphur emitted from a plasma of electron density 10^{17} cm^{-3} and temperature $28500 \text{ }^\circ\text{K}$. These have been compared with results of measurements performed by Platiša, Popović, Dimitrijević and Konjević on a low pressure pulsed arc. Good overall agreement has been obtained for both ionization stages, in confirmation of our earlier conclusions based on a similar comparison for oxygen ion lines. The present calculations have been compared with calculations based upon two simplified models of Griem, and the classical-path approximation of Sahal-Bréchet. Our calculated widths are in better agreement with experiment than with values obtained from the first two models; for the two multiplets where comparison is possible, good agreement is found with the widths obtained by Sahal-Bréchet. We conclude that the present model whereby the effective Gaunt factor is calculated, is capable of predicting reliable values for the Stark widths of isolated ion lines. Comparison with experiment (for S(III)) indicates that, provided a sufficiently complete set of perturbing levels is used in the calculations, the present formula for \bar{g} may also be used for below-threshold energies in the determination of the elastic contribution to the broadening. For S(IV), an ambiguity remains in this regard, owing chiefly to a scarcity of available experimental data.

INTRODUCTION

In a recent study of the Stark broadening of isolated lines emitted by singly- and doubly-ionized oxygen¹, it was found that very good agreement on the whole was obtained between the calculated line widths and the results of measurements performed on a pulsed arc plasma by Platiša et al.² The comparison was interpreted as support for a recently derived expression³ for the effective Gaunt factor in line broadening calculations, notably in the range of above-threshold perturber energies. For below-threshold energies, relevant for the calculation of the elastic contributions to the broadening,⁴⁻⁶ some ambiguity remained¹ as to the direct applicability of the formula.³

In view of the present scarcity of reliable theoretical data⁷ for comparison with measurements of the widths of isolated ion lines from multiply-charged emitters,⁸ our intention is to continue the present programme^{1,3,9} aimed at developing a reliable semiclassical technique for such computations, of accuracy comparable with that of the earlier work on singly-charged ions by Jones, Bennett and Griem^{10,11} (JBG). The value of this work lies in the increasing importance of the spectra from multiply-charged ions for the study of dense, hot astrophysical and laboratory plasmas.^{10,12}

The recent measurements performed by Platiša et al.¹³ of the Stark broadening of isolated lines from doubly- and

281

triply-ionized sulphur are of particular interest for two reasons. Firstly, S(III) and O(III) ions are homologous, and therefore trends and regularities occurring in the oscillator strengths¹⁴ of the two atomic systems can be expected to play a similar role in the Stark broadening of their respective spectra.^{15,16} Therefore, it would seem reasonable to suppose that the good agreement reported earlier between theory¹ and measurement² for O(III) should be found similarly in the present case. Secondly, comparison between the recent results¹³ for S(III) and S(IV) and theoretical widths derived from the semi-empirical¹⁷ (SE) and simplified semiclassical¹⁸ (SC) formulae of Griem (see eqn. (526) of Ref.(10)) have yielded agreement far inferior to that generally reported for the spectra of the singly-charged ions^{10,11}. For S(III), the ratios of measured (W_m) to calculated (W_e) electron impact widths (FWHM) were reported as:¹³

$$\frac{W_m}{W_e}(\text{SE}) = 1.67 \pm 0.05$$

$$\frac{W_m}{W_e}(\text{SC}) = 0.74 \pm 0.04 ,$$

for sixteen lines from eight multiplets. In contrast, the classical-path calculations of Sahal-Bréchet¹⁷ (SB) for multiplet nos. (4) and (5) are found to yield (after appropriate wavelength scaling and correction for temperature) excellent agreement with experiment:

$$\frac{W_m}{W_e}(\text{SB}) = 0.90 \pm 0.03 ,$$

for four lines where comparison is possible. (This accuracy is indeed comparable with that claimed for the JBG calculations.¹¹)

Now the various difficulties connected with the use of the semi-empirical approximation of Griem¹⁷ have been discussed in detail by one of us.^{7,16,19} These are (mainly) the lack of reliable threshold values for \bar{g} and (often) the oversimplification of the radiator structure. While the latter can be corrected for by incorporation of the appropriate coupling scheme for the bound electrons,^{16,20,21} improvement in the \bar{g} values requires a different approach to the problem.^{1,3,9} In the later semiclassical model of Griem¹⁰ (see eqn.(526) of Ref.(10)), the \bar{g} values are improved semi-empirically, but the structural details of the radiator system are again omitted. In this equation, in addition, the effects of curvature of the perturber trajectory are not properly accounted for; allowance for such effects is vital for the derivation of an analytical formula for \bar{g} .^{1,3}

The aims of the present paper are the following:

- (i) to test the hypothesis regarding similarities in the Stark broadening of homologous radiators¹⁵;
- (ii) to show that the \bar{g} formula obtained recently³ is reliable for species with charge $(Z-1) \geq 2$;
- (iii) to elucidate further the nature of the elastic contributions to the broadening, thereby testing the applicability of the \bar{g} formula³ below threshold.

203

THEORY

Our calculations are based upon the following expression^{2,1} obtained from the Baranger⁴ theory of electron impact broadening:

$$W_e^{if} = \frac{\alpha \lambda^2 a_0^2}{\sqrt{\pi}} N_e \left(\frac{E_H}{kT} \right)^{1/2} \left\{ \sum_{i'} \frac{\langle \Omega(i, i') \rangle}{\tilde{\omega}_i} + \sum_{f'} \frac{\langle \Omega(f, f') \rangle}{\tilde{\omega}_f} \right\}. \quad (1)$$

The line width (FWHM) is expressed in wavelength (λ) units in terms of perturber concentration (N_e) and temperature (T) as a summation over the various collisional processes (strength Ω) which are responsible for the broadening. The spectral line λ corresponds to a radiative transition between level i (statistical weight $\tilde{\omega}_i$) and level f (statistical weight $\tilde{\omega}_f$); the collisional processes depend upon the location in the term scheme for the radiator of the various "perturbing" levels i' and f' to which collision-induced transitions from i and f can occur.

The average indicated in parentheses denotes³

$$\langle \Omega(i, i') \rangle = \int_{z_{i',i}}^{\infty} \Omega(i, i') \exp(-z) dz \quad (2)$$

in the case of inelastic collisions ($E_{i'} - E_i > 0$), and

$$\langle \Omega(i, i') \rangle = \int_0^{\infty} \Omega(i, i') \exp(-z) dz \quad (3)$$

in the case of superelastic collisions ($E_{i'} - E_i < 0$), where the parameters $z, z_{i',i}$ are given in terms of the incident electron speed (v) by

$$z = \frac{mv^2}{2kT} \quad \text{and} \quad z_{i',i} = \frac{\Delta E_{i',i}}{kT},$$

with $\Delta E_{i',i} = |E_{i'} - E_i|$.

The elastic contributions to the broadening⁴ are now simply incorporated by extrapolating the inelastic terms in eqn. (2) below threshold,^{5,6} i.e. by replacing $z_{i',i}$ in eqn. (2) by zero. There is some ambiguity,^{2,2} however, as to the form of Ω applicable in the classical-path calculations to below-threshold energies, since this is dependent upon the nature of resonances whose properties should be studied quantum mechanically.^{2,3} (It is interesting to compare results obtained by the use of two different semiclassical corrections for resonances in Ref. (22)).

We now go over to a semiclassical formulation in which only direct collision (i.e. non-exchange) contributions are retained, and of these we consider explicitly only the dipole terms. In that case,^{2,4}

$$\Omega(i, i') = \frac{8\pi}{3^{3/2}} \bar{g}(i, i') \frac{S(J, J')}{a_0^2 e^2} \quad (4)$$

where \bar{g} denotes the effective Gaunt factor and $S(J, J')$ the atomic line strength.

The derivation³ of a quasi-classical expression for \bar{g} has been outlined in Ref. (1). In terms of incident perturber energy, the parameters

$$x = \sqrt{\frac{\frac{1}{2}mv^2}{\Delta E_{i',i}}}, \quad y = \sqrt{\frac{E_H}{\Delta E_{i',i}}}$$

enable \bar{g} for an ion of charge $(Z-1)$ to be written as

$$\bar{g} = \frac{\sqrt{3}}{2\pi} \ln \left[\frac{1 + \frac{4x^6}{(Z-1)^2 y^2} \phi^4}{1 + \frac{x^2}{(Z-1)^2 y^2} \left[1 + d_{i',i}^2 \left(1 + \frac{x^2}{y^2} + \frac{2(Z-1)}{d_{i',i}} \right) - \frac{(Z-1)^2 y^2}{x^2} \right]} \right] \quad (5)$$

$$\bar{g} = \frac{\sqrt{3}}{2\pi} \ln \left[\frac{1 + \frac{4x^6}{(Z-1)^2 y^2} \phi^4}{1 + \frac{x^2}{(Z-1)^2 y^2} \left[1 + d_{i',i}^2 \left(\frac{x^2}{y^2} + \frac{2(Z-1)}{d_{i',i}} \right) \right]} \right] \quad (6)$$

where the latter expression replaces the former in the low energy region

$$x^2 \lesssim (Z-1)^2 y^2 / d_{i',i}^2 \quad (7)$$

The curvature correction factor ϕ obeys the cubic equation

$$\phi^3 - \phi - (Z-1)y/x^3 = 0 \quad (8)$$

and $d_{i',i}$ is related to the dipole moment of the atomic system by²⁵

$$d_{i',i} = \left[\frac{1}{3} \frac{\lambda_{ij}}{2l+1} R_{i',i}^2 \right]^{1/2} \quad (9)$$

The additional contribution to the broadening from strong collisions¹⁰ which are not explicitly accounted for by eqns.(4)-(6), is given by (FWHM, in wavelength units)

$$W_s = \frac{2}{\sqrt{\pi}} \alpha \lambda^2 a_0^2 N_e \left(\frac{E_H}{kT} \right)^{1/2} \left[1 + 2(Z-1) \bar{d}_{i',i} + \left(1 + \frac{kT}{E_H} \right) \bar{d}_{i',i}^2 \right] \quad (10)$$

The bar denotes an average over the various collision-induced transitions $|i\rangle \rightarrow |i'\rangle$ which contribute to the line width. As discussed in Ref.(1), only the collision-induced transitions

associated with the upper state of the line are included in W_s , and this width is added to the dipole contribution from eqns. (4)-(6) to make up the electron impact width W_e .

The contribution to the broadening from ion perturbers should be very small.¹⁰ In order to verify this, the simplified formula¹⁰ applicable to quadrupole interactions has been applied to each line. This may be written (FWHM, in wavelength units)

$$W_i^q = \frac{2\alpha \lambda^2 a_0^2}{Z^2} \sum_p N_p Z_p \left(n_i^{*2} - n_f^{*2} \right)^2 \quad (11)$$

where N_p and $Z_p e$ are the perturber concentration and charge, respectively. The n_i^* , n_f^* are effective principal quantum numbers for the upper and lower levels. The condition of quasi-neutrality in the plasma enables one to substitute above

$$N_e = \sum_p N_p Z_p \quad (12)$$

Perturber correlations are not explicitly included in the present calculation. In all cases, the impact parameter cut-offs for perturber trajectories^{1,3} lie well within the Debye radius. [Equivalently, $\Delta E_{i',i} \gg \hbar \omega_p$, where ω_p is the electron plasma frequency.] The use of such cut-offs therefore justifies the approximation of isolated lines broadened by impact of unshielded perturbers²⁶.

RADIATOR STRUCTURE

As mentioned above, the ions S(III) and O(III) (for which calculations have recently been performed¹) are homologous. The present study therefore involves the computation of rather similar collision-induced transitions to those in Ref.(1). In the present case, a major difficulty was, however, the absence of several terms of importance from the atomic energy level tables.²⁷ The missing levels could be supplemented from the paper of Dynefors and Martinson,²⁸ from which we obtained the levels $3d^3 F_4^0$, $3d^3 F_3^0$ and $4d^3 P_2^0$ of S(III). In the latter case, the remaining members of the term were taken to have the same energy on the basis of the discussion given on pp.200,201 of Ref.(29). The terms $5p^3 S$, $5p^3 P$, $5p^3 D$, $4f^3 D$, $4f^3 F$, $4f^3 G$ of the same ion were located by simple quantum defect estimates.²⁹ In the case of S(IV), the level $5p^2 P_{3/2}$ was obtained from Ref.(28) and the position of the other member of the doublet derived by simple scaling of the spin-orbit coupling parameter with effective principal quantum number.²⁹ The values of the respective ionization energies were taken from Ref.(30).

In spite of the incompleteness of the term system as listed,^{27,28} one can easily see that configuration interaction is present in S(III), as also in O(III). For example, in the case of the $3p\ 3d$ configuration, the term splitting occurs in the ratio

$$\frac{(P - F)}{(F - D)} = 7.66$$

as compared with the theoretical value²⁹ derived for pure-configuration, LS coupling, of 0.55, indicating appreciable perturbation of the $3p\ 3d\ ^3P^0$ and $3p\ 3d\ ^3D^0$ terms by the corresponding terms in the $3s\ 3p^3$ configuration. (In the case of O(III), the corresponding value of the term splitting parameter for the $2p\ 3d$ configuration is 1.30.) It should, however, be noted that in all cases of interest, $\Delta E_{i,i}$ and $\Delta E_{f,f}$ are appreciable compared with kT . Therefore, the relevant Gaunt factors do not greatly exceed their threshold values, and in view of the sum rules that come into play for the line strengths,^{25,29} one can conveniently ignore the possibility of mixing of the pure-configuration, LS coupled wave functions for both S(III) and S(IV).

For S(IV), the last statement may seem paradoxical in view of the discussion in Ref.(9) of the importance of accounting for configuration mixing in the case of the ion Sn(II), to which it has qualitative structural similarities. In the latter case, it was necessary to allow for mixing of the wave functions corresponding to the terms denoted by $5p^2\ ^2D$ and $5d\ ^2D$ in order to compute correctly the excitation rate from the $6p\ ^2P^0$ levels.⁹ The corresponding terms in S(IV) would be those denoted by $3p^2\ ^2D$, $3d\ ^2D$ and $4p\ ^2P^0$. With the term energies represented by their designation,²⁹ the following two parameters show the important quantitative difference to be expected from the effects of configuration mixing in the two ions:

$$\frac{4p\ ^2P^0 - 3p^2\ ^2D}{4p\ ^2P^0 - 3d\ ^2D} = 1.943 \quad [S(IV)]$$

and

$$\frac{6p^2 p^0 - 5p^2 {}^2D}{6p^2 p^2 - 5d^2 {}^2D} = 44.07 [\text{Sn(II)}] .$$

It is in details of this kind that the expectation of trends and regularities on the basis of homologous structure^{14,15} can be misleading. In the final analysis, each particular atomic system must be treated as a unique structure.

Lastly, it should be pointed out that it was necessary in certain lines to consider the ground term system explicitly among the perturbing levels. Since this contains two equivalent active electrons, some modification was required of the "usual" expression for the line strength applicable to transitions involving a single electron. From Sobel'man²⁵ one readily derives the appropriate relation for the corresponding (emission) oscillator strength as

$$f(3p\ 3d + 3p^2) = \frac{5}{6} f(3d + 3p) .$$

RESULTS

In Table I, results of our calculations are presented for the electron impact widths of all spectral lines of S(III) and S(IV) whose widths have been measured by Platiša et al.¹³ In the calculation of the line strengths occurring in eqn.(4), the LS coupling scheme has been adopted, and the radial integrals occurring in the dipole matrix elements have been calculated by the Coulomb approximation,^{31,32} which we expect to be sufficiently accurate in all cases except that discussed at the end of the previous section. This case yields, however, only a minor contribution to the line width.

After each transition are listed in order: the measured width (W_m , FWHM), two values of the electron impact width (W_e) calculated by the present theory applied in two ways (see below); the fractional contribution to the line width from strong collisions (W_s/W_e) expressed as a percentage; the fractional contribution to the line width from the inelastic part of the weak (i.e. non-strong) interactions (W_{in}/W_e) expressed as a percentage; the fractional contribution from the elastic part of the weak interactions (W_{el}/W_e) expressed as a percentage. These three percentages should thus in all cases add up to unity.

The next column gives an estimate of the importance of the neglected contribution to the broadening from ion perturbers also in percent, as calculated from eqn.(11). Next is given the completeness parameter (χ) reduced to percent, which

indicates the degree of completeness of the subset of perturbing levels actually employed in the calculation. This parameter is calculated (also in the Coulomb approximation^{31,32}) from the reduced matrix elements^{25,29}

$$\chi = \frac{1}{2J+1} \frac{\sum_{i'} \left| \langle i' | \frac{r}{a_0} | i \rangle \right|^2}{(R_{n\ell})^2} \quad (13)$$

where $R_{n\ell}$ is given in terms of the effective principal quantum number (n^*) and orbital angular momentum (ℓ) of the radiating electron (coordinate r) by²⁹

$$(R_{n\ell})^2 = \frac{n^{*2}}{2Z^2} [5n^{*2} + 1 - 3\ell(\ell+1)] \quad (14)$$

for an ion of charge $(Z-1)$. The first value of χ in each row applies to the perturbing levels for the upper state, the second to perturbing levels for the lower state.

As discussed in an earlier paper on oxygen ion lines,¹ the major problem pertaining to the present model concerns the elastic contribution⁴ to the broadening, which is in theory accounted for by extrapolation of the effective Gaunt factors into the range of below-threshold energies.^{5,6} The proper choice of analytical continuation of the \bar{g} function employed here into the domain of below-threshold energies is not directly obtainable from our semiclassical derivation.³ In our previous study,¹ two appreciably different methods of extrapolation were chosen; however, owing mainly to the limited amount of data available, comparison with experimental results did not yield an unambiguous answer as to the more suitable approximation.

In an endeavour to resolve this question, both methods have again been employed. In the first, eqn.(5) or (6) is simply employed in the given form for below-threshold energies, the Maxwellian average in eqn.(2) being cut off at the value

$$z_{\min} = \frac{mv^2}{2kT}$$

such that $\bar{g} = 0$, this point being solved for numerically (Method I). In the second method, the threshold value \bar{g}_{th} is employed for all $0 \leq z \leq z_{1,i}$, as proposed by Griem¹⁷ (Method II).

The inelastic contribution to the broadening (W_{in}) thus consists of the sum of (2) and (3) for all inelastic plus superelastic collision-induced transitions. The elastic contribution is obtained from the Maxwellian sum of all integrals of the type

$$\int_{z_{\min}}^{z_{1,i}} \Omega(i,i') \exp(-z) dz \quad ,$$

using either Method I or Method II.

Some of the threshold values of \bar{g} for S(III), obtained from the present theory, are listed in Table III and Table IV. These values contain no contribution from strong collisions. It may be of interest to compare them with the corresponding threshold values tabulated in Ref.(1) for the homologous ion O(III). In the present calculation, it was found that while curvature of the perturber trajectory plays an important role, the \bar{g} values are relatively insensitive to the accuracy with which interpolation is applied to the tabulated Bates-Damgaard

factors^{11,12} occurring in the radial integrals. This tends to enhance the accuracy of our tabulated \bar{g} values.

DISCUSSION

The present results for the widths of isolated lines from S(III) and S(IV) are compared in Table II with values computed¹³ by the semi-empirical approximation of Griem¹⁷ and the later semi-classical approximation of Griem¹⁰ [Eqn.(526) of Ref.(10)]. In addition, four electron impact widths calculated by Sahal-Bréchet¹⁸ have been included, after appropriate correction for the actual plasma conditions applicable to the measurements. The latter values are found to lie between those calculated by Methods I and II, and compare very favourably with experiment, except that they are systematically larger than the experimental values. This would in itself not be too serious, except for the fact that Sahal-Bréchet has calculated rather larger contributions to the broadening (by a factor ~ 2 or more) from ion perturbers than our simple estimates suggest.

Some criticism of the semi-empirical¹⁷ and semi-classical approximation [Ref.(10), eqn.(526)] has been outlined in earlier papers^{7,9}. The major points of disagreement concerned the omission of details of the radiator structure, and more seriously the question of reliability of the \bar{g} values proposed in these works, particularly for ionization stages $Z \geq 3$. In the present work, our calculated widths showed in general the same trends within multiplets as the measured values. This provided a

useful check that the accuracy claimed for the experimental line widths (errors within $\pm 18\%$) was a safe if conservative margin of error. The experimental errors involved in the plasma diagnostics,¹³ have not been included in our comparison.

In Table V, the overall comparison is presented between the average ratios of measured (W_m) to calculated (W_e) line widths as obtained from the various theoretical approaches. Both methods discussed in this paper are strongly favoured above the calculated values from Ref.(13). In attempting to decide between Method I and Method II, one should note that completeness of the set of perturbing levels (χ) appears to play some role in the choice. For those lines of S(III) involving higher values of χ , Method I tends to be favoured. [In the earlier case of O(III), the amount of data was insufficient to enable this choice to be made.¹]

Since only one line width from the spectrum of S(IV) was measured, no firm conclusions can be drawn for this ion except to note that our two calculated values again agree rather better with experiment than those from Ref.(13).

As far as the effective Gaunt factors in Tables III and IV are concerned, we have again found as in Ref.(1) poor agreement with the values proposed on p.273 of Ref.(10). In particular, we do not obtain threshold values for $\Delta n = 0$ transitions that are systematically appreciably larger than the values for $\Delta n \neq 0$ transitions.

Lastly, it will be noted that our assessment of the percentage contribution to the broadening from strong collisions, while similar to that found in Ref.(1), is appreciably smaller than that calculated in most cases by both Griem¹⁰ and Sahal-

288

Bréchet.¹⁸ On the one hand, this appears not to be too serious since our choice of lower impact parameter cut-off is completely consistent³ with the calculation of W_s . On the other hand, this may simply be due to a different demarcation¹ between the "strong" and "weak" regimes used in these models. It would be interesting in the future to examine this question in more detail.

CONCLUSIONS

The conclusions reached from the present study tend to confirm in large measure the findings in Ref.(1), and provide additional insight into the proper treatment of the elastic contributions to the broadening. Subject to confirmation from further investigations in testing the present model against other experimental data, we advance the following:

- (i) The analytical Gaunt factor derived earlier¹ by suitable incorporation of curvature effects, can be used for accurate computation of the Stark widths of isolated lines emitted by ions up to ionization stage $Z = 3$ with confidence, and tentatively up to $Z = 4$.
- (ii) Where good statistics are available for comparison purposes, the experimental results indicate a preference for calculations in which the elastic contributions to the broadening are determined by application of the \bar{q} formula without modification in the regime of below-threshold energies (Method I). However, extrapolation of the \bar{q} factors below threshold as a constant (Method II) appears an adequate procedure, in the sense that the widths obtained are still more accurate than those predicted by the semi-empirical¹⁷ or semi-classical (Ref.(10), eqn.(526)) approximations.

- (iii) Explicit allowance for details of the radiator structure (details of angular momenta of the bound electrons and precise energies of individual levels) is a useful procedure, in that the confirmation of measured variations of line widths within multiplets lends confidence in both the precision of theory and the accuracy of experiment.
- (iv) The negative "interference" terms which contribute to the strong collision term¹ appear to be adequately accounted for by assuming that these cancel fully the term corresponding to eqn.(10) for the lower state of the line. The good agreement shown in Table I would not be possible unless this were a good approximation.
- (v) The actual importance of the contribution to the broadening from ion perturbers is difficult to assess from the present comparison between theory and experiment, in the sense that of the various theories compared in Table II and Table V, a greater number predict systematically larger widths on the basis of electron impact broadening alone, than were measured in Ref.(13). In the case of the first version of the present theory (Method I), however, an additional contribution of some - 3% from ion perturbers could be suggested to account for the remaining discrepancies between theory and experiment. While this seems a reasonable order of magnitude, it cannot nevertheless be proposed with confidence since rather larger errors could be ascribed to both the experiment¹³ (from the line width determination as well as the diagnostics) and certain aspects of the theory as discussed above.

REFERENCES

1. J.D. HEY and P. BREGER, *JQSRT* (to be published).
2. M. PLATIŠA, M.V. POPOVIĆ and N. KONJEVIĆ, *Astron. Astrophys.* 45, 325 (1975).
3. J.D. HEY, Unpublished report, University of Cape Town (1979).
4. M. BARANGER, *Phys. Rev.* 112, 855 (1958).
5. M. GAILITIS, *Sov. Phys. J.E.T.P.* 17, 1328 (1963).
6. O. BELY, *Phys. Rev.* 185, 79 (1969).
7. J.D. HEY, *JQSRT* 18, 649 (1977).
8. M. DIMITRIJEVIĆ and N. KONJEVIĆ, *JQSRT* 20, 223 (1978).
9. J.D. HEY and P. BREGER, *JQSRT*, (in press).
10. H.R. GRIEM, *Spectral Line Broadening by Plasmas*. Academic Press, New York (1974).
11. W.W. JONES, *Phys. Rev.* A7, 1826 (1973).
12. E. KÄLLNE, L.A. JONES and A.J. BARNARD, *JQSRT*, 22, 589 (1979).
13. M. PLATIŠA, M. POPOVIĆ, M. DIMITRIJEVIĆ and N. KONJEVIĆ, *JQSRT*, 22, 333 (1979).

14. W.L. WIESE, M.W. SMITH and B.M. MILES, *Atomic Transition Probabilities*, Vol.II, NSRDS-NBS 22, Washington, DC (1969).
15. J. PURIĆ, L. ĆIRKOVIĆ and J. LABAT, *Fizika* 6, 211 (1974).
16. J.D. HEY, *JQSRT*, 17, 721 (1977).
17. H.R. GRIEM, *Phys. Rev.* 165, 258 (1968).
18. S. SAHAL-BRÉCHOT, *Astron. Astrophys.* 2, 322 (1969).
19. J.D. HEY, *JQSRT*, 18, 425 (1977).
20. J.D. HEY, *JQSRT*, 20, 403 (1978).
21. J.D. HEY and M. BLAHA, *JQSRT*, 20, 557 (1978).
22. C. FLEURIER, S. SAHAL-BRÉCHOT and J. CHAPELLE, *JQSRT*, 17, 595 (1977).
23. M.J. SEATON, *J. Phys. B.: Atom. Molec. Phys.*, 2, 5 (1969).
24. M.J. SEATON, *Atomic and Molecular Processes*, Chapter 11, (Edited by D.R. Bates). Academic Press, New York (1962).
25. I.I. SOBEL'MAN, *Introduction to the Theory of Atomic Spectra*. Pergamon Press, Oxford (1972).
26. M. BARANGER, *Atomic and Molecular Processes*, Chapter 13 (Edited by D.R. Bates). Academic Press, New York (1962).

290

27. C.E. MOORE, *Atomic Energy Levels Vol.I*, NSRDS-NBS 35, Washington, DC (1971).
28. B.I. DYNEFORS and I. MARTINSON, *Physica Scripta* 17, 123 (1978).
29. E.U. CONDON and G.H. SHORTLEY, *The Theory of Atomic Spectra*. Cambridge University Press (1951).
30. R.L. KELLY and L.J. PALUMBO, *Atomic and Ionic Emission Lines below 2000 Angstroms*. Naval Research Laboratory Washington, DC (1973).
31. D.R. BATES and A. DAMGAARD, *Phil. Trans. Roy. Soc. London (Ser.A)* 242, 101 (1949).
32. G.K. OERTEL and L.P. SHOMO, *Astrophys. J. Suppl.* 16, 175 (1968).

TABLE I Comparison between measured (W_m) and calculated (W_e) widths (FWHM) of isolated lines of S(III) and S(IV) from the indicated transitions, for electron density $N_e = 10^{17} \text{ cm}^{-3}$ and temperature $T = 28500 \text{ K}$. The measurements have been taken from Ref. 13. The strong (W_s), inelastic (W_{in}) and elastic (W_e) contributions to the width are listed as percentages. The importance of the neglected contribution to the broadening from ion perturbers is estimated by W_{ion} . The completeness parameter is denoted by χ . For each case, two sets of results are given: the first obtained by Method I and the second by Method II (see the text).

Ion	Transition Array	Designation	Unshifted $\lambda(\text{\AA})$ (Air)	$W_m^o(\text{\AA})$	$W_e^o(\text{\AA})$	$\frac{W_s}{W_e}(\%)$	$\frac{W_{in}}{W_e}(\%)$	$\frac{W_{el}}{W_e}(\%)$	$\frac{W_{ion}}{W_e}(\%)$	$\chi(\%)$	$\frac{W_m}{W_e}$	
S(III)	3p(² P ^o)3d - 3p 4p	³ P ₂ ^o - ³ P ₁	3370.4	0.149	0.131 0.162	43.4 35.0	41.7 33.6	14.8 31.3	1.5 1.2	99/58	1.14 0.92	
		¹ P ₁ ^o - ¹ P ₀	3387.1	0.151	0.132 0.163	43.3 34.9	41.8 33.7	14.9 31.4	1.5 1.2	99/58	1.14 0.93	
		³ D ₃ ^o - ³ P ₂	3928.6	0.173	0.182 0.226	42.1 33.9	42.7 34.3	15.2 31.8	1.2 0.9	98/66	0.95 0.77	
		¹ D ₂ ^o - ³ P ₁	3983.8	0.169	0.188 0.233	42.3 34.0	42.6 34.3	15.1 31.6	1.1 0.9	99/66	0.90 0.73	
	3p(² P ^o)4s - 3p 4p	³ P ₁ ^o - ³ D ₁	4332.7	0.245	0.237 0.300	37.9 29.9	42.9 33.9	19.2 36.2	0.8 0.7	92/94	1.03 0.82	
		³ P ₂ ^o - ³ D ₂	4361.5	0.24	0.238 0.302	37.4 29.4	43.2 34.0	19.4 36.6	0.8 0.7	92/94	1.04 0.82	
		¹ P ₁ ^o - ³ P ₁	3832.0	0.198	0.202 0.253	36.3 29.0	45.5 36.4	18.2 34.5	1.0 0.8	99/94	0.98 0.78	
		³ P ₂ ^o - ³ P ₁	3899.1	0.192	0.209 0.262	36.3 29.0	45.5 36.4	18.2 34.6	1.0 0.8	99/94	0.92 0.73	
		³ P ₁ ^o - ³ S ₁	3662.0	0.182	0.185 0.232	37.2 29.7	44.1 35.2	18.6 35.1	1.1 0.9	98/94	0.98 0.78	
		3p(² P ^o)4p - 3p 4d	¹ D ₁ - ³ F ₃ ^o	2856.0	0.206	0.192 0.221	34.7 30.2	53.5 46.5	11.8 23.3	3.2 2.8	89/92	1.07 0.93
			³ D ₃ - ³ F ₃ ^o	2863.5	0.202	0.199 0.228	35.3 30.9	53.3 46.6	11.4 22.5	3.1 2.7	88/91	1.02 0.85
			³ D ₁ - ³ F ₂ ^o	2872.0	0.200	0.188 0.217	33.8 29.2	53.9 46.7	12.3 24.1	3.2 2.8	89/92	1.06 0.92
	³ D ₁ - ³ D ₁ ^o		2718.9	0.202	0.171 0.196	30.1 26.2	58.1 50.7	11.8 23.1	3.7 3.2	87/92	1.18 1.03	
		³ D ₃ - ³ D ₃ ^o	2756.9	0.206	0.184 0.209	31.9 28.0	56.9 49.9	11.2 22.1	3.5 3.1	87/91	1.12 0.99	
		³ P ₁ - ³ D ₂ ^o	2950.2	0.210	0.213 0.244	29.8 26.1	58.8 51.5	11.4 22.5	3.1 2.7	87/99	0.99 0.86	
		³ P ₂ - ³ D ₁ ^o	2964.8	0.212	0.221 0.251	30.7 26.9	58.2 51.1	11.1 22.0	3.1 2.7	87/98	0.96 0.84	
S(IV)		3s ² (³ S)4s - 3s ² 4p	² S _{1/2} - ² P _{1/2} ^o	3097.5	0.116	0.102 0.130	51.4 40.3	31.4 24.6	17.2 35.0	0.7 0.5	97/96	1.14 0.89

TABLE II

Comparison between the electron impact widths (FWHM) calculated by Methods I and II (see text) for the indicated S(III) and S(IV) lines, and the corresponding values from Ref. 13 calculated by the semi-empirical (SE) and semi-classical (SC) models of Griem. Also given are the widths calculated by Sahal-Br  chet (SB) for certain of these transitions, and the measured widths (W_m) from Ref. 13, scaled to the same plasma conditions as in Table I.

Ion	Transition Array	Designation	Unshifted λ (�) (Air)	W_e^0 (�) (I)	W_e^0 (�) (II)	W_e^0 (�) (SE)	W_e^0 (�) (SC)	W_e^0 (�) (SB)	W_m^0 (�)	
S(III)	3p($^2P^0$)3d - 3p 4p	$^3P_2^0 - ^3P_1$	3370.4	0.131	0.162	0.080	0.147		0.149	
		$^3P_1^0 - ^3P_0$	3387.1	0.132	0.163	0.080	0.147		0.151	
		$^3D_3^0 - ^3P_2$	3928.6	0.182	0.226	0.114	0.206		0.173	
		$^3D_2^0 - ^3P_1$	3983.8	0.188	0.233	0.114	0.206		0.169	
	3p($^2P^0$)4s - 3p 4p	$^3P_0^0 - ^3D_1$	4332.7	0.237	0.300	0.165	0.416	0.259	0.245	
		$^3P_2^0 - ^3D_2$	4361.5	0.238	0.302	0.165	0.416	0.263	0.247	
		$^3P_0^0 - ^3P_1$	3832.0	0.202	0.253	0.135	0.345	0.222	0.198	
		$^3P_2^0 - ^3P_1$	3899.1	0.209	0.262	0.135	0.345	0.229	0.192	
		$^3P_1^0 - ^3S_1$	3662.0	0.185	0.232	0.127	0.325		0.182	
	3p($^2P^0$)4p - 3p 4d	$^3D_2 - ^3F_3^0$	2856.0	0.192	0.221	0.112	0.273		0.206	
		$^3D_3 - ^3F_4^0$	2863.5	0.199	0.228	0.112	0.273		0.202	
		$^3D_1 - ^3F_2^0$	2872.0	0.188	0.217	0.112	0.273		0.200	
		$^3D_1 - ^3D_1^0$	2718.9	0.171	0.196	0.106	0.257		0.202	
		$^3D_3 - ^3D_1^0$	2756.9	0.184	0.209	0.106	0.257		0.206	
		$^3P_1 - ^3D_2^0$	2950.2	0.213	0.245	0.125	0.304		0.210	
		$^3P_2 - ^3D_1^0$	2964.8	0.221	0.251	0.125	0.304		0.212	
	S(IV)	3s 2 (1S)4s - 3s 2 4p	$^2S_{1/2} - ^2P_{1/2}^0$	3097.5	0.102	0.130	0.071	0.196		0.116

TABLE III

Effective Gaunt factors for several collision-induced transitions in S(III), applicable to electron perturbers incident at threshold energy.

Transition	\bar{g}		
	4s - 4p	4s - 5p	5s - 4p
ns 3P - np 3S	0.211	0.418	0.297
- np 3P	0.212	0.417	0.300
- np 3D	0.214	0.387	0.310
	4p - 3d	4p - 4d	5p - 4d
np 3S - nd 3P	0.299	0.218	
np 3P - nd 3P	0.297	0.219	
- nd 3D	0.286	0.220	0.233
np 3D - nd 3P	0.291	0.222	
- nd 3D	0.280	0.223	0.228
- nd 3F	0.336	0.221	0.235

TABLE IV

Effective Gaunt factors for several collision-induced transitions in S(III), applicable to electron perturburbers incident at threshold energy.

Transition	\bar{g}	
	3d - 4f	4d - 4f
nd ³ P - nf ³ D	0.285	
nd ³ D - nf ³ D	0.276	0.206
- nf ³ F	0.276	0.206
nd ³ F - nf ³ D		0.208
- nf ³ F		0.208
- nf ³ G		0.208
	3p ² - 3d	3p ² - 4s
np ² ³ P - nd ³ P	0.293	
- nd ³ D	0.293	
- ns ³ P		0.419

TABLE V

Comparison between the average ratio of measured to calculated (FWHM) electron impact widths for S(III) lines and values obtained by other authors. The indicated uncertainties are standard errors of the mean, and do not implicitly include the experimental uncertainties in electron concentration and temperature stated in Ref. 13. This reference is the source of all measured widths.

Method	Author	Reference	$\frac{W_m}{W_e}$
Method I	Hey (1979)	Present	1.03 ± 0.02
Method II	Hey (1979)	Present	0.86 ± 0.02
Semi-Empirical	Griem (1968)	Ref. 13	1.67 ± 0.05
Semi-Classical	Griem (1974)	Ref. 13	0.74 ± 0.04
Semi-Classical	Sahal-Bréchet (1969)	Ref. 18	0.90 ± 0.03

APPENDIX IV: Data files BATES. and BATES2.

File BATES. contains selected values of the Bates-Damgaard factor for s-p, p-d and d-f transitions. For $\Delta n^* > 1.3$ and $\Delta n^* < -1$, where one defines:

$$\Delta n^* = n_{l_>}^* - n_{l_<}^*$$

the Bates-Damgaard factors are set to zero.

File BATES2. contains selected values of the Bates-Damgaard factor for s-p, p-d, d-f, f-g and g-h transitions. Again, values for $\Delta n^* > 1.3$ and $\Delta n^* < -1$ are regarded as zero.

The values for s-p, p-d and d-f transitions are from Griem (1964), and for the f-g and g-h transitions the tables by Oertel and Shomo (1968) have been used.

In the listings below, the values are read sequentially from left to right.

File BATES.

.40000000-002	.45000000-001	.98000000-001	.16300000	.24100000	.32800000	.42400000	.52400000
.62400000	.72000000	.80800000	.88400000	.94300000	.98300000	1.0000000	.99400000
.96400000	.91100000	.83700000	.74700000	.64300000	.53100000	.41500000	.30000000
.19200000	-.15000000-001	.28000000-001	.84000000-001	.15400000	.23500000	.32700000	.42500000
.52700000	.62900000	.72500000	.81300000	.88800000	.94600000	.98400000	1.0000000
.99200000	.96100000	.90800000	.83500000	.74500000	.64200000	.53100000	.41700000
.30400000	.19800000	-.26000000-001	.18000000-001	.77000000-001	.14800000	.23200000	.32500000
.42500000	.52800000	.63100000	.72800000	.81600000	.89100000	.94800000	.98500000
1.0000000	.99200000	.96000000	.90700000	.83300000	.74400000	.64200000	.53200000
.41900000	.30700000	.20200000	.18200000	.24200000	.31100000	.38800000	.47200000
.55900000	.64800000	.73400000	.81400000	.88500000	.94400000	.98700000	1.0110000
1.0160000	1.0000000	.96300000	.90700000	.83400000	.74600000	.64600000	.54000000
.43100000	.32400000	.22200000	.12900000	.55000000-001	.11700000	.19000000	.27300000
.36400000	.46100000	.56000000	.65700000	.75000000	.83300000	.90300000	.95700000
.99300000	1.0070000	1.0000000	.97100000	.92100000	.85200000	.76700000	.67000000
.56400000	.45500000	.34600000	.24200000	.14700000	.16000000-001	.75000000-001	.14600000
.22900000	.32100000	.42000000	.52200000	.62300000	.72000000	.80800000	.88400000
.94300000	.98400000	1.0030000	1.0000000	.97500000	.92800000	.86200000	.77900000
.68300000	.57800000	.46900000	.36000000	.25500000	.15800000	.31300000	.38900000
.47100000	.55700000	.64400000	.73100000	.81300000	.88800000	.95200000	1.0040000
1.0400000	1.0580000	1.0580000	1.0380000	1.0000000	.94400000	.87200000	.78600000
.69100000	.58800000	.48300000	.37900000	.27900000	.18600000	.10500000	.11300000
.19000000	.27600000	.37000000	.46900000	.56900000	.66800000	.76100000	.84500000
.91600000	.97200000	1.0100000	1.0280000	1.0240000	1.0000000	.95500000	.89200000
.81300000	.72200000	.62100000	.51500000	.40900000	.30500000	.20900000	.12200000
.51000000-001	.12300000	.20600000	.29800000	.39700000	.50000000	.60300000	.70300000
.79400000	.87400000	.93800000	.98500000	1.0120000	.17000000-001	1.0000000	.96200000
.90400000	.82900000	.74000000	.64100000	.53500000	.42800000	.32300000	.22400000
.13400000							

File BATES2.

.40000000-002	.45000000-001	.98000000-001	.16300000	.24100000	.32800000	.42400000	.52400000
.62400000	.72000000	.80800000	.88400000	.94300000	.98300000	1.0000000	.99400000
.96400000	.91100000	.83700000	.74700000	.64300000	.53100000	.41500000	.30000000
.19200000	- .15000000-001	.28000000-001	.84000000-001	.15400000	.23500000	.32700000	.42500000
.52700000	.62900000	.72500000	.81300000	.88800000	.94600000	.98400000	1.0000000
.99200000	.96100000	.90800000	.83500000	.74500000	.64200000	.53100000	.41700000
.30400000	.19800000	- .26000000-001	.18000000-001	.77000000-001	.14800000	.23200000	.32500000
.42500000	.52800000	.63100000	.72800000	.81600000	.89100000	.94800000	.98500000
1.0000000	.99200000	.96000000	.90700000	.83300000	.74400000	.64200000	.53200000
.41900000	.30700000	.20200000	.18200000	.24200000	.31100000	.38800000	.47200000
.55900000	.64800000	.73400000	.81400000	.88500000	.94400000	.98700000	1.0110000
1.0160000	1.0000000	.96300000	.90700000	.83400000	.74600000	.64600000	.54000000
.43100000	.32400000	.22200000	.12900000	.55000000-001	.11700000	.19000000	.27300000
.36400000	.46100000	.56000000	.65700000	.75000000	.83300000	.90300000	.95700000
.99300000	1.0070000	1.0000000	.97100000	.92100000	.85200000	.76700000	.67000000
.56400000	.45500000	.34600000	.24200000	.14700000	.16000000-001	.75000000-001	.14600000
.22900000	.32100000	.42000000	.52200000	.62300000	.72000000	.80800000	.88400000
.94300000	.98400000	1.0030000	1.0000000	.97500000	.92800000	.86200000	.77900000
.68300000	.57800000	.46900000	.36000000	.25500000	.15800000	.31300000	.38900000
.47100000	.55700000	.64400000	.73100000	.81300000	.88800000	.95200000	1.0040000
1.0400000	1.0580000	1.0580000	1.0380000	1.0000000	.94400000	.87200000	.78600000
.69100000	.58800000	.48300000	.37900000	.27900000	.18600000	.10500000	.11300000
.19000000	.27600000	.37000000	.46900000	.56900000	.66800000	.76100000	.84500000
.91600000	.97200000	1.0100000	1.0280000	1.0240000	1.0000000	.95500000	.89200000
.81300000	.72200000	.62100000	.51500000	.40900000	.30500000	.20900000	.12200000
.51000000-001	.12300000	.20600000	.29800000	.39700000	.50000000	.60300000	.70300000
.79400000	.87400000	.93800000	.98500000	1.0120000	.17000000-001	1.0000000	.96200000

.90400000	.82900000	.74000000	.64100000	.53500000	.42800000	.32300000	.22400000
.13400000	.43340000	.52050000	.61010000	.70000000	.78760000	.87000000	.94440000
1.0081000	1.0584000	1.0933000	1.1111000	1.1107000	1.0917000	1.0545000	1.0000000
.93000000	.84690000	.75360000	.65320000	.54910000	.44500000	.34420000	.24970000
.16410000	.89700000-001	.17060000	.25960000	.35610000	.45750000	.56060000	.66230000
.75880000	.84680000	.92270000	.98360000	1.0270000	1.0510000	1.0546000	1.0373000
1.0000000	.94400000	.87140000	.78530000	.68900000	.58620000	.48080000	.37670000
.27750000	.18630000	.10580000	.89000000-001	.17060000	.26240000	.36190000	.46620000
.57150000	.67420000	.77040000	.85620000	.92820000	.98330000	1.0192000	1.0342000
1.0275000	1.0000000	.95210000	.88600000	.80460000	.71120000	.60970000	.50410000
.39840000	.29660000	.20220000	.11790000	.54510000	.64000000	.73450000	.82590000
.91170000	.98910000	1.0555000	1.1084000	1.1459000	1.1664000	1.1688000	1.1527000
1.1185000	1.0671000	1.0000000	.91940000	.82810000	.72890000	.62510000	.52020000
.41720000	.31920000	.22890000	.14850000	.79500000-001	.22700000	.32580000	.43010000
.53690000	.64280000	.74440000	.83810000	.92070000	.98890000	1.0402000	1.0727000
1.0850000	1.0766000	1.0479000	1.0000000	.93480000	.85480000	.76320000	.66350000
.55940000	.45460000	.35270000	.25700000	.17020000	.94600000-001	.12660000	.21690000
.31610000	.42120000	.52900000	.63560000	.73720000	.83000000	.91040000	.97520000
1.0217000	1.0480000	1.0532000	1.0369000	1.0000000	.94400000	.87120000	.78470000
.68800000	.58490000	.47950000	.37560000	.27670000	.18610000	.10630000	

BIBLIOGRAPHY

- ALDER, K.; BOHR, A.; HUUS, T.;
MOTTelson, D.; WINTHER, A.
1956 'Study of Nuclear Structure by Electromagnetic
Excitation with accelerated Ions' in Rev. Mod.
Phys., Vol. 28, p. 432
- ARYA, A.P.
1971 Fundamentals of Atomic Physics. Allyn and Bacon
Inc., Boston
- BARANGER, M.
1958a 'Simplified Quantum Mechanical Theory of Pressure
Broadening' in Phys. Rev., Vol. 111, p. 481
- BARANGER, M.
1958b 'Problem of Overlapping Lines in the Theory of
Pressure Broadening' in Phys. Rev., Vol. 111, p. 494
- BARANGER, M.
1958c 'General Impact Theory of Pressure Broadening'
in Phys. Rev., Vol. 112, p. 855
- BARANGER, M.
1962 'Spectral Line Broadening in Plasmas' Ch.13 in
Atomic and Molecular Processes (ed. Bates : 1962)
- BARNES, K.S.; PEACH, G.
1970 'The Shape and Shift of the Resonance Lines of
Ca⁺ perturbed by Electron Collisions' in
J. Phys. B., Vol. 3, p. 350
- BATES, D.R.
1962 Atomic and Molecular Processes. Academic Press,
New York
- BATES, D.R.;
DANGAARD, A.
1949 'The Calculation of the Absolute Strengths of
Spectral Lines' in Phil. Trans. R. Soc. London,
Vol. A242, p. 101
- BEHRINGER, K.; THOMA, P.
1978 'Electron Impact Widths of some ArII Multiplets'
in JQSRT, Vol. 20, p. 615
- BELY, O.
1969 'Line Broadening Theory for Positive Ions' in
Phys. Rev., Vol. 185, p. 79
- BELY, O.; GRIEM, H.R.
1970 'Quantum-Mechanical Calculation for the Electron
Impact Broadening of the Resonance Lines of Singly
Ionised Mg' in Phys. Rev., Vol. A1, p. 97
- BELY, O.; PETRINI, D.
1970 'Excitation of Li-like Ions by Electron Impacts'
in Astron. Astrophys., Vol. 6, p. 318
- BETHE, H.A.
1930 'Zur Theorie des Durchgangs schneller Korpuskular-
strahlen durch Materie' in Ann. der Physik,
Vol. 5, p. 325
- BETHE, H.A.;
SALPETER, E.E.
1957 Quantum Mechanics of One- and Two-electron Atoms.
Springer Verlag, Berlin

- BLAHA, M.
1969 'Effective Gaunt Factors for Excitation of Positive Ions by Electron Collisions in simplified CB Approximation' in Astrophys. J., Vol. 157, p. 473
- BLAHA, M.
1972 'Excitation of Mg⁺ by Electron Collisions' in Astron. Astrophys., Vol. 16, p. 437
- BLAHA, M.; DAVIS, J.
1978 'Electron Impact Excitation of highly charged Sodium-like Ions' in JQSRT, Vol. 19, p. 227
- BOGEN, P.
1972 'Pressure Broadening of Multiply Ionised Carbon Lines' in Z. für Naturforschung, Vol. 27, p. 210
- BREENE, R.G. (Jr.)
1957 'Line Shape' in Rev. Mod. Phys., Vol. 29, p. 94
- BRETON, C.;
DE MICHELIS, C.;
NATTIOLI, M.
1978 'Ionisation Equilibrium and Radiative Cooling of a High Temperature Plasma' in JQSRT, Vol. 19 p. 367
- BRINK, D.M.;
SATCHEL, G.R.
1962 Angular Momentum. Oxford University Press, London
- BURGESS, D.D.;
FANCETT, B.C.;
PEACOCK, N.J.
1967 'Vacuum ultra-violet Emission Spectra from Laser Produced Plasmas' in Proc. Phys. Soc., Vol. 92, p. 805
- BURKE,
HOISEWITSCH,
1976 Atomic Processes and Application. North-Holland Pub. Co., Amsterdam
- CONDON, E.U.;
SHORTLEY, G.H.
1935 The Theory of Atomic Spectra. Cambridge University Press, London
- COOPER, J.
1966 'Plasma Spectroscopy' in Rep. Prog. Phys., Vol. 29, p. 35
- COOPER, J.; OERTEL, G.K.
1967 'Stark Broadening of Isolated Ion Lines in a Plasma' in Phys. Rev. Letters, Vol. 18, p. 985
- COOPER, J.; OERTEL, G.K.
1969 'Electron Impact Broadening of Isolated Lines of Neutral Atoms in a Plasma' in Phys. Rev., Vol. 180, p. 286
- COWAN, R.D.;
ANDREW, K.L.
1965 'Coupling Considerations in Two-electron Spectra' in J. Opt. Soc. Am., Vol. 55, p. 502
- DAVIS, J.
1974 'Effective Gaunt Factors for Electron Impact Excitation for Multiply charged N and O Ions' in JQSRT, Vol. 14, p. 549

- DAVIS, J.; KEPPLE, P.C.;
BLAHA, M.
1976 'Electron Impact Excitation Coefficients for Laboratory and Astrophysical Plasmas' in JQSRT, Vol. 16, p. 1043
- DAVIS, J.; KEPPLE, P.C.;
BLAHA, M.
1977 'Line Strengths, Collision Strengths and Excitation Rates for Multiply-charged Silicon Ions' in JQSRT, Vol. 18, p. 535
- DE WITT COLEMAN, C.;
BOZMAN, W.R.;
HEGGERS, W.F.
1960 Table of Wavenumbers. Vol. I, NBS Monograph 3, U.S. Department of Commerce, Washington D.C.
- DIMITRIJEVIĆ, M.S.;
GRUJIĆ, P.
1978 'Long Range Potentials and Stark Broadening of Neutral Lines' in JQSRT, Vol. 19, p. 407
- DIMITRIJEVIĆ, M.S.;
KONJEVIĆ, N.
1978 'On the Temperature Dependence of Gaunt Factors' in JQSRT, Vol. 20, p. 223
- DIMITRIJEVIĆ, M.S.;
KONJEVIĆ, N.
1980a 'Stark Widths of doubly- and triply-ionised Atom Lines', to be published in JQSRT
- DIMITRIJEVIĆ, M.S.;
KONJEVIĆ, N.
1980b 'On the Stark Broadening of Ionised Nitrogen Lines', (unpub. Manuscript)
- DIMITRIJEVIĆ, M.S.;
KONJEVIĆ, N.
1980c 'Modified Semi-empirical Formula for the Electron-Impact Width of Ionised Atom Lines: Theory and Applications' to be published in Proc. 5th ICSLS, Berlin
- DYNEFORS, B.I.;
MARTINSON, I.
1978 'Beam Foil Studies of Ionised Sulfur' in Physica Scripta, Vol. 17, p. 123
- FEYNMAN, R.P.
1951 'An Operator Calculus having Applications in Quantum Electrodynamics' in Phys. Rev., Vol. 84, p. 108
- FLEURIER, C.;
SAHAL-BRECHOT, S.;
CHAPELLE, J.
1977 'Stark Profiles of some Ion Lines of Alkaline Earth Elements' in JQSRT, Vol. 17, p. 595
- FOLEY, H.M.
1946 'The Pressure Broadening of Spectral Lines' in Phys. Rev., Vol. 69, p. 616
- FOWLER, R.H.
1924 'Statistical Equilibrium with Special Reference to the Mechanism of Ionisation by Electronic Impacts' in Phil. Mag., Vol. 56-47, p. 257

- FUHR, J.R.; MILLER, B.J.;
MARTIN, G.A.
1978
Bibliography on Atomic Transition Probabilities.
NBS Special Publication 505, U.S. Department of
Commerce, Washington D.C.
- GAİLITIS, M.
1963
'Behaviour of Cross-Sections near Threshold of a
new Reaction in the Case of a Coulomb Attraction
Field' in Soviet Phys. JETP, Vol. 17, p. 1328
- GAUNT, J.A.
1930
'Continuous Absorption'
in Phil. Trans., Vol. A229, p. 163
- GELL-MANN, M.;
GOLDBERGER, H.L.
1953
'The Formal Theory of Scattering' in Phys. Rev.,
Vol. 91, p. 398
- GRIEM, H.R.
1962a
'Stark Broadening of Isolated Spectral Lines from
Heavy Elements in a Plasma' in Phys. Rev.,
Vol. 128, p. 515
- GRIEM, H.R.
1962b
'Wing Formulae for Stark-broadened Hydrogen and
Hydrogenic Lines' in Astrophys. J., Vol. 136, p. 422
- GRIEM, H.R.
1964
Plasma Spectroscopy. McGraw-Hill, New York
- GRIEM, H.R.
1966
'Electron-impact Broadening of Isolated Ion
Lines' in Phys. Rev. Letters, Vol. 17, p. 509
- GRIEM, H.R.
1968
'Semi-empirical Formulae for the Electron Impact
Widths and Shifts of Isolated Ion Lines in
Plasmas' in Phys. Rev., Vol. 165, p. 258
- GRIEM, H.R.
1970/71
'Effects of Resonances on the Electron Impact
Broadening of Ion Lines' in Comm. Atom. Molec. Phys.
Vol. 2, p. 147
- GRIEM, H.R.
1974
Spectral Line Broadening by Plasmas.
Academic Press, New York
- GRIEM, H.R.; KOLB, A.C.;
SHEN, K.Y.
1959
'Stark Broadening of Hydrogen Lines in a Plasma'
in Phys. Rev., Vol. 116, p. 4
- GRIEM, H.R.;
BARANGER, H.; KOLB, A.C.;
BERTEL, G.K.
1962
'Stark Broadening of neutral Helium Lines in a
Plasma' in Phys. Rev., Vol. 125, p. 177
- HAGAN, L.
1977
Bibliography on Atomic Energy Levels and Spectra.
NBS Special Publication 363, Supplement 1,
U.S. Department of Commerce, Washington D.C.
- HAGAN, L.; MARTIN, W.C.
1972
Bibliography on Atomic Energy Levels and Spectra.
NBS Special Publication 363, U.S. Department of
Commerce, Washington D.C.

- HAUER, A.
1980 'Diagnosis of high Density Laser compressed Plasma using Spectral Line Profiles' to be published in Proc.5th ICSSL, Berlin
- HEBB, H.H.; MENZEL, D.H.
1940 'Physical Processes in Gaseous Nebulae' in Astrophys.J., Vol. 92, p. 408
- HEITLER, W.
1954 The Quantum Theory of Radiation.
3rd.rev.ed., Oxford University Press, London
- HERZBERG, G.
1937 Atomic Spectra and Atomic Structure.
Dover Publications, New York
- HEY, J.D.
1976a 'Criteria for LTE in non-hydrogenic Plasmas' in JQSRT, Vol. 16, p. 69
- HEY, J.D.
1976b 'Estimates of Stark Broadening of Nitrogen Ion Lines' in JQSRT, Vol. 16, p. 575
- HEY, J.D.
1977a 'The role of the Oscillator Strength in the determination of Plasma Densities' in JQSRT, Vol. 17, p. 721
- HEY, J.D.
1977b 'Estimates of Stark Broadening of some ArIII and ArIV Lines' in JQSRT, Vol. 17, p. 729
- HEY, J.D.
1977c 'Estimates of Stark Broadening of some SiII Lines' in JQSRT, Vol. 18, p. 425
- HEY, J.D.
1977d 'On the Stark Broadening of isolated Lines of FII and ClIII by Plasmas' in JQSRT, Vol.18, p. 649
- HEY, J.D.
1978 'On the Variation of Spectral Line Widths within Stark-broadened Multiplets' in JQSRT, Vol.20, p. 403
- HEY, J.D.; BRYAN, R. J.
1977 'Estimates of Stark Broadening of Oxygen Ion Lines' in JQSRT, Vol.17, p. 221
- HEY, J.D.; BLAHA, M.
1978 'Stark Broadening of Nitrogen Ion Lines from States of high Orbital Angular Momentum' in JQSRT, Vol. 20, p. 557
- HEY, J.D.; BREGER, P.
1980a 'Stark Broadening of Isolated Lines emitted by Singly-ionised Tin' in JQSRT, Vol. 23, p. 311
- HEY, J.D.; BREGER, P.
1980b 'Calculated Stark Widths of Oxygen Ion Lines' in press, JQSRT
- HEY, J.D.; BREGER, P.
1980c 'Calculated Stark Widths of Isolated SIII and SiV Lines' in press, JQSRT
- HEY, J.D.; BREGER, P.
1980d 'Stark Broadening of Isolated Ion Lines by Plasmas: Theory' to be pub. in Proc.5th ICSSL, Berlin

- HEY, J.D.; BREGER, P.
1980e 'Stark Broadening of Isolated Ion Lines by Plasmas: Application of Theory' to be pub. in Proc. 5th ICSSL, Berlin
- HOLTSMARK, J.
1919 'Über die Verbreiterung von Spektrallinien' in Annalen der Physik, Vol. 58, p. 577
- HUDDLESTONE, R.H.;
LEONARD, S.L.
1965 Plasma Diagnostic Techniques.
Academic Press, New York
- HUI LI
1972 'Zeeman effect of PII' in J. Opt. Soc. Am., Vol. 62,
p. 12
- JONES, W.W.; BENETT, S.N.;
GRIEM, H.R.
1971 University of Maryland Technical Report. No. 71-123
- JONES, W.W.; HILLER, M.
1974 'Stark Broadening of Germanium' in Phys. Rev.,
Vol. A10, p. 1803
- KÄLLNE, E.; JONES, L.;
BARNARD, A.
1979 'Experimental Study of Stark Broadening of
Nitrogen Ion Lines from a Theta Pinch Plasma'
in JQSRT, Vol. 22, p. 589
- KELLY, R.L.; PALUMBO, L.J.
1973 Atomic and Ionic Emission Lines below 2000 Å.
Naval Research Laboratory, Washington D.C.
- KONJEVIĆ, H.; ROBERTS, J.R.
1976 'A Critical Review of the Stark Widths and Shifts
of Spectral Lines from Non-Hydrogenic Atoms' in
J. Phys. Chem. Ref. Data, Vol. 5, p. 209
- KONJEVIĆ, N.; WIESE, W.L.
1976 'Experimental Stark Widths and Shifts for Non-
Hydrogenic Spectral Lines of Ionised Atoms (A
Critical Review and Tabulation of Selected Data)'
in J. Phys. Chem. Ref. Data, Vol. 5, p. 259
- KONJEVIĆ, N.;
DIHITRIJEVIĆ, M.S.
1980 'On the systematic Trends of Stark Broadening
Parameters of Isolated Lines in Plasmas' to be
published in Proc. 5th ICSSL, Berlin
- KWU-REPORT
1973 Energy Sources and their Prospects,
Kraftwerk Union Annual Report, KWU 266-101,
Federal Republic of Germany
- KRAMERS, H.A.
1923 'On the Theory of X-Ray Absorption and of the
continuous X-Ray Spectrum' in Phil. Mag.,
Vol. 46, p. 836
- LEWIS, M.
1961 'Stark Broadening of Spectral lines by High-
Velocity Charged Particles' in Phys. Rev.,
Vol. 121, p. 501
- LITTLEWOOD, D.E.
1958 A University Algebra.
Dover Publications, New York

- LOCHTE-HOLTGREVEN, W.
1968 Plasma Diagnostics.
North-Holland Pub.Co., Amsterdam
- LORENTZ, H.A.
1906 'The Absorption and Emission Lines of Gaseous Bodies' in Proc.Roy.Acad.Sci.(Amsterdam), Vol. 8, p. 591
- MARR, G.V.
1968 Plasma Spectroscopy.
Elsevier Pub. Co., Essex
- MASSEY, H.S.W.
1956 'Theory of the Scattering of Slow Electrons' in Rev.Mod.Phys., Vol. 28, p. 199
- HAZURE, A.; NOLLEZZ, G.
1978 'Application of the Model Microfield Method to Stark Profiles of Alkali Metal Resonance Lines' in Z.Naturforschung, Vol. 33a, p. 1575
- MERZBACHER, E.
1961 Quantum Mechanics. 2nd ed., John Wiley & Sons, Inc., New York
- HEWE, R.
1972 'Interpolation Formulae for the Electron Impact Excitation of Ions in the H, He, Li and Ne Sequences' in Astron.Astrophys., Vol. 20 p. 215
- MIHALAS, D.
1970 Stellar Atmospheres.
W.H.Freeman and Co., San Francisco
- MILLER, H.H.; ROIG, R.A.;
BENOTSON, R.D.
1979 'Experimental Transition Probabilities and Stark Broadening Parameters of Neutral and Singly Ionised Tin' in Phys.Rev., Vol. A20, p. 499
- MILMAN, A.S.
1978 'Calculation of Optical Depths from an Integral of the Voigt Function' in JQSRT, Vol. 20, p. 593
- HILNE, E.A.
1924 'Statistical Equilibrium in relation to the Photo-electric Effect and its Application to the Determination of Absorption Coefficients' in Phil.Mag., Vol. S6-47, p. 209
- MOORE, C.E.
1958 Atomic Energy Levels. Vol III, NBS Circular no. 467, U.S.Department of Commerce, Washington D.C.
- MOORE, C.E.
1970 Selected Tables of Atomic Spectra, NSRDS-NBS 3, Section 3, U.S.Department of Commerce, Washington D.C.
- MOORE, C.E.
1971a Atomic Energy Levels. Vol.I, NSRDS-NBS 35, U.S.Department of Commerce, Washington, D.C.
- MOORE, C.E.
1971b Selected Tables of Atomic Spectra. NSRDS-NBS 3, Section 4, U.S.Department of Commerce, Washington D.C.

- MOORE, C.E.
1975
Selected Tables of Atomic Spectra. NSRDS-NBS 3, Section 5, U.S. Department of Commerce, Washington D.C.
- MOTT, N.F.; MASSEY, H.S.W.
1965
The Theory of Atomic Collisions. 3rd. ed. Oxford University Press, London
- ORTEL, G.K.; SHOMO, L.P.
1968
'Tables for the calculation of Radial Multipole Matrix Elements by the Coulomb Approximation' in *Astrophys. J. Suppl.*, Vol. 16, p. 175
- PETRINI, D.
1970
'The Electron Excitation Rate of the green Coronal Line 5303Å' in *Astron. Astrophys.*, Vol. 9 p. 392
- PLATIŠA, M.; POPVIĆ, M.;
DIMITRIJEVIĆ, N.;
KONJEVIĆ, N.
1975
'Stark Broadening of AIII and AIV Lines' in *Z. Naturforschung*, Vol. 30a, p. 212
- PLATIŠA, M.; POPOVIĆ, M.;
KONJEVIĆ, N.
1975
'Stark Broadening of OII and OIII Lines' in *Astron. Astrophys.*, Vol. 45, p. 463
- PLATIŠA, M.;
DIMITRIJEVIĆ, N.;
POPOVIĆ, N.; KONJEVIĆ, N.
1977
'Stark Broadening of FII and CIIII Lines' in *Astron. Astrophys.*, Vol. 54, p. 837
- PLATIŠA, M.; POPOVIĆ, M.;
DIMITRIJEVIĆ, N.;
KONJEVIĆ, N.
1979
'Stark Broadening of SIII and SIV Lines' in *JQSRT*, Vol. 22, p. 333
- PURIĆ, J.; CIRKOVIĆ, L.J.;
LABAT, J.
1974
'Regularities in Stark Broadening Parameters' in *Fizika*, Vol. 6, p. 211
- PURIĆ, J.;
DIMITRIJEVIĆ, N.S.;
LAKICEVIĆ, I.S.
1978
'Some Regularities within the Stark Widths of Resonance Lines of Alkali-like Homologous Atoms and Ions' in *Physics Letters*, Vol. 67A, p. 189
- PURIĆ, J.;
LAKICEVIĆ, I.S.;
GLAVONJIĆ, V.
1979a
'Some Regularities within the Stark Widths and Shifts of Resonance Lines of Neutral Atoms from He to Ca' in *Journal de Physique, Colloque C7*, supplément au no. 7, Tome 40, p. C7-795
- PURIĆ, J.;
LAKICEVIĆ, I.S.;
GLAVONJIĆ, V.
1979b
'Some Regularities within the Stark Widths and Shifts of Resonance Lines of Singly Charged Ions from He to Ca' in *Journal de Physique, Colloque C7* supplément au no. 7, Tome 40, p. C7-835
- PURIĆ, J.;
LAKICEVIĆ, I.S.;
GLAVONJIĆ, V.
1980
'Stark Width and Shift dependence on the Ionisation Potential' in *Physics Letters*, Vol. 76A, p. 128

- SAHAL-BRECHOT, S.
1969a 'Impact Theory of the Broadening and Shift of Spectral lines due to Electrons and Ions in a Plasma I' in Astron.Astrophys., Vol. 1, p. 91
- SAHAL-BRECHOT, S.
1969b 'Impact Theory of the Broadening and Shift of Spectral Lines due to Electrons and Ions in a Plasma II' in Astron.Astrophys., Vol. 2, p. 322
- SCHIFF, L. I.
1968 Quantum Mechanics. 3rd.ed.
McGraw Hill, Tokyo
- SEATON, M. J.
1955 'Cross-Sections for 2s-2p Transitions in H and 3s-3p Transitions in Na produced by Electron and by Proton Impact' in Proc.Phys.Soc., Vol. 68, p. 457
- SEATON, M. J.
1958 'Thermal Inelastic Collision Processes' in Rev.Mod.Phys., Vol. 30, p. 979
- SEATON, M. J.
1962a 'The Theory of Excitation and Ionisation by Electron Impact', Ch. 11 in Atomic and Molecular Processes (ed. Bates: 1962)
- SEATON, M. J.
1962b 'The Impact Parameter Method for Electron Excitation of Optically allowed Atomic Transitions' in Proc.Phys.Soc., Vol. 79, p. 1105
- SEATON, M. J.
1969 'Quantum defect Theory VII Analysis of Resonance Structures' in J.Phys.B., Vol. 2, p. 5
- SEATON, M. J.
1975 'Electron Impact Excitation of Positive Ions' in Advances Atom.Molec.Phys., Vol. 11
- SEATON, M. J.; STOREY, P.
1976 'Di-electronic Recombination' in Atomic Processes and Applications (ed. Burke and Moiseiwitsch: 1976)
- SHORE, D. W.; MENZEL, D. H.
1968 Principles of Atomic Spectra.
John Wiley and Sons, New York
- SOBEL'MAN, I. I.
1972 Introduction to the Theory of Atomic Spectra.
Pergamon Press, Braunschweig
- SPITZER, L.
1940 'Impact Broadening of Spectral Lines' in Phys.Rev., Vol. 58, p. 348
- THOMAS, L. H.
1927 'The Calculation of Atomic Fields' in Proc.Camb.Phil.Soc., Vol. 23, p. 542
- TOLMAN, R. C.
1948 The Principles of Statistical Mechanics.
Oxford University Press, London
- TRAVING, G.
1968 'Interpretation of Line Broadening and Line Shift' Ch. 2 in Plasma Diagnostics, (ed. Lochte-Holtgreven: 1968)

- VAN REGEMORTER, H.
1960 'Electron Impact Excitation of positive Ions: Application to Ca⁺ 4s-4p and 3d-4p' in MNRAS, Vol. 121, p. 213
- VAN REGEMORTER, H.
1962 'Rate of Collisional Excitation in Stellar Atmospheres' in Astrophys. J., Vol. 136, p. 906
- VOLONTE, S.
1978 'Polarisation Shift effect in high-density Plasmas' in J. Phys. D: Appl. Phys., Vol. 11, p. 1615
- WARNER, B.
1968a 'Atomic Oscillator Strengths I' in MNRAS, Vol. 139, p. 1
- WARNER, B.
1968b 'Atomic Oscillator Strengths II' in MNRAS, Vol. 139, p. 103
- WARNER, B.
1968c 'Atomic Oscillator Strengths III' in MNRAS, Vol. 139, p. 115
- WARNER, B.
1968d 'Line Strengths in two-electron Spectra' in MNRAS, Vol. 139, p. 273
- WEISSKOPF, V.
1933 'Zur Theorie der Kopplungsbreite und der Stossdämpfung' in Z. für Physik, Vol. 75, p. 287
- WIESE, W. L.
1965 'Line Broadening', Ch. 6 of Plasma Diagnostic Techniques (ed. Huddleston and Leonard: 1965)
- WIESE, W. L.; WEISS, A. U.
1968 'Regularities in Atomic Oscillator Strengths' in Phys. Rev., Vol. 175, p. 50
- WIESE, W. L.; SMITH, M. W.; NILES, B. H.
1969 Atomic Transition Probabilities. Vol. II, NSRDS-NBS 22, U.S. Department of Commerce, Washington D.C.
- WUJEC, T.; MUSIELOK, J.
1976 'Measurement of Absolute Transition Probabilities of SnI and SnII Lines by Method of Emission Spectroscopy' in Astron. Astrophys., Vol. 50, p. 405
- WUJEC, T.; WENIGER, S.
1977 'Atomic Transition Probabilities for SnI, SnII and ClI Lines in the 5300-6850 Å wavelength Range' in JQSRT, Vol. 18, p. 509
- YOUNGER, S. H.
1979 'Collision Strengths and Gaunt factors for highly ionised Atoms of the Copper Isoelectronic Sequence' in JQSRT, Vol. 22, p. 155
- YOUNGER, S. H.
1980 'Electron Impact Excitation of the Resonance Transitions of highly ionized Atoms of the Be, Mg, and Zn isoelectronic Sequences' in JQSRT, Vol. 23, p. 489
- YOUNGER, S. H.; WIESE, W. L.
1979 'An Assessment of the effective Gaunt Factor Approximation' in JQSRT, Vol. 22, p. 161
- ZURRO, B.; CAMPOS, J.; SÁNCHEZ DEL RÍO, C.
1973 'Lifetimes of some excited Levels of ArI' in Physics Letters, Vol. 43A, p. 527